Appendix A

R4 Model Documentation

Appendix A – Section 1

INTRODUCTION

The Chino groundwater basin is about 220 square miles in area. The surface watershed surrounding the basin is about 530 square miles including Chino Basin, Arlington Basin and portion of Temescal Basin as shown in Figure A1-1. This appendix summarizes the calculation of areal recharge for the Chino Basin that is used as input to the MODFLOW groundwater model. Historical areal recharge is estimated using a model that is comprised of three modules: Rainfall-Runoff (R-R), Router, and Root Zone module. This model is referred to as the R4 model and developed by Wildermuth Environmental, Inc (WEI).

The origin of this model can be traced to the Chino Basin Water Conservation District and the Chino Basin Watermaster. These agencies wanted to estimate the volume of stormwater recharge in the Chino Basin that occurred in recharge basins, flood retention basins, and unlined streams. WEI developed a daily simulation model to estimate runoff, route the runoff through the Chino Basin drainage system, calculate recharge on a daily basis, and produce reports that summarized recharge performance. This model was initially developed in 1994 for the western portion of the Chino Basin (Mark J. Wildermuth, 1995) and was expanded to the entire Chino Basin in 1996 (WEI, 1998). Subsequently, it was used in the Chino Basin to estimate the recharge performance of new basins and the recharge benefits of improved basin maintenance (Black and Veatch, 2001). The model was then expanded to include water quality simulations and was applied to the Wasteload Allocation Investigation for the Santa Ana Watershed (WEI, 2002). After the root zone simulation module was added, the model was successfully used to estimate areal recharge from precipitation, return flows from urban and agricultural land uses, and stormwater percolation in the recharge basins and channel systems of several groundwater basins for which WEI has developed groundwater models—Chino Basin (WEI, 2003), Beaumont Basin (WEI, 2006) and Arlington Basin (WEI, 2006).

Figure A1-2 is a simplified flowchart that documents and summarizes the key steps followed in the R4 model. The rainfall is the most important input data to drive the R-R module. Daily rainfall data have been collected for the period of 1921 to 2006. The R-R model process daily rainfall data and produce daily storm water discharge and surface infiltration data for each sub-drainage area. The Router module routes the storm water discharge and other flows, such as boundary inflow and point discharge, along the stream and recharge/retention basin network and calculates outflow. It also calculates ground percolation from stream and recharge/retention basins. The Root Zone module reads the infiltration data outputs of the R-R model, calculates applied water for irrigated lands, calculates evapotranspiration requirements, and estimates root zone percolation to the groundwater basin. The output data from the Router and Root Zone modules are processed to create areal recharge data used in the groundwater model. The following sections describe each module in detail.

RUNOFF MODULE

A2-1 INPUT PARAMETERS FOR THE RUNOFF MODULE

This section describes the input data required for the runoff model. These input data are listed below and followed by a brief description:

Geographic Information Data:

- Digital Elevation Model (DEM) : A representation of ground surface topography
- Storm water Drainage Master Plan
- Hydrologic Sub-Area (HSA)
- Hydrologic Soil Coverage
- Historical Land Use Data

Daily Hydrologic Data:

- Rainfall

Parameters:

- Runoff Curve Number

The surface water drainage, or watershed, delineation was based on a digital elevation model and drainage master plans from the counties and cities within the watershed boundary. The watershed of the modeling area is part of the Upper Santa Ana River Watershed west of the Riverside Narrows. This watershed is approximately 530 square miles. This modeling area was divided into 126 sub-drainage areas called Hydrologic Sub-Areas (HSA). The complete watershed and the sub-drainages are shown in Figure A2-1.

The hydrologic soil type delineations for the watershed were based on the Soil Conservation Service (SCS) maps and classifications. Soil surveys for the area are contained in the *Soil Survey of San Bernardino County, Southwestern Part* (SCS, 1977), *Soil Survey of Western Riverside County* (SCS, 1971), and the *Soil Survey of the Pasadena Area, California* (SCS, 1917). The SCS soil classification system rates soils by runoff potential as shown in Table A2-1. Figure A2-2 shows the areal distribution of the hydrologic soil types.

The land use data, which consist of data from the Department of Water Resources (DWR) and the Southern California Association of Governments (SCAG), were obtained from the

Santa Ana Watershed Project Authority (SAWPA). The DWR land use data, which range from 1933 to 1984, are grouped into nine land use classifications. The land use data (survey years 1990 and 2000) are in Anderson Code, a more detailed land use classification. Table A2-2 lists the year of the land use survey and the source of the data, and Table A2-3 summarizes the data. DWR land use data were grouped into nine land use types and digitized for SAWPA basin plan upgrade task force (JMM, 1989). WEI reviewed these land use types as well as SCAG land use data and added four more types to create thirteen land use types, as shown in Table A2-3. Table A2-4 shows the Anderson Land Use Code and its conversion into 13 land use types. Figures A2-3 through A2-10 show land time history for the period of 1933 to 2000 that was used in the R4 model. To reflect the rapid land use development in the last few years, the 2000 land use map was updated with a 2006 aerial photograph as shown in Figure A2-11. For the planning period, land use map according to the following assumptions:

a) The surrounding mountain area will remain the same.
b) The riparian area along the Santa Ana River and Prado Basin will remain the same.
c) The developed urban area will remain the same.
d) The undeveloped urban and agricultural areas will be developed as urban residential area.
e) Only agricultural area in Prado Basin will remain the same.

Twenty-four rain gauges were used in the analysis. These gauges are typically well spaced across the watershed, and the majority have complete records during the simulation period. Daily rainfall data were obtained from San Bernardino and Riverside Counties. The stations that were used are listed in Table A2-5. Gauge locations and Thiessen polygons are shown in Figure A2-12. To derive the daily mean areal precipitation (MAP), the Thiessen polygon method was applied to the gauge network across the watershed. The MAP is assumed uniform and given the value of the gauge associated with each polygon if the HSA is within a Thiessen polygon. IF the HSA lies over multiple Thiessen polygons, a weighting factor based on the proportional area is multiplied by each gauge value corresponding to each polygon.

The hydrologic soil types and land uses were used to develop runoff curve number (CN) tables. The CNs reflect the abilities of soils in retaining rainfall from storm events Which correspond to lower values for well draining sandy soils and higher values for poor draining silty clay soils. Table A2-6 lists the initial CN estimates for land uses and soil types. These data were based on the recommended values in the hydrology manuals of the San Bernardino County Flood Control District (SBCFCD) and the Riverside County

Flood Control and Water Conservation District (RCFC&WCD) and TR-55.

A2-2 RUNOFF MODULE THEORY AND METHODS

The primary method used to estimate rainfall-runoff is the SCS method. The National Engineering Handbook, Section 4, Chapter 10 (SCS, 1985) illustrates the derivation of the rainfall-runoff relationship, which is known as the SCS Method This relationship among rainfall, runoff, and retention can be expressed mathematically from the hypothesis that the ratio of potential quantities is equal to the ratio of actual quantities, that is:

$$\frac{F}{S} = \frac{Q}{P - I_a}$$

Where F = the actual retention after runoff begins
S = the potential maximum retention after runoff begins (S > F)
Q = the actual runoff or rainfall excess
I_a = the initial abstraction
P = the actual rainfall (P>Q)

The total mass balance of the storm can be written as:

$$P = Q + (F + I_a)$$

This equation states that the total rainfall is the sum of runoff and retention. The equation can be rearranged as:

$$F = (P - I_a) - Q$$

Solving for the total storm runoff (Q) results in the runoff equation:

$$Q = \frac{(P - I_a)^2}{(P - I_a) + S}$$

This is the basic rainfall-runoff relationship used in SCS method. Figure A2-13 illustrates the relationship between the SCS method variables. Notice that runoff does not occur during the initial abstraction.

The initial abstraction (I_a)consists of interception, infiltration during early parts of the storm, and surface depression storage. It was assumed to be a function of the maximum potential retention (S). The SCS has empirical established that the I_a is related to S as:

$$I_a = 0.2S$$

By substituting I_a in the basic rainfall-runoff equation:

$$Q = \frac{(P - 0.2S)^2}{P + 0.8S} \qquad when\, P > I_a$$

The empirical relationship between the CN and the potential retention is given by:

$$CN = \frac{1000}{10 + S}$$

The practical implication of this equation is that CN approaches 100 when S approaches zero (retention is negligible), and CN approaches zero when S approaches infinity.

The rainfall-runoff data do not fit the CN runoff concept precisely due to variability of rainfall intensity and duration, total rainfall, soil moisture conditions, cover density, stage of growth, and temperature. Subsequently, this variability is accounted for by adjusting the CN number of normal Antecedent Runoff Condition (ARC) accordingly. The ARC is divided into three classes: I for dry conditions, II for normal conditions, and III for wet conditions. The National Engineering Handbook, part 630, Chapter 10 (NEH, 2000), contains a table of empirically determined CNs for three ARCs, which have been plotted in Figure A2-14.

Several equations have been developed to fit the CNs for different ARCs. Limbrunner et al (2005) quote the work of Haith et al (1987) for CNs that correspond to different ARCs:

$$CN_1 = \frac{CN_2}{2.334 - 0.01334 * CN_2}$$

$$CN_3 = \frac{CN_2}{0.4036 + 0.0059 * CN_2}$$

Limbrunner et al (2005) suggest an interpolation between CN_1 and CN_3, using soil moisture retention capacity:

$$CN(t) = (CN_3 - CN_1) * \frac{S(t)}{S_{max}} + CN_1$$

Where *S*(*t*) is a variable that represents unsaturated zone soil storage at time *t*, and S_{max} is the maximum allowable unsaturated soil storage under dry conditions. The storage variable is tracked on a daily basis such that *CN*(*t*) can be tracked on a daily basis.

A2-4 SUMMARY

The Runoff Module is used to determine two key elements of areal recharge: the actual runoff volume and the rainfall abstraction. Runoff was calculated with the SCS method and imported into the Router Module for routing flows through the Chino Basin. The rainfall abstraction was imported into the Root Zone Module to calculate the amount of water that infiltrates the root zones.

ROUTER MODULE

The Router Module collects daily discharge from the hydrologic areas specified in the Runoff Module, boundary inflows, and other points of discharge (e.g., discharged recycling plant to the stream system), then routes the water through the drainage system. The USGS maintains several stream gauge stations on tributary streams that are within or contribute to the study area. Table A3-1 lists these stations as well as some stations that are not currently maintained, but were used in this analysis; in some cases, historical records were used from stream gauges that are no longer in service. The daily stream flow data for watersheds that are tributary to the study area are used as input data to the Router module and for stations within the study area, the stream flow data are used for calibration of the router modules.

The drainage system is represented by nodes and links. A node collects flows from upstream tributary links; add and accept runoff from HSA's, boundary inflows, and point discharge; and send totalized flows through the downstream link.

There are five types of links in the router module that are used to route discharge through the stream reaches in the system:

- Type 1 – Open Channels with Trapezoidal Sections
- Type 2 – Open Channels with Elevation-Width-Flow Rate Rating Tables
- Type 3 – Closed Conduits
- Type 4 – Retention/Recharge Basins
- Type 5 – Diversions

A3-1 OPEN CHANNEL LINKS

Open channel links are used to route flows between nodes and to estimate stream bottom percolation. There are two types of open channel links: Type 1 (trapezoidal), and Type 2 (elevation-width rating curve links). For Type 1, Manning's equation is used to estimate average stream width and elevation. For Type 2, a predetermined rating curve is used to estimate average stream widths and elevations, based on flow rate.

In Manning's equation, the flow is represented as:

$$Q_s = \frac{1.49}{n} A R^{2/3} S_b^{1/2}$$

Where Q_s = the flow rate (cfs)
n = the roughness coefficient
A = the cross-sectional area
R = the hydraulic radius (cross-sectional area divided by wetted perimeter)
S_b = the channel bottom slope

For a trapezoidal section with a known bottom width (B) and known left (s_l) and right (s_r) side slopes, the stream top width (T) can be expressed as:

$$T = B + y(s_l + s_r)$$

The cross-sectional area (A) as:

$$A = y(B + \frac{s_l + s_r}{2} y)$$

And the wetted perimeter (P) as:

$$P = B + y(\sqrt{(1 + s_l^2)} + \sqrt{(1 + s_r^2)}$$

Substituting A and P, the Manning's equation can be written as:

$$Q_s = \frac{1.49}{n}\left[\left[y(B + \frac{s_l + s_r}{2} y)\right]\right]^{5/3} \left[B + y(\sqrt{(1 + s_l^2)} + \sqrt{(1 + s_r^2)}\ \right]^{-2/3} S_b^{1/2}$$

For the given daily average flow (Q_s), the equation is iteratively solved using Newton's method for the average depth (y), and stream width (T) can be estimated.

The daily stream bottom percolation in a link can be estimated with the following equation:

$$Q_{sp} = L * T * P_v$$

Where Q_{sp} = stream bottom percolation (ft^3/day)
L = the length of the stream link (ft)
T = the top width of the stream link (ft)
p_v = the vertical percolation rate (ft/day)

Table A3-2 lists the roughness coefficients for selected channel characteristics.

For the rating table stream sections, the relationship of daily average flow versus average width is specified as input data to the Router Module. This feature is useful for a stream section wherein the cross-section is irregular, such as the lower portion of the Santa Ana River. The information needed to obtain the average width was obtained from the HEC-RAS flood prediction model that was developed for the Santa Ana River.

A3-2 TYPE 3 CLOSED CONDUITS

Closed conduit links represent closed storm drain pipes. These links are assumed to have no infiltration properties.

A3-4 TYPE 4 RETENTION/RECHARGE BASINS

Retention/Recharge basins are simulated for flood peak attenuation and groundwater recharge purposes. These basins are represented by rating curves that relates water surface elevation to surface area, and discharge.
The mass balance equation for a retention/recharge basin can be expressed as:

$$S_t - S_{t-1} = I_t - Ev_t - Qp_t - Qc_t - Qs_t$$

Where S_t = the storage at the end of time step *t*
I_t = the total inflow during time step *t*
Ev_t = evaporation
Qp_t = percolation
Qc_t = controlled conduit outflow
Qs_t = spillway outflow

Recharge basins are simulated by solving the continuity equation. It is based on an assumption that is used for the Modified Puls method of reservoir routing. The water level in the basin is horizontal; thus, eliminating the momentum of flow. For mathematical stability, the model adjusts the simulation time steps, comparing the basin storage volume and inflow rate up to a maximum of 240 time steps per day.

A3-5 TYPE 5 DIVERSION LINKS

Diversion links represent stream diversions out of a node. These links are simulated with rating tables that divert flow as a function of the total flow at the link.

ROOT ZONE MODULE

A4-1 THEORY AND METHODS

The Root Zone Module calculates the amount of water that passes through the root zone and into the unsaturated zone. To complete this simulation, soil moisture, estimates of irrigation water requirements for agricultural and urban areas, and deep percolation below the root zone are tracked on a daily basis.

The Root Zone Module requires the following input data:

- The crop coefficients of the land use types
- The soil characteristics for field capacity, the wilting point, and the critical soil moisture for irrigation
- Daily rainfall infiltration to root zone from the runoff model
- Daily reference evapotranspiration

There is one evaporation station near the study area with long period of record. This station, the Puddingstone Reservoir station, is maintained by the County of Los Angeles, Department of Public Works and has a period of record that ranges from 1948 to present. Within this period of record, two years of data are missing: 1991 and 1994. For modeling purposes these missing data were estimated using long-term average evaporation data. The historical evaporation data are shown in Figure A4-1.

On a daily time step, the Root Zone Module calculates the mass balance for areas with identical soil and land use types in a hydrologic area as:

$$SM_{t+1} = SM_t + I_t + AW_t - ET_t - DP_t$$

Where SM_t = soil moisture storage at time t
I_t = rainfall infiltration to root zone during the period t to $t+1$
AW_t = applied water to for irrigation during the period t to $t+1$
ET_t = evapotranspiration during the period t to $t+1$
Dp_t = deep percolation below root zone during the period t to $t+1$

The daily rainfall infiltration for each area of specified land use and soil type in a drainage area that is an output from the Runoff Module is taken as input to the Root Zone Module. The soil moisture in storage is tracked on a daily basis by the model as a state variable.

Evapotranspiration

Evapotranspiration (ET) is the loss of water to the atmosphere from the combined processes of evaporation (from soil and plant surfaces) and transpiration (from plant tissues). The ET of specific plants can be estimated using data from the California Irrigation Management Information System (CIMIS) for reference crops (grass or alfalfa) and crop coefficients for plants. ET from a standardized grass surface is commonly denoted as ET_o, and ET from a standardized alfalfa surface is denoted as ET_r (CIMIS, ET Overview).

CIMIS maintains 204 stations in California and two stations in the proximity of the study area (Station 082 in Claremont and Station 044 at the University of California Riverside. The Claremont station data was used in this project.

The Claremont station has historical data that begins in 1989, as shown in Figure A4-2. To extend the data back in time, two options were considered: (1) develop an annual cycle from the recorded data and repeat the cycle for missing years, or (2) develop a relationship with the evaporation data of a station with a longer recording period and extend the data based on this relationship. The latter method to conserves more temporal variability aspects of ET and was assumed to be a more accurate method of estimating historic ET. Figure A4-3 shows the relationship between the Claremont Station ET_o data and Puddingstone Reservoir evaporation data. ET is about 77% of pan evaporation with a 0.72 correlation coefficient as shown in Figure A4-3.

Water requirements for agricultural crops and turf grasses have been established in laboratory and field studies by measuring plant water loss. The total amount of water lost during a specific period of time gives an estimate of the amount that needs to be resupplied by irrigation. This evapotranspiration loss is estimated as follows:

$$ET_c = K_c * ET_o$$

A crop coefficient (K_c) is used with ET_o to estimate the evapotranspiration rate of a specific crop. The crop coefficient is a dimensionless number. Crop coefficients vary by many factors including crop type and the stage of growth. Coefficients for annual crops vary widely through a season: annual crops have small coefficients in their early stages and large coefficients when they are at full cover. Crop coefficient data are available from CIMIS. In a previous study conducted by the California Department of Water Resources

(DWR), evapotranspiration data was used to estimate monthly crop coefficients for each land use type. These coefficients were used in this model and are listed in Table A4-1.

For land use that is classified as barren land, bare soil evaporation and its corresponding K_c value were used. The monthly K_c values for bare soil were obtained from a K_c curve for bare soil in Fresno, California (Snyder, 2007).

Applied Irrigation

The applied irrigation water is calculated for irrigated land use types when soil moisture drops below the critical soil moisture as:

$$AW_t = (FC_s - SM_t) / E_{ir}$$
$$SM_c = WP_s + (FC_s - WP_s) * F_s$$

Where AW_t = the applied irrigation water

FC_s = the field capacity for soil type s – the maximum soil moisture that soil type s can hold against

WP_s = the wilting point for soil type s – the minimum soil moisture that plants can take water from soil

E_{ir} = irrigation efficiency

SM_s = the critical soil moisture, below which the evapotranspiration by plants declines

F_s = the multiplier for critical soil moisture

Figure A4-4 illustrates the relationship between soil moisture, wilting point, field capacity, critical soil moisture, and evapotranspiration. Critical soil moisture is sometimes described with allowable depletions (Hanson, 1995), below which the crop yield reduces. The allowable depletion is frequently expressed as a percent of the total available soil moisture. Hanson (1995) contains a table of allowable depletions for various crop types, which vary from 30% for potatoes to 70% for wheat.

The total rooting depth is an important factor in estimating the total amount of water available to plants for evapotranspiration. Rooting depth information was collected from several references (UCCE & CADWR, 2000). This information is provided in Table A4-2.

Irrigation efficiency is imperative in calculating the total volume of applied water to irrigated land and deep percolation below the root zone. Irrigation efficiency is the beneficial use of applied water by plants (UCCE&DWR, 2000). The following formula defines irrigation efficiency mathematically:

Irrigation Efficiency (%) = Beneficially Used Water / Total Water Applied x 100

An efficiency of 100% would mean that all of the applied water is used by plants, which is not attainable or desirable. Irrigation efficiency is dependent on irrigation method. For this project, the irrigation efficiency was assumed to be 75% for urban areas and 65% for irrigated agricultural land use.

A4-2 SUMMARY

The root zone module runs on a daily time step and calculates deep percolation using all the input variables described above. The output data from this model include monthly data of deep percolation from each drainage area, urban water applied to each drainage area, and agricultural water applied to each drainage area.

RECHARGE ESTIMATION

After the Runoff, Router, and Root Zone module runs are completed in series, the output files can be summarized as monthly, quarterly or annual data for the following:

- Stream bottom percolation (Router)
- Storm water recharge from recharge basins (Router)
- Deep percolation below root zone (Root Zone)

For groundwater modeling, each of these exports from the R4 Model now become imports for various the Unsaturated flow model and or MODFLOW packages such as the Recharge Package, River Package, Stream Package, and or Flow Head Boundary Package

REFERENCES

Carsel, R.F. and R.S. Parrish, 1988. Developing joint probability distributions of soil water retention characteristics, *Water Resources Research*, 24(5): 755-769, May 1988

Chow, V. T., Maidment, D. R, Mays, L. W. (1988). *Applied hydrology*. McGraw-Hill Inc., New York.

Hanson, Blaine and Larry Schwankl, 1995, *Surface Irrigation*, University of California Irrigation Program, University of California, Davis

Haith, D.A. and L.L. Shoemaker, Generalized Watershed Loading Functions for stream flow nutrients, *Water Resources Bulletin*, 23(3), 1987.

Limbrunner, James F., Richard M. Vogel, and Steven C Chapra, Chapter 22 A Parsimonious Watershed Model *in Watershed Models* Edited by Vijay P. Singh and Donald K. Frevert, December 2005

Mark J. Wildermuth, Water Resources Engineers. 1995. *Annual Recharge Estimates at Chino Basin Water Conservation District Spreading Basins*. October 1995.

Snyder, R.L., M. Orang, S. Matyac, and S. Eching, Crop Coefficients, Regents of University of California, Last Update March 2, 2007

TR-55, 1986. Urban Hydrology for Small Watersheds, US Department of Agriculture, Soil Conservation Service.

UCCE and CADWR, 2000, *A guide to Estimating Irrigation Water Needs of Landscape Plantings in California*, University of California Cooperative Extentions and California Department of Water Resources, August 2000

US EPA, 1999 *Data Collection for the Hazardous Waste Identification Rule, Section 7.0 Soil Data* EPA, Office of Solid Waste, October 1999

Wildermuth Environmental, Inc. 1998. *Phase 1 Recharge Master Plan*, January 1998

Wildermuth Environmental, Inc. 2003. *Modeling Report for the Chino Basin Dry-Year Yield Program. Optimum Basin Management Program.* Prepared for Chino Basin Water Master and Inland Empire Utilities Agency under a Subcontract Agreement with Black & Veatch Corp. July 2003

Wildermuth Environmental, Inc. 2006. *Integrated Regional Water Management Program for the San Timoteo Watershed*, Prepared for San Timoteo Watershed Management Authority and State Water Resources Control Board, January 2006.

Wildermuth Environmental, Inc. 2006. *Feasibility Study for the expansion of the Arlington Desalter System*, Prepared for Western Municipal Water District, August 2007.

Table A2-1
Soil Conservation Service Soil Classifications

Hydrologic Soil Type	Description
A	Low runoff potential. Soils having high infiltration rates even when thoroughly wetted and consisting chiefly of deep, well to excessively drained sands or gravels. These soils have a high rate of water transmission.
B	Soils having moderate infiltration rates when thoroughly wetted and consisting chiefly of moderately deep to deep, moderately well to well drained soils with moderately fine to moderately coarse textures. These soils have a moderate rate of water transmission.
C	Soils having slow infiltration rates when thoroughly wetted and consisting chiefly of soils with a layer that impedes downward movement of water, or soils with moderately fine to fine texture. These soils have a slow rate of water transmission.
D	High runoff potential. Soils having very slow infiltration rates when thoroughly wetted and consisting chiefly of clay soils with a high swelling potential, soils with a permanent high water table, soils with a clay pan or clay layer at or near the surface, and shallow soils over nearly impervious material. These soils have a very slow rate of water transmission.

Table A2- 2
Land Use Survey Data

Survey Year	Origin of Data
1933	DWR
1949	DWR
1957	DWR
1963	DWR
1975	DWR
1984	DWR
1990	SCAG
2000	SCAG
2006	WEI
2025	WEI

Table A2- 3
Land Use Types and Curve Numbers for Hydrologic Soil Types

Class	Land Use Type Description	Hydrologic Soil Type A	Hydrologic Soil Type B	Hydrologic Soil Type C	Hydrologic Soil Type D
1	Non-Irrigated Field Crops, Pasture, Fruits and Nuts	72	81	88	91
2	Irrigated Field Crops, Pasture, Fruits and Nuts	67	78	85	89
3	Irrigated and Non-Irrigated Citrus	44	65	77	82
4	Irrigated Vineyard	33	58	72	79
5	Non-Irrigated Vineyard	57	73	82	86
6	Dairies and Feedlots	38	61	74	80
7	Urban Residential	32	56	69	75
8	Special Impervious	98	98	98	98
9	Native Vegetation	56	73	82	86
10	Low density Urban Residential	32	56	69	75
11	Commercial	32	56	69	75
12	Industrial	32	56	69	75
13	Barren (graded) Land	78	86	91	93
	Impervious Area	98	98	98	98

Note:

1. Earlier land use survey data from Departement of Water Resourses were grouped and digitized into nine land use types (first nine from top) by (JMM, 1989).
2. Southern California Area Governments (SCAG) land use data were mapped to thirteen land use types by WEI.
3. Classes from 1-12 consider only irrigated Area

Table A2-4
1990 and 2000 Land Use Code Conversion

Anderson Land Use Classification	Description	WEI Land Use Types
1000	URBAN OR BUILT-UP	
1100	Residential	
1110	Single Family Residential	7
1111	High Density Single Family Residential	7
1112	Low Density Single Family Residential	10
1120	Multi-Family Residential	7
1121	Mixed Multi-Family Residential	7
1122	Duplexes and Triplexes	7
1123	Low-Rise Apartments, Condos, Townhouses	7
1124	Medium-Rise Apartments and Condos	7
1125	High-Rise Apartments and Condos	7
1130	Mobile Homes and Trailer Parks	7
1131	Trailer Parks and Mobile Home Courts, High Density	7
1132	Trailer Parks and Mobile Home Courts, Low Density	7
1140	Mixed Residential	7
1150	Rural Residential	10
1151	Rural Residential High Density	10
1152	Rural Residential Low Density	10
1200	Commercial and Services	11
1210	General Office Use	11
1211	Low - Medium Rise Major Office Use	11
1212	High Rise Major Office Use	11
1213	Skyscrapers	11
1220	Retail Stores and Commercial Services	11
1221	Regional Shopping Mall	11
1222	Retail Centers	11
1223	Modern Strip Development	11
1224	Older Strip Development	11
1230	Other Commercial	11
1231	Commercial Storage	11
1232	Commercial Recreation	11
1233	Hotels and Motels	11
1244	Attended Pay Public Parking Facilities	11
1240	Public Facilities	11
1241	Government Offices	11
1242	Police and Sheriff Stations	11
1243	Fire Stations	11
1244	Major Medical Health Care Facilities	11
1245	Religious Facilities	11
1246	Other Public Facilities	11
1247	Non-Attended Public Parking Facilities	11
1250	Special Use Facilities	11
1251	Correctional Facilities	11
1252	Special Care Facilities	11
1253	Other Special Use Facilities	11

Table A2-4
1990 and 2000 Land Use Code Conversion

Anderson Land Use Classification	Description	WEI Land Use Types
1260	Educational Institutions	11
1261	Pre-Schools/Day Care Centers	10
1262	Elementary Schools	10
1263	Junior or Intermediate High Schools	10
1264	Senior High Schools	10
1265	Colleges and Universities	10
1266	Trade Schools	10
1270	Military Installations	10
1271	Base (Built-up Area)	10
1272	Vacant Area	9
1273	Air Field	8
1300	Industrial	12
1310	Light Industrial	12
1311	Manufacturing and Assembly	12
1312	Motion Picture	11
1313	Packing Houses and Grain Elevators	12
1314	Research and Development	12
1320	Heavy Industrial	12
1321	Manufacturing	12
1322	Petroleum Refining and Processing	12
1323	Open Storage	12
1324	Major Metal Processing	12
1325	Chemical Processing	12
1330	Extraction	9
1331	Mineral Extraction-Other than gas and oil	9
1332	Mineral Extraction-Oil and gas	9
1400	Transportation, Communications, and Utilities	8
1410	Transportation	8
1411	Airports	8
1412	Railroads	9
1413	Freeways	8
1414	Park and Ride Lots	8
1415	Bus Terminals and Yards	8
1416	Truck Terminals	8
1417	Harbor Facilities	NA
1418	Navigation Aids	NA
1420	Communication Facilities	
1430	Utility Facilities	8
1431	Electrical Power Facilities	9
1432	Solid Waste Disposal Facilities	8
1433	Liquid Waste Disposal Facilities	8
1434	Water Storage Facilities	8
1435	Natural Gas and Petroleum Facilities	8
1436	Water Transfer Facilities	9
1437	Improved Flood Waterways and Structures	9
1438	Mixed Wind Energy Generation and Percolation Basin	8
1440	Maintenance Yards	8
1450	Mixed Transportation	8
1460	Mixed Transportation and Utility	8

Table A2-4
1990 and 2000 Land Use Code Conversion

Anderson Land Use Classification	Description	WEI Land Use Types
1500	Mixed Commercial and Industrial	11
1600	Mixed Urban	7
1700	Under Construction	13
1800	Open Space and Recreation	9
1810	Golf Courses	2
1820	Local Parks and Recreation	2
1830	Regional Parks and Recreation	2
1840	Cemeteries	2
1850	Wildlife Preserves and Sanctuaries	9
1860	Specimen Gardens and Arboreta	2
1870	Beach Parks	NA
1880	Other Open Space and Recreation	13
1900	Urban Vacant	13
2000	AGRICULTURE	2
2100	Cropland and Improved Pasture Land	2
2110	Irrigated Cropland and Improved Pasture Land	2
2120	Non-Irrigated Cropland and Improved Pasture Land	1
2200	Orchards and Vineyards	4
2300	Nurseries	3
2400	Dairy and Intensive Livestock	6
2500	Poultry Operations	5
2600	Other Agriculture	2
2700	Horse Ranches	2
3000	VACANT	13
3100	Vacant Undifferentiated	9
3200	Abandoned Orchards and Vineyards	9
3300	Vacant With Limited Improvements	9
4000	WATER	8
4100	Water, Undifferentiated	8
4200	Harbor Water Facilities	NA
4300	Marina Water Facilities	NA
4400	Water Within a Military Installation	NA
4500	Area of Inundation	8

Table A2-5
Rainfall Monitoring Stations

Station ID	Name/Location	Location		Elevation	Source of Data
		Latitude	Longitude	ft()	
1026	Ontario Fire Station	34.06	117.65	986	SBCFCD
1034	Claremont Pomona College	34.1	117.72	1196	SBCFCD
1019	Upland - Chappel	34.14	117.68	1609	SBCFCD
1021	Mira Loma Space Center	34.03	117.54	827	SBCFCD
1067	Chino Substation - Edison	33.98	117.68	670	SBCFCD
1079	Chino - Imbach	33.97	117.6	642	SBCFCD
1085	San Antonio Heights C.D.F.	34.16	117.65	1901	SBCFCD
1175	Alta Loma Forney	34.12	117.59	1865	SBCFCD
2017	Fontana 5N (Getchell)	34.18	117.44	2020	SBCFCD
2194	Fontana Union Water Company - Townsite	34.1	117.44	1289	SBCFCD
2005	Declez	34.08	117.49	900	SBCFCD
2037	Lytle Creek Ranger Station	34.23	117.48	2730	SBCFCD
2159	Lytle Creek At Foothill Boulevard	34.11	117.33	1225	SBCFCD
2198	San Bernardino City - Lytle Creek	34.12	117.35	1225	SBCFCD
007	Arlington	33:55:01	-117:26:31	805	RCFCD&WCD
044	Corona North	33:54:07	-117:33:40	638	RCFCD&WCD
100	La Sierra	33:55:07	-117:29:12	712	RCFCD&WCD
102	Lake Mathews	33:51:10	-117:27:15	1400	RCFCD&WCD
177	Riverside East	33:58:02	-117:20:40	986	RCFCD&WCD
178	Riverside North	34:00:10	-117:22:40	800	RCFCD&WCD
179	Riverside South	33:57:04	-117:23:15	840	RCFCD&WCD
250	Woodcrest	33:53:05	-117:21:01	1557	RCFCD&WCD
265	Indian Hills	33:58:48	-117:27:10	840	RCFCD&WCD
035	Chase & Taylor	33:50:42	-117:34:28	1055	RCFCD&WCD

Table A3-1
USGS Stream Gauge Stations in the Area

Site Number	Site name	Location	
		Latitude	Longitude
11066460	Santa Ana River at MWD Crossing Ca	33°58'07"	117°26'51"
11066500	Santa Ana River at Riverside Narows near Arlington Ca	33°57'53"	117°27'55"
11072000	Temescal Creek near Corona Ca	33°50'29"	117°30'37"
11072100	Temescal Creek Above Main Street at Corona Ca	33°53'21"	117°33'43"
11072200	Temescal Creek at Corona Ca	33°53'46"	117°34'50"
11073360	Chino Creek at Schaefer Avenue near Chino Ca	34°00'14"	117°43'34"
11073495	Cucamonga Creek near Mira Loma Ca	33°58'58"	117°35'55"
11074000	Santa Ana River below Prado Dam Ca	33°53'00"	117°38'40"

Table A3-2
Manning's Roughness Coefficients, N

Channel Material	n
Neat cement, smooth metal	0.010
Ordinary concrete, asphalted cast iron	0.013
Cast-iron pipe	0.015
Smooth earth	0.018
Corrugated metal pipe	0.022
Natural channel in good condition	0.025
Natural channel with stones and weeds	0.035
Natural channel in very poor condition	0.060

Table A4-1
Estimated Growing Season Evapotranspiration For Principal Crops - South Coast, Coastal Valleys And Plains

Crop	Month												
	Jan	Feb	Mar	Apr	May	Jun	Jul	Aug	Sep	Oct	Nov	Dec	Total
Potential ET	1.8	2.4	3.1	3.8	4.5	5.1	5.5	5.5	4.5	3.4	2.6	2.2	44.4
Alfalfa			2.9	3.4	4.1	4.8	5.3	5.6	4.6	3.5			34.2
Deciduous Orchard			1.8	2.7	3.8	4.6	5.2	5.2	4.1	1.3			28.7
Pasture (Improved)			3.1	3.8	4.5	5.1	5.5	5.5	4.5	3.4			35.4
Strawberries	1.8	2.4	3.1	3.1	1.4			1.1	3.6	3.4	2.6	2.2	24.7
Subtropical Orchard	1.8	2.4	1.8	2.3	2.7	3.1	3.3	3.3	2.7	2.1	2.6	2.2	30.3
Tomatoes (Market)			0.9	2.9	5.1	5.8	5.2	3.5	1.7				25.1

Reproduced from CA DWR Bulleltin 113-3, "Vegetative Water Use in California", 1974,

Table A4-2

Effective Root Depths that Contain Approximately 80 Percent Root System in a Deep, Uniform, Well-Drained Soil Profile

Crop	Root depth (ft)	Crop	Root depth (ft)
Alfalfa	4.0 to 6.0	Lettuce	0.5 to 1.5
Almonds	2.0 to 4.0	Lucerne	4.0 to 6.0
Apple	2.5 to 4.0	Oats	2.0 to 2.5
Apricot	2.0 to 4.5	Olives	2.0 to 4.0
Artichoke	2.0 to 3.0	Onion	1.0
Asparagus	6.0	Parsnip	2.0 to 3.0
Avocado	2.0 to 3.0	Passion fruit	1.0 to 1.5
Banana	1.0 to 2.0	Pastures (annual)	1.0 to 2.5
Barley	3.0 to 3.5	Pastures (perennial)	1.0 to 2.5
Bean (dry)	1.5 to 2.0	Pea	1.5 to 2.0
Bean (green)	1.5 to 2.0	Peach	2.0 to 4.0
Beans (lima)	3.0 to 5.0	Pear	2.0 to 4.0
Beet (sugar)	1.5 to 2.5	Pepper	2.0 to 3.0
Beet (table)	1.0 to 1.5	Plum	2.5 to 4.0
Berries	3.0 to 5.0	Potato (Irish)	2.0 to 3.0
Broccoli	2.0	Potato (sweet)	2.0 to 3.0
Brussel sprout	2.0	Pumpkin	3.0 to 4.0
Cabbage	2.0	Radish	1.0
Cantaloupe	2.0 to 4.0	Safflower	3.0 to 5.0
Carrot	1.5 to 2.0	Sorghum (grain and sweet)	2.0 to 3.0
Cauliflower	2.0	Sorghum (silage)	3.0 to 4.0
Celery	2.0	Soybean	2.0 to 2.5
Chard	2.0 to 3.0	Spinach	1.5 to 2.0
Cherry	2.5 to 4.0	Squash	2.0 to 3.0
Citrus	**2.0 to 4.0**	Strawberry	1.0 to 1.5
Coffee	3.0 to 5.0	Sugarcane	1.5 to 3.5
Corn (grain and silage)	2.0 to 3.0	Sudangrass	3.0 to 4.0
Corn (sweet)	L5 to 2.0	Tobacco	2.0 to 4.0
Cotton	2.0 to 6.0	Tomato	2.0 to 4.0
Cucumber	1.5 to 2.0	Turnip (white)	1.5 to 2.5
Eggplant	2.5	Walnuts	5.5 to 8.0
Fig	3.0	Watermelon	2.0 to 3.0
Flax	2.0 to 3.0	Wheat	2.5 to 3.5
Grapes	**1.5 to 3.0**		

'Soil and plant environmental factors often offset normal root development. Soil density, pore

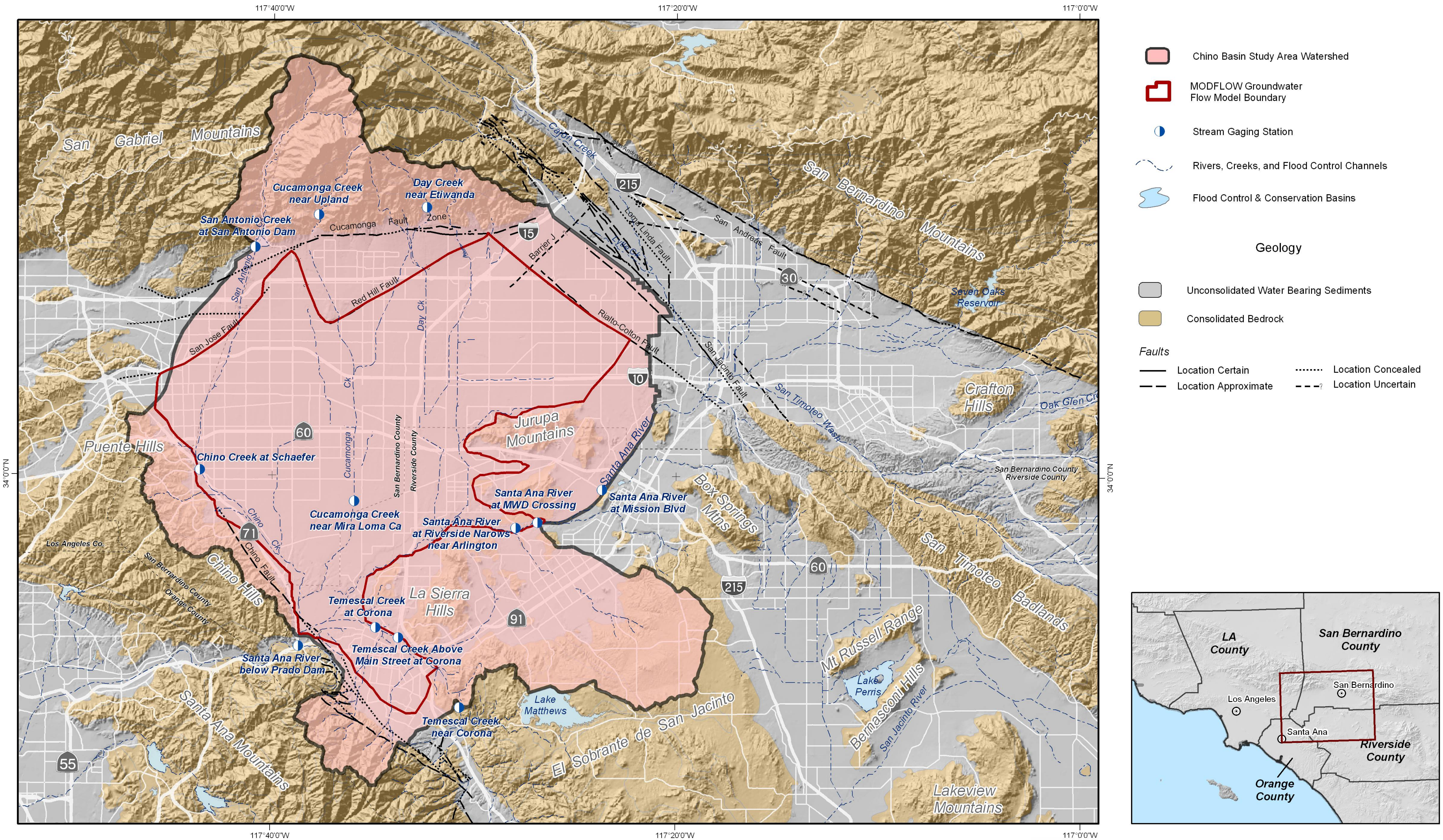

Produced by:

WILDERMUTH™ ENVIRONMENTAL INC.

23692 Birtcher Drive
Lake Forest, CA 92630
949.420.3030
www.wildermuthenvironmental.com

Author: FIB/MJC
Date: 20071004
File: Figure_A1-1.mxd

CHINO BASIN WATERMASTER — Partners in Basin Management

2007 CBWM Groundwater Model Documentation
and Evaluation of the Peace II Project Description

R4 Model Documentation

Chino Basin Study Area Watershed Boundary

Figure A1-1

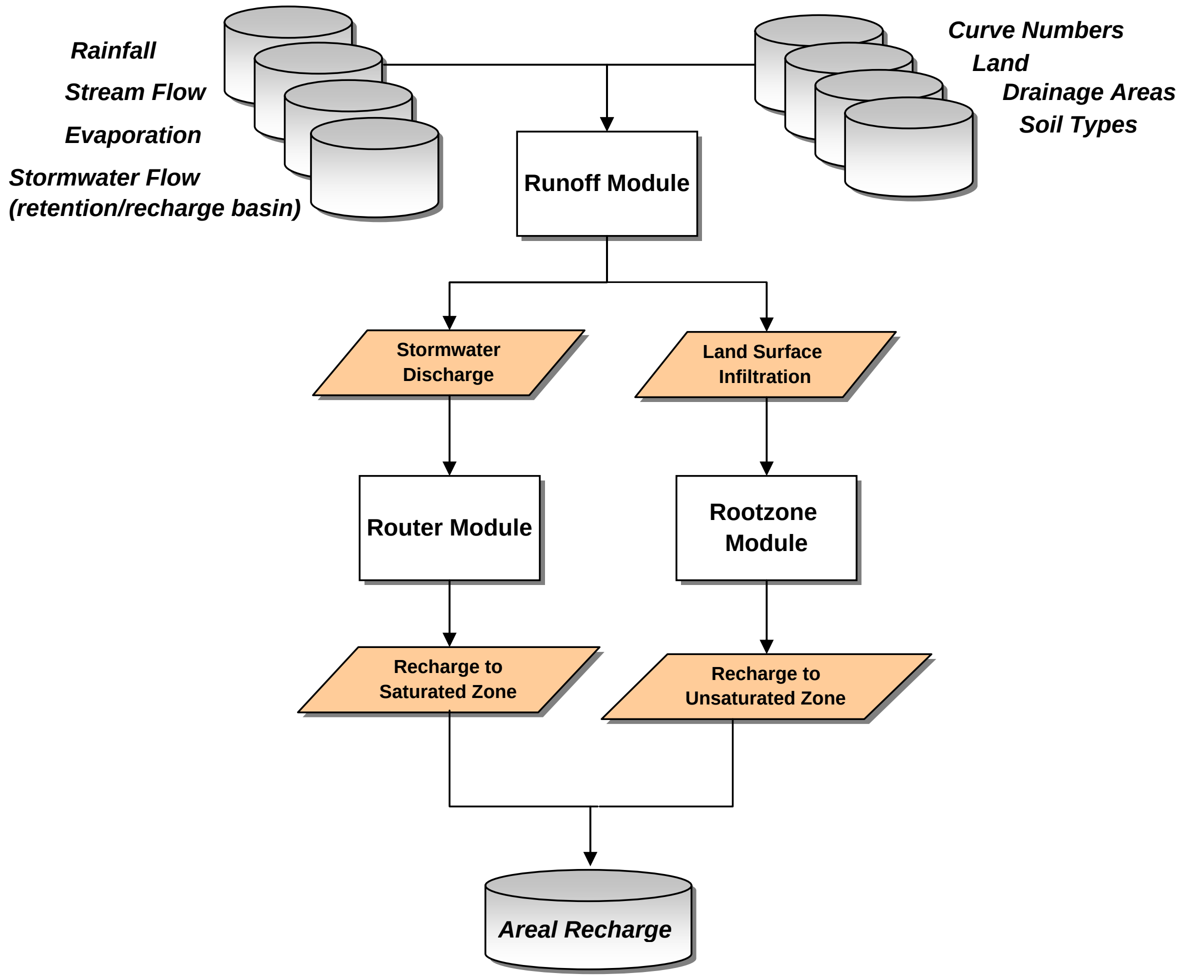

Figure A1-2 Flow Diagram of the R4 Process

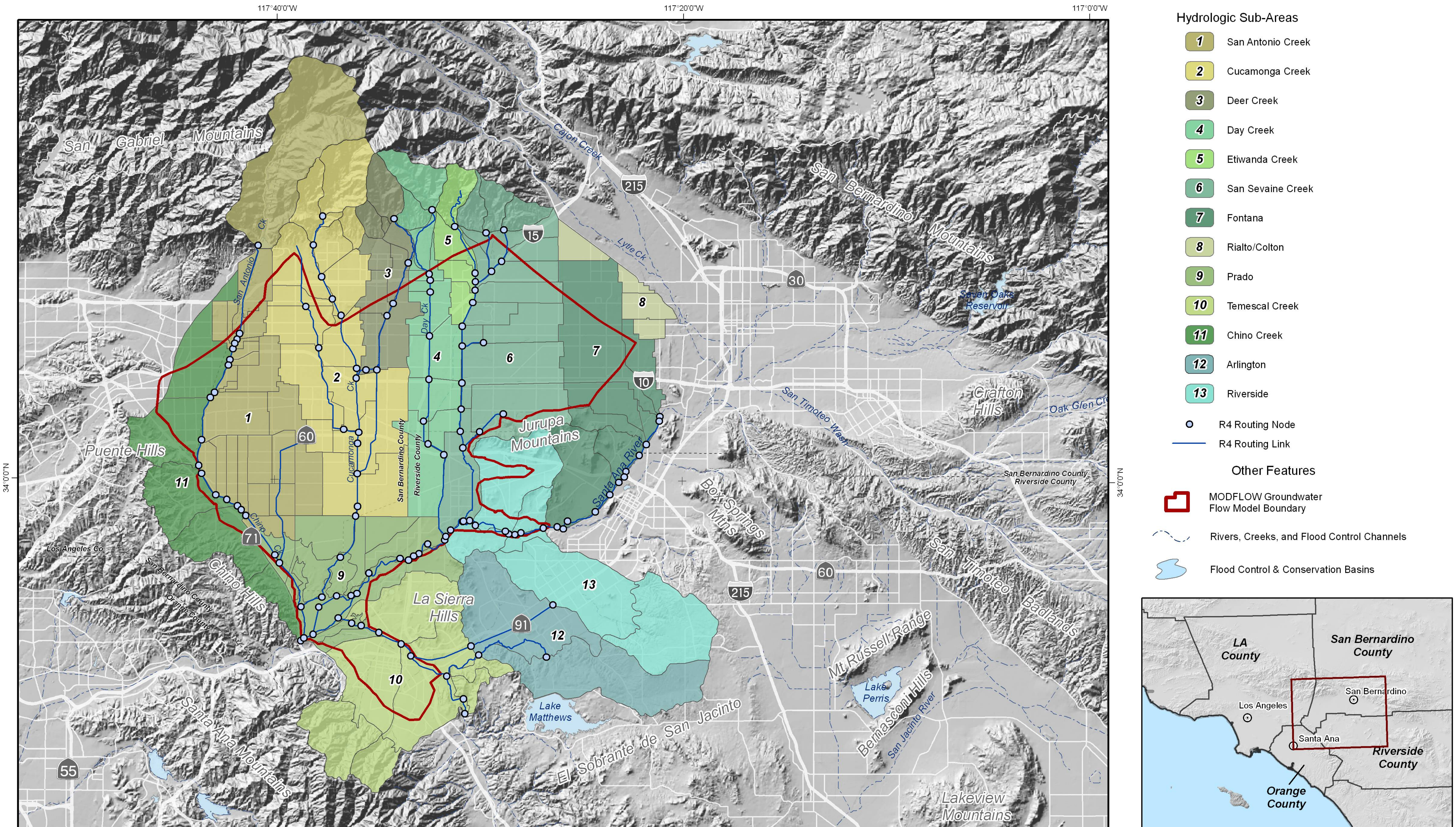

Hydrologic Sub-Areas

- 1 San Antonio Creek
- 2 Cucamonga Creek
- 3 Deer Creek
- 4 Day Creek
- 5 Etiwanda Creek
- 6 San Sevaine Creek
- 7 Fontana
- 8 Rialto/Colton
- 9 Prado
- 10 Temescal Creek
- 11 Chino Creek
- 12 Arlington
- 13 Riverside
- R4 Routing Node
- R4 Routing Link

Other Features

- MODFLOW Groundwater Flow Model Boundary
- Rivers, Creeks, and Flood Control Channels
- Flood Control & Conservation Basins

Produced by:

WILDERMUTH ENVIRONMENTAL INC.

23692 Birtcher Drive
Lake Forest, CA 92630
949.420.3030
www.wildermuthenvironmental.com

Author: FIB/MJC

Date: 20071004

File: Figure_A2-1.mxd

0 2 4 Miles

0 2 4 6 KM

2007 CBWM Groundwater Model Documentation and Evaluation of the Peace II Project Description

R4 Model Documentation

Study Area Hydrologic Drainage

Figure A2-1

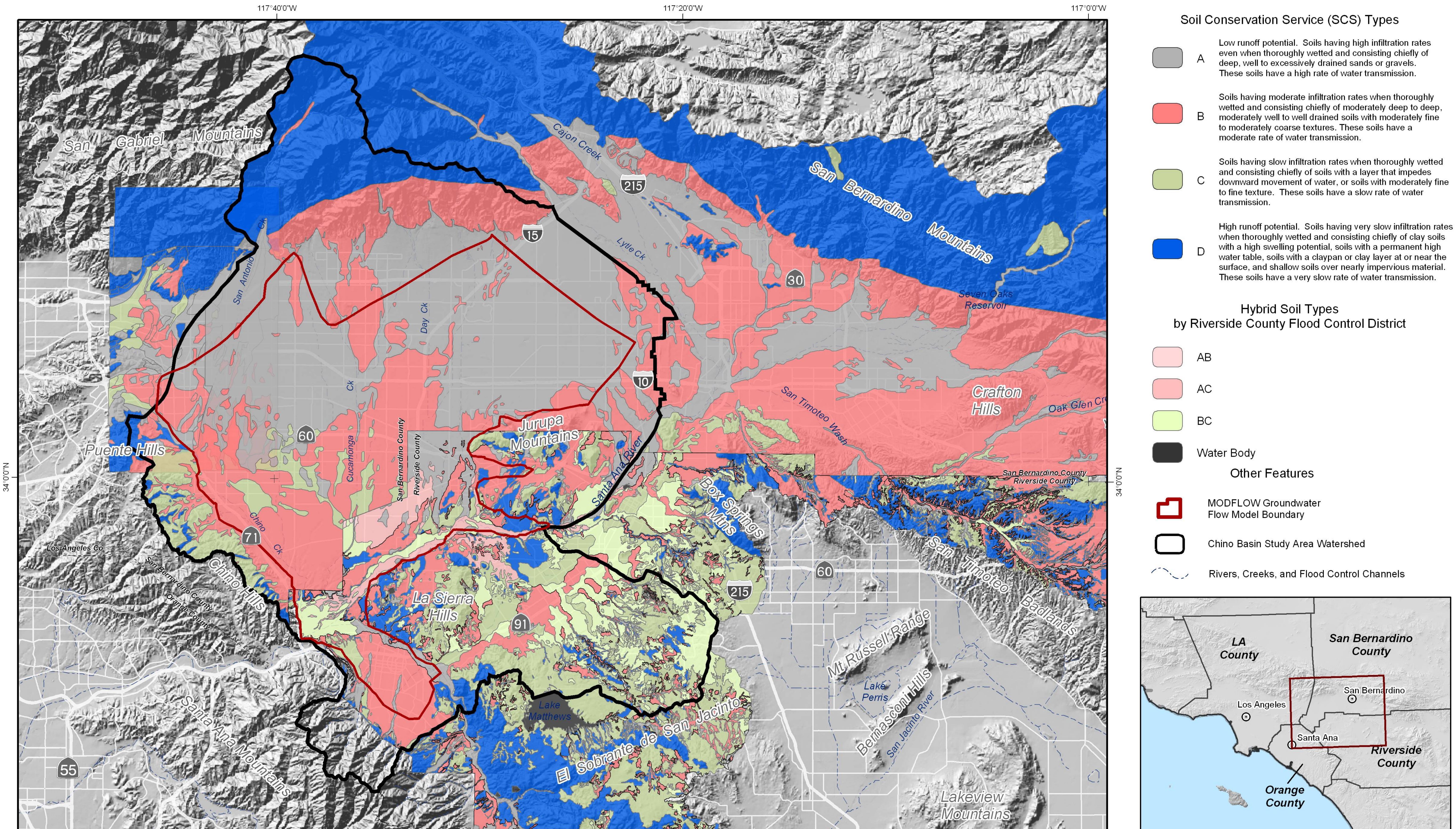

Produced by:
WILDERMUTH ENVIRONMENTAL INC.
23692 Birtcher Drive
Lake Forest, CA 92630
949.420.3030
www.wildermuthenvironmental.com

Author: FIB/MJC
Date: 20071004
File: Figure_A2-2.mxd

0 2 4 Miles
0 2 4 6 KM

CHINO BASIN WATERMASTER
Partners in Basin Management

2007 CBWM Groundwater Model Documentation and Evaluation of the Peace II Project Description

R4 Model Documentation

SCS Hydrologic Soil Types

Figure A2-2

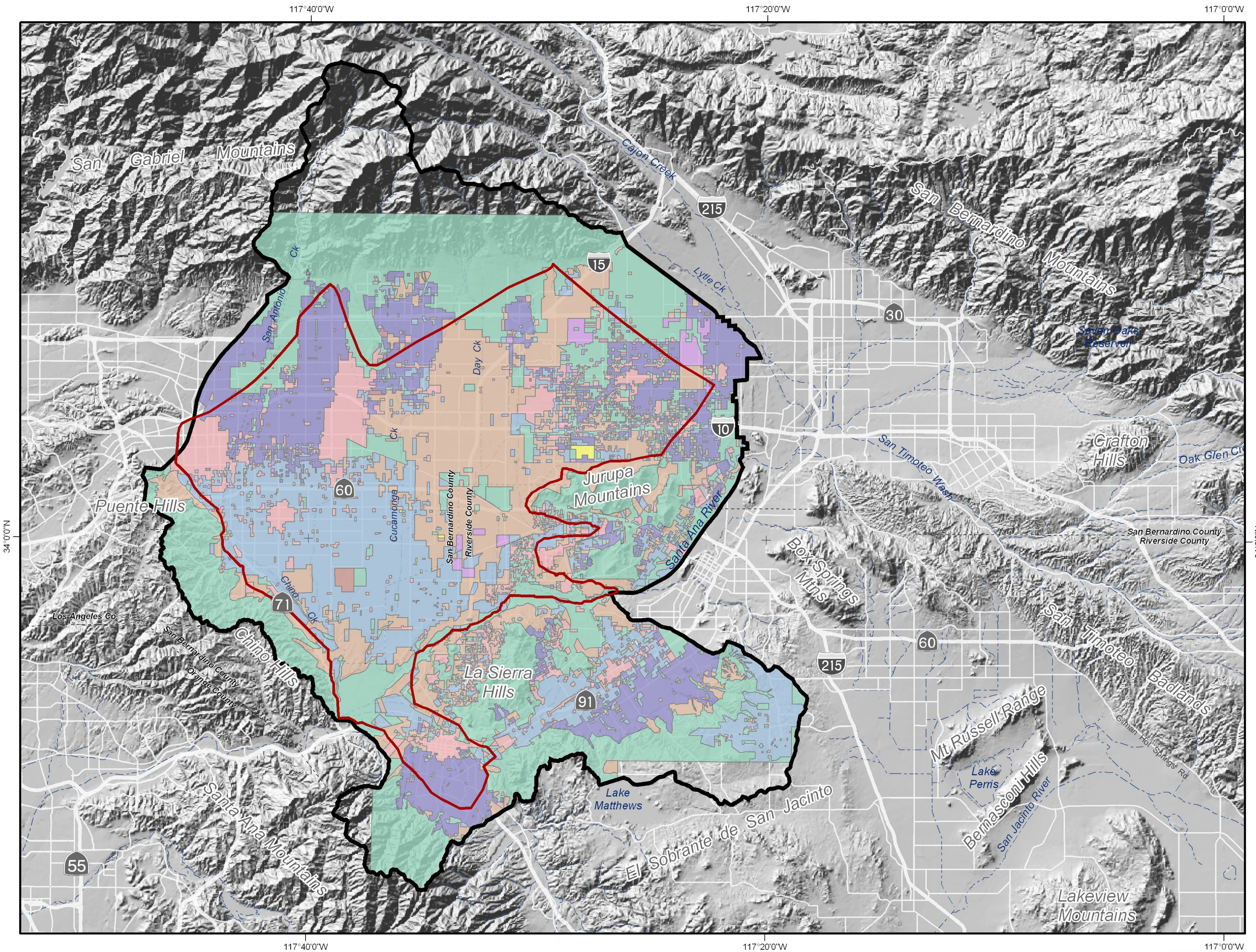

Land Use

- Non-Irrigated Field Crops, Pasture, Fruit and Nuts
- Irrigated Field Crops, Pasture, Fruit and Nuts
- Irrigated and Non-Irrigated Citrus
- Irrigated Vineyard
- Non-Irrigated Vineyard
- Dairies and Feedlots
- Urban Residential
- Special Impervious
- Native Vegetation

Other Features

- MODFLOW Groundwater Flow Model Boundary
- Chino Basin Study Area Watershed
- Rivers, Creeks, and Flood Control Channels

Produced by:

WILDERMUTH™ ENVIRONMENTAL INC.
23692 Birtcher Drive
Lake Forest, CA 92630
949.420.3030
www.wildermuthenvironmental.com

Author: FIB/MJC
Date: 20071004
File: Figure_A2-3.mxd

0 2 4 Miles
0 2 4 6 KM

2007 CBWM Groundwater Model Documentation and Evaluation of the Peace II Project Description
R4 Model Documentation

1933 Land Uses in the Chino Area

Figure A2-3

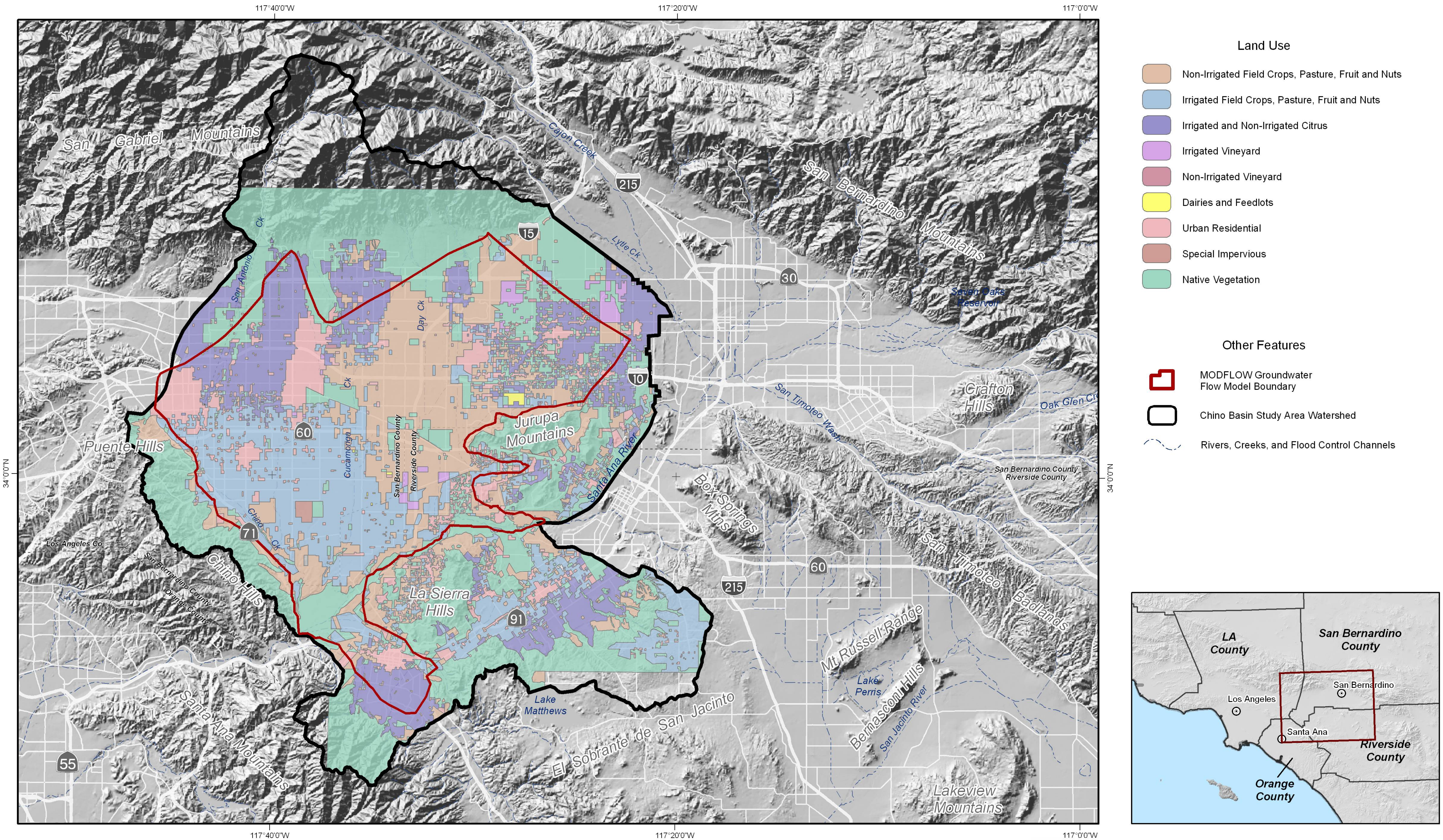

Produced by:

WILDERMUTH™ ENVIRONMENTAL INC.

23692 Birtcher Drive
Lake Forest, CA 92630
949.420.3030
www.wildermuthenvironmental.com

Author: FIB/MJC
Date: 20071004
File: Figure_A2-4.mxd

0 2 4 Miles
0 2 4 6 KM

CHINO BASIN WATERMASTER — Partners in Basin Management

2007 CBWM Groundwater Model Documentation and Evaluation of the Peace II Project Description

R4 Model Documentation

1949 Land Uses in the Chino Area

Figure A2-4

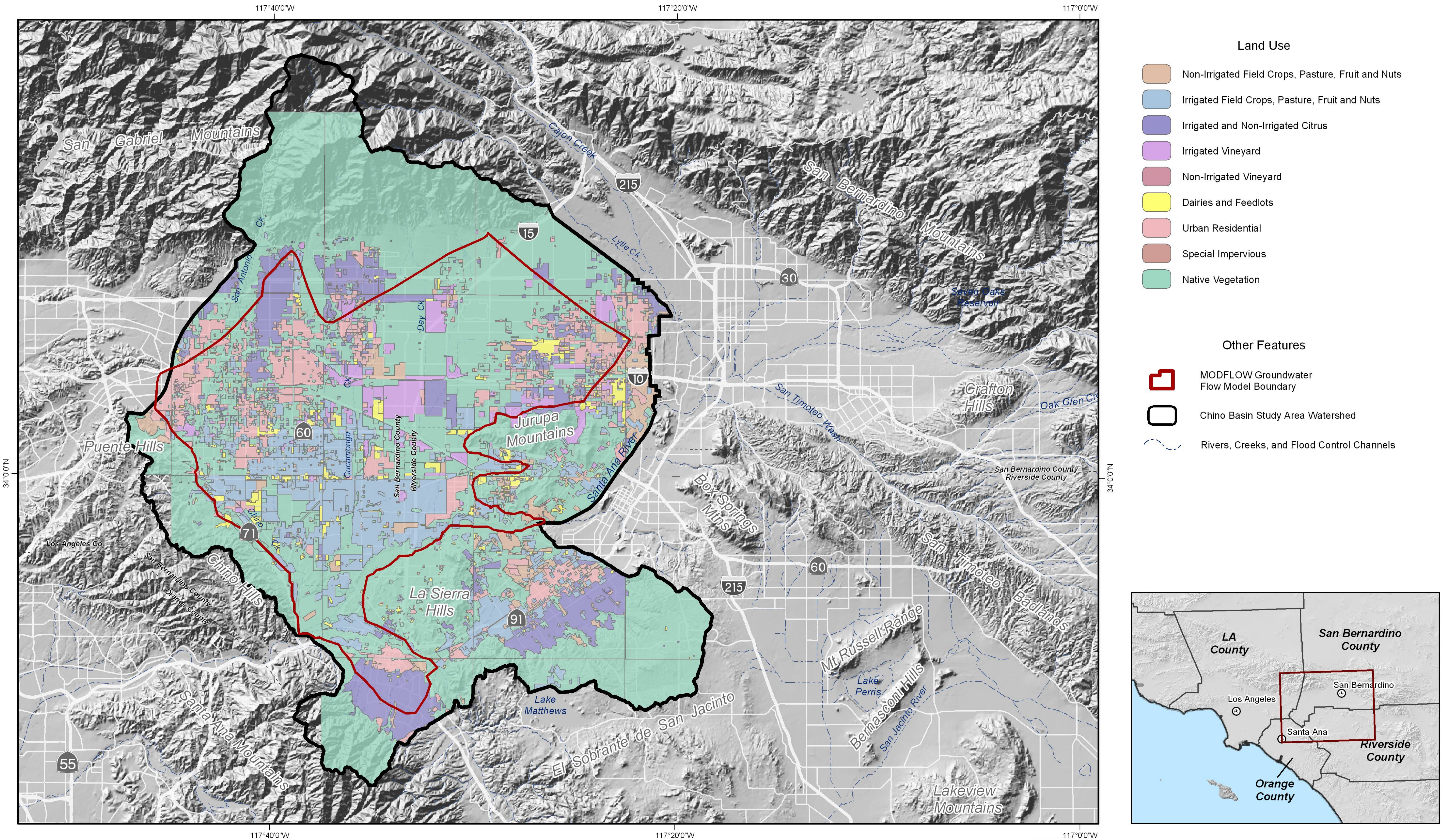

Produced by:

WILDERMUTH ENVIRONMENTAL INC.

23692 Birtcher Drive
Lake Forest, CA 92630
949.420.3030
www.wildermuthenvironmental.com

Author: FIB/MJC
Date: 20071004
File: Figure_A1-6.mxd

2007 CBWM Groundwater Model Documentation and Evaluation of the Peace II Project Description

R4 Model Documentation

1957 Land Uses in the Chino Area

Figure A2-5

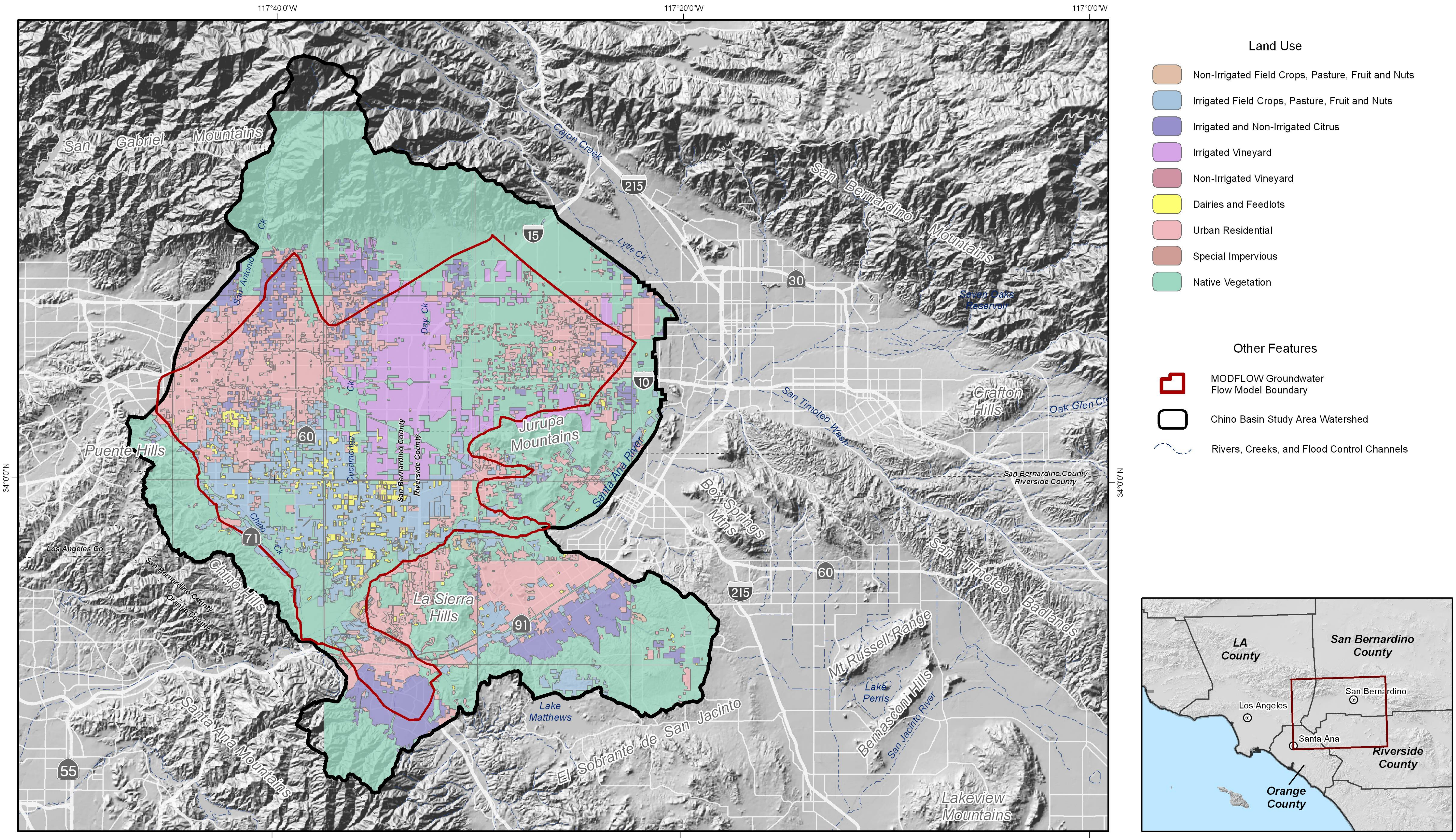

Produced by:

WILDERMUTH™ ENVIRONMENTAL INC.
23692 Birtcher Drive
Lake Forest, CA 92630
949.420.3030
www.wildermuthenvironmental.com

Author: FIB/MJC
Date: 20071004
File: Figure_A2-6.mxd

0 2 4 Miles
0 2 4 6 KM

CHINO BASIN WATERMASTER — Partners in Basin Management

2007 CBWM Groundwater Model Documentation and Evaluation of the Peace II Project Description

R4 Model Documentation

1963 Land Uses in the Chino Area

Figure A2-6

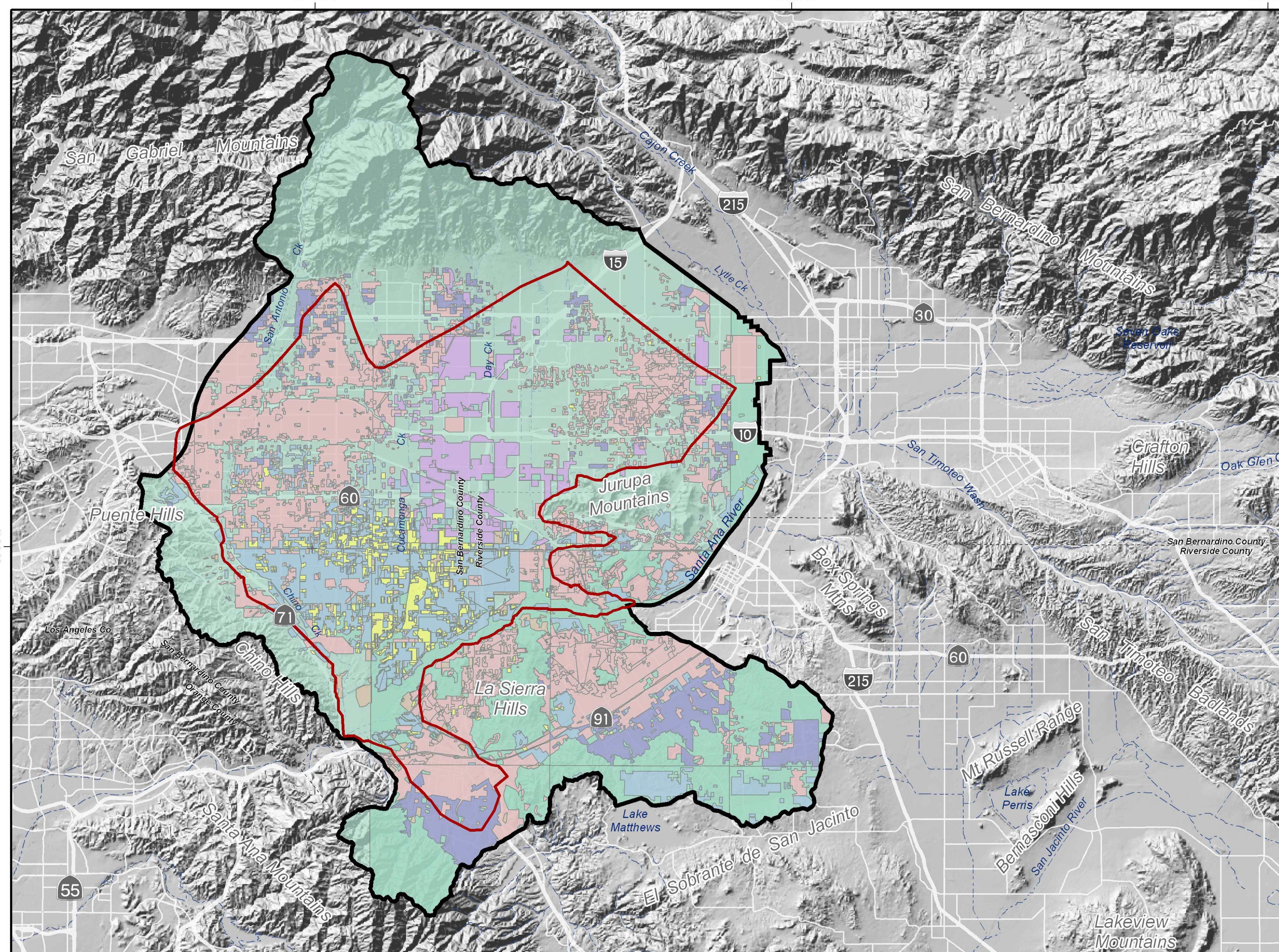

Land Use

- Non-Irrigated Field Crops, Pasture, Fruit and Nuts
- Irrigated Field Crops, Pasture, Fruit and Nuts
- Irrigated and Non-Irrigated Citrus
- Irrigated Vineyard
- Non-Irrigated Vineyard
- Dairies and Feedlots
- Urban Residential
- Special Impervious
- Native Vegetation

Other Features

- MODFLOW Groundwater Flow Model Boundary
- Chino Basin Study Area Watershed
- Rivers, Creeks, and Flood Control Channels

Produced by:

WILDERMUTH™ ENVIRONMENTAL INC.
23692 Birtcher Drive
Lake Forest, CA 92630
949.420.3030
www.wildermuthenvironmental.com

Author: FIB/MJC
Date: 20071004
File: Figure_A2-7.mxd

0 2 4 Miles
0 2 4 6 KM

CHINO BASIN WATERMASTER — Partners in Basin Management

2007 CBWM Groundwater Model Documentation and Evaluation of the Peace II Project Description

R4 Model Documentation

1975 Land Use

Figure A2-7

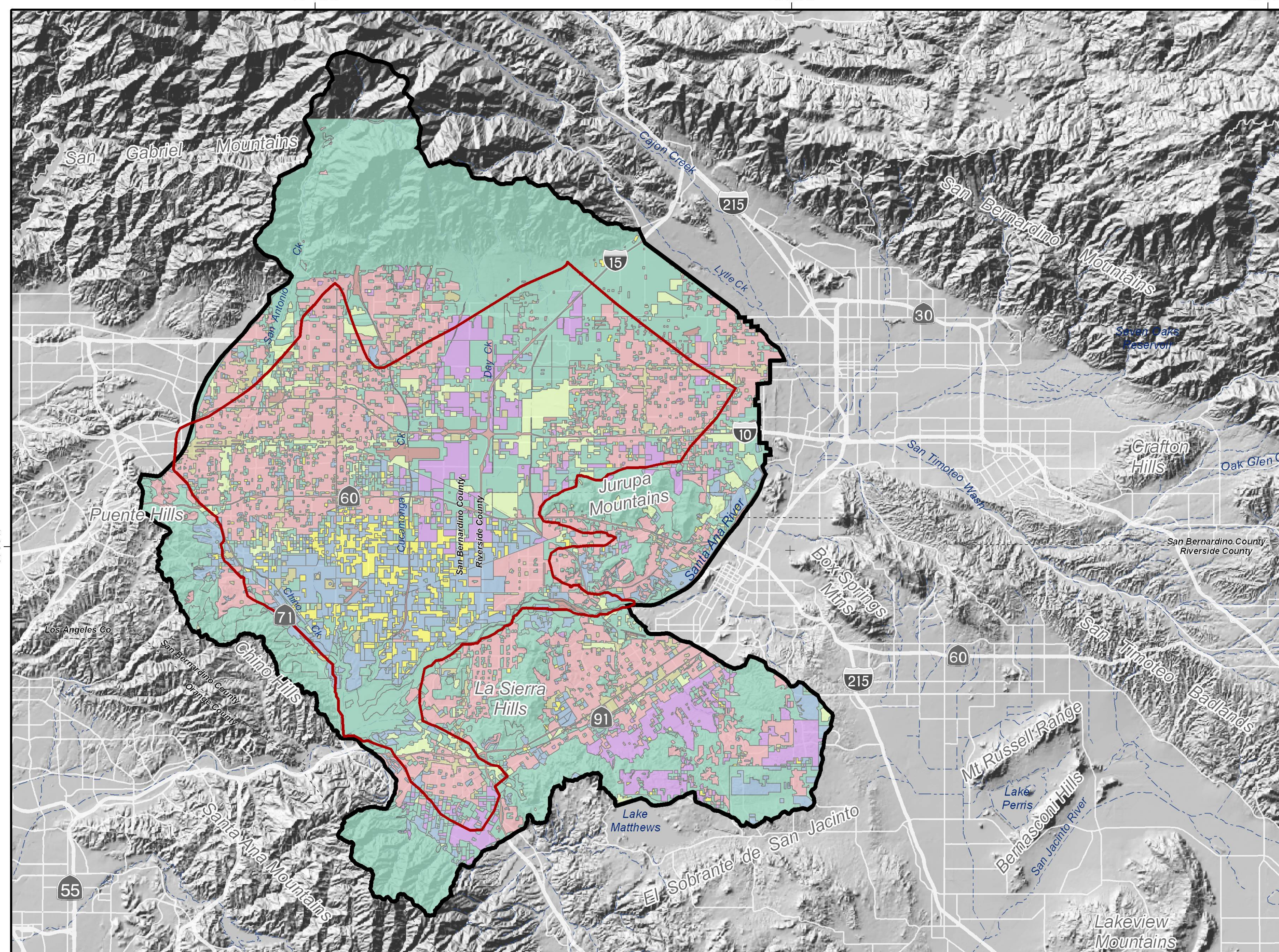

Land Use

- Non-Irrigated Field Crops, Pasture, Fruit and Nuts
- Irrigated Field Crops, Pasture, Fruit and Nuts
- Irrigated and Non-Irrigated Citrus
- Irrigated Vineyard
- Non-Irrigated Vineyard
- Dairies and Feedlots
- Urban Residential
- Special Impervious
- Native Vegetation

Other Features

- MODFLOW Groundwater Flow Model Boundary
- Chino Basin Study Area Watershed
- Rivers, Creeks, and Flood Control Channels

Produced by:

WILDERMUTH™ ENVIRONMENTAL INC.
23692 Birtcher Drive
Lake Forest, CA 92630
949.420.3030
www.wildermuthenvironmental.com

Author: FIB/MJC
Date: 20071004
File: Figure_A2-8.mxd

0 2 4 Miles
0 2 4 6 KM

CHINO BASIN WATERMASTER — Partners in Basin Management

2007 CBWM Groundwater Model Documentation and Evaluation of the Peace II Project Description

R4 Model Documentation

1984 Land Uses in the Chino Area

Figure A2-8

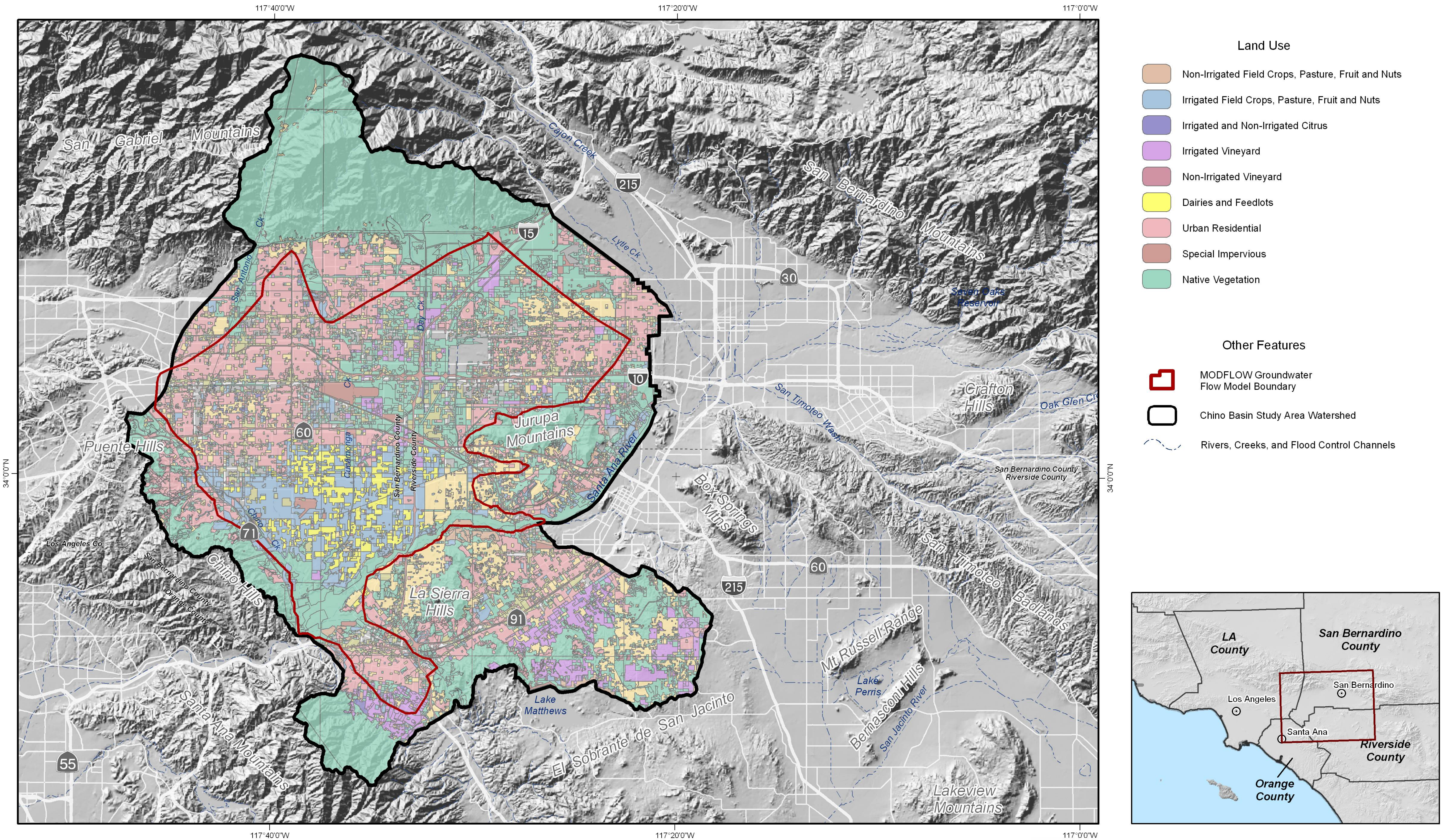

Produced by:

WILDERMUTH™ ENVIRONMENTAL INC.
23692 Birtcher Drive
Lake Forest, CA 92630
949.420.3030
www.wildermuthenvironmental.com

Author: FIB/MJC
Date: 20071004
File: Figure_A2-9.mxd

0 2 4 Miles
0 2 4 6 KM

CHINO BASIN WATERMASTER — Partners in Basin Management

2007 CBWM Groundwater Model Documentation and Evaluation of the Peace II Project Description

R4 Model Documentation

1990 Land Use

Figure A2-9

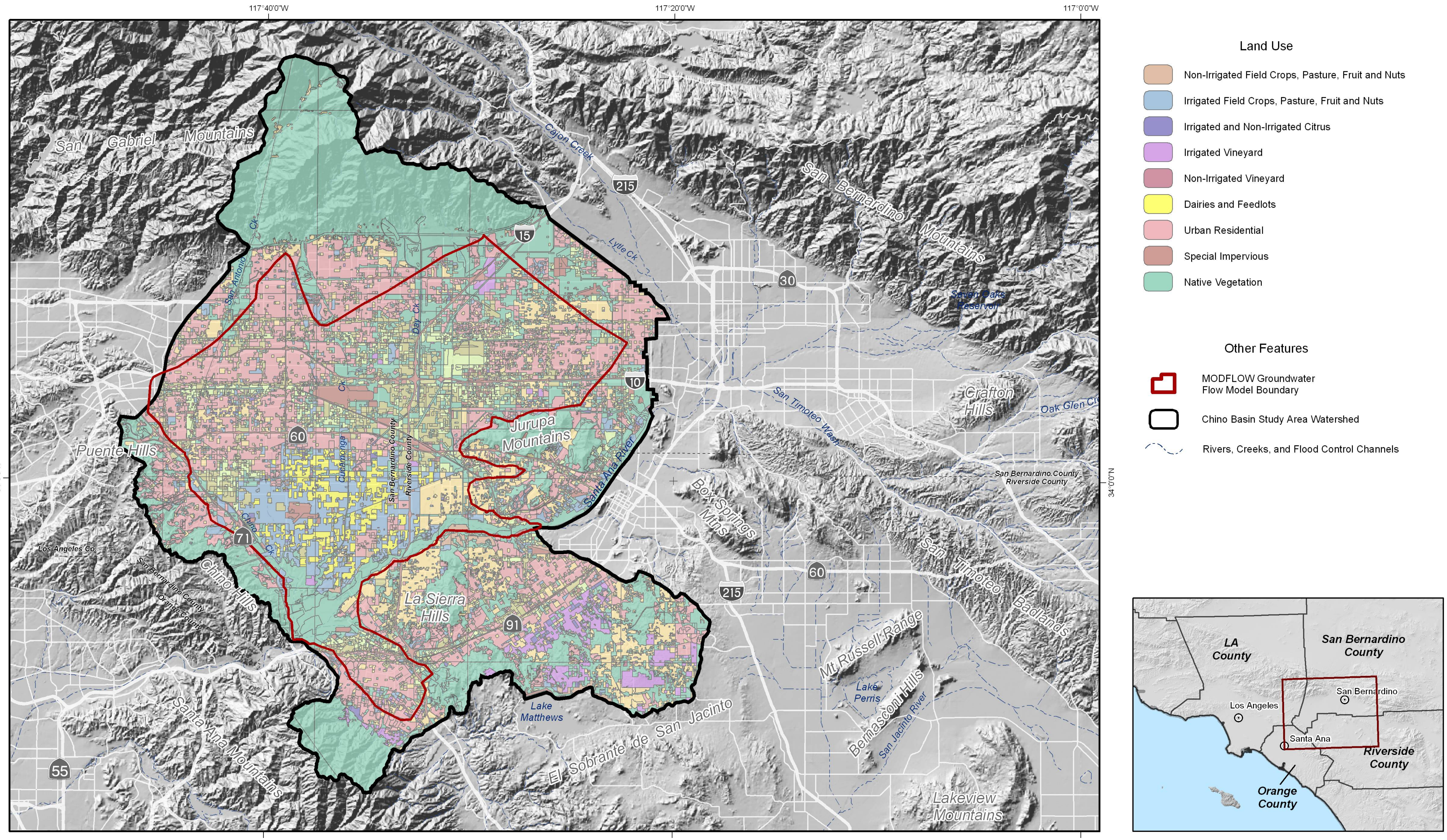

Produced by:

WILDERMUTH™ ENVIRONMENTAL INC.
23692 Birtcher Drive
Lake Forest, CA 92630
949.420.3030
www.wildermuthenvironmental.com

Author: FIB/MJC
Date: 20071004
File: Figure_A2-10.mxd

0 2 4 Miles
0 2 4 6 KM

CHINO BASIN WATERMASTER — Partners in Basin Management

2007 CBWM Groundwater Model Documentation and Evaluation of the Peace II Project Description

R4 Model Documentation

2000 Land Uses in th Chino Area

Figure A2-10

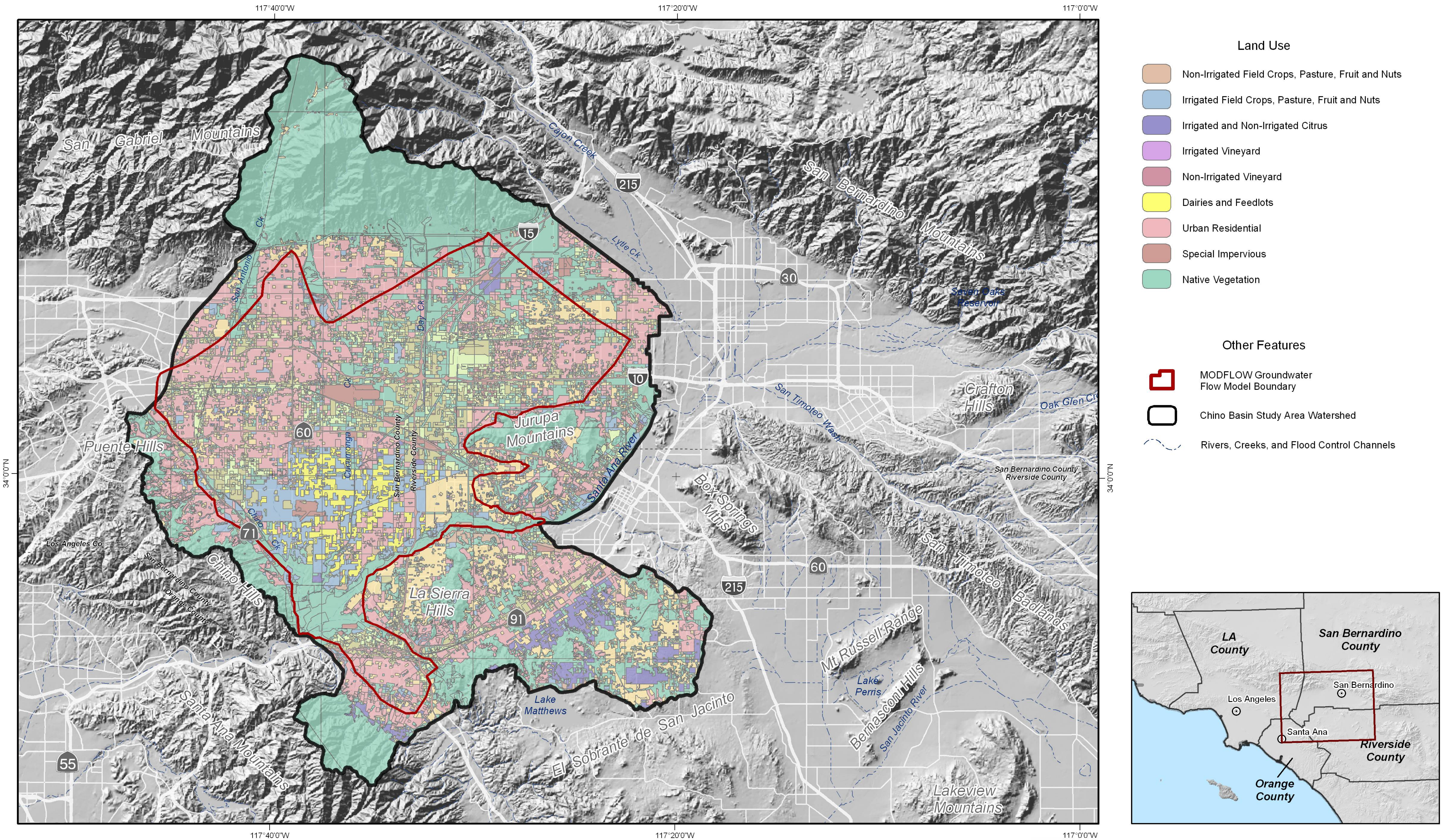

Produced by:

WILDERMUTH™ ENVIRONMENTAL INC.

23692 Birtcher Drive
Lake Forest, CA 92630
949.420.3030
www.wildermuthenvironmental.com

Author: FIB/MJC
Date: 20071108
File: Figure_A2-11.mxd

0 2 4 Miles
0 2 4 6 KM

2007 CBWM Groundwater Model Documentation and Evaluation of the Peace II Project Description

R4 Model Documentation

2006 Land Uses in th Chino Area

Figure A2-11

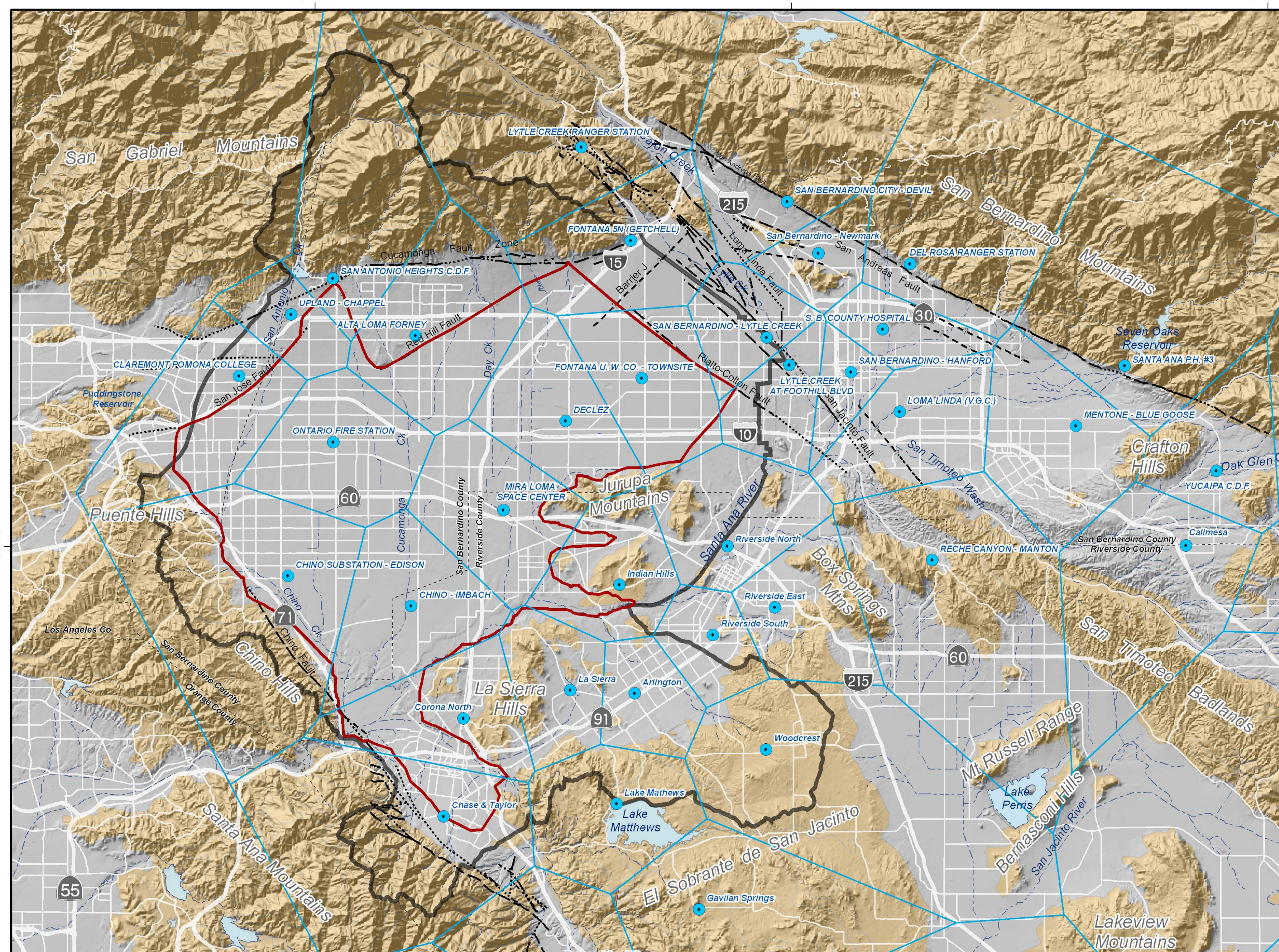

- Precipitation Station
- Thiessen Polygons (Precipitation Monitoring Station Area of Influence)
- Chino Basin Study Area Watershed
- MODFLOW Groundwater Flow Model Boundary
- Rivers, Creeks, and Flood Control Channels
- Flood Control & Conservation Basins

Geology

- Unconsolidated Water Bearing Sediments
- Consolidated Bedrock

Faults

- Location Certain
- Location Approximate
- Location Concealed
- Location Uncertain

0 2 4 Miles
0 2 4 6 KM

Produced by:
WILDERMUTH ENVIRONMENTAL INC.
23692 Birtcher Drive
Lake Forest, CA 92630
949.420.3030
www.wildermuthenvironmental.com

Author: FIB/MJC
Date: 20071004
File: Figure_A2-12.mxd

2007 CBWM Groundwater Model Documentation and Evaluation of the Peace II Project Description

R4 Model Documentation

Location of Precipitation Stations and Thiessen Polygons

Figure A2-12

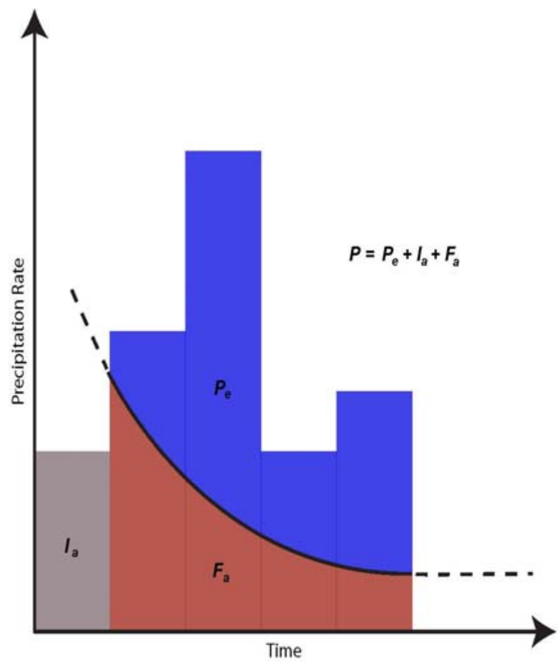

Figure A2-13 Relationship between the SCS method variables (After Chow et al, 1988)

I_a = initial abstractions, P_e = rainfall excess, F_a = continuing abstraction, P = total rainfall.

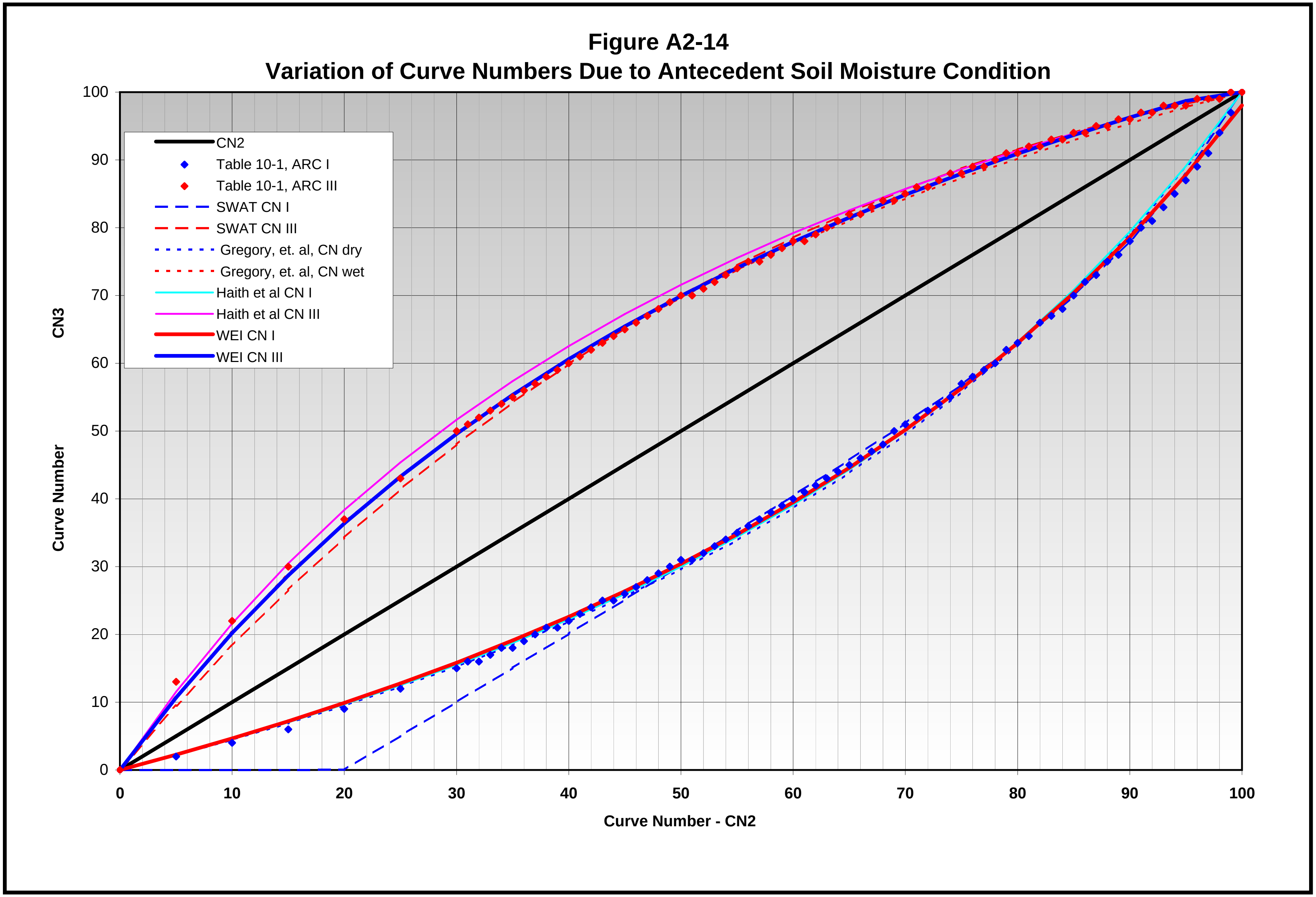

Figure A2-14
Variation of Curve Numbers Due to Antecedent Soil Moisture Condition
CN3
Curve Number
Curve Number - CN2
0
10
20
30
40
50
60
70
80
90
100
CN2
Table 10-1, ARC I
Table 10-1, ARC III
SWAT CN I
SWAT CN III
Gregory, et. al, CN dry
Gregory, et. al, CN wet
Haith et al CN I
Haith et al CN III
WEI CN I
WEI CN III

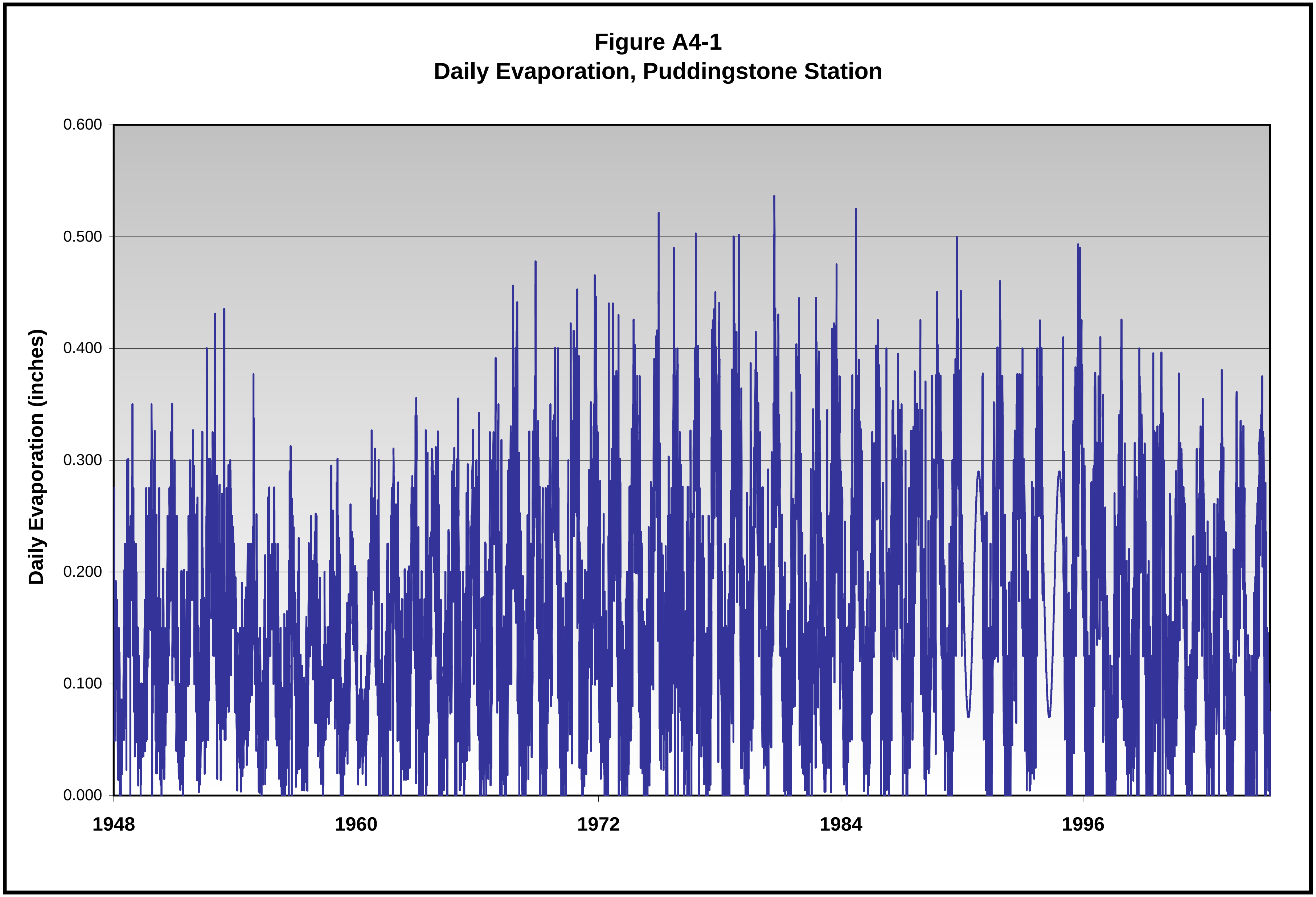
Figure A4-1
Daily Evaporation, Puddingstone Station
Daily Evaporation (inches)
0.600
0.500
0.400
0.300
0.200
0.100
0.000
1948
1960
1972
1984
1996

Figure A4-2
CIMIS ETo Data - Claremont Station

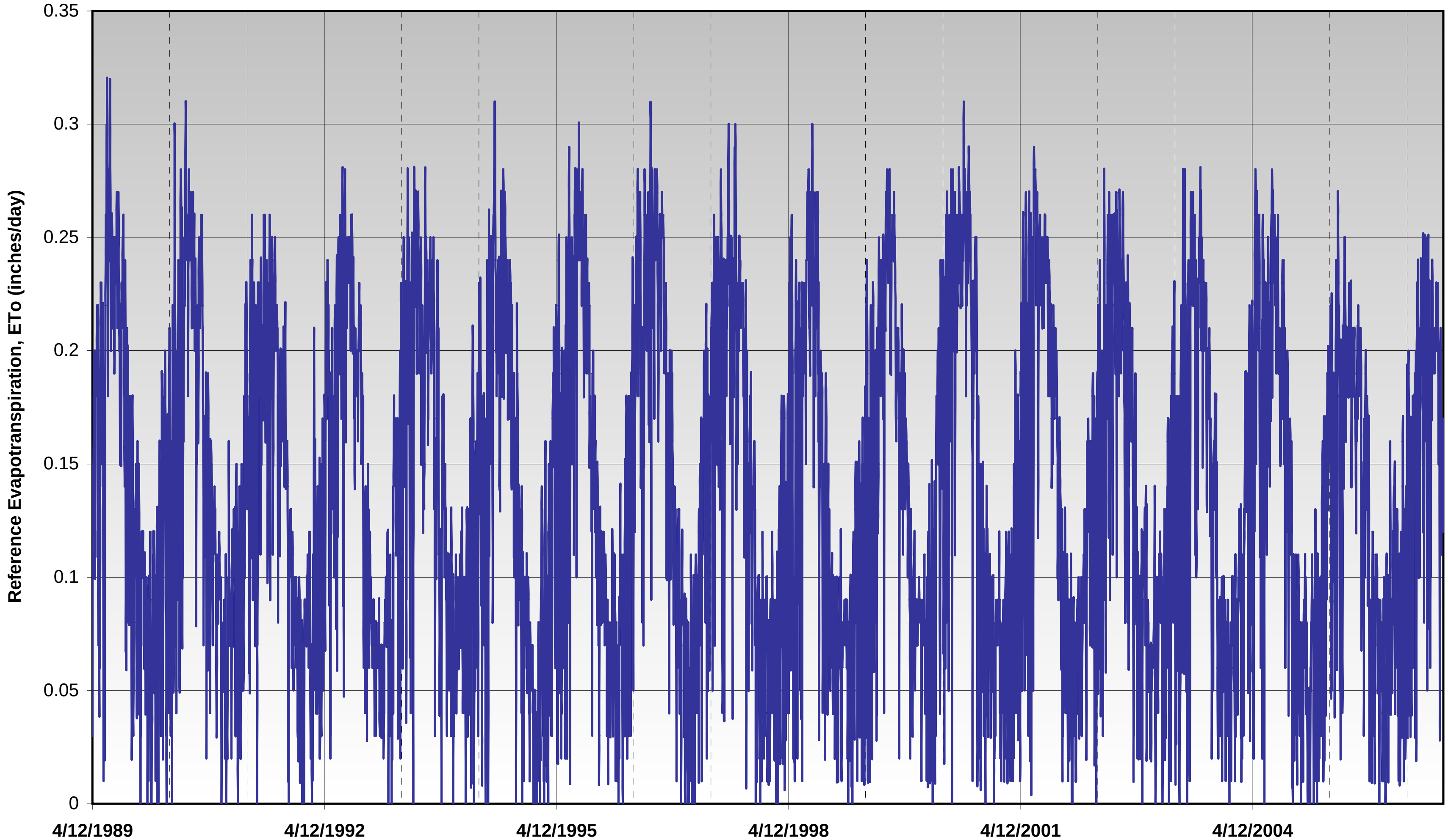

Tables&figures_AppendixA_v2.xls

WILDERMUTH ENVIRONMENTAL INC.

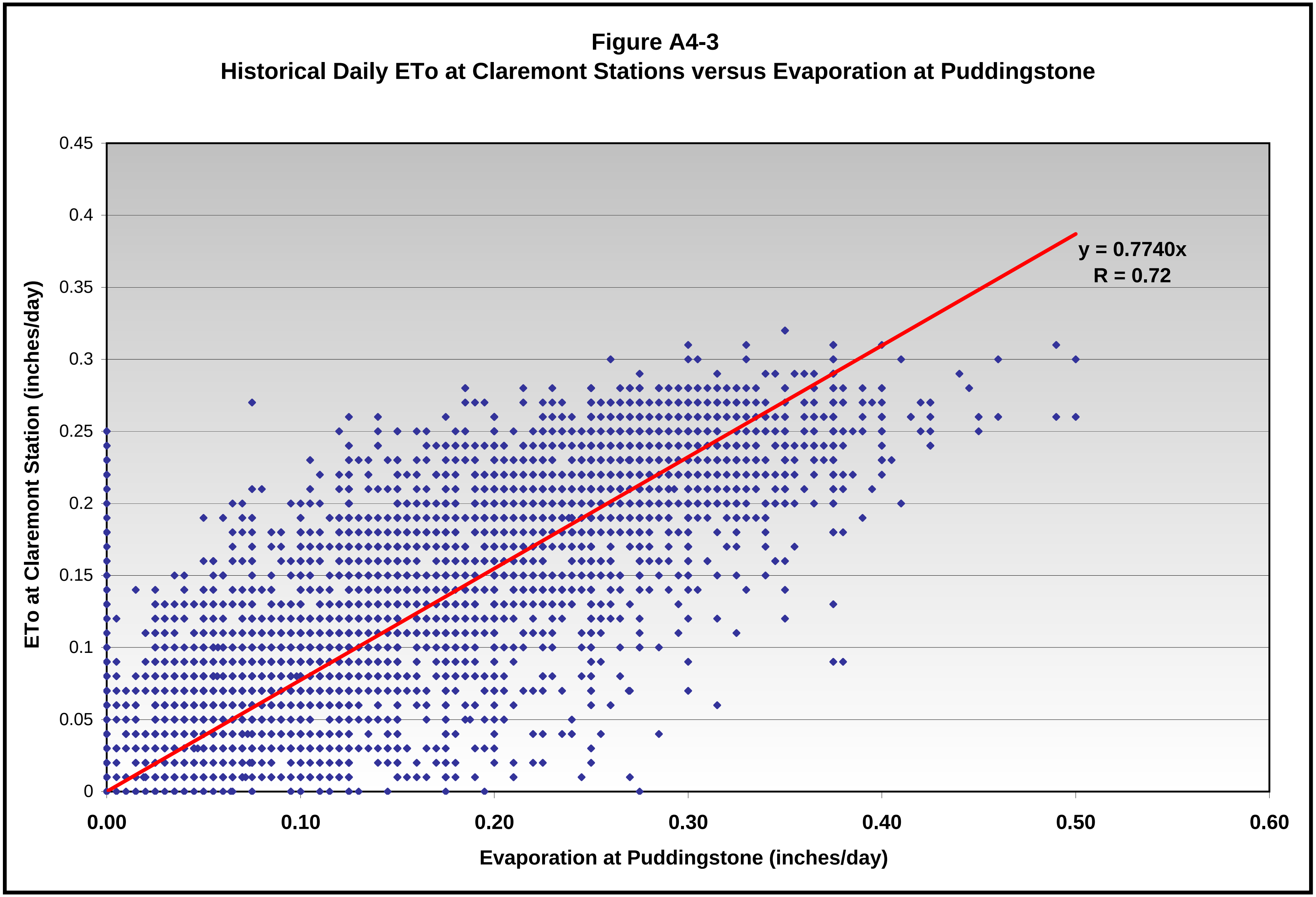

Figure A4-3
Historical Daily ETo at Claremont Stations versus Evaporation at Puddingstone
ETo at Claremont Station (inches/day)
0.45
0.4
0.35
0.3
0.25
0.2
0.15
0.1
0.05
0
y = 0.7740x
R = 0.72
0.00
0.10
0.20
0.30
0.40
0.50
0.60
Evaporation at Puddingstone (inches/day)

Figure A4-4
Illustration of Relationship between Evapotranspiration Rate and Soil Moisture

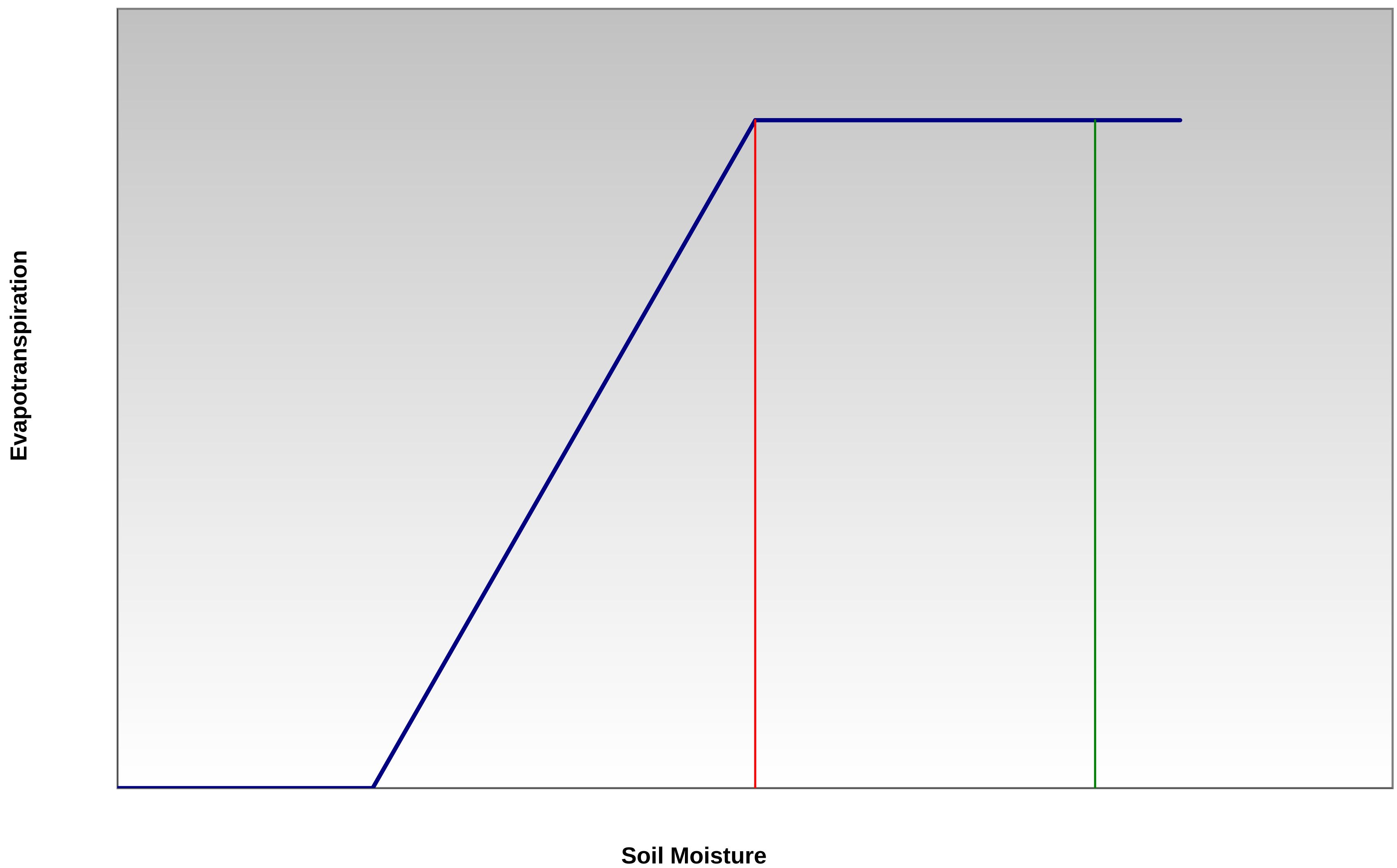

Appendix B

Unsaturated Flow Recharge for the Chino Basin Documentation

INTRODUCTION

This report documents the model construction and underlying assumptions of the unsaturated flow and transport model used for the Chino Basin. The purpose of this model is to quantify the travel time of infiltrating recharge water from the land surface to the water table. The results of this model will be used to apply an appropriate travel time, or lag time, to water that is recharged at the land surface such that the groundwater system can be simulated more accurately. It should be noted that this model is for unsaturated flow only. Water that is recharged via stream channels or recharge basins and other saturated recharge events were not considered in this evaluation.

The modeling process consists of four key steps. These steps are listed below and discussed in depth herein:

- Determine boundary conditions, that consists of input water from rainfall and irrigation
- Quantify vadose zone flow properties
- Determine solute transport parameters
- Conduct and review simulations

These key steps were followed for seven modeling locations, or points, within the active groundwater model domain. The processing of unsaturated flow and transport models is extremely computer intensive; therefore, seven representative modeling points were selected within the active groundwater model domain. The seven sites were selected based on site lithology, surface land use, and depth to groundwater. The travel time of infiltrating recharge water at each of these modeling points will be used within the calibration process to determine the travel time for recharge water across the active groundwater model domain.

B1.1 REGIONAL CLIMATE

The climate in the Chino Basin area is characterized by warm, dry summers, low precipitation, and mild winters. The average daily winter temperature is 51 degrees Fahrenheit (ºF), while the average daily summer temperature is 75 ºF. Throughout the year, temperatures range from a low near 20 ºF during the winter to a high of over 100 ºF during the summer. Most of the precipitation occurs between November and March, and there is practically no rainfall during the summer months. Summer thunderstorms occur in the mountains but do not contribute significantly to runoff. In the Chino Basin area, the mean annual precipitation ranges from 13 inches near Prado Dam to 25 inches at the base of the San Gabriel Mountains. In these mountains, the average annual rainfall has reached as high as 40 inches with extremes ranging between 40 and 200 percent of normal. In nearly all months, evaporation exceeds precipitation. Relative humidity averages 45 percent year round, 40 to 70 percent in winter, and 10 to 20 percent in summer.

There are 28 rainfall stations in and around the Chino Basin, as shown on Figure B1-1. The recorded daily precipitation data from some of these stations can be traced back as early as the year 1900. Figure B1-2 shows the measured annual rainfall at the Ontario Fire Station gage, a precipitation station at the center of the basin. Table B1-2 shows the average annual rainfall increases from Prado Dam (Chino – Imbach gage) to the foothills of the San Gabriel Mountains (San Antonio Heights C.D.F gage, Upland–Chappel gage), or from south to north.

B1.2 EVAPOTRANSPIRATION

Evapotranspiration (ET) is the loss of water to the atmosphere through the combined processes of evaporation and transpiration. Many factors affect ET, including weather parameters, such as solar radiation, air temperature, relative humidity, and wind speed; soil factors, such as soil texture, structure, density, and chemistry; and plant factors, such as plant type, root depth, foliar density, height, and stage of growth. Although ET can be measured using devices, such as lysimeters, estimating ET using analytical and empirical equations is a common practice because measurement methods are expensive and time consuming. Many ET equations were developed by correlating measured ET to measured weather parameters that directly or indirectly affect ET. Since there are so many factors that affect ET, it is difficult to formulate an equation that can produce estimates of ET under different sets of conditions. ET is often calculated from a grass surface with prevailing conditions and adjusted by crop coefficients to estimate the ET of other vegetation. ET from a standardized grass surface is commonly denoted as ET_o.

There are many theoretical and empirical equations for estimating ET_o. The model used by the California Irrigation Management Information System (CIMIS) is the Penman's equation, modified by Pruitt and Doorenbos (Proceedings of the International Round Table Conference on Evapotranspiration, Budapest, Hungary, 1977). The Modified Penman employs a wind function. Instead of daily weather data, the CIMIS version uses hourly weather data to calculate ET_o. Hourly averages of weather data were used in the unsaturated flow model to calculate an hourly ET_o value. To calculate daily ET_o, the 24 hour ET_o values (midnight to midnight) are summed. Air temperature, wind speed, and relative humidity are measured directly at each weather station. Vapor pressure is calculated from relative humidity and air temperature. Figure B1-3 shows the calculated daily ET_o in Claremont. As one would anticipate, the ET_o is high in the summer when evaporation and plant transpiration are highest and low in the winter when plant species are less active. What is more, the value changes from as low as zero to as high as 0.30 inches per day.

B1.3 SOIL AND LAND USE

Soils in the Chino Basin are largely derived from the alluvial materials. The Chino Basin consists of an arid, fan-shaped plain of permeable sandy soils and deep aggregates, sloping to the southwest. Consequently, they are generally light, sandy, highly permeable, and easily eroded. Large boulder fields occur at the mouths of major canyons in San Gabriel Mountains. Soils around the perimeter of the upper valleys are rocky while those in the middle and lower areas consist primarily of finer sands and silts.

The distribution of soil types, as classified by the Natural Resource Conservation Service (NRCS) based on the soil's runoff potential, is shown in Figure B1-4**.** The four hydrologic soils groups—A, B, C, and D—are characterized by the following features:

- Group A is sand, loamy sand, or sandy loam. It has low runoff potential and high infiltration rates even when thoroughly wetted.
- Group B is silt loam or loam. It has a moderate infiltration rate when thoroughly wetted.
- Group C is sandy clay loam. It has low infiltration rates when thoroughly wetted.
- Group D is clay loam, silty clay loam, sandy clay, silty clay, or clay. This kind of soil has the highest runoff potential. It has very low infiltration rates when thoroughly wetted.

The soils in the upstream area of the Chino Basin, near the foothills of the San Gabriel Mountains, belong to Group A while most of the soils in the southern end of the basin are Group B soils or mixed soils from Groups A to C.

Based on the historical land use of these soil types, empirical parameters can be estimated for predicting direct runoff or infiltration from rainfall excess.

B1.4 FEATURES OF THE VADOSE ZONE

The vadose zone, which is also termed the unsaturated zone, is the portion of the soil profile between the land surface and the phreatic zone, or the zone of saturation. It extends from the top of the ground surface to the water table. Figure B1-5 is a depth to water contour map (vadose zone thickness contour map) for the Chino Basin in 2004. Figures B1-6 through B1-13 show the soil profiles at the modeled locations inside the

Chino Basin. The features of the vadose zone in Chino Basin can be summarized as follows:

- The thickness of the unsaturated zone ranges from as low as 0 feet (near Prado Basin) to as high as 1000 feet (in the north Chino Basin).
- The vadose zone consists of complicated interbedded coarse and fine alluvium material with lithology ranging from clay to gravel sand.
- The vadose zone soils in the north side of the Basin consist primarily of sand-grained and gravel-grained materials while those in the middle and lower areas consist of interbedded finer sands, silts, and clay.

The lithology of the vadose zone is based on well completion reports of wells within the basin. In these well completion reports, soils are grouped using the Unified Soil Classification System (USCS).

Table B1-1
Precipitation Statistics for Measurements Recorded at Stations in or near the Chino Basin

Statistics	Ontario Fire Station	Claremont Pomona College	Upland - Chappel	Mira Loma Space Center	Chino Substation -Edison	Chino - Imbach	San Antonio Heights C.D.F.	Alta Loma - Forney	Fontana Union Water Company - Townsite	Declez
Mean	16.24	18.48	19.51	11.98	15.18	12.3	20.66	20.74	17.51	13.08
Median	14.56	17.31	18.41	11.19	13.98	11.34	19.89	18.8	15.64	12.22
Standard Deviation	7.41	8.02	8.52	5.14	6.83	5.45	9.07	9.1	7.56	5.68
Range	33.06	32.12	34.81	23.45	32.44	26.19	44.39	41.24	33.23	23.23
Minimum	3.94	5.5	5.86	3.55	3.94	3.43	4.6	6.65	5.09	3.98
Maximum	37	37.62	40.67	27	36.38	29.62	48.99	47.89	38.32	27.21

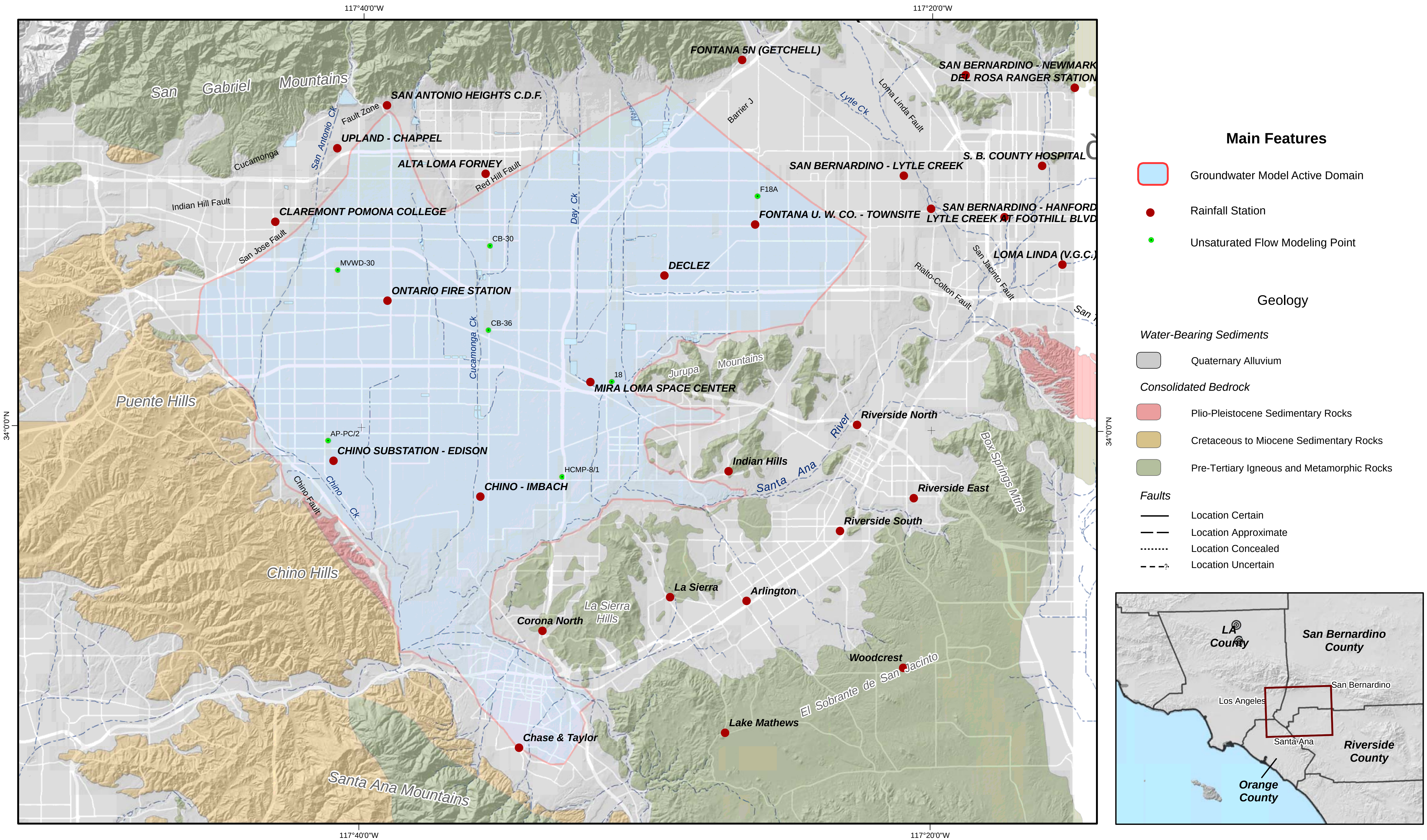

Produced by:

WILDERMUTH ENVIRONMENTAL INC
23692 Birtcher Drive
Lake Forest, CA 92630
949.420.3030
www.wildermuthenvironmental.com

Author:FIB
Date: 20070815
File: Rainfall_Station_FigB1-1.mxd

Appendix B
Chino Basin Unsaturated Flow Model Documentation

Rainfall Stations and Unsaturated Flow and Transport Simulation Points

Figure B1-1

Figure B1-2
Measured Annual Rainfall at the Ontario Fire Station

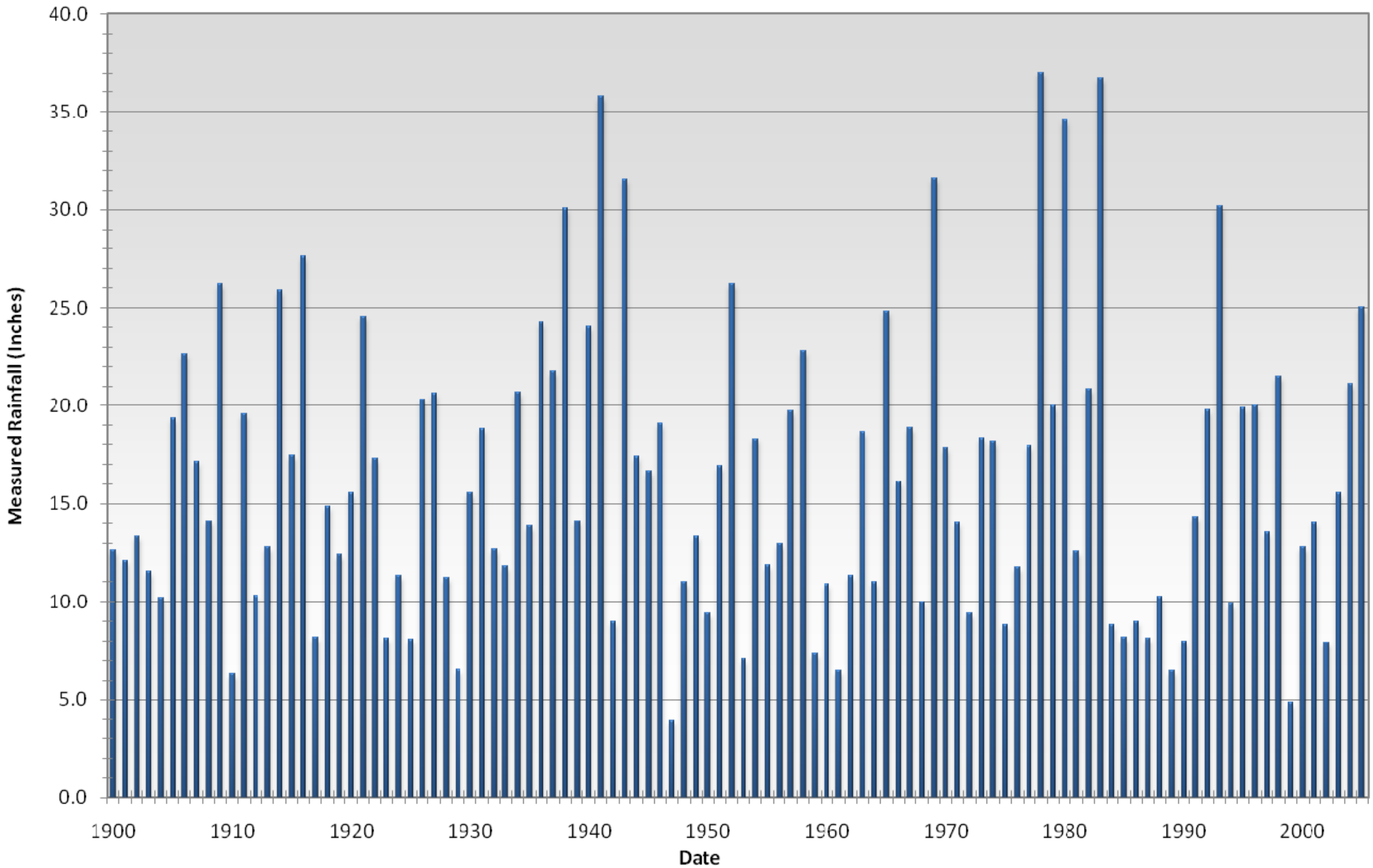

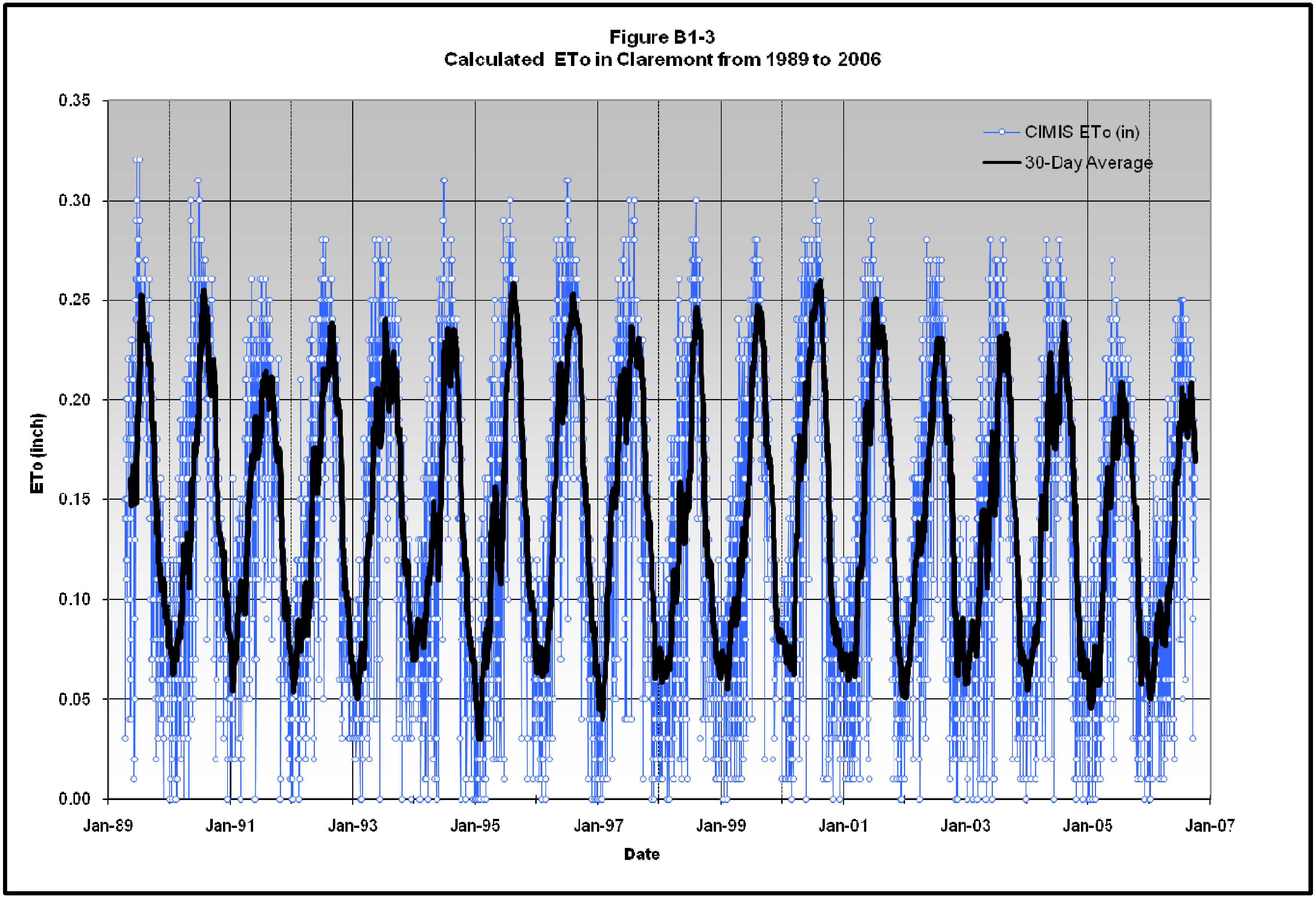
Figure B1-3
Calculated ETo in Claremont from 1989 to 2006
0.35
0.30
0.25
0.20
0.15
0.10
0.05
0.00
ETo (inch)
CIMIS ETo (in)
30-Day Average
Jan-89
Jan-91
Jan-93
Jan-95
Jan-97
Jan-99
Jan-01
Jan-03
Jan-05
Jan-07
Date

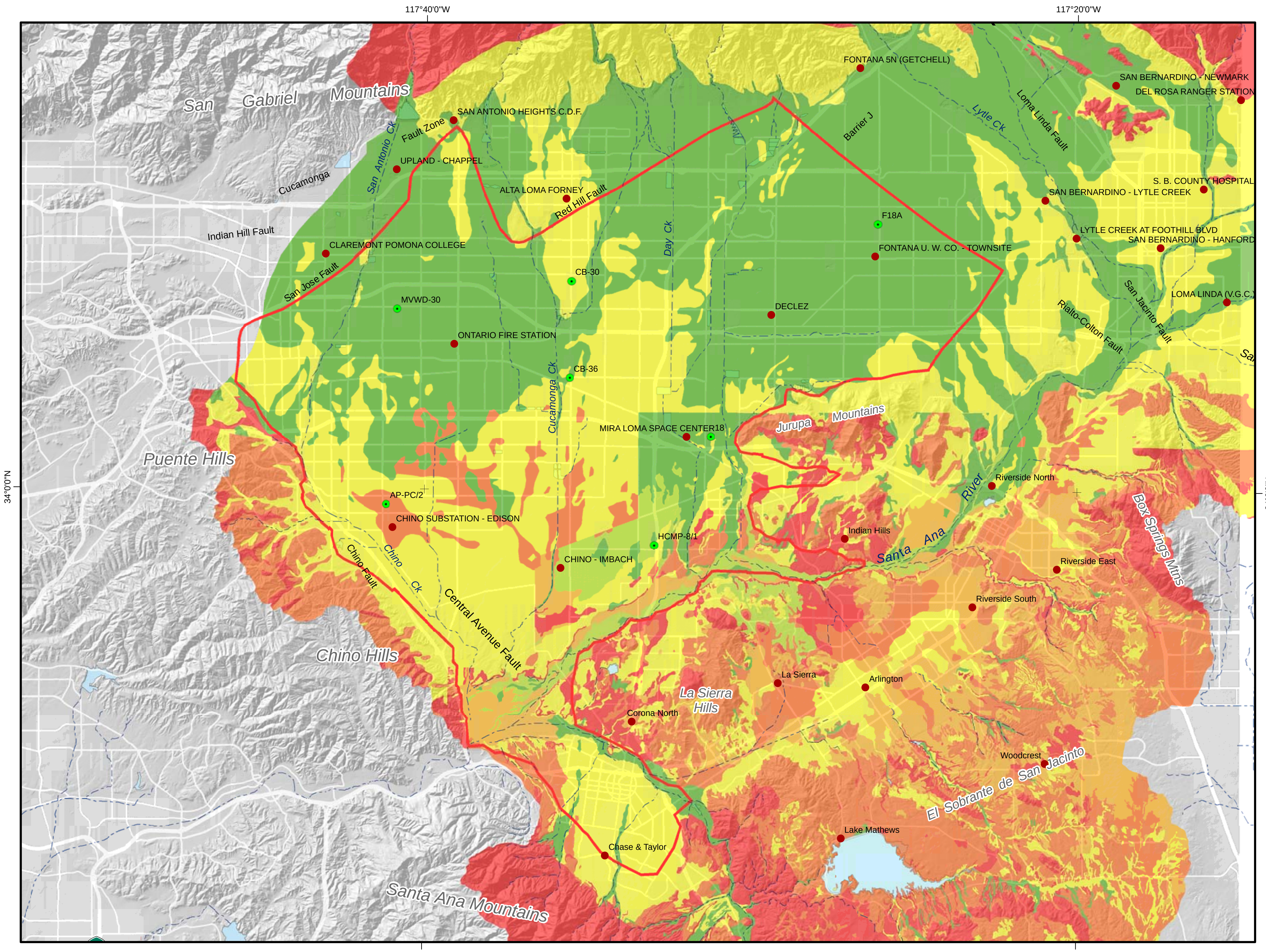

Main Features

- Rainfall Station
- Unsaturated Flow Modeling Point
- Modeling Domain

Hydrologic Soil Group

- **A** — Low runoff potential. Soils having high infiltration rates even when thoroughly wetted and consisting chiefly of deep, well to excessively drained sands or gravels. These soils have a high rate of water transmission.
- **AB** — Hybrid Soil Types by Riverside County Flood Control District
- **AC** — Hybrid Soil Types by Riverside County Flood Control District
- **B** — Soils having moderate infiltration rates when thoroughly wetted and consisting chiefly of moderately deep to deep, moderately well to well drained soils with moderately fine to moderately coarse textures. These soils have a moderate rate of water transmission.
- **BC** — Hybrid Soil Types by Riverside County Flood Control District
- **C** — Soils having slow infiltration rates when thoroughly wetted and consisting chiefly of soils with a layer that impedes downward movement of water, or soils with moderately fine to fine texture. These soils have a slow rate of water transmission.
- **D** — High runoff potential. Soils having very slow infiltration rates when thoroughly wetted and consisting chiefly of clay soils with a high swelling potential, soils with a permanent high water table, soils with a claypan or clay layer at or near the surface, and shallow soils over nearly impervious material. These soils have a very slow rate of water transmission.

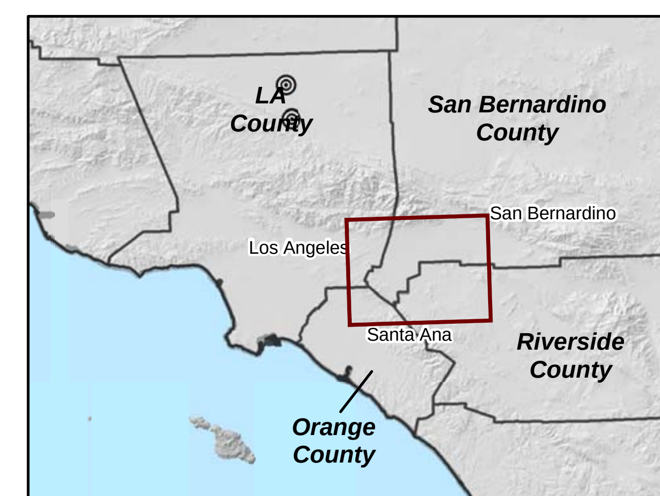

Produced by:
WILDERMUTH ENVIRONMENTAL INC
23692 Birtcher Drive
Lake Forest, CA 92630
949.420.3030
www.wildermuthenvironmental.com

Author: FIB
Date: 20070815
File: Soil_Group_FigB1-4.mxd

0 1 2 3 4 Miles
0 2 4 6 KM

Inland Empire Utilities Agency

Appendix B
Chino Basin Unsaturated Flow Model Documentation

The Distribution of Hydrologic Soil Group in Chino Basin Area

Figure B1-4

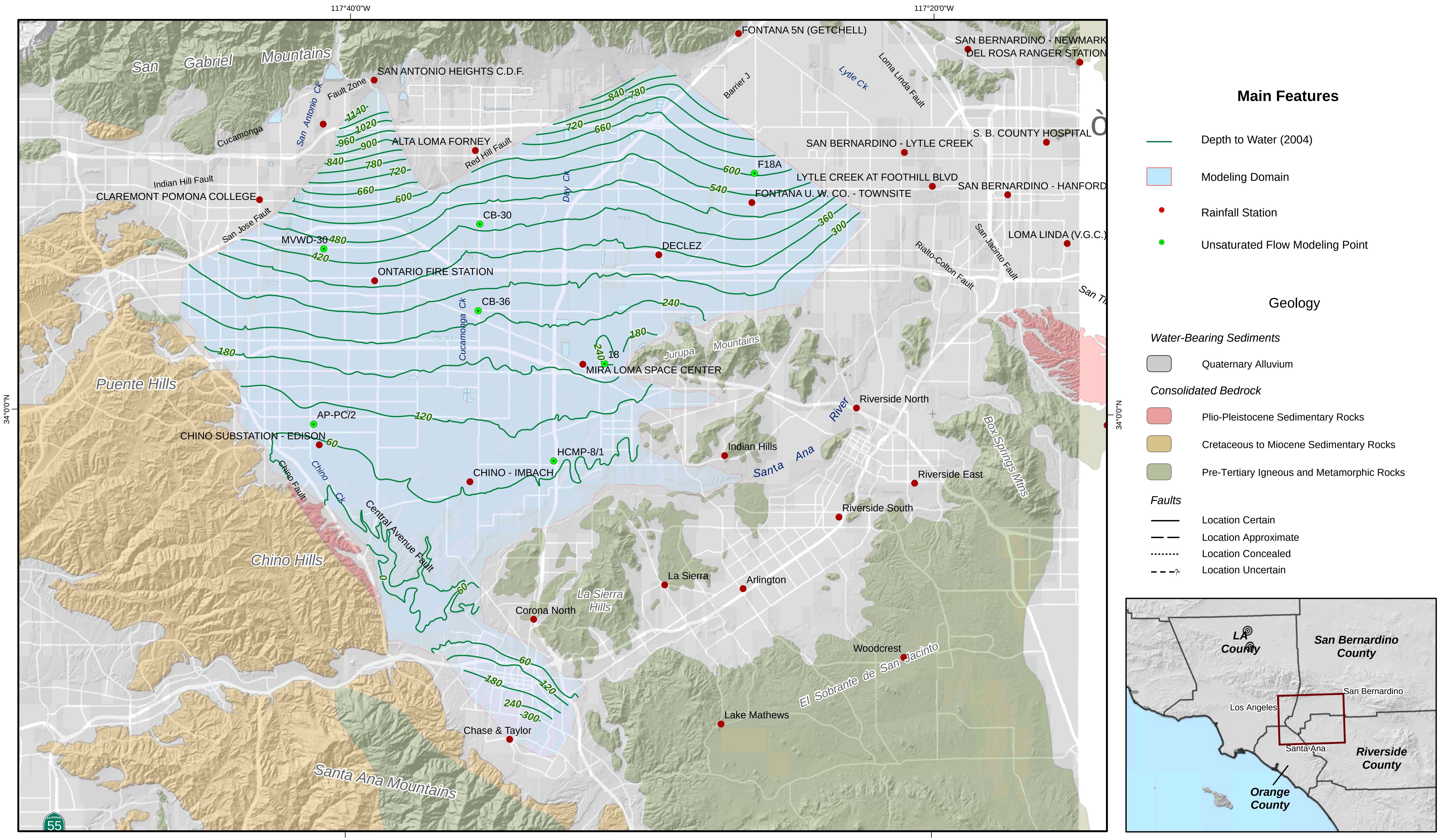

Main Features

- Depth to Water (2004)
- Modeling Domain
- Rainfall Station
- Unsaturated Flow Modeling Point

Geology

Water-Bearing Sediments

- Quaternary Alluvium

Consolidated Bedrock

- Plio-Pleistocene Sedimentary Rocks
- Cretaceous to Miocene Sedimentary Rocks
- Pre-Tertiary Igneous and Metamorphic Rocks

Faults

- Location Certain
- Location Approximate
- Location Concealed
- Location Uncertain

0 1 2 3 4 Miles

0 2 4 6 KM

Produced by:

WILDERMUTH ENVIRONMENTAL INC

23692 Birtcher Drive
Lake Forest, CA 92630
949.420.3030
www.wildermuthenvironmental.com

Author: MC,FIB

Date: 20070815

File: DTW_FigB1-5.mxd

Inland Empire Utilities Agency

Appendix B

Chino Basin Unsaturated Flow Model Documentation

Depth to Water in Chino Basin 2004

Figure B1-5

MODEL THEORY AND METHODS

Many factors influence unsaturated groundwater flow, such as rainfall, the condition of the soil's surface and its vegetation cover, evapotranspiration, soil land use, the properties of soils, and the moisture distribution of soils in the unsaturated zone. This section describes the theory and methods of estimating the amount of water that reaches the unsaturated zone and how it percolates to the groundwater table.

The methods applied for this unsaturated flow model differ slightly from those applied for the recharge and runoff model that calculates recharge and runoff for the entire Chino Basin. The rational for this difference is the distinction between the calculation for runoff and recharge for an entire basin and the recharge and runoff for a localized point in a basin.

B2.1 CALCULATION OF RAINFALL ABSTRACTIONS

In 1972, the U.S. Soil Conservation Service (now referred to as the NRCS) suggested an empirical model for rainfall abstractions, based on the potential for soil to absorb a certain amount of moisture. On the basis of field observations, soil potential storage (S) (inches) was related to a curve number (CN), which is a characteristic of the soil type, land use, and the initial degree of saturation known as the antecedent moisture condition.

For the normal antecedent moisture condition (AMC II), the value of S is defined by the empirical expression:

$$S = \frac{1000}{CN} - 10 \qquad (2.1)$$

For dry (AMC I) or wet conditions (AMC III), the equivalent curve numbers can be computed as follows, respectively:

$$CN(I) = \frac{4.2CN(II)}{10 - 0.058CN(II)} \qquad (2.2)$$

and

$$CN(III) = \frac{23CN(II)}{10 + 0.13CN(II)} \qquad (2.3)$$

The range of antecedent moisture conditions for each class is shown in the Table B2-1.

The effective rainfall is computed with the following equation:

$$P_e = \frac{(P - I_a)^2}{P - I_a + S} \tag{2.4}$$

Where
P_e is the effective precipitation or excess rainfall or direct runoff,
P is rainfall,
I_a is the initial abstraction, and
S is the soil's potential storage or retention.

Through the study of results from many small experimental watersheds, the effective precipitation is computed with the following equation:

$$P_e = \frac{(P - 0.2S)^2}{P + 0.8S} \tag{2.5}$$

Once the effective precipitation is obtained, the total rainfall abstraction (initial abstraction I_a + continuing abstraction F_a) can be computed as follows:

$$I_a + F_a = P - P_e \tag{2.6}$$

B2.2 REQUIRED IRRIGATION WATER

When groundwater flow in the vadose zone is to be simulated, all water resources should be taken into account. For example, the return flow of irrigation water is an important source in the Chino Basin. The irrigation water need can be quantified with the following equation:

$$ET_{crops} = ET_o \times K_{crops} \tag{2.7}$$

Where
ET_{crops} is the amount of water required by crops,
ET_o is the reference water use or called reference evapotranspiration, and
K_{crops} is the crop coefficient.

The actual irrigation water is thus determined as follows:

$$Irrigation\ need = \frac{ET_{crop}}{DU} \tag{2.8}$$

Where DU is the distribution uniformity or irrigation efficiency.

Rainfall would be considered to be 100% uniform because all of the areas of a particular site would receive an equivalent depth of precipitation. Irrigation sites in the Chino Basin have an assumed irrigation DU of 80%.

B2-3 UNSATURATED FLOW EQUATION

The Richards' equation is the standard governing equation for simulating groundwater flow in an unsaturated zone. The equation is expressed as follows:

$$\sum_{i=1}^{3} \frac{\partial}{\partial x_i}\left(K(h)\frac{\partial h}{\partial x_i} \right) + G = \frac{\partial \theta}{\partial t} \tag{2.9}$$

To solve this equation, knowledge of the relationships between hydraulic conductivity (*K*), water content (*θ*), and pressure head (*h*) are essential. The relationship between pressure head and volumetric water content for a particular soil is known as a soil-water characteristic curve or a soil-water retention curve. Certain empirical expressions can be used to relate the water content of a soil to its pressure head. The most frequently used expressions are those proposed by Brooks and Corey (1964) and by van Genuchten (1980).

The Brooks and Corey models (1964) for soil-water retention and unsaturated hydraulic conductivity are:

$$\frac{\theta - \theta_r}{\theta_s - \theta_r} = \left(\frac{h_b}{h} \right)^{\lambda} \qquad h > h_b \tag{2.10}$$

$$K = K_s \left(\frac{h_b}{h} \right)^{(2+3\lambda)} = K_s \left(\frac{\theta - \theta_r}{\theta_s - \theta_r} \right)^{3+\frac{2}{\lambda}} \tag{2.11}$$

Where
θ is soil volumetric water content;
θ_r and θ_s are residual and saturated water content, respectively;
h_b is air-entry suction;
h is capillary suction;
λ is a pore size distribution index;
K is hydraulic conductivity; and

K_s is saturated hydraulic conductivity.
For $h < h_b$, $\theta = \theta_s$, and $K = K_s$.

The van Genuchten equations (1980) for soil-water retention and unsaturated hydraulic conductivity are:

$$\frac{\theta - \theta_r}{\theta_s - \theta_r} = \left[\frac{1}{1+(\alpha h)^n}\right]^m \quad (2.12)$$

$$K = K_s \frac{\left[1-(\alpha h)^{n-1}\left[1+(\alpha h)^n\right]^{1/n-1}\right]^2}{\left[1+(\alpha h)^n\right]^{0.5(1-1/n)}} \quad (2.13)$$

or

$$K = K_s \left(\frac{\theta - \theta_r}{\theta_s - \theta_r}\right)^{1/2} \left\{1-\left[1-\left(\frac{\theta - \theta_r}{\theta_s - \theta_r}\right)^{1/m}\right]^m\right\}^2 \quad (2.14)$$

Where α and n are so-called van Genuchten parameters and $m = 1 - 1/n$.

Figures B2-1 and B2-2 show the relationship between water content and tension (capillary suction) and how hydraulic conductivity varies with changes of water content or tension.

The Brooks-Corey parameters can be approximately converted to van Genuchten parameters, based on the following conversion equations (van Genuchten, 1980):

$$\lambda = n - 1 \quad (2.15)$$
$$h_b = 1/\alpha \quad (2.16)$$

The Brooks-Corey soil-water retention model provides good results for soils with a narrow pore-size distribution (Brooks and Corey, 1964). However, it is not effective at reproducing observed soil-water retention behavior for undisturbed field soils with wide pore-size distributions, particularly near full saturation (van Genuchten and Nielsen, 1985). The Brooks-Corey model describes only the portion of the curve for capillary suction larger than air-entry suction, and its discontinuous behavior prohibits the model from reproducing the smooth transition between unsaturated and saturated conditions. The van Genuchten soil-water retention model permits a representation of the total water-retention curve for a wider variety of soil types (van Genuchten and Nielsen, 1985).

Richards' equation is the standard governing equation for describing groundwater flow in an unsaturated zone. As stated above, to solve this equation, knowledge of the relationships between hydraulic conductivity (*K*), water content (θ), and pressure head (*h*) is essential. And, the van Genuchten model (1980) is the most acceptable model for describing such relationships.

B2.4 SOIL PROFILES HYDRAULIC PROPERTIES

Soil hydraulic properties are essential for simulating water flow and solute transport in the subsurface. There are no measurements of the soil hydraulic properties of the Chino Basin. Fortunately, however, the values of hydraulic parameters vary systematically with USDA soil textural class (McCuen et al. 1981). In other words, each soil class has its own hydraulic properties, which allows for the appropriate values of the hydraulic parameters to be determined, based on soil class. Several databases have been developed for this purpose, including RAWLS (Rawls et al., 1982), ROSETTA (Schaap and Leij, 1998), and CARSEL (Carsel and Parrish, 1988).

The RAWLS database was compiled from about 30 sources in the United States and contains 5,401 samples. Rawls et al. (1982) published a table of mean Brooks-Corey parameter estimates and their standard deviations for 11 USDA soil texture classes.

The ROSETTA database was pooled from the AHUJA, UNSODA, and RAWLS databases. The AHUJA database contains 393 samples for water retention and K_s. The UNSODA database (Leij et al., 1996) contains 791 entries with water retention as well as unsaturated and saturated hydraulic conductivity data from many international sources. The ROSETTA database contains 2,134 water retention samples and 1,306 samples of K_s. Based on the ROSETTA database, Schaap and Leij (1998) provide mean retention parameter values and K_s for 12 USDA soil classes.

The CARSEL database contains 15,737 soil textural samples that were collected by the Natural Resources Conservation Service (formerly SCS) from 42 states. The database does not contain measured hydraulic parameters. Based on the Rawls-Brakensiek regressions (1985), coupled with Monte Carlo simulations, Carsel and Parrish (1988) used the database to derive probability distributions for saturated volumetric water content (θ_s), residual volumetric water content (θ_r), saturated hydraulic conductivity (K_s), and van Genuchten's parameters (α and n) on the basis of twelve USDA soil textural classes.

Wang (2002) and Wang et al. (2003) demonstrated that mean hydraulic parameter estimates that are based on the generic database that was published by Carsel and Parrish (1988) allow for a much better reproduction of observed water contents than estimates that are based on the RAWLS or ROSETTA databases. Therefore, the mean hydraulic estimates from CARSEL were used to represent the hydraulic properties of the soil classes in the Chino Basin, as shown in Table B2-2.

In the United States, there are two systems under which soils are likely to be classified: (1) the Unified Soil Classification System (USCS) and (2) the US Department of Agriculture (USDA) System. The differences between these two classifications are:

- The USCS was developed to describe the engineering properties of soils. This system classifies soil types into 15 categories, which are based on particle (grain) size and response to physical manipulation at various water contents.

- The USDA system classifies soil types into 12 categories, based entirely on particle size and fraction. This system is extensively used by US soil scientists.

As noted in the Section B1.5 of this report, the lithological descriptions of vadose zone soil profiles in Chino Basin well completion reports are based on the USCS. The soil hydraulic properties for each texture class in the aforementioned national soil databases were derived from the USDA system. So, it is necessary to find a bridge between USCS and USDA soil classifications.

Fuller (1978) developed a comparison of the USDA system and USCS. Based on soil textures, part of the USDA system can be compared directly to the USCS. Strictly speaking, however, the two systems are not directly comparable. The soil texture designation in the USDA system is based solely on the amount of sand-, silt-, and clay-sized particles, and USCS soil types are determined by both the amount of certain sized soil particles as well as on the soil's response to physical manipulation at varying water contents. Correlations between the USDA soil textures and USCS soil types are presented in Table B2-3. From these correlations, appropriate soil hydraulic parameter values can be assigned to the soil types that are classified in the USCS.

B2.5 SOLUTE TRANSPORT PARAMETERS

A solute transport model was used for particle tracking purposes only. All solute parameters were set the same as water (e.g., a retardation of 1.0). Solute transport during transient water flow in a variably saturated soil can be written as:

$$\frac{\partial \theta RC}{\partial t} = \frac{\partial}{\partial x_i}\left(\theta D_{ij}\frac{\partial C}{\partial x_j}\right) - \frac{\partial\left(\theta v_i C\right)}{\partial x_i} + W \qquad (2.17)$$

Where R is a retardation factor and D_{ij} is an effective dispersion tensor.

For return flows of irrigation water, the retardation factor is set to 1.0, indicating no reaction between percolation flow and soils.

Because typical soils are not homogeneous, all water does not travel at the same velocity and mixing occurs along the flow path. This mixing, or mechanical dispersion, results in a dilution of the solute at the advancing edge of flow. In addition, an advancing solute or flow will also tend to spread in directions normal to the direction of flow because the flow paths can diverge at the pore scale. The amount of mechanical dispersion is a function of the average linear velocity, and the coefficient of mechanical dispersion is defined as the product of dispersivity (α), which is a property of the medium, and the average linear velocity (v):

$$D = \alpha v + D^* \qquad (2.18)$$

Where D^* is molecular diffusion coefficient.

Due to solute mixing along the direction of the flow path and in directions normal to the flow path, there are two parameters—longitudinal and transverse dispersivity—to measure mixing.

For coarse sand in the dry Chino Basin climate, the longitudinal dispersivity values range from 0.01 meters (m) to 0.1 m (Wang, 2002). There is paucity of data in the literature on the relationship of longitudinal to transverse dispersivity. From the few field studies available, the ratio is in the range of 6 to 20 (i.e. Anderson, 1979; Klotz et al., 1980). Based on a less conservative consideration for contaminant transport, the longitudinal and transverse dispersivity in this study were set to 0.1 m. In general, a molecular diffusion coefficient could be regarded as a small constant value or can be set to zero because its influence is insignificant when compared to the other factors.

B2.6 COMPUTER CODE

The HYDRUS2D (Simunek et al., 1998) computer model was used to simulate unsaturated flow and solute transport in the Chino Basin. This program is a finite element model for simulating the movements of water, heat, and multiple solutes in variably saturated media. The program numerically solves the Richards' equation for saturated-unsaturated flow and the Fickian-based advection-dispersion equations for heat and solute transport. This program can be used to analyze water and solute movement in unsaturated, partially saturated, or fully saturated porous media.

B2.7 INITIAL CONDITIONS

The initial soil moisture condition in the unsaturated zone has a great impact on unsaturated flow. The vadose zone is partially saturated, and hydraulic conductivity values vary greatly if capillary pressure or water content changes, as shown in Figures B2-1 and B2-2. These figures illustrate that regardless of soil type, hydraulic conductivity increases with water content while tension decreases. The initial model conditions were obtained using two-step simulations:

- The first simulation conducted was a simulation wherein a 50-year steady-state water infiltration rate was applied to establish the first-step initial condition in the year 1900. The constant application rate is 1.0 feet/year from the ground surface; this value is an approximate estimate of the net infiltration rate under the root zone of irrigation land in the Chino Basin.

- The second simulation conducted was a 30-year (1900 to 1930) transient simulation. The historical recorded daily rainfall data from nearby measurement stations, computed rainfall abstraction and evapotranspiration data, and irrigation water data were applied at the ground surface. The results of this simulation are then used as the soil moisture distribution from the ground surface to groundwater table is the initial condition at the simulation points in the year 1930.

B2.8 BOUNDARY CONDITIONS

The ground surface was set as an atmospheric boundary. The inputs for this atmospheric boundary include: the daily rainfall abstraction data, calculated from Equation 2-6; the daily evaporation data, which is the product of the reference evaporation and crop coefficient, and the required irrigation water, calculated from Equation 2-8. In addition, the lowest soil capillary pressure was set slightly higher than the wilt point, and the highest soil pressure was set to zero, which indicates that there was no ponding during the irrigation period.

B2.9 MODEL DOMAIN AND GRID

The unsaturated flow model is two dimensional; therefore, six locations were selected within the Chino Basin based on known geology, spatial location within the basin, and depth to water. A coupled unsaturated flow/transport model was run for each of these locations. The modeling domain of each is from the ground surface to a depth below the groundwater table. Each location is shown in Figure B2-3 and briefly discussed below.

- Well AP-PC/2 is located in the City of Chino in the southwestern portion of the Chino Basin. Depth to water is approximately 80 feet.

- Well CB-30 is located in the northern portion of the Chino Basin. The vadose zone mainly consists of sand and gravel. Depth to water is approximately 420 feet.
- Well CB-36 is located in the center of the Chino Basin. The vadose zone mainly consists of sands and clays. Depth to water is approximately 260 feet.
- Well F-18A is located to the northeast of the Chino Basin. The vadose zone mainly consists of gravelly sand with several layers of sandy clay. Depth to water is approximately 590 feet.
- Well HCMP-8/1 is located in the southern portion of the Chino Basin near the Santa Ana River. The thickness of the vadose zone in this location is small, and the vadose zone mainly consists of sandy silt with several layers of clay. Depth to water is approximately 80 feet.
- The Mira Loma Space Center site is located in the eastern portion of the Chino Basin. The vadose zone features gravel and sand deposits with several layers of soft clay. Depth to water is approximately 200 feet.
- Well MVWD-30 is located in the western portion of the Chino Basin. The vadose zone consists of sand with gravel and silt. As a result, soil saturation is quite low in the vadose zone. Depth to water is approximately 440 feet.

Vadose zone thickness varies greatly in the Chino Basin, ranging from more than 500 feet in the north to less than 100 feet in the south near Prado reservoir. Correspondingly, the model domain varies based on the thickness of the vadose zone.

The grid increment is uniform, and the triangle grid cell is fine with a length of 3 feet horizontally and vertically. One of the model grids is illustrated in Figure B2-4.

Table B2-1
Classification of Antecedent Moisture Classes (AMC)
for the SCS Method of Rainfall Abstractions*

AMC Group	Total 5-Day Antecedent Rainfall (Inches)	
	Dormant Season	Growing Season
I	<0.5	<1.4
II	0.5-1.1	1.4-2.1
III	>1.1	>2.1

*Adapted from Jury et al., 1991

Table B2-2
Hydraulic Parameter Estimates for USDA Soil Types[1, 2]

USDA Soil Type	θ_r (cm³ /cm³)	θ_s (cm³ /cm³)	α (1/cm)	n (--)	K_s (cm/hr)
Sand	0.045 (0.010)	0.43 (0.06)	0.145 (0.029)	2.68 (0.29)	29.70 (15.60)
Loamy sand	0.057 (0.010)	0.41 (0.09)	0.124 (0.043)	2.28 (0.27)	14.59 (11.36)
Sandy loam	0.065 (0.017)	0.41 (0.09)	0.075 (0.037)	1.89 (0.17)	4.42 (5.63)
Loam	0.078 (0.013)	0.43 (0.10)	0.036 (0.021)	1.56 (0.11)	1.04 (1.82)
Silt	0.034 (0.010)	0.46 (0.11)	0.016 (0.007)	1.37 (0.05)	0.25 (0.33)
Silt loam	0.067 (0.015)	0.45 (0.08)	0.020 (0.012)	1.41 (0.12)	0.45 (1.23)
Sandy clay loam	0.100 (0.006)	0.39 (0.07)	0.059 (0.038)	1.48 (0.13)	1.31 (2.74)
Clay loam	0.095 (0.010)	0.41 (0.09)	0.019 (0.015)	1.31 (0.09)	0.26 (0.70)
Silty clay loam	0.089 (0.009)	0.43 (0.07)	0.010 (0.006)	1.23 (0.06)	0.07 (0.19)
Sandy clay	0.100 (0.013)	0.38 (0.05)	0.027 (0.017)	1.23 (0.10)	0.12 (0.28)
Silty clay	0.070 (0.023)	0.36 (0.07)	0.005 (0.005)	1.09 (0.06)	0.02 (0.11)
Clay	0.068 (0.034)	0.38 (0.09)	0.008 (0.012)	1.09 (0.09)	0.20 (0.42)

1. Wang, 2002
2. Standard Deviations Are Provided in Parentheses

Table B2-3
Corresponding USDA and USCS Soil Classifications*

Soil Texture	Soil Type
Gravel, very gravelly loamy sand	GP, GW, GM
Sand, coarse sand, fine sand	SP, SW
Loamy gravel, very gravelly sand loam, very gravelly loam	GM
Loamy sand, gravelly loamy sand, very fine sand	SM
Gravelly loam, gravelly sandy clay loam	GM, SC
Sandy loam, fine sandy loam, loamy very fine sand, gravelly sandy loam	SM
Silt loam, very fine sandy clay loam	ML
Loam, sandy clay loam	ML, SC
Silty clay loam, clay loam	CL
Sandy clay, gravelly clay loam, gravelly clay	SC, GC
Very gravelly clay loam, very gravelly sandy clay loam, very gravelly silty clay loam, very gravelly silt clay and clay	GC
Silty clay, clay	CH
Muck and peat	PT

*Fuller, 1978

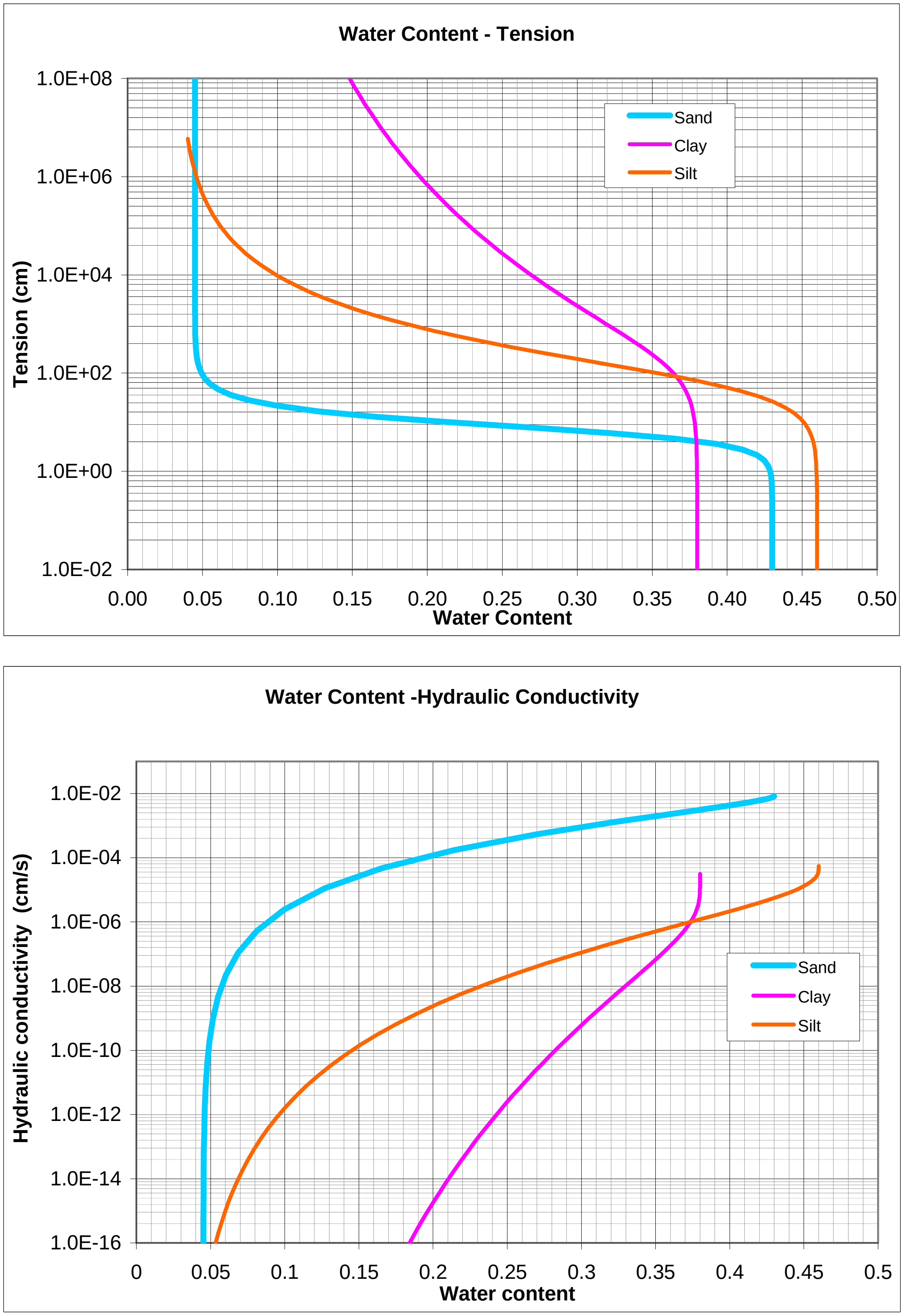

Figure B2-1
Typical soil water retention curves for sand, clay, and silt;
hydraulic conductivity varies greatly with changes of water content (Brooks and Corey, 1964)

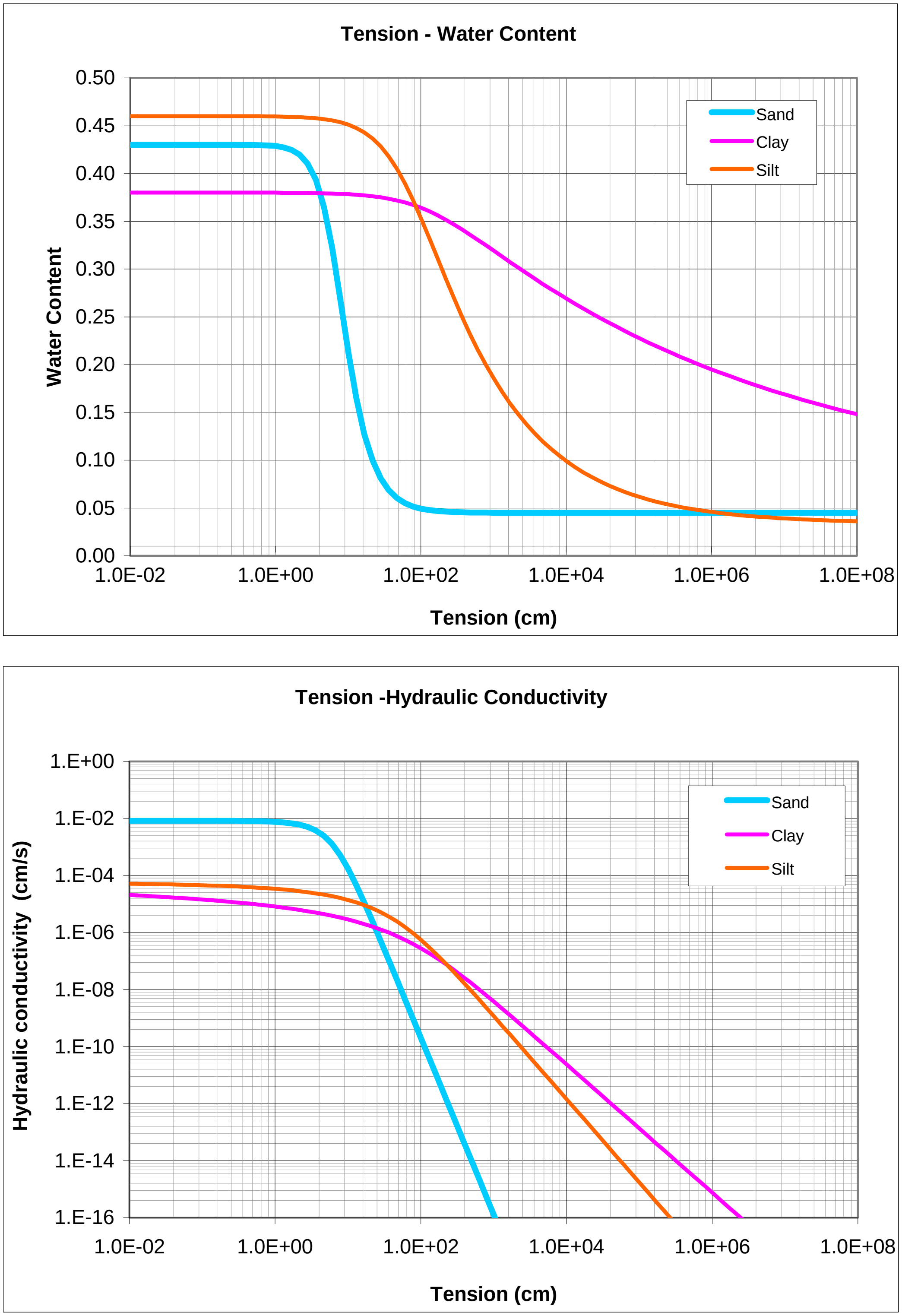

Figure B2-2

Typical soil water retention curves for sand, clay, and silt; hydraulic conductivity varies with changes of tension (capillary suction) (Brooks and Corey, 1964)

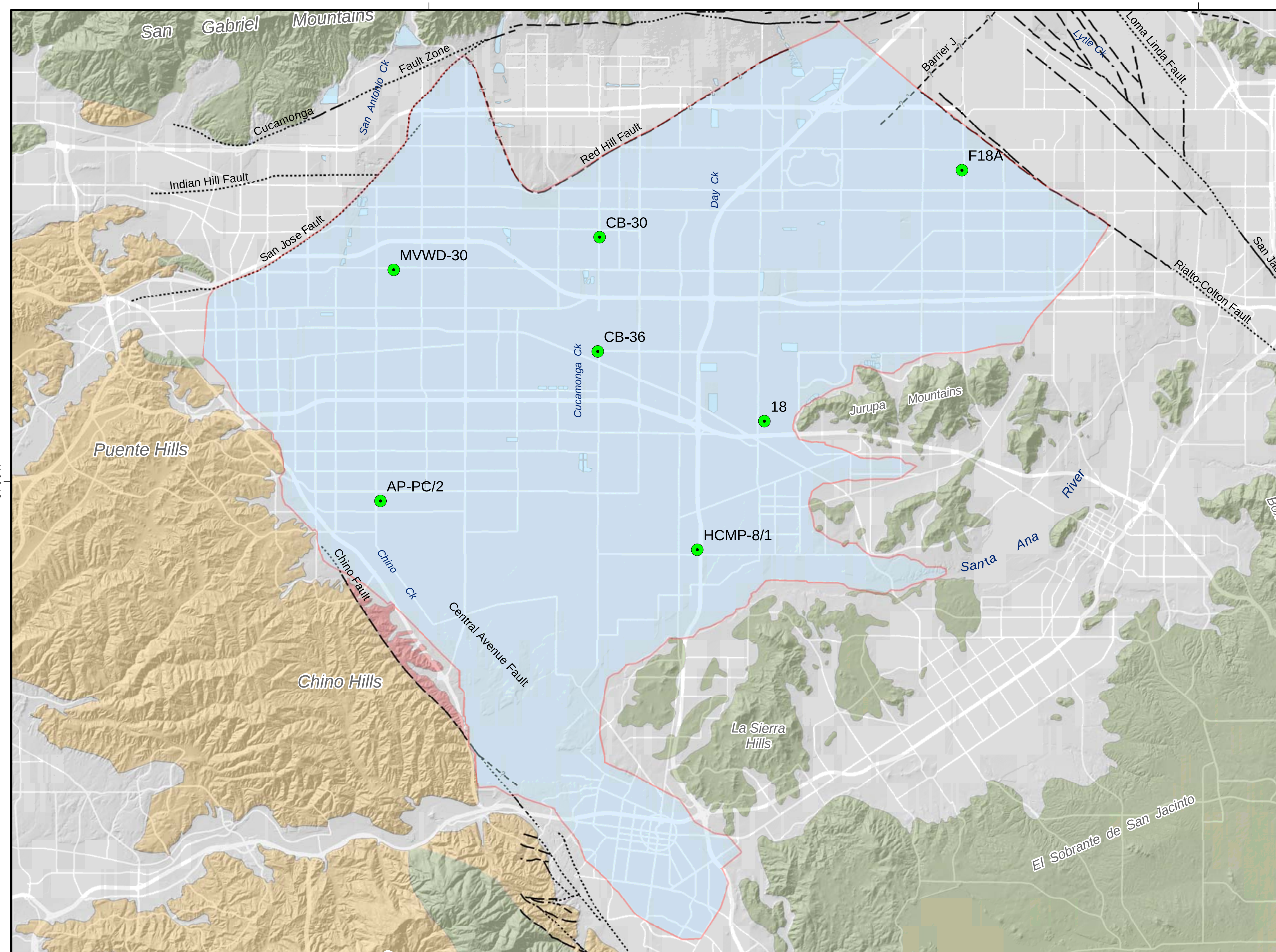

Main Features

- Active Groundwater Model Domain
- Unsaturated Flow Model Locations

Geology

Water-Bearing Sediments

- Quaternary Alluvium

Consolidated Bedrock

- Plio-Pleistocene Sedimentary Rocks
- Cretaceous to Miocene Sedimentary Rocks
- Pre-Tertiary Igneous and Metamorphic Rocks

Faults

- Location Certain
- Location Approximate
- Location Concealed
- Location Uncertain

0 1 2 3 4 Miles

0 2 4 6 KM

Produced by:
WILDERMUTH ENVIRONMENTAL INC
23692 Birtcher Drive
Lake Forest, CA 92630
949.420.3030
www.wildermuthenvironmental.com

Author: FIB
Date: 20070816
File: UFMpoints_FigB2-3.mxd

Appendix B
Chino Basin Unsaturated FLow Model Documentation

Unsaturated Flow Modeling Points

Figure B2-3

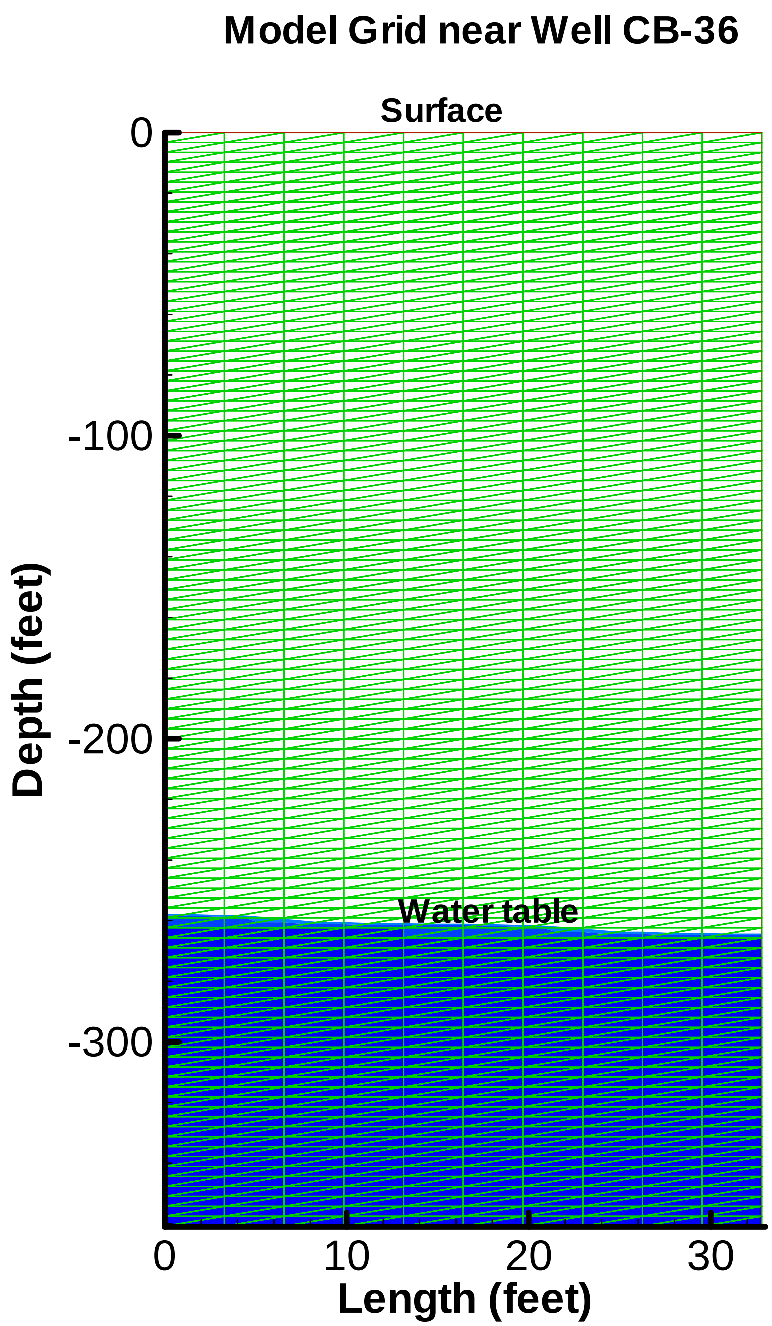

Figure B2-4
Model grid in the location nearby well CB-36 (not to scale)

SIMULATION RESULTS

B3.1 SIMULATIONS AT AP-PC/2

To track solute transport with the source (i.e. irrigation return flow) from the ground surface to the water table, a coupled unsaturated flow and solute transport simulation was conducted. Well AP-PC/2 is located in the City of Chino in the southwestern portion of Chino Basin. The vadose zone consists of interbedded sand and clay layers. The left side of Figure B3-1 shows the initial soil moisture distribution in 1930, and the right side of the figure shows the initial solute concentration, which was set to zero along the soil profile. Due to the interbedded distribution of coarse- and fine-grained soils in the vadose zone, soil-water saturation was not linearly distributed with depth and varied greatly in the different soil layers. In general, the saturation is low in coarse-grained soils (i.e. sand) and high in fine-grained soils (i.e. clay and silt). Figure B3-1 also shows the location of the groundwater table at depths of 85-88 feet below the ground surface. Below the groundwater table, the soil is fully saturated, and the saturation value is 1.0.

Figures B3-2 through B3-5 show water flow and solute transport in the vadose zone. One year after the modeling started, the front of the solute reached 15 feet in depth. In another words, the breakthrough time was about one year at 15 feet of depth. The front of the solute reached 30-40 feet of depth in five years and 60-75 feet of depth in ten years. Fourteen years after the simulation started, the solute reached the groundwater table. In contrast to solute concentration, the change of soil saturation along the soil profile was relatively small. The reasons for this are:

- The initial soil moisture was not completely dry. The soil water saturation and its distribution along the soil profile, in any given year, were the result of a long-term soil water balance; the soil moisture in vadose zone cannot be completely dry.
- The factors that influenced unsaturated flow did not change significantly after 1930; although, the effects of historical heavy rainfall events can be observed from these plots.

The simulation indicated that it would take about 14 years (breakthrough time) for the solute to reach the groundwater table. However, this does not mean that the infiltration water caused by rainfall and irrigation return flows needs 14 years to impact the saturated zone. As discussed above, the initial soil moisture along the soil profile was not completely dry. Thus, the incoming infiltration water replaced the water initially present in the soil and pushed it ahead of the front like a piston. The calculated breakthrough time indicates approximately how long it would take to replace the water between the ground surface and the groundwater table (the entire vadose zone). Nevertheless, when the incoming infiltration water replaced half of the pore volume, an equivalent amount of the water volume was pushed to the deeper unsaturated zone and began to recharge the saturated zone. Therefore, the impact time of incoming infiltration water is about half of the breakthrough time. The lag time is about 7 years at this location.

B3.2 SIMULATIONS AT CB-30

Well CB-30 is located in the northern portion of the Chino Basin. The vadose zone mainly consists of sand and gravel. Figure B3-6 shows the initial soil moisture distribution and the solute concentration in the year 1930. The saturation distribution reflects the layering of different soil classes. Saturation is low in coarse-grained soils and high in fine-grained soils. This plot also shows the location of the groundwater table at depths of 431-434 feet below the ground surface. Below the groundwater table, the soil is fully saturated with a saturation value of 1.0.

Figures B3-7 through B3-12 show water flow and solute transport in the vadose zone beginning in 1930. The simulation indicated that it would take about 42 years (breakthrough time) for the solute to reach the groundwater table from the ground surface. As discussed in the previous section, the impact of incoming infiltration water on the saturated zone lags, or is delayed, by about half of the breakthrough time. The lag time is thus about 21 years in this location.

B3.3 SIMULATIONS AT CB-36

Well CB-36 is located in the middle of the Chino Basin. The vadose zone mainly consists of sand, clay, and mixed sand and clay. Figure B3-13 shows the initial soil moisture distribution and the solute concentration in the year 1930. The saturation distribution is a reflection of the layered soil classes. Saturation is low in coarse-grained soils and high in fine-grained soils. This plot also shows the location of the groundwater table at depths of 260-263 feet below the ground surface. Below the groundwater table, the soil is fully saturated with a saturation value of 1.0.

Figures B3-14 through B3-17 show water flow and solute transport in the vadose zone beginning in 1930. The simulation indicated that it would take about 25 years (breakthrough time) for the solute to reach the groundwater table from the ground surface. Consequently, the impact of incoming infiltration water on the saturated zone lags about half of the breakthrough time. The lag time is thus about 12 years in this location.

B3.4 SIMULATIONS AT F-18A

Well F-18A is located to the northeast of Chino Basin. The vadose zone mainly consists of gravelly sand with several layers of sandy clay. Figure B3-18 shows the initial soil moisture distribution and solute concentration in the year 1930. The initial saturation shows a layering of distributed soil classes. This plot also shows the location of the groundwater table at a depth of 580 feet below the ground surface. Below the groundwater table, soil is fully saturated with a saturation value of 1.0.

Figures B3-19 through B3-23 show water flow and the solute transport in the vadose zone beginning in 1930. The simulation indicated that it would take about 62 years (breakthrough time) for the solute to reach the groundwater table. Consequently, the lag time of the infiltration flow is about 31 years in this location.

B3.5 SIMULATIONS AT HCMP-8/1

Well HCMP-8/1 is located in the south side of Chino Basin near the Santa Ana River. The thickness of the vadose zone at this location is quite small, mainly consisting of sandy silt with several layers of clay. Figure B3-24 shows the initial soil moisture distribution and the solute concentration in the year 1930. The initial saturation plot shows several clay layers in the vadose zone. This plot also shows the location of the groundwater table at a depth of 85 feet below the ground surface. Below the groundwater table, soil is fully saturated with a saturation value of 1.0.

Figures B3-25 through B3-27 show water flow and the solute transport in the vadose zone beginning in 1930. The simulation indicated that it would take about 14 years (breakthrough time) for the solute to reach the groundwater table from the ground surface. Consequently, the lag time of the infiltration flow is about 7 years.

B3.6 SIMULATIONS AT MIRA LOMA

This unsaturated flow simulation point is located at the Mira Loma Space Center in the eastern portion of the Chino Basin. The vadose zone features gravel and sand deposits with several layers of soft clay. Figure B3-28 shows the initial soil moisture distribution and the solute concentration in the year 1930. The layer-distributed saturation shows these soft clay layers in the vadose zone. This plot also shows the location of the groundwater table at 211 feet below the ground surface. The soil underneath the groundwater table is fully saturated with a saturation value of 1.0.

Figures B3-29 through B3-31 show water flow and the solute transport in the vadose zone beginning in 1930. The simulation indicated that it would take about 19 years (breakthrough time) for the solute to reach the groundwater table from the ground surface. Consequently, the lag time of the infiltration flow is about 9-10 years.

B3.7 SIMULATIONS AT MVWD-30

Well MVWD-30 is located in the Monte Vista Water District in the he western portion of the Chino Basin.. The vadose zone is consists of sand with gravel and silt. As a result, soil saturation is quite low in the vadose zone, as shown in Figure B3-32. As was done at the other locations, the initial solute concentration was set to zero in the year 1930. This plot also shows the location of the groundwater table at a depth of 434 feet below the ground surface. The soil underneath the groundwater table is fully saturated with a saturation value of 1.0.

Figures B3-33 through B3-35 show water flow and the solute transport in the vadose zone beginning in 1930. The simulation indicated that it would take about 34 years (breakthrough time) for the solute to reach the groundwater table from the ground surface. Consequently, the lag time of infiltration flow is about 17 years.

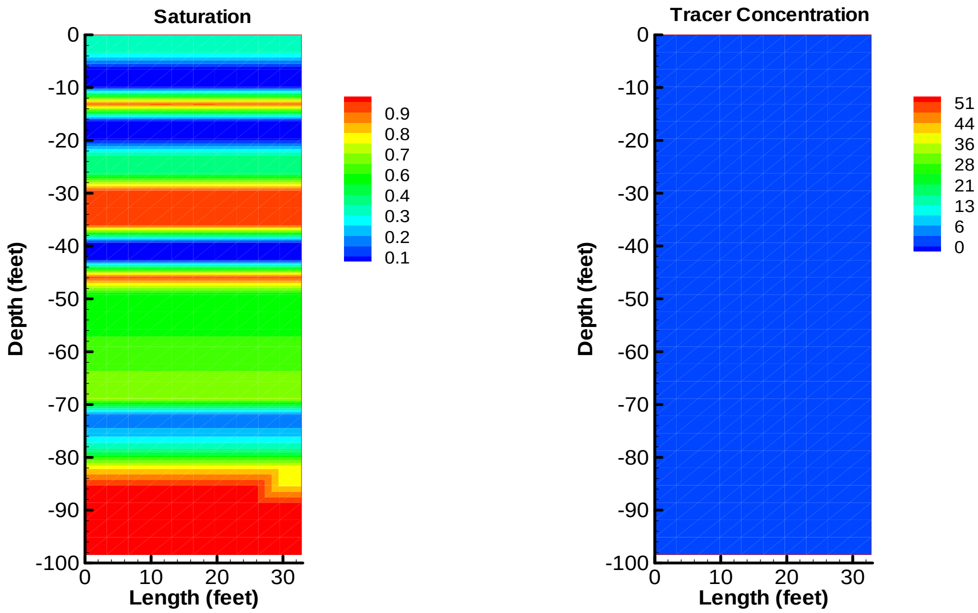

Figure B3-1
The initial saturation and solute concentration at the location AP-PC/2 (Saturation = fraction saturated, Concentration = mg/L)

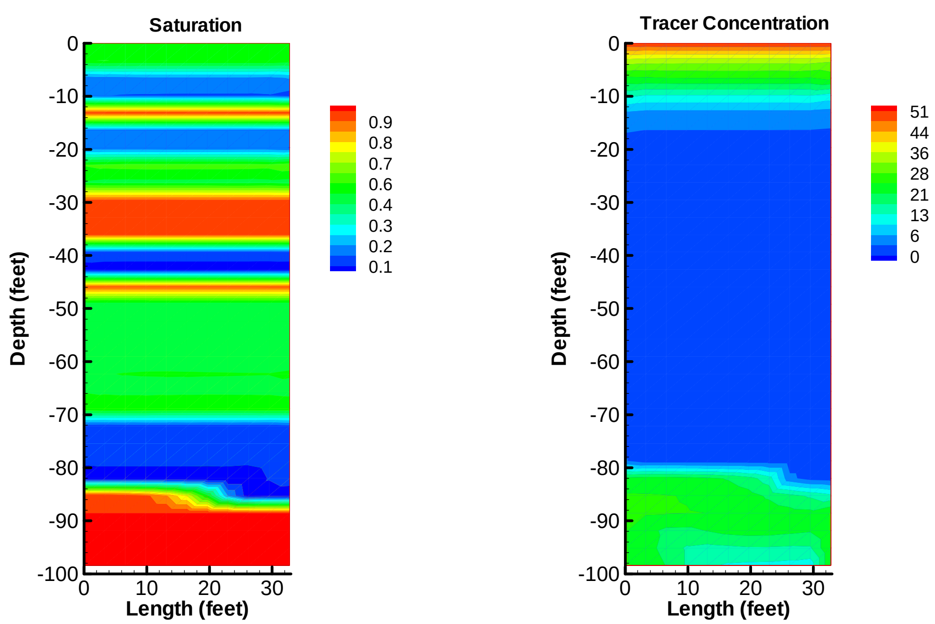

Figure B3-2
The saturation and solute concentration one year after the modeling started at the location AP-PC/2 (Saturation = fraction saturated, Concentration = mg/L)

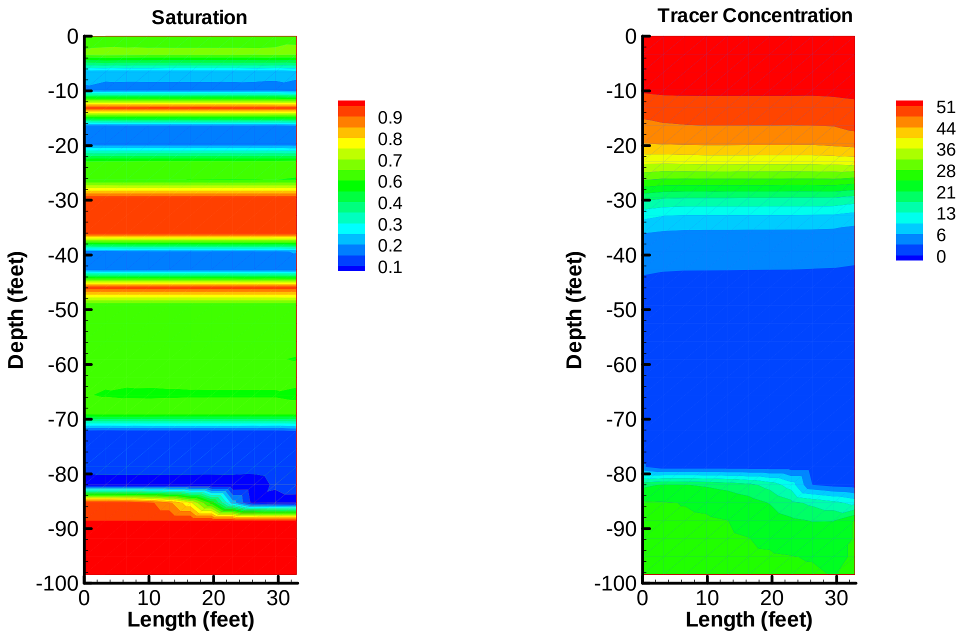

Figure B3-3
The saturation and solute concentration five years after the modeling started at the location AP-PC/2 (Saturation = fraction saturated, Concentration = mg/L)

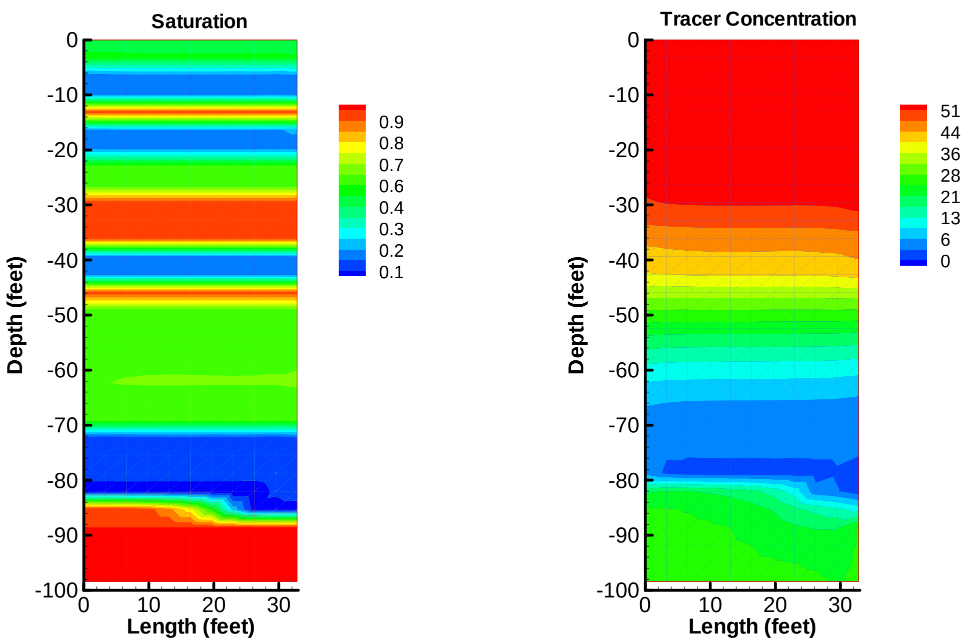

Figure B3-4
The saturation and solute concentration 10 years after the modeling started at the location AP-PC/2 (Saturation = fraction saturated, Concentration = mg/L)

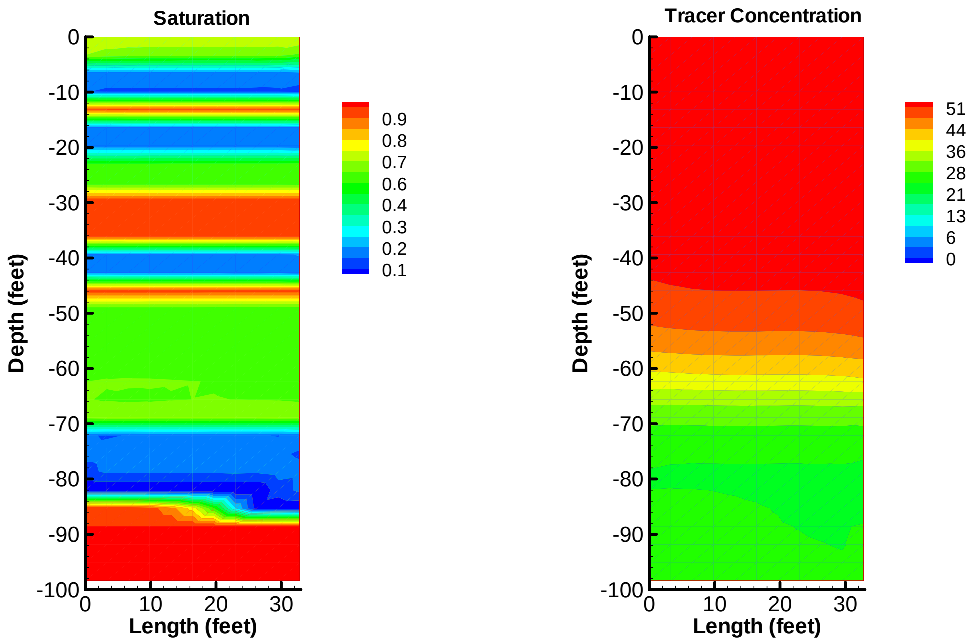

Figure B3-5
The saturation and solute concentration 14 years after the modeling started at the location AP-PC/2 (Saturation = fraction saturated, Concentration = mg/L)

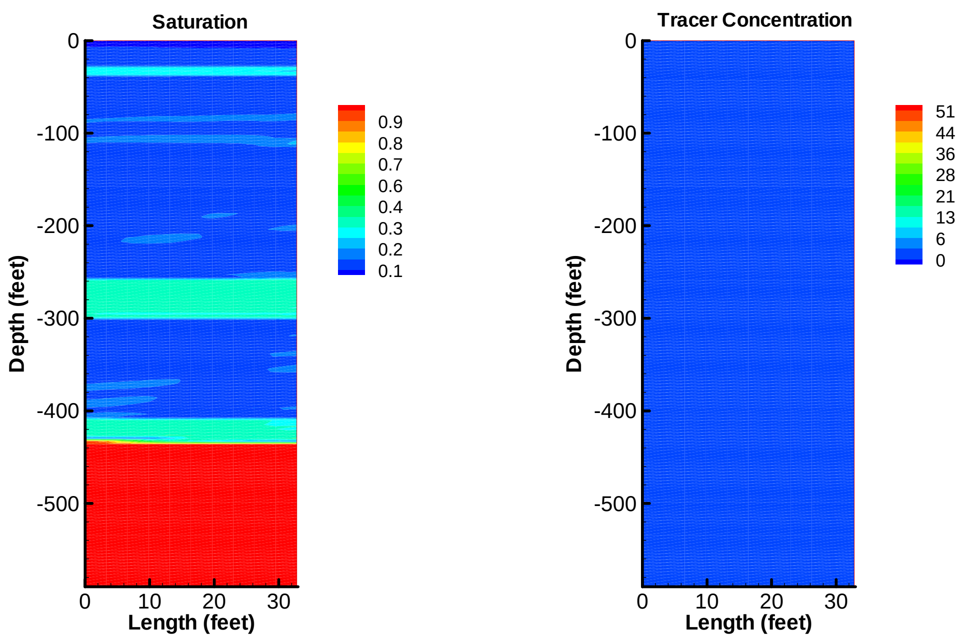

Figure B3-6
The initial saturation and solute concentration at the location CB-30 (Saturation = fraction saturated, Concentration = mg/L)

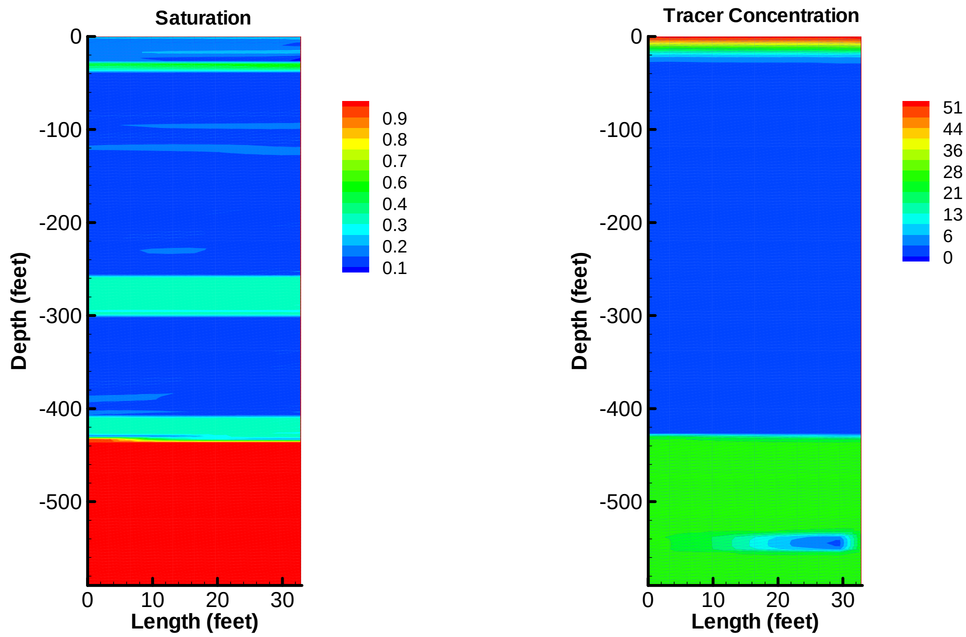

Figure B3-7
The saturation and solute concentration one year after the modeling started at the location CB-30
(Saturation = fraction saturated, Concentration = mg/L)

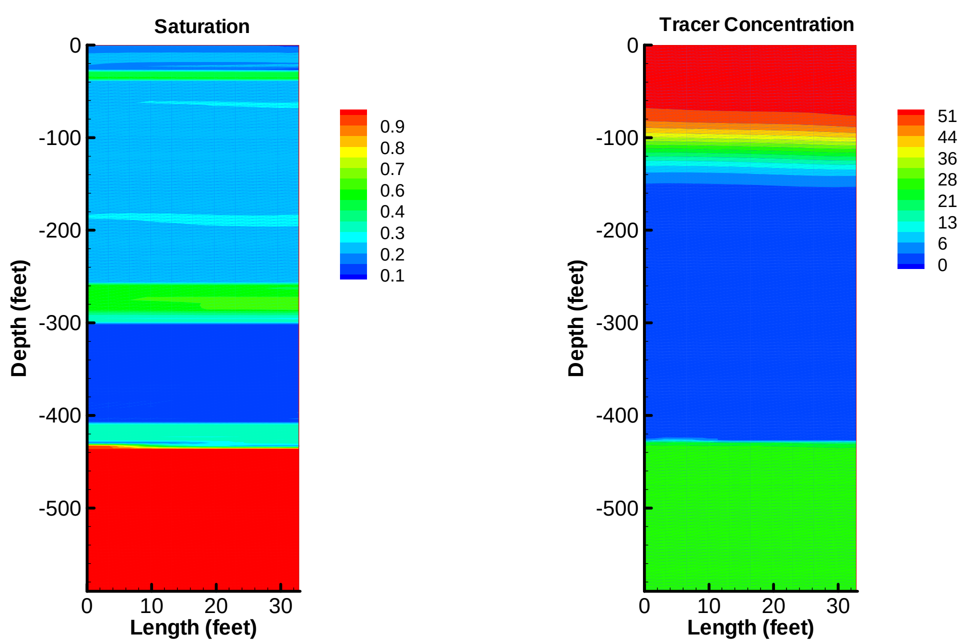

Figure B3-8
The saturation and solute concentration 10 years after the modeling started at the location CB-30
(Saturation = fraction saturated, Concentration = mg/L)

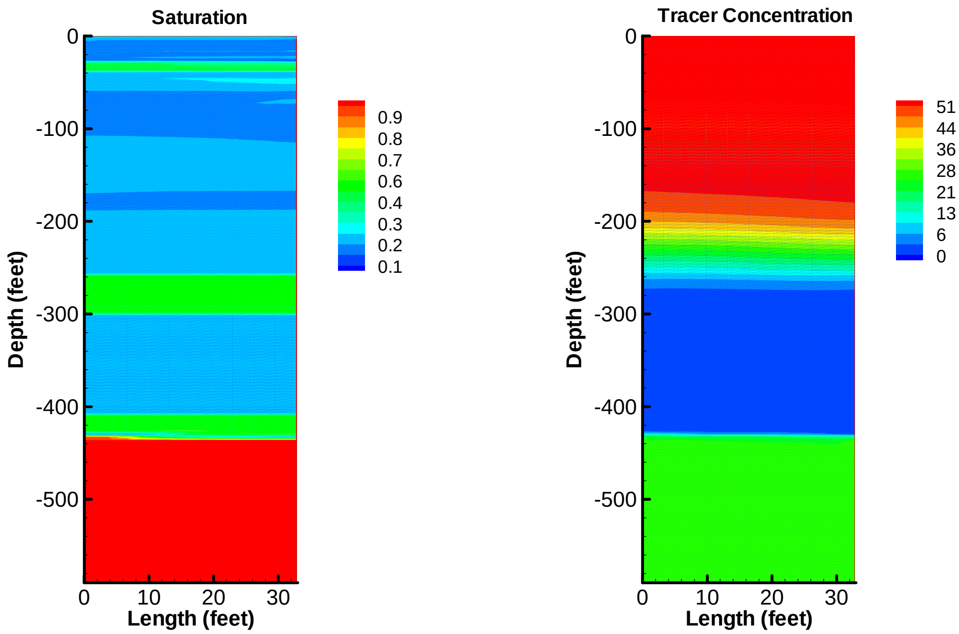

Figure B3-9
The saturation and solute concentration 20 years after the modeling started at the location CB-30 (Saturation = fraction saturated, Concentration = mg/L)

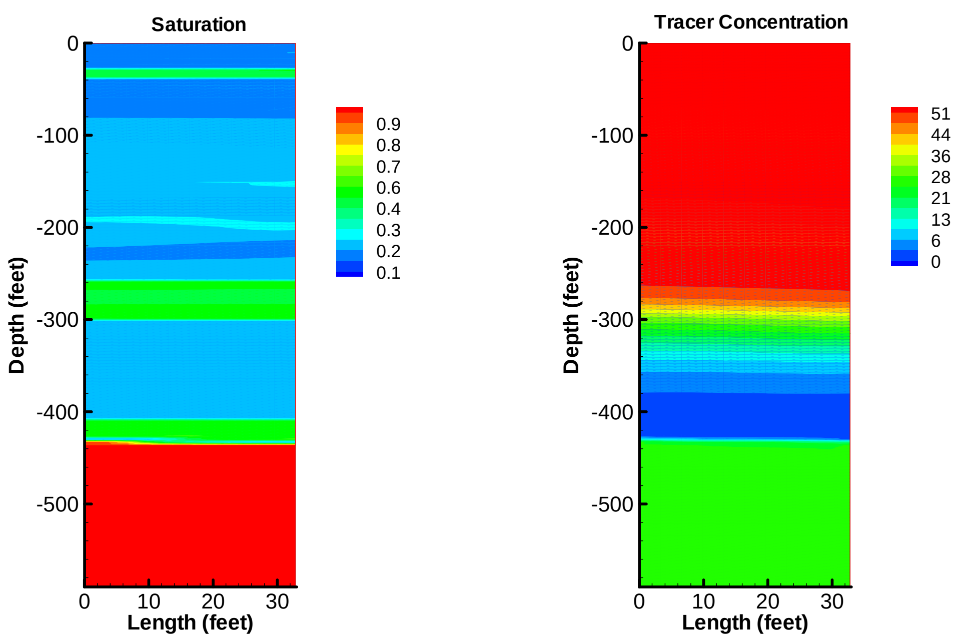

Figure B3-10
The saturation and solute concentration 30 years after the modeling started at the location CB-30 (Saturation = fraction saturated, Concentration = mg/L)

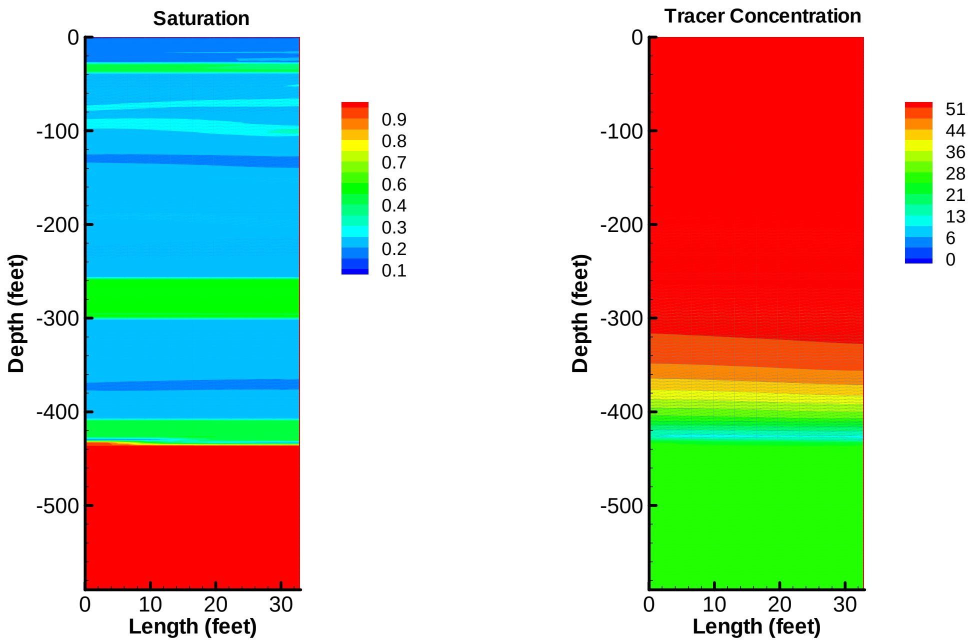

Figure B3-11
The saturation and solute concentration 40 years after the modeling started at the location CB-30
(Saturation = fraction saturated, Concentration = mg/L)

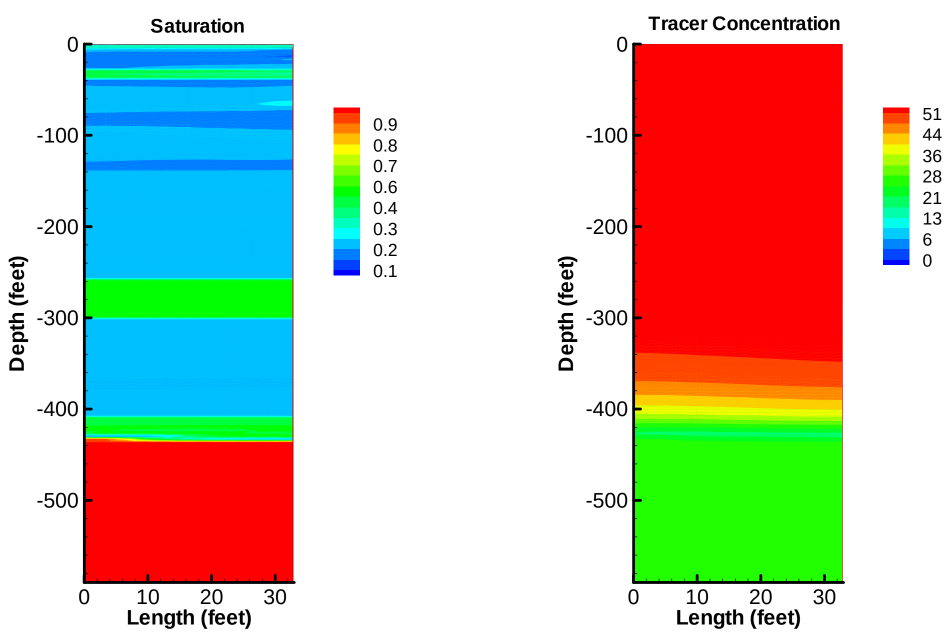

Figure B3-12
The saturation and solute concentration 42 years after the modeling started at the location CB-30
(Saturation = fraction saturated, Concentration = mg/L)

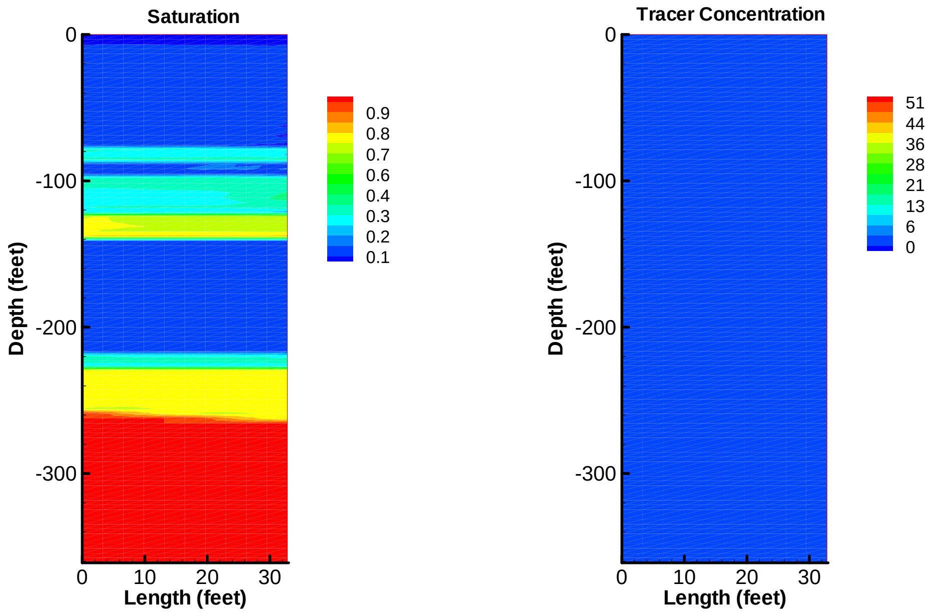

Figure B3-13
The initial saturation and solute concentration at the location CB-36 (Saturation = fraction saturated, Concentration = mg/L)

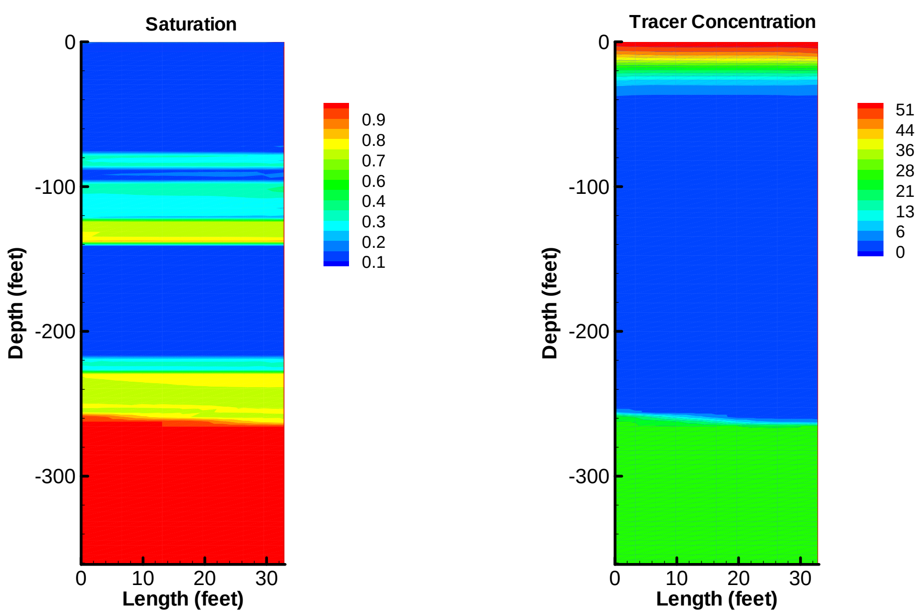

Figure B3-14
The saturation and solute concentration one year after the modeling started at the location CB-36 (Saturation = fraction saturated, Concentration = mg/L)

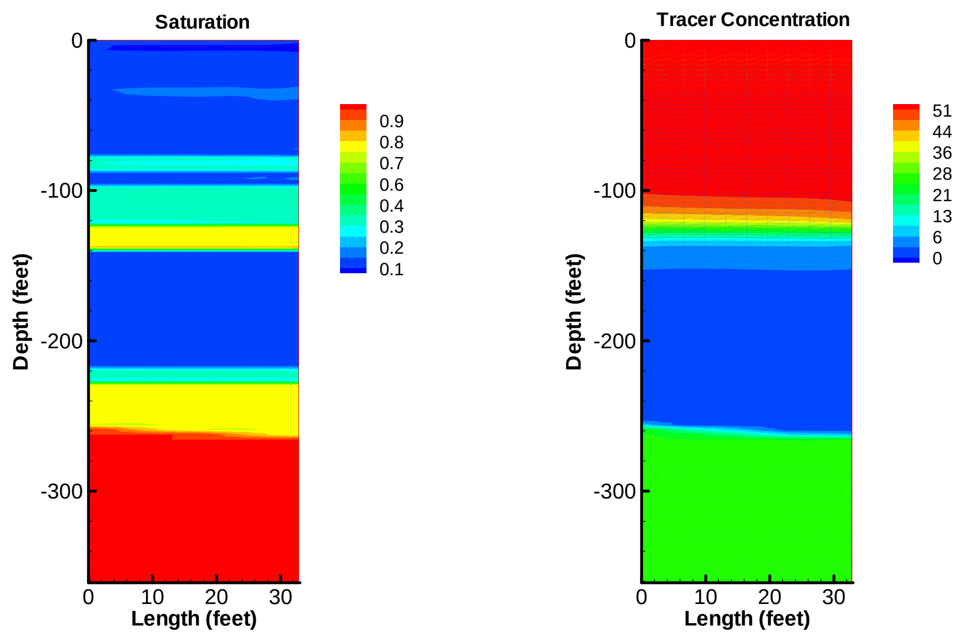

Figure B3-15

The saturation and solute concentration 10 years after the modeling started at the location CB-36 (Saturation = fraction saturated, Concentration = mg/L)

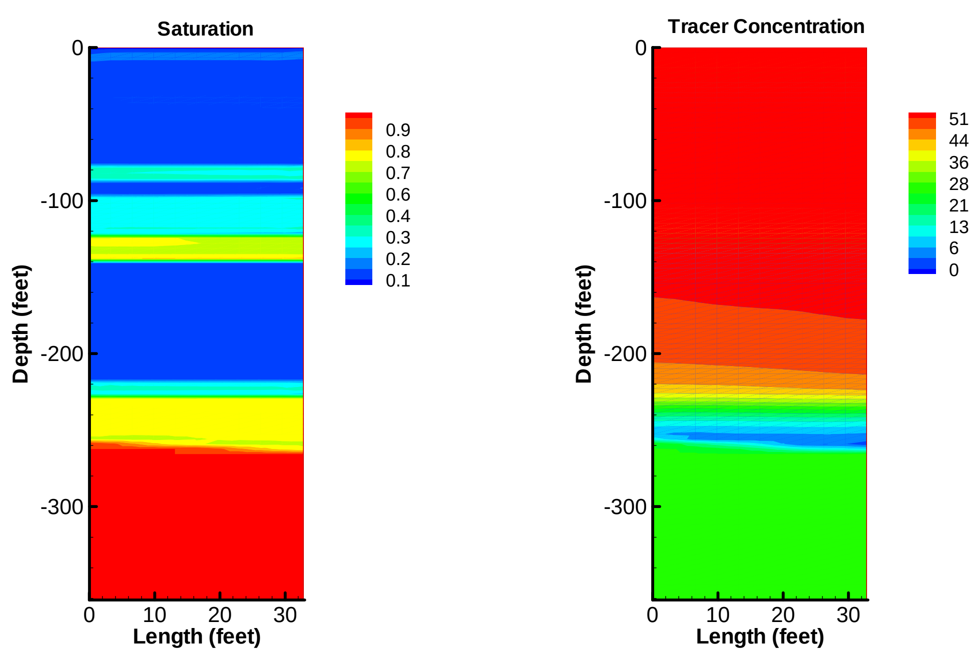

Figure B3-16

The saturation and solute concentration 20 years after the modeling started at the location CB-36 (Saturation = fraction saturated, Concentration = mg/L)

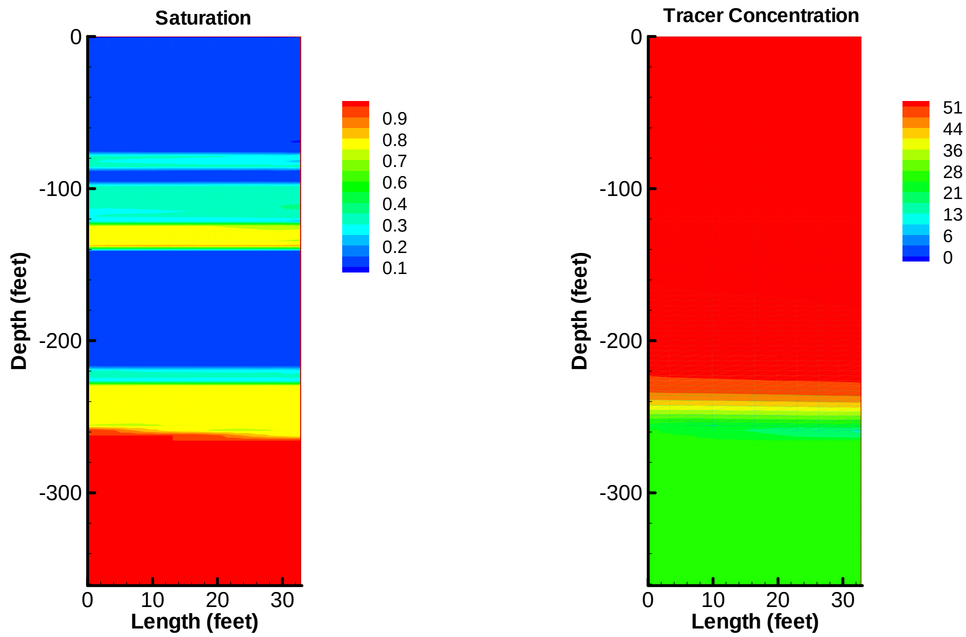

Figure B3-17
The saturation and solute concentration 25 years after the modeling started at the location CB-36
(Saturation = fraction saturated, Concentration = mg/L)

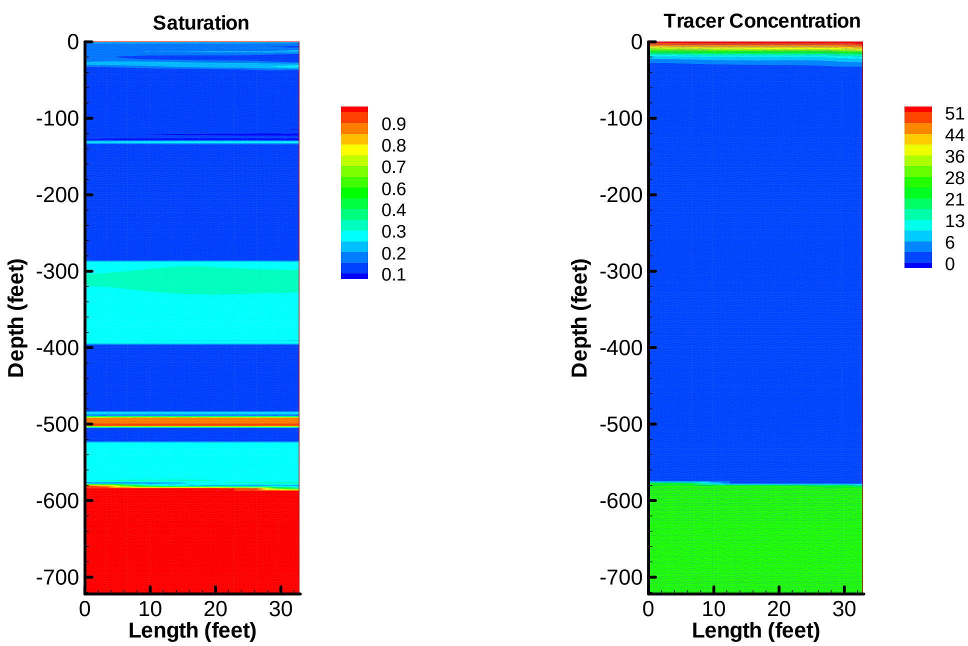

Figure B3-17
The saturation and solute concentration 25 years after the modeling started at the location CB-36
(Saturation = fraction saturated, Concentration = mg/L)

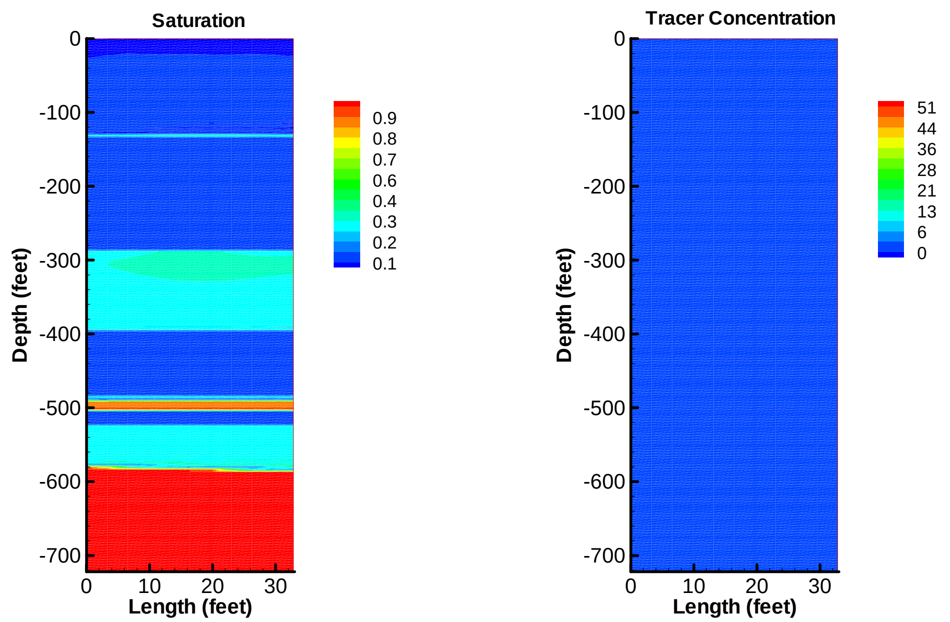

Figure B3-18
The initial saturation and solute concentration at the location F-18A (Saturation = fraction saturated, Concentration = mg/L)

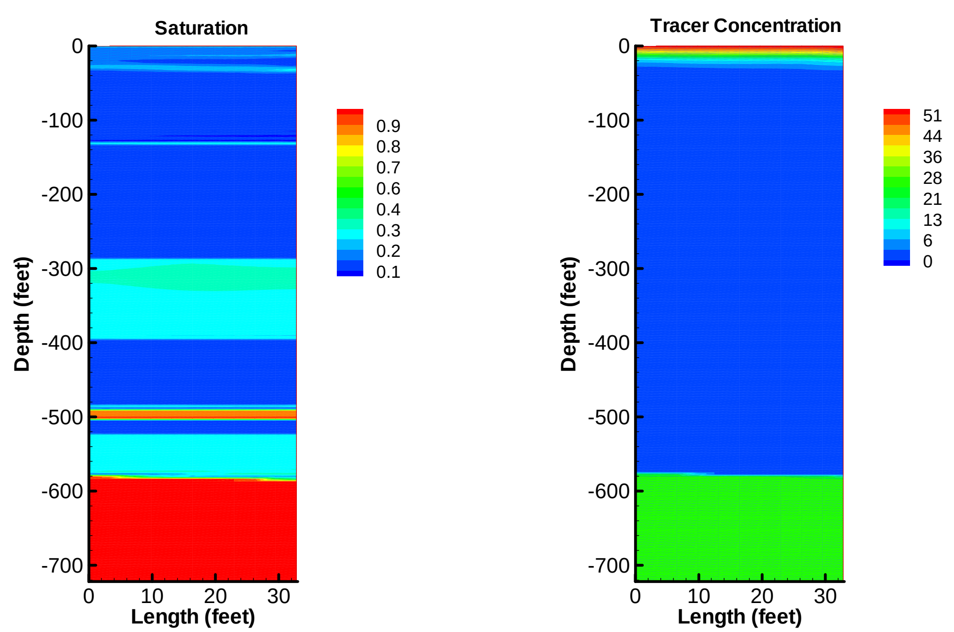

Figure B3-19
The saturation and solute concentration one year after the modeling started at the location F-18A (Saturation = fraction saturated, Concentration = mg/L)

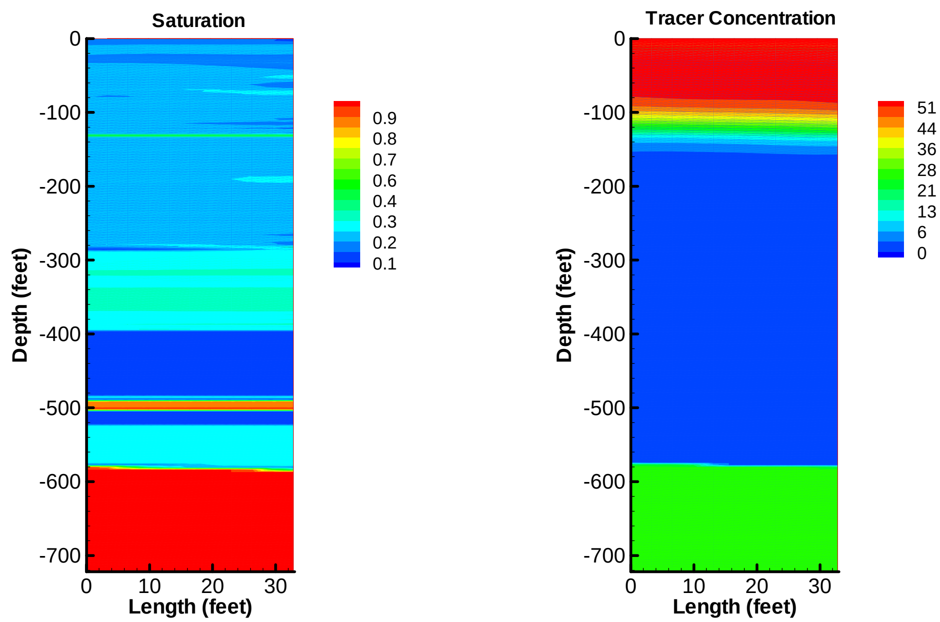

Figure B3-20
The saturation and solute concentration 10 years after the modeling started at the location F-18A
(Saturation = fraction saturated, Concentration = mg/L)

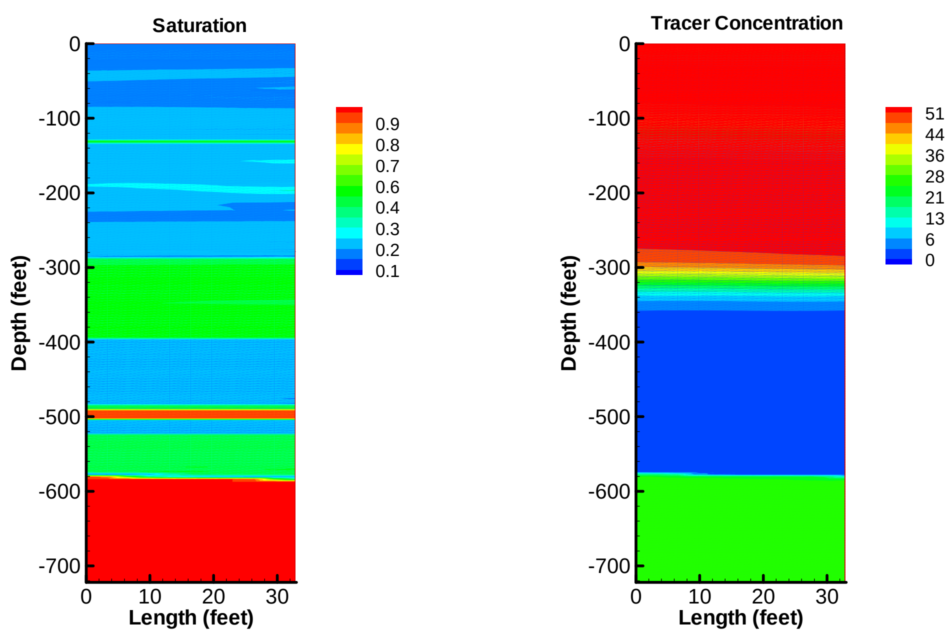

Figure B3-21
The saturation and solute concentration 30 years after the modeling started at the location F-18A
(Saturation = fraction saturated, Concentration = mg/L)

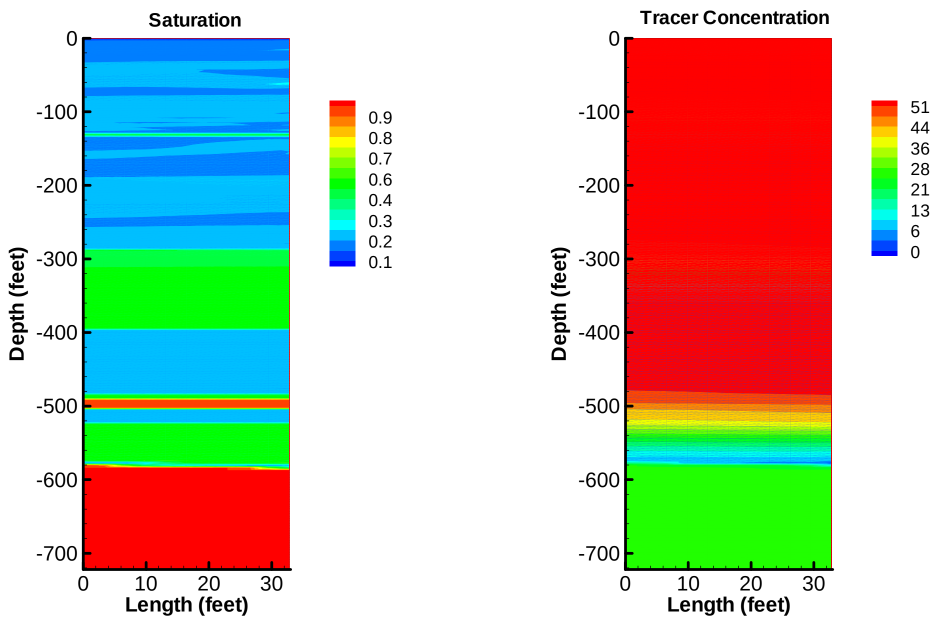

Figure B3-22
The saturation and solute concentration 60 years after the modeling started at the location F-18A (Saturation = fraction saturated, Concentration = mg/L)

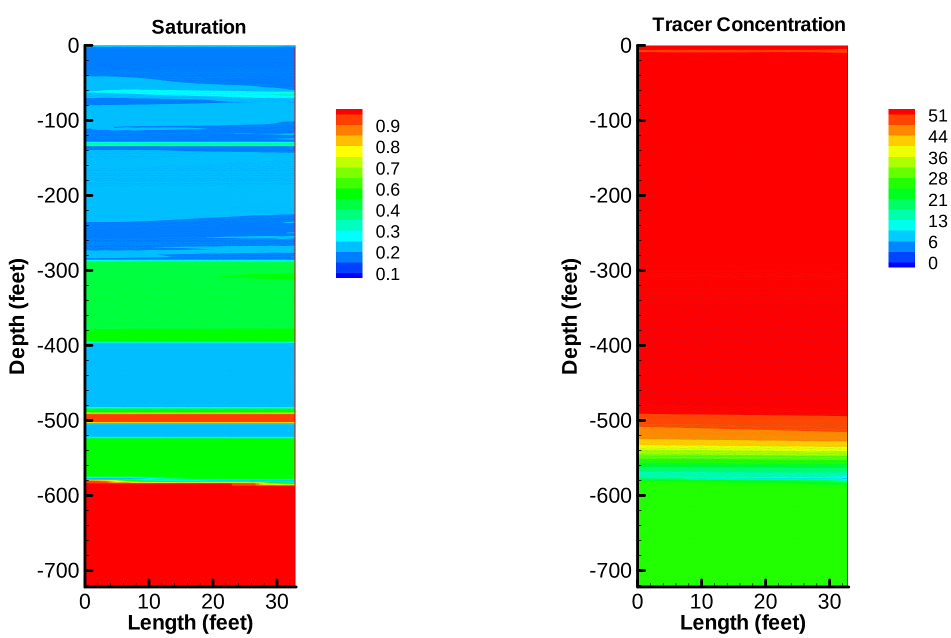

Figure B3-23
The saturation and solute concentration 62 years after the modeling started at the location F-18A(Saturation = fraction saturated, Concentration = mg/L)

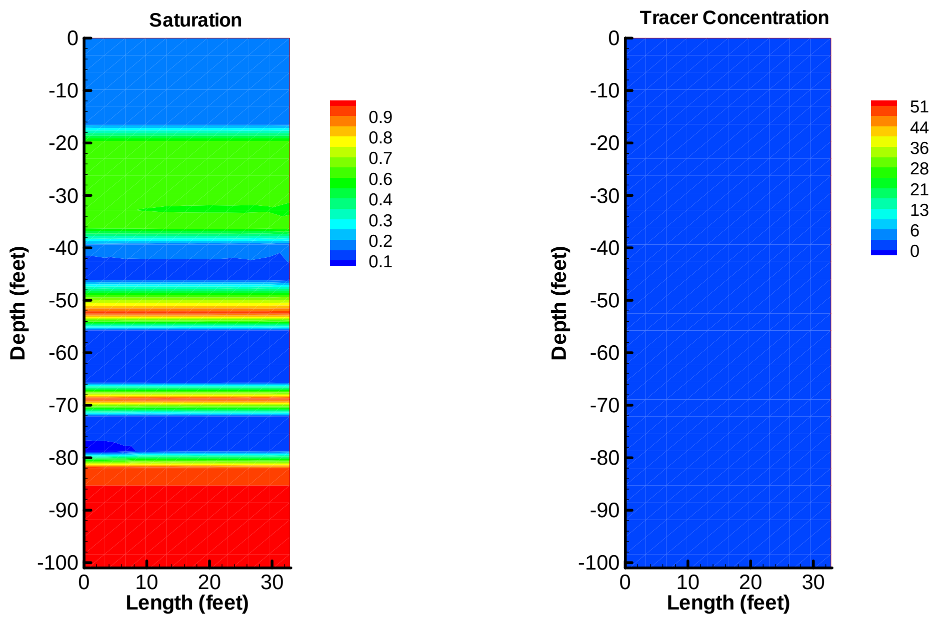

Figure B3-24
The initial saturation and solute concentration at the location HCMP-8/1 (Saturation = fraction saturated, Concentration = mg/L)

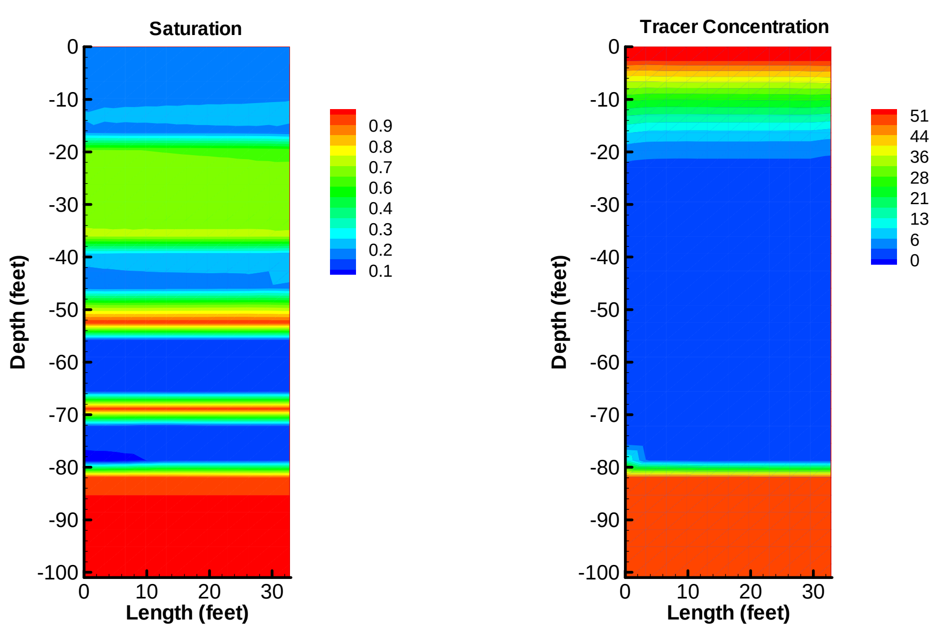

Figure B3-25
The saturation and solute concentration one year after the modeling started at the location HCMP-8/1 (Saturation = fraction saturated, Concentration = mg/L)

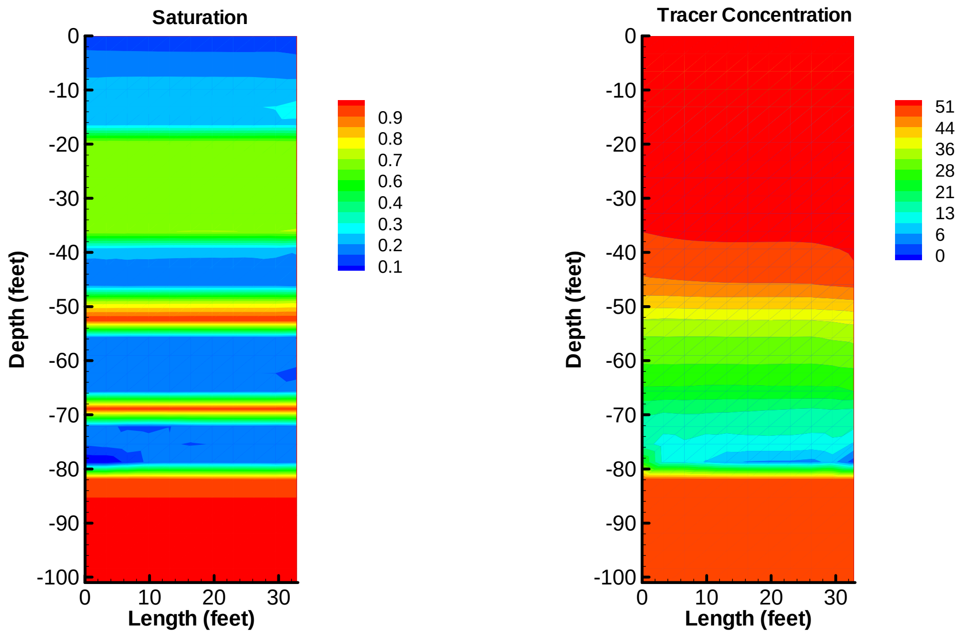

Figure B3-26
The saturation and solute concentration 10 years after the modeling started at the location HCMP-8/1 (Saturation = fraction saturated, Concentration = mg/L)

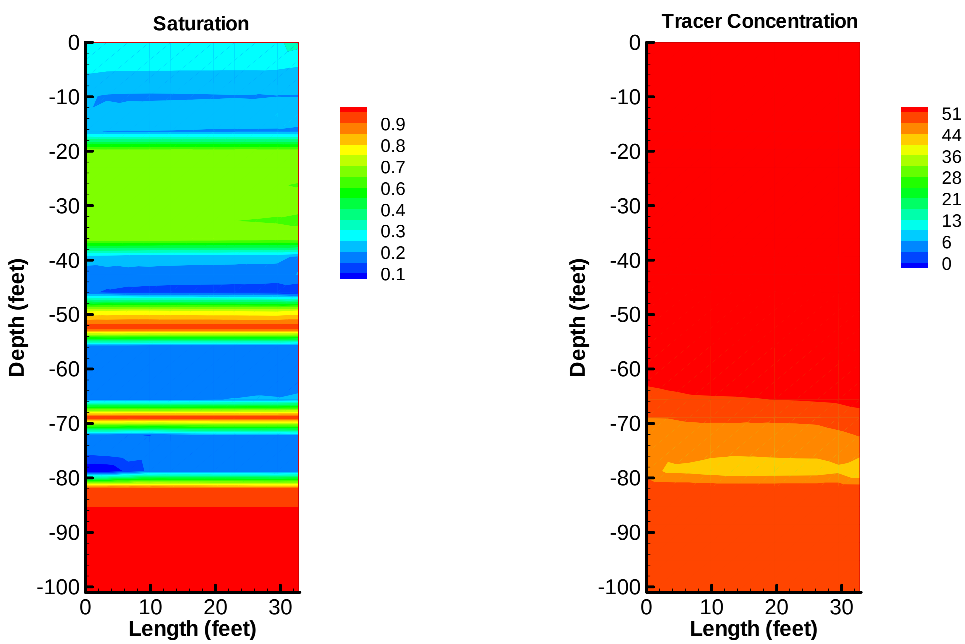

Figure B3-27
The saturation and solute concentration 14 years after the modeling started at the location HCMP-8/1 (Saturation = fraction saturated, Concentration = mg/L)

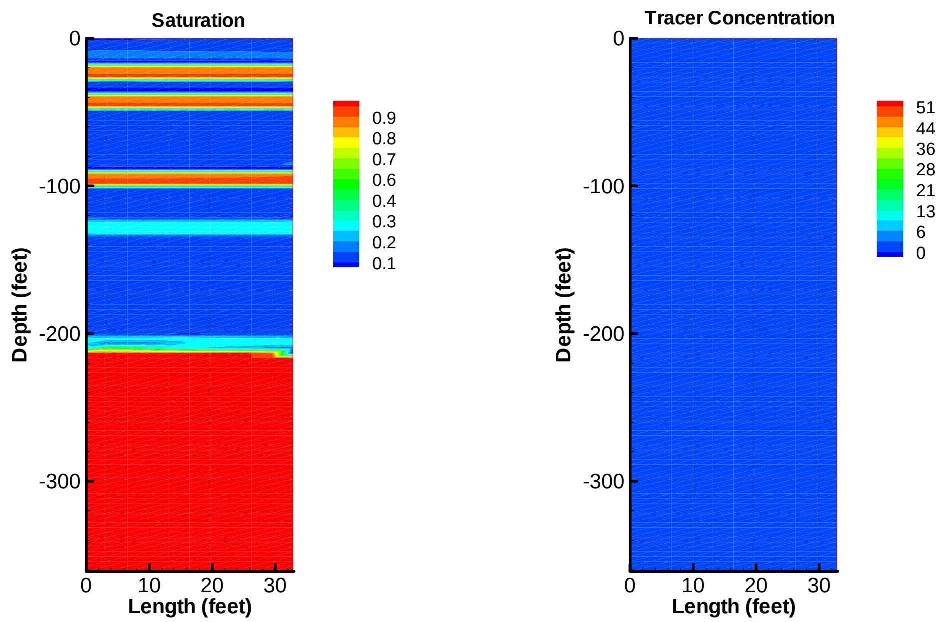

Figure B3-28
The initial saturation and solute concentration at the location Mira Loma (Saturation = fraction saturated, Concentration = mg/L)

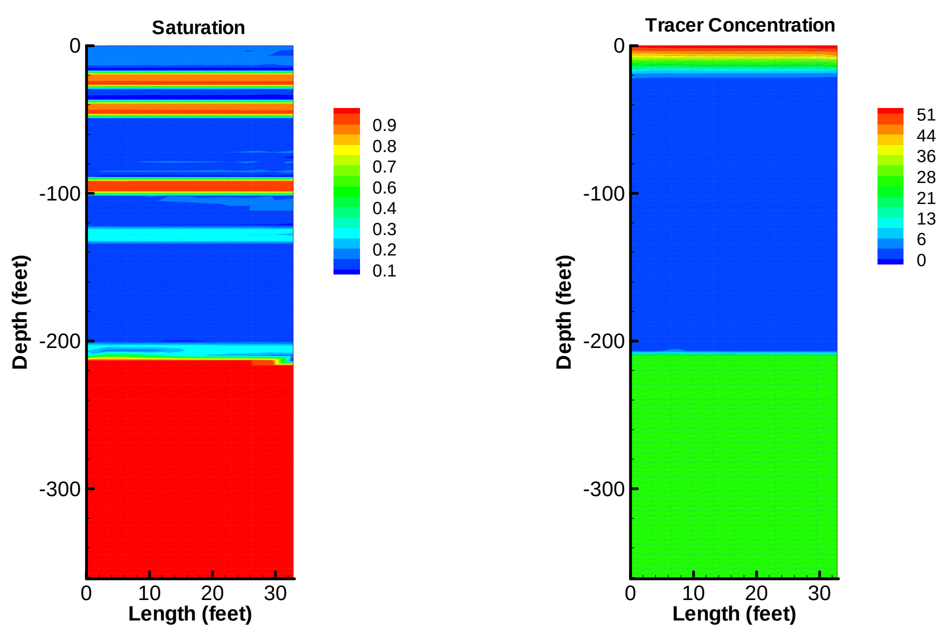

Figure B3-29
The saturation and solute concentration 1 year after the modeling started at the location Mira Loma (Saturation = fraction saturated, Concentration = mg/L)

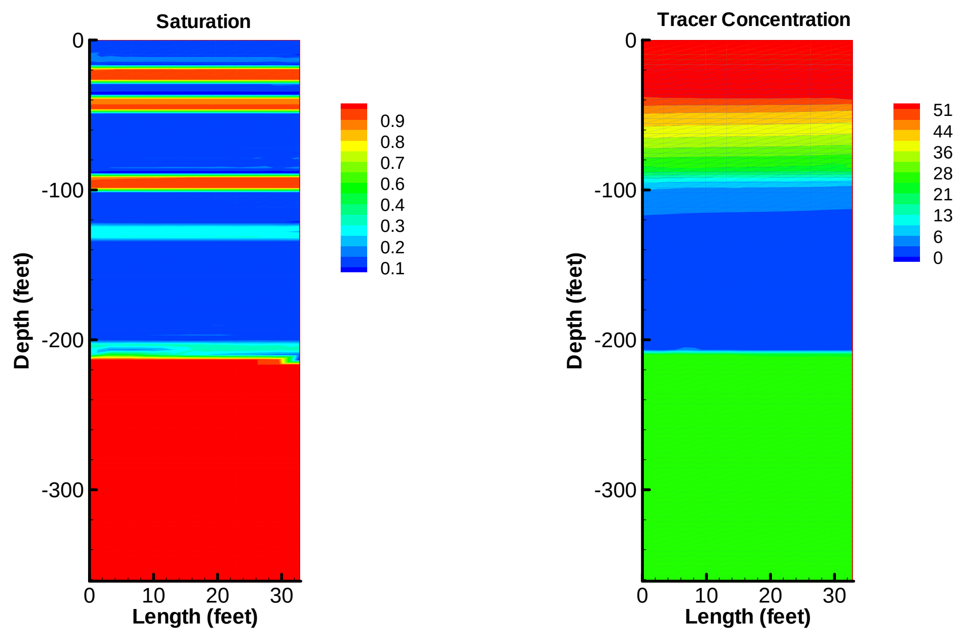

Figure B3-30
The saturation and solute concentration 10 years after the modeling started at the location Mira Loma (Saturation = fraction saturated, Concentration = mg/L)

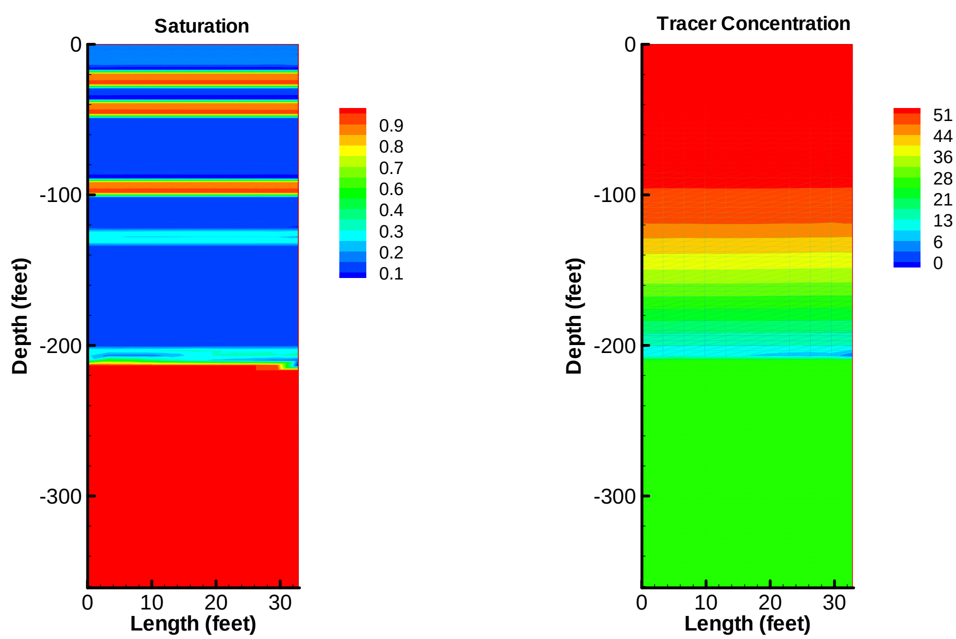

Figure B3-31
The saturation and solute concentration 19 years after the modeling started at the location Mira Loma (Saturation = fraction saturated, Concentration = mg/L)

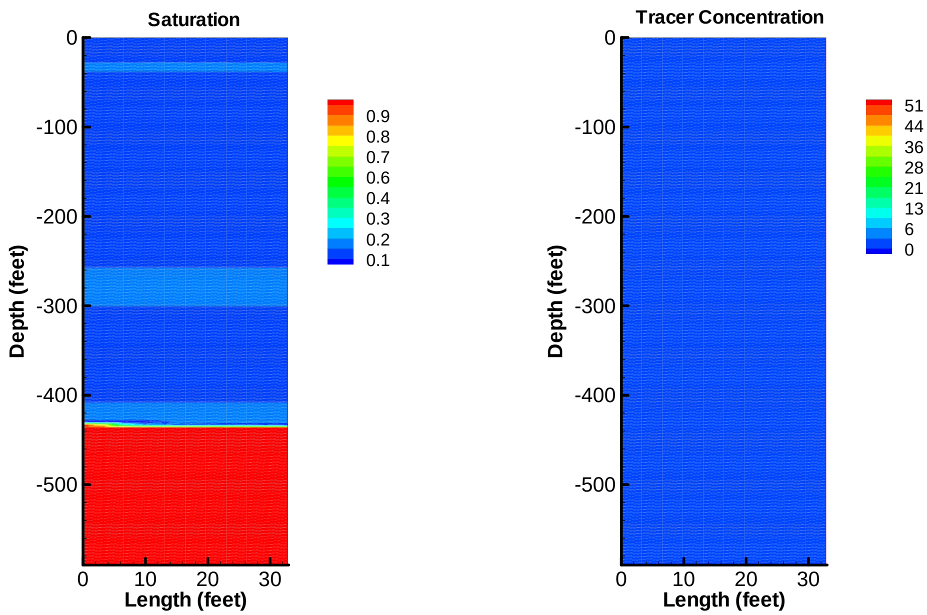

Figure B3-32
The initial saturation and solute concentration at the location MVWD-30 (Saturation = fraction saturated, Concentration = mg/L)

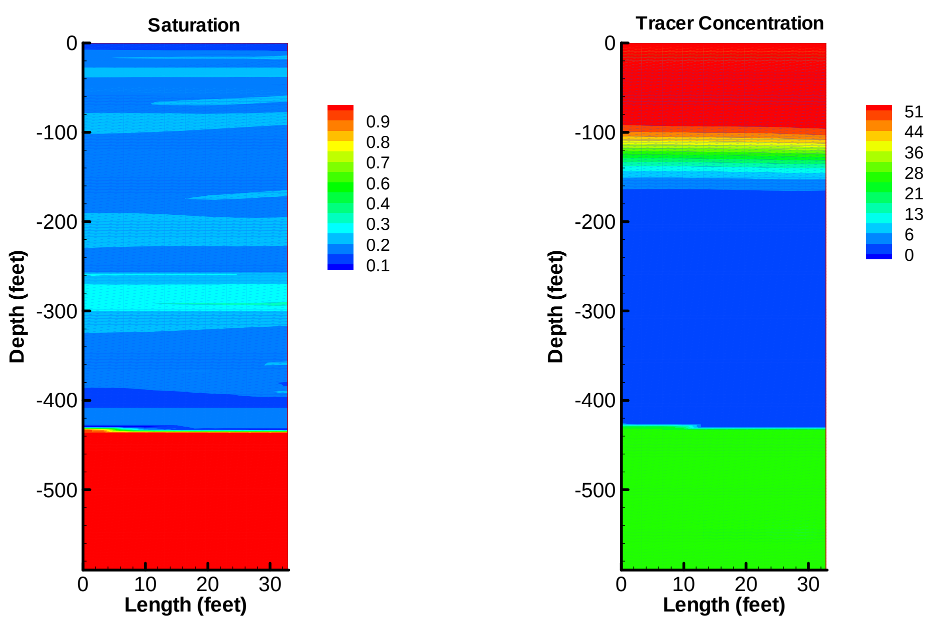

Figure B3-33
The saturation and solute concentration 10 years after the modeling started at the location MVWD-30 (Saturation = fraction saturated, Concentration = mg/L)

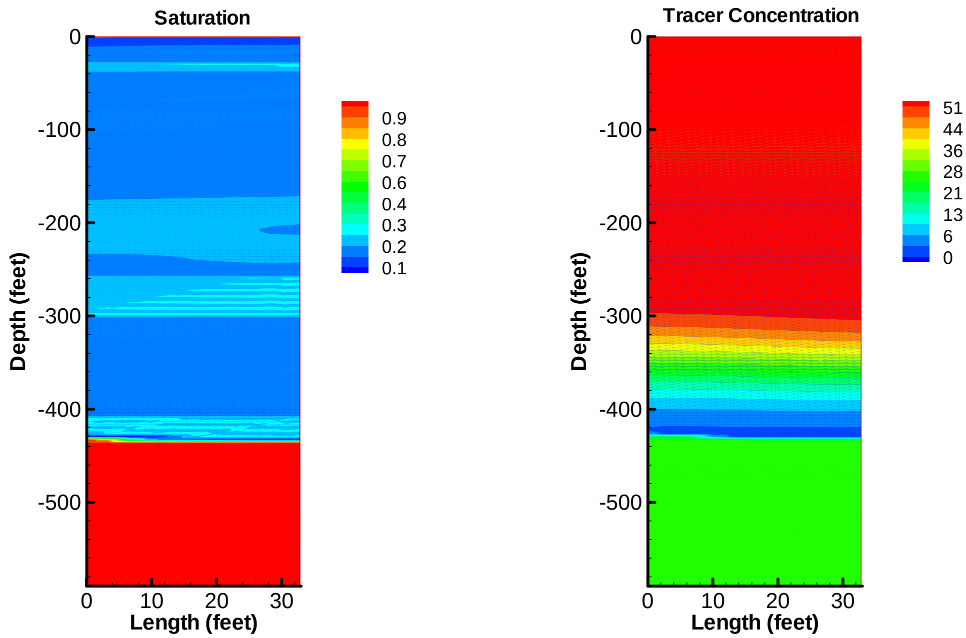

Figure B3-34
The saturation and solute concentration 30 years after the modeling started at the location MVWD-30

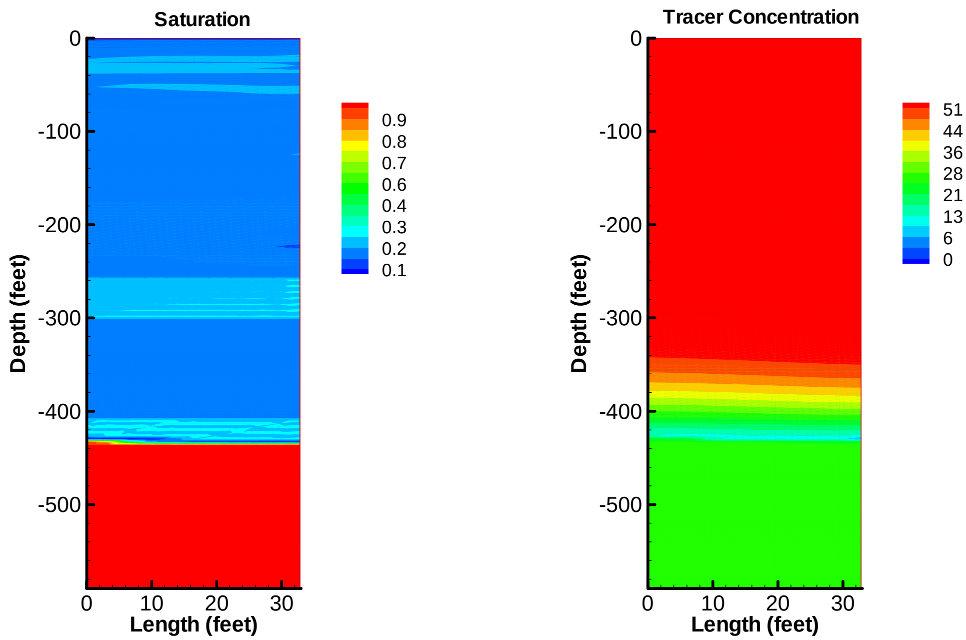

Figure B3-35
The saturation and solute concentration 34 years after the modeling started at the location MVWD-30

B4-1 SUMMARY

Although many factors affect unsaturated flow and solute transport in the vadose zone, only two factors play major roles in the Chino Basin. Factors, such as rainfall, irrigation, evaporation, and the condition of the surface soil only play minor roles in affecting lag time. As a matter of fact, evaporation and irrigation do not change much spatially within the Chino Basin. Although rainfall varies greatly over time and the north side of the basin receives slightly more rainfall than the southern portion, evaporation in the Chino Basin, in general, exceeds precipitation. Past heavy rainfall events have sped up unsaturated flow and solute transport, but this impact is quite uniformly spatial. The major factors that affect flow and transport are the thickness of the unsaturated zone and the properties of the soil materials in the vadose zone; both factors differ significantly from one location to another.

Figure B4-1 is a generalized lag time contour map of the Chino Basin that was created based on the point simulation results, the depth of the groundwater table, and lithologic descriptions from well completion reports. This figure provides a general, graphical display of lag times within the Chino Basin; moreover, there is a gradation of lag times across the basin that is not expressed by the polygons in this figure.

B4-2 CONCLUSIONS

The following major conclusion have arisen from the unsaturated flow and solute transport simulations for the Chino Basin:

- For the deep percolation flow caused by irrigation and rainfall, the vadose zone thickness is the most important factor that affects the breakthrough time (the travel time for a solute to reach the groundwater table from the ground surface). The second most important factors are soil type and variation in vadose zone.

- The breakthrough time for a solute (i.e. return flow) to reach the groundwater table from the ground surface ranges from more than 60 years in the northern region of the Chino Basin to less than one year in the southern region near the Prado Basin. Water quality simulations should take this difference into account.

- The impact of the infiltration of water from the ground surface on the saturated zone lags about half of the breakthrough time. The lag time ranges from more than 30 years in the northern portion of the Chino Basin to less than one year in the southern portion.

- Calculating the rainfall abstraction is important when simulating unsaturated flow and solute transport. Otherwise, all rainfall, no matter how heavy, would infiltrate the ground because the daily rainfall rate is always less than soil vertical hydraulic conductivity in the Chino Basin.

- Unsaturated flow and solute transport modeling results cannot be used to extrapolate stream and recharge basin percolation rates; that is, the infiltration rates of streams and basins are saturated flow. For saturated flow the infiltration rate is a multiple of the saturated hydraulic conductivity and the unit gradient. In such cases, breakthrough time and impact lag time can be much less than a year in the Chino Basin. The results from this modeling work are only applied to recharged water from applied water and precipitation which percolate to the saturated water table via unsaturated flow conditions.

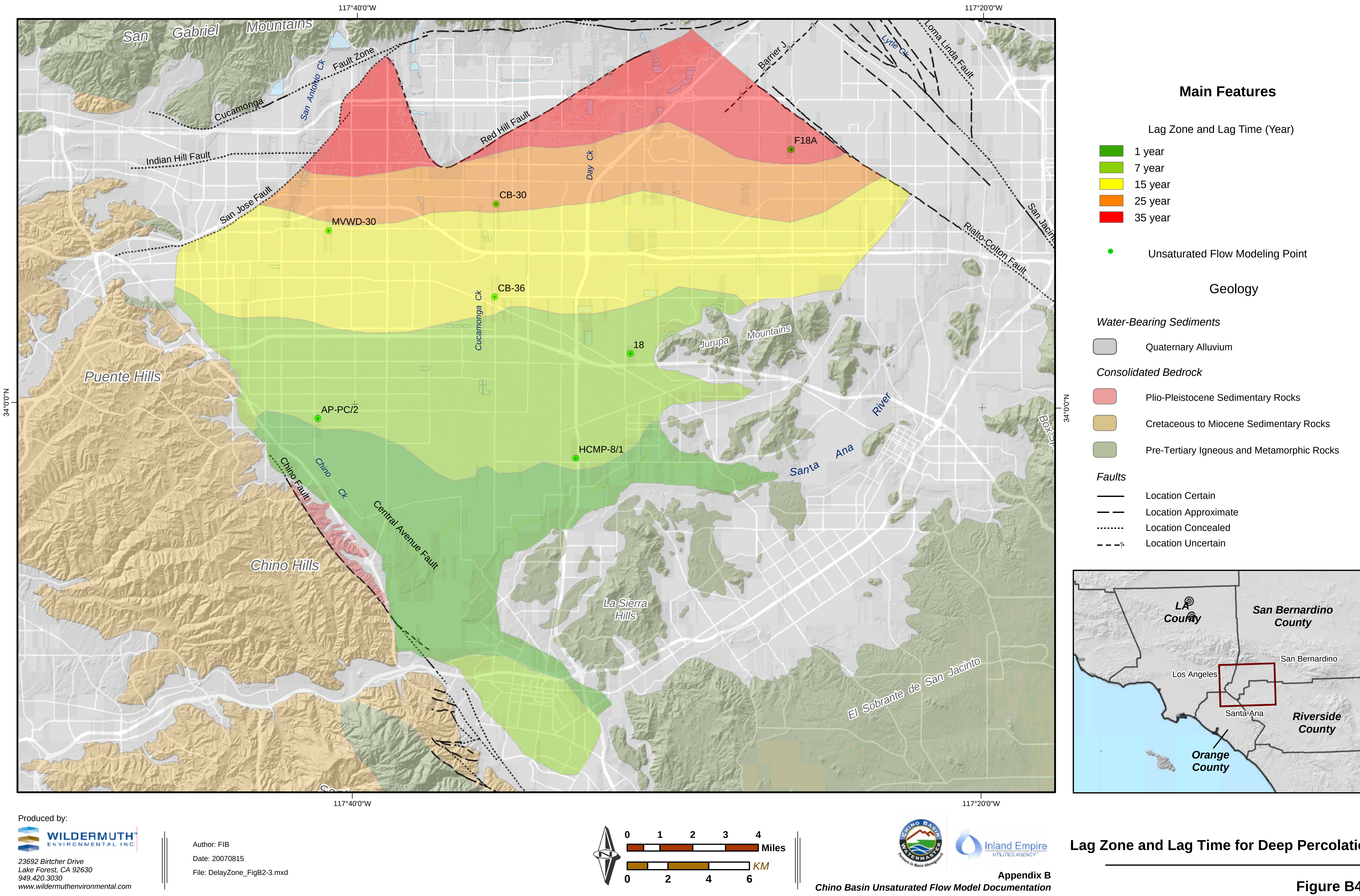

Produced by:
WILDERMUTH ENVIRONMENTAL INC
23692 Birtcher Drive
Lake Forest, CA 92630
949.420.3030
www.wildermuthenvironmental.com

Author: FIB
Date: 20070815
File: DelayZone_FigB2-3.mxd

Appendix B
Chino Basin Unsaturated Flow Model Documentation

Lag Zone and Lag Time for Deep Percolation

Figure B4-1

REFERENCES

Anderson, M.P., 1979, Using models to simulate the movement of contaminants through groundwater systems, CRC Critical Reviews in Environmental Control 9(2), 97-156.

Brooks, R. H., and A. T. Corey, Hydraulic properties of porous media, Hydrol. Pap., Colorado State Univ., Fort Collins, 3: 1–27, 1964.

Carsel, R. F., and R. S. Parrish, Developing joint probabil-ity distributions of soil water retention characteristics, Wat . Resour. Res., 24(5): 755-770, 1988.

Fuller, W. H. 1978. Investigations of Landfill Leachate Pollutant Attenuation by Soils. EPA-600/2-78/158, U. S. Environmental Protection Agency, Cincinnati, OH.

Jury, W.A., W.R. Gardner, and W.H. Garner, Soil Physics, John Wiley & Sons, 1991.

Klotz D, Seiler K-P, Moser H, Neumaier F. 1980. Dispersivity and velocity relationship from laboratory and field experiments. Journal of Hydrology, 45. No.3

Leij, F. J., W. J. Alves, and M. T. van Genuchten, The UNSODA unsaturated soil hydraulic database, EPA, Ada, OK., 1996.

McCuen, R.H., W. J. Rawls, and D.L. Brakensiek, Statistical-analysis of the brooks-corey and the green-ampt parameters across soil textures, Water Resour. Res., 17(4): 1005-1013, 1981.

Rawls, W. J., and D. L. Brakensiek, Prediction of soil water properties for hydrologic modeling, In Proceedings, Watershed Management in the Eighties, pp. 293-299, American Society of Civil Engineering, New York, 1985.

Rawls, W. J., D. L. Brakensiek, and K. E. Saxton, Estimation of soil water properties, Trans. ASAE, 25(5): 1316-1320, 1982.

Schaap, M.G., and F.J. Leij, Database Related Accuracy and Uncertainty of Pedotransfer Functions, Soil Science, 163(10): 765-779, 1998.

Simunek, J., M. Sejna, and M.T. van Genuchten, The HYDRUS-2D Software Package for Simulating the One-Dimensional Movement of Water, Heat, and Multiple Solutes in Variably-Saturated Media, Version 2.0, pp. 178, U.S. Salinity Laboratory, Riverside, CA, 1998.

van Genuchten, M. T., A closed-form equation for predicting the hydraulic conductivity of unsaturated soils, Soil Sci Soc Am J., 44(5): 892–898, 1980.

van Genuchten, M.T., and D. R. Nielsen, On describing and predicting the hydraulic-properties of unsaturated soils, Ann. Geophys., 3(5): 615-627 1985.

Wang, W., Uncertainty Analysis of Groundwater Flow and Solute Transport in Unsaturated-Saturated Soil: Maricopa Case, Ph.D. Dissertation, University of Arizona, 2002.

Wang, W., S. P. Neuman, T. Yao, and P. Wierenga, “Simulation of Large-Scale Field Infiltration Experiments using a Heirachy of Models Based on Public, Generic, and Site Data.” Vadose Zone Journal, 2:297-312. 2003.

Wang, W., S. P. Neuman, T. Yao, and P. Wierenga, “Comparative Simulations of a Large-Scale Field Infiltration Experiment, PROCEEDINGS.” TOUGH Symposium 2003, Lawrence Berkeley National Laboratory, Berkeley, California. 2003.

Appendix C

Evapotranspiration Analysis of the Prado Basin, Santa Ana River, California

Evapotranspiration Analysis
Of the Prado Basin
Santa Ana River, California

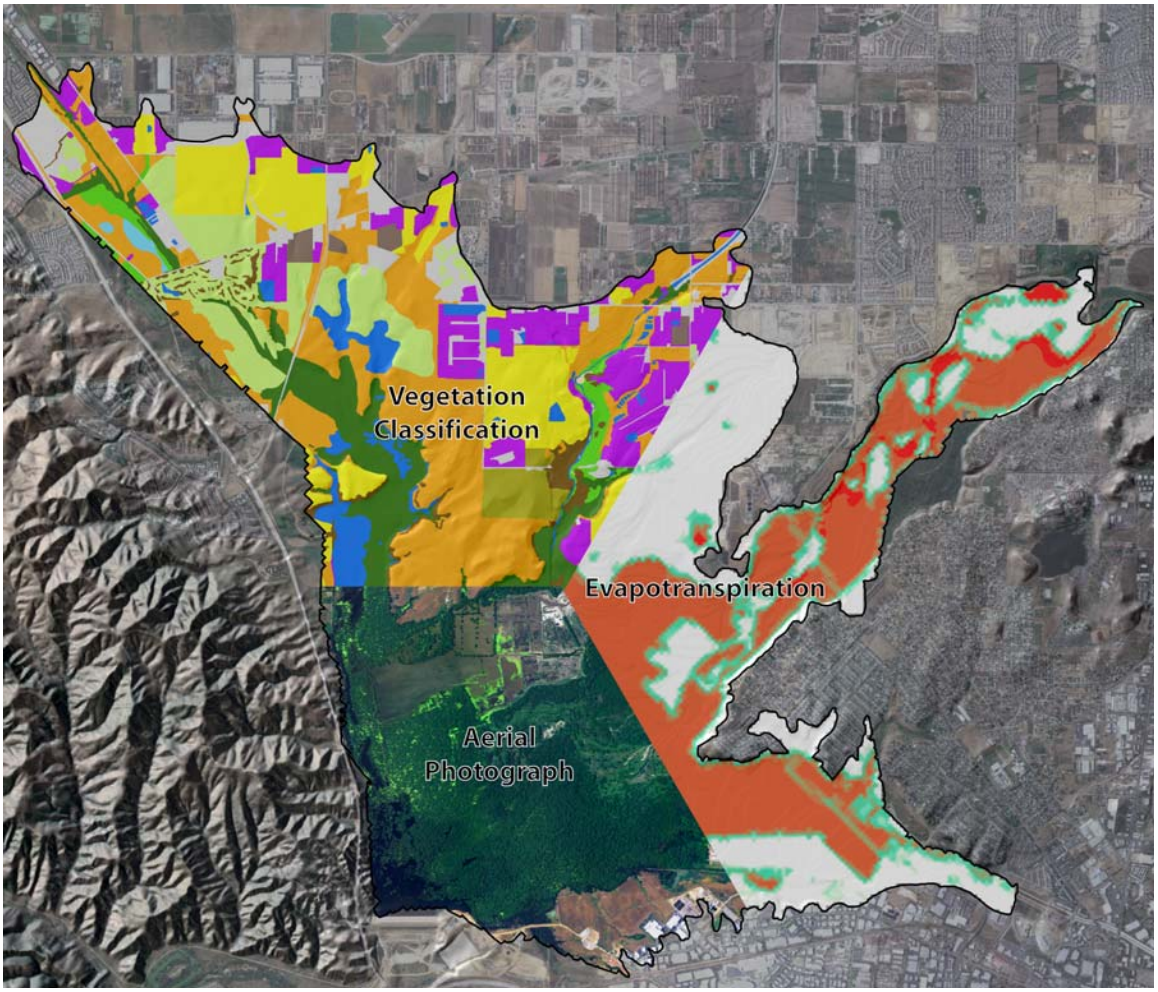

Prepared for:

Wildermuth Environmental, Inc.
23692 Birtcher Drive
Lake Forest, CA 92630

Prepared by:

Merkel & Associates, Inc.
5434 Ruffin Road
San Diego, CA 92123
(858) 560-5465

November 2007

TABLE OF CONTENTS

LIST OF FIGURES

LIST OF TABLES

INTRODUCTION

Merkel & Associates, Inc. (M&A) has been retained by Wildermuth Environmental, Inc. to conduct analyses to determine the evapotranspiration (ET) rates within the Prado Basin (Figure 1) in association with water budget modeling for the basin. To accomplish this effort, M&A mapped and characterized vegetation, obtained reference ET rates (ET_o) for local weather stations, and developed ET rates for vegetation communities based on vegetation characterization and ET_o rates for the region. Using the calculated ET rates, evapotranspiration demand was calculated for the basin on a water quarter and grid basis that allowed use in the Wildermuth modeling effort. This document summarizes the methods employed and results of these analyses.

BACKGROUND

Evapotranspiration (ET) is the sum of both evaporation of free water and plant transpiration (Allen et al. 2005). This accounts for the movement of water to the air from soil, bodies of water, and through stomata in the leaves of plants. The method used for calculation of ET in the Prado Basin study site is as follows: the Prado Basin was mapped by individual vegetation units for the years 1974, 1984, and 2006 and split into cells (cell data was provided by Wildermuth Environmental, Inc.); ET values for each vegetation unit were either obtained from published data or calculated using reference evapotranspiration (ET_o) rates and a calculated landscape coefficient. The total area of each vegetation unit (i.e., vegetation polygon) was calculated; individual ET values were multiplied by the area of corresponding vegetation polygons, and the resulting ET values were summed within each cell to obtain a single ET value for each model grid cell within the watershed. ET was determined for each cell by water year quarter by the summation of daily ET values within each quarter.

METHODS

VEGETATION MAPPING

Vegetation maps were created using the ESRI® ArcMap™ GIS software package by the digitizing of aerial photos for the years 1974, 1984, and 2006 at a scale of 1:12,000. The 1974 and 1984 aerial photos provided by Wildermuth Environmental, Inc. are not georectified images and thus have not been geometrically corrected for topographic relief, lens distortion, or camera tilt. This results in unavoidable distortion in area calculations of digitized features. These variations, however, are not considered to result in significant differences in accuracy for our calculations. The historical aerial photos were georeferenced with ArcMap™, resulting in a spatial accuracy of approximately 25 m or better at the resolution of interpretation. A single black and white aerial photo was available for the year 1974. For 1984, a total of six black and white aerial photos provided incomplete cover of the study area. Where gaps existed in the coverage, data from 1974 were used to complete the 1984 vegetation map. For the year 2006, digitizing was completed using a color orthorectified aerial photo with a 1-meter resolution. Groundtruthing of the 2006 vegetation map was carried out through field truthing that included in-situ observations of each vegetation type. A total of 15 unique vegetation types were identified within the study area. These classification units were employed during each of the mapping years (Figures 2-4).

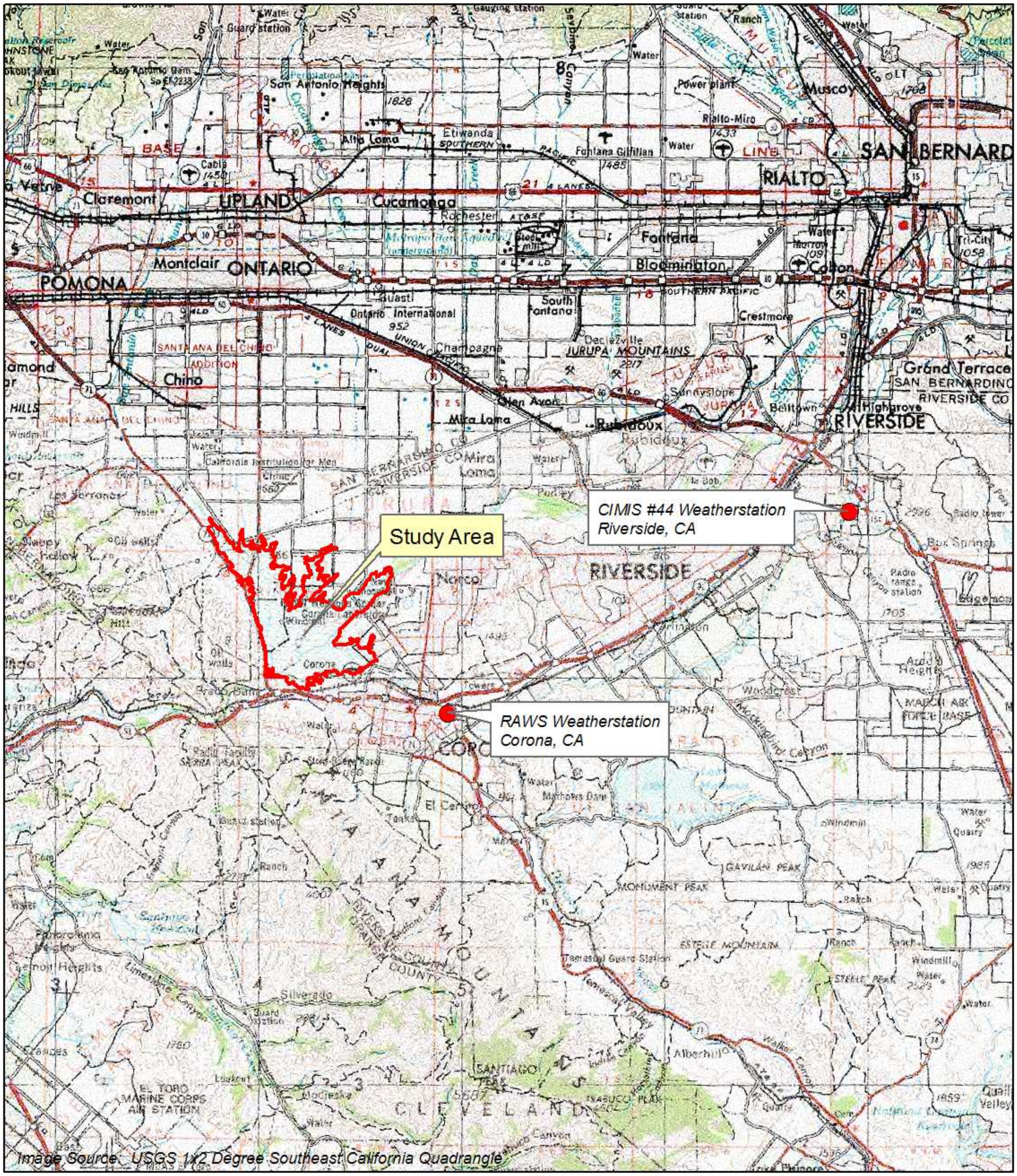

Miles 0 1 2 3

Project Vicinity Map

Prado Basin

Figure 1

Merkel & Associates, Inc.

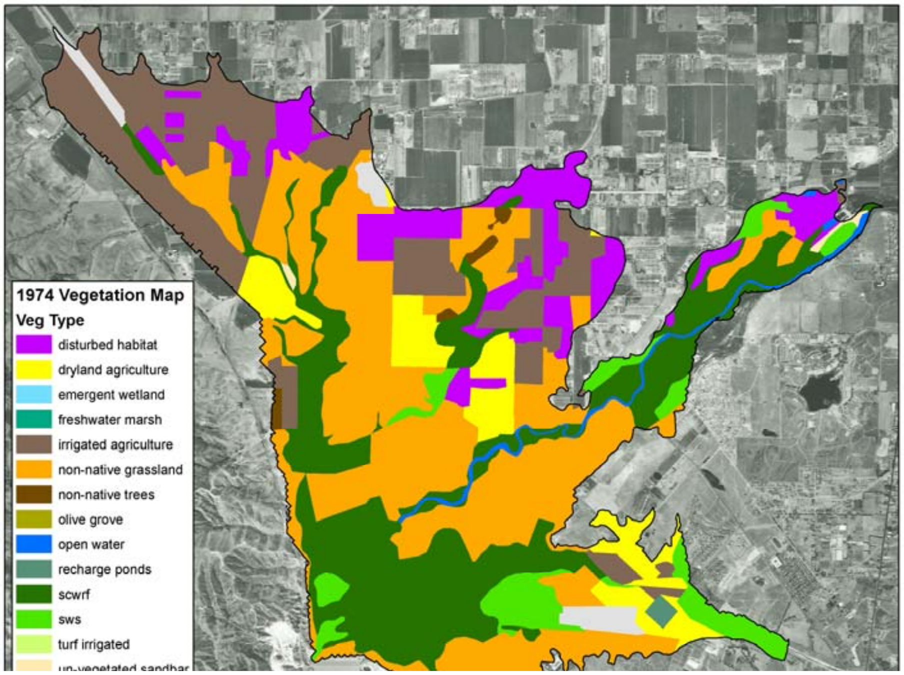

Figure 2. 1974 Vegetation Map for Prado Basin

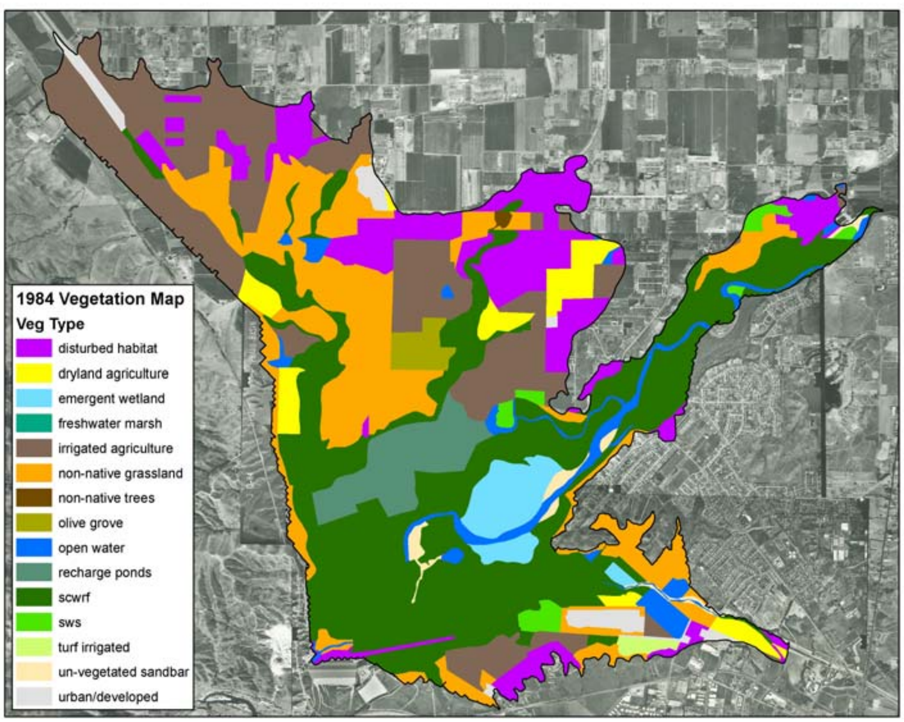

Figure 3. 1984 Vegetation Map for Prado Basin

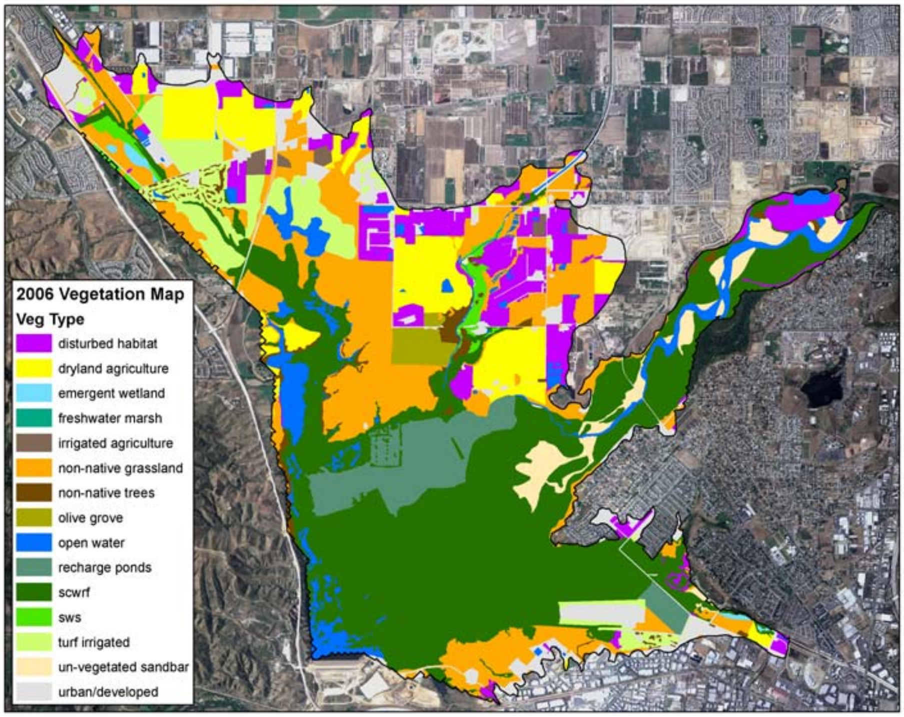

Figure 4. 2006 Vegetation Map for Prado Basin

Several habitat changes have been observed within the basin over the past two decades. Perhaps the most pronounced the increase in southern cottonwood willow riparian forest, the new occurrence of irrigated turf lands, and the decrease in irrigated agriculture (Figure 5).

REFERENCE EVAPOTRANSPIRATION (ET_O)

Calculated reference evapotranspiration rates ($ET_{o,}$) derived from weather station data, is publicly available from both the Western Regional Climate Center (WRCC) and the California Irrigation Management Information System (CIMIS). These estimates of ET_o approximate the evapotranspiration (ET) of a short, cool-season grass that is not water stressed (Snyder et al. 1989). For this study, monthly ET_o values were averaged over all available years to obtain average monthly values in inches per month. These values were converted to feet per day and used to calculate actual evaportranspiration (ET_c).

The weather station in closest proximity to Prado Basin is the National Weather Service's Cooperative Remote Automated Weather Station (RAWS) located in Corona, California (N 33^0 52' 28", W 117^0 32' 57", NAD 83), approximately 5.2 miles east of the Prado Basin dam (Figure 1). Monthly weather data and associated reference evapotranspiration (ET_o) from this station are available from August 2001 to the present.

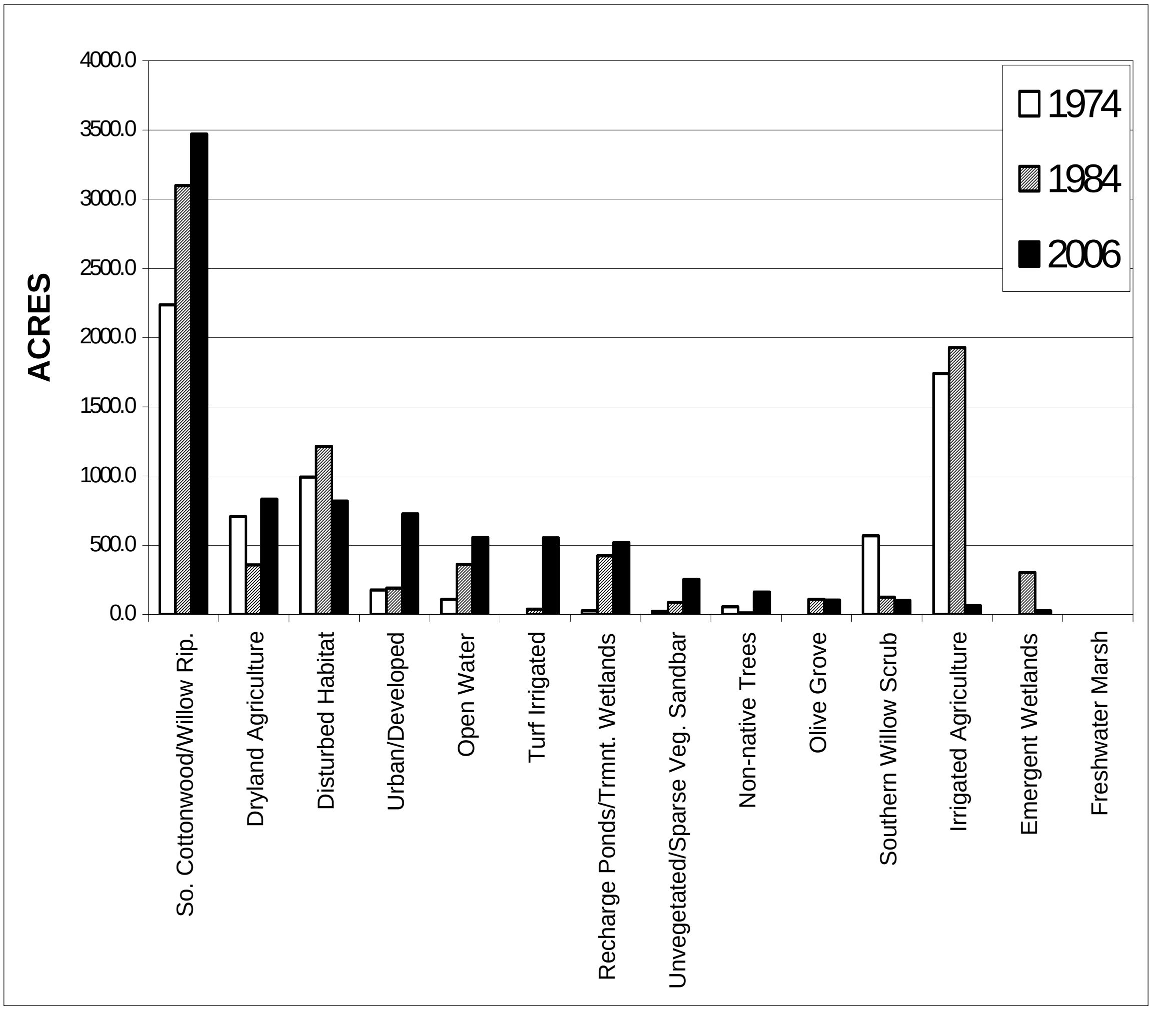

Figure 5. Habitat composition changes from 1974 through 2006.

In order to determine whether this relatively short record could serve as base line data for the extrapolation for a longer period of time (30 years), a nearby station with a much longer record was examined and analyzed for variance between station and stability of measured data across timeframes. The CIMIS weather station # 44, located at U.C. Riverside (N 33^0 57' 54", W 117^0 20' 08", NAD 83) (Figure 1), approximately 18 miles east-northeast of the Prado Basin dam has been active since June 02, 1985. Neither station has collected data for the full 30-year period desired by Wildermuth for modeling purposes. For this reason, analyses have been conducted to explore the degree of variability between stations and within station data. A plot of both Corona and Riverside monthly averaged ET_o values for 2001 to the present indicate that, although differences exist between the two curves with higher ET_o values in summer months than Riverside, both stations capture the same seasonal trends in ET_o and exhibit comparable ET_o ranges (Figure 6).

A comparison of Riverside 7-year monthly averaged ET_o values with Riverside monthly averaged ET_o for the 22 year average from 1985 to the present indicate that the shorter record provides a reasonable representation of historical ET_o with the region and for the time period of interest (Figure 7). Furthermore, a plot of monthly ET_o from 1985 to the present suggests that seasonal variations of ET_o have not changed significantly over the last 22 years with the region (Figure 8). Thus, the 7-year record of ET_o from the Corona weather station is believed to be representative of Prado Basin ET_o for the 30 year time period of interest.

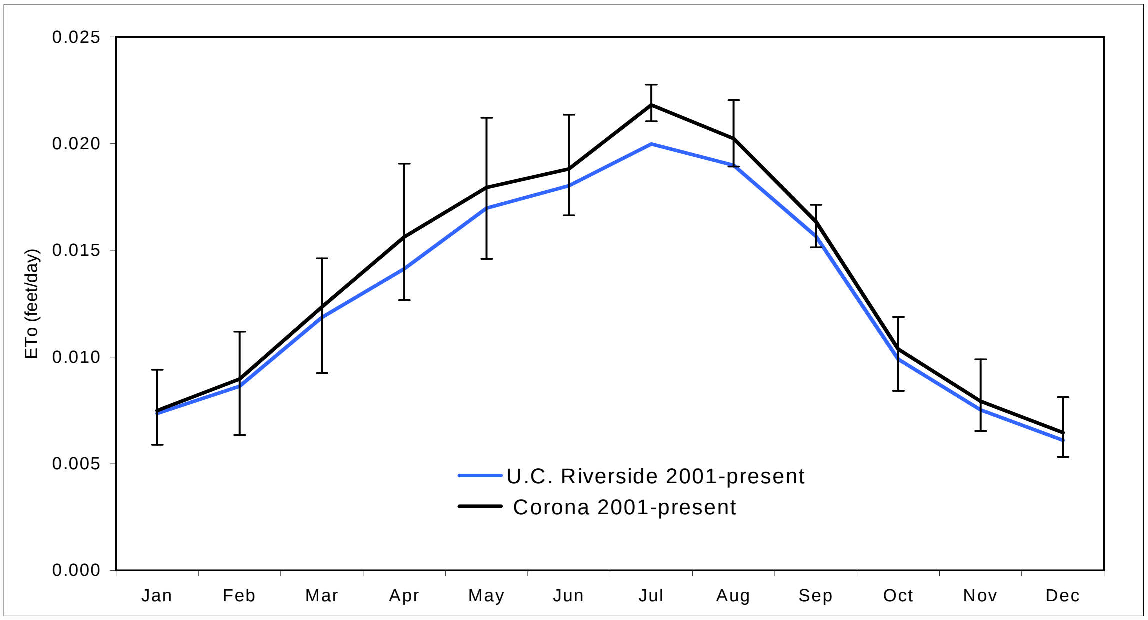

Figure 6. Comparison of ET_o from Corona weather station with U.C. Riverside weather station for the time period of 2001 to the present.

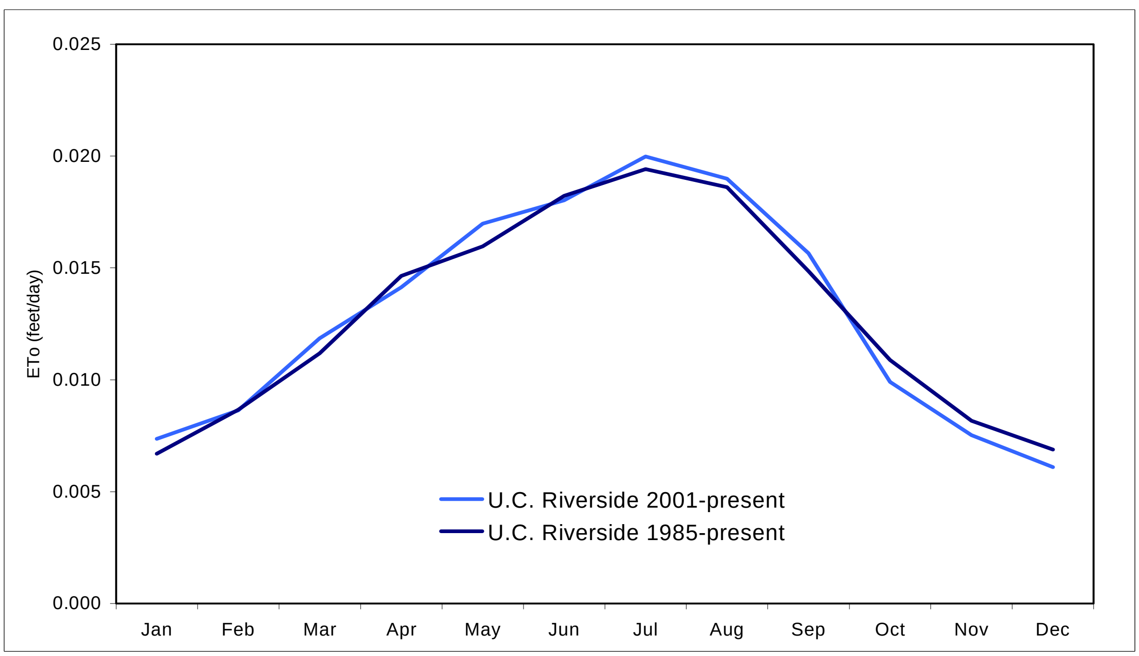

Figure 7. Comparison of ET_o from U.C. Riverside weather station for 2001-present and 1985-present.

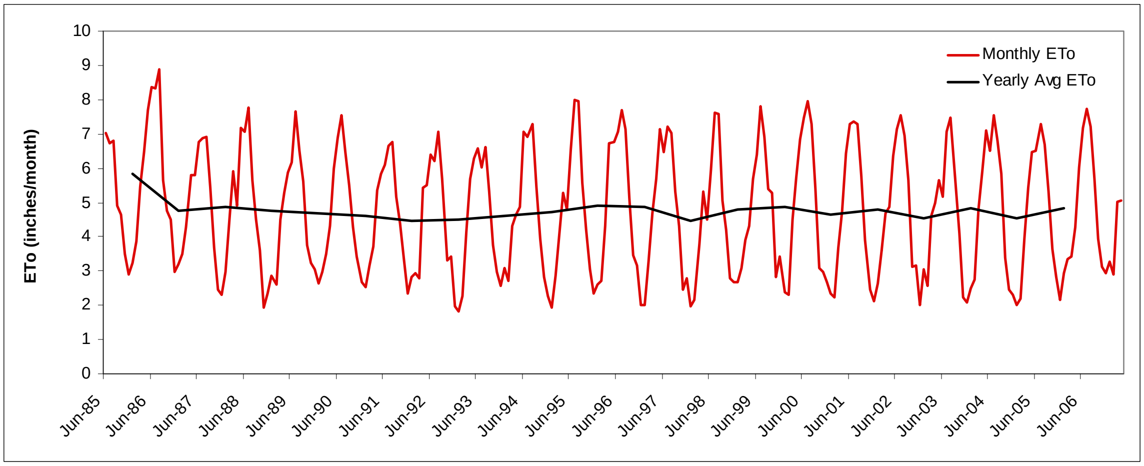

Figure 8. Plot of monthly ET_o values and yearly averaged ET_o values from U.C. Riverside weather station for the time period of June 1985 to present.

Finally, to examine the overall stability of the monthly ET_o values over a long period, the U.C. Riverside station data was again explored to develop a plot of the mean and standard deviations from the mean, along with the monthly maximum and minimum values (Figure 9). This plot suggests significant stability of the monthly mean values over time for the present region. The maximum deviations in ET_o values were generally less than two standard deviations from the mean value. Further, the maximum single deviation during the 22-year record period was less than 24% greater than the mean for the month, and the maximum standard deviation range for any given month is only ±12% from the mean. Based on the relatively tight deviation about the mean for the long-term record period, there is little reason to suggest that the mean monthly ET_o value is inappropriate for long-term modeling applications.

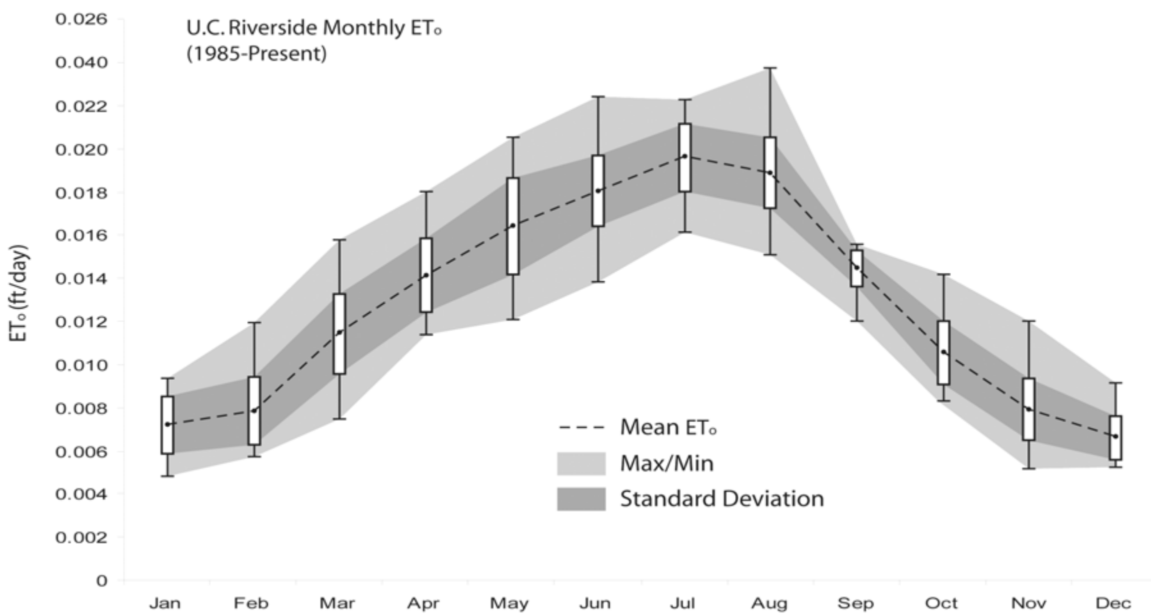

Figure 9. Plot of mean monthly ET_o values along with standard deviation and maximum-minimum monthly ranges for ET_o values from U.C. Riverside weather station for the 22-year time period of June 1985 to present.

ACTUAL EVAPOTRANSPIRATION (ET_C)

Monthly values of actual evapotranspiration rates (ET_c) for each vegetation type were obtained from published data when available. For the vegetation types *sparsely-vegetated sandbar* and *disturbed habitat*, ET_c values for bare soil were obtained from the Irrigation Training and Research Center (ITRC) Report 03-001 titled "California Crop and Soil Evapotranspiration" (ITRC 2003). The data obtained from this publication represent "…the consolidation of results from thousands of annual ET simulations." The Prado Basin falls within zones 6 and 9 of the California Department of Water Resources (DWR) Reference Evapotranspiration zones. Monthly values from the "typical year" tables for these zones were averaged in order to obtain monthly values used for this study. For the vegetation type *irrigated agriculture*, monthly values were also obtained from ITRC (2003) and calculated in the same process described above except alfalfa values were used in place of bare soil. A combination of alfalfa and bare soil were used to calculate ET_c values for the vegetation types *dryland agriculture* and *non-native grassland*. It was assumed that alfalfa is representative of the two vegetation types from November to May during the rainy season and that bare soil is representative during the dry season from June to October. For the *turf irrigated* vegetation type, the calculated ET_o values were used. In order to calculate open water ET, pan evaporation values from the Western Regional Climate Center (WRCC) for the Riverside Citrus Experimental Station were used. The data include monthly averaged pan evaporation ET from 1948-2005. As suggested by the WRCC, the ET values were multiplied by 0.75 in order to adjust for effects such as radiation on the side walls of the pan and heat exchanges with the pan material, thus providing a better estimate of evaporation from naturally existing surfaces. Crop coefficient values (K_c) were derived from published ET values by dividing published ET by the monthly averaged ET_o discussed in the previous section. This is a valid method for calculation of K_c because for a given vegetation type K_c is a constant that does not change regardless of climatic conditions. By converting ET values to K_c values the data can then be used to calculate ET for any time period where ET_o data are available. For the *olive grove* vegetation unit K_c was obtained from the Crop Coefficient Multiple Model (Snyder 2007).

Published ET_c values were not available for *non-native trees*, *emergent wetland*, *freshwater marsh*, *southern cottonwood willow riparian forest*, and *southern willow scrub*. For these vegetation types monthly ET_c was calculated using averaged monthly ET_o values and landscape coefficients (K_L) using the equation:

$$ET_c = ET_o \times K_L$$ (Costello et al., 2000)

It should be noted that crop coefficient (K_c) refers to a value determined from field research, whereas landscape coefficient (K_L) refers to a value calculated using the equation:

$$K_L = k_s \times k_d \times k_{mc}$$ (Costello et al., 2000)

Unique K_L values were derived from species (k_s), density (k_d), and microclimate crop factors (k_{mc}). Values for k_s were obtained from the Water Use Classification of Landscape Species (Costello and Jones 2000). For each vegetation unit, factors were determined for both a growing season (March through October) and a non-growing season (November through February). This distinction was made in an effort to account for variations in plant phenology between warm-dry summers, and cool-wet winters. The warm and dry 'growing season' is characterized by high production and rapid growth. During the 'non-growing season' cool and wet conditions result in more moderate vegetation growth. It should be noted that these categories were not used explicitly, but rather as general guides, as several of the plant species found within Prado Basin have evolved to take advantage of growth and development during what is defined here as the 'non-growing' season. One example is the understory vegetation within the *Southern Cottonwood Willow Riparian Forest*. During the period of willow dormancy, an herbaceous understory of annuals and drought deciduous perennial plants grow, flower, and set seed or die-back coincident with the leaf-out period of the canopy woodland trees. This herbaceous community has differing ET demands than the overstory trees and thus community ET_c values represent the cumulative demand for all aspects of the community through the full year.

HABITAT BY HABITAT ET_C CALCULATIONS

The following pages of this section summarize the habitats existing within the Prado Basin and outline the calculations of monthly ET_c values for each. In cases where the habitat is supported by imported or extracted water applied surfically, as is the case with *turf irrigated*, *irrigated agriculture*, or *urban/developed*, no ET_c values were calculated as these are understood to be addressed elsewhere in the basin model by Wildermuth Environmental as import or extraction supply and not groundwater.

Following the calculation of monthly ETc values, these were aggregated and averaged by water quarters based on the calendar year, resulting in four water quarter ETc values for each unique habitat type (Table 1). January through March constitutes Water Quarter (WQ) 1. April through June constitutes WQ2, and so forth.

Table 1. Community evapotranspiration rate (ET_c) for the Prado Basin

Habitat Class	**Mean ET (ft/day) By Water Quarter**			
	WQ 1	**WQ 2**	**WQ 3**	**WQ 4**
	Jan01-Mar31	***Apr01-Jun30***	***Jul01-Sep30***	***Oct01-Dec31***
Un-vegetated Sandbar	0.00238	0.00022	0.000487	0.002805
Disturbed Habitat	0.00238	0.00022	0.000487	0.002805
Dryland Agriculture	0.00793	0.01027	0.000487	0.00411
Irrigated Agriculture	0	0	0	0
Turf Irrigated	0	0	0	0
Non-native Grassland	0.00793	0.01027	0.000487	0.00411
Non-native Trees	0.00536	0.01135	0.012655	0.004596
Olive Grove	0.00768	0.01397	0.015575	0.006601
Emergent Wetland	0.00411	0.01397	0.015575	0.003485
Freshwater Marsh	0.00774	0.01886	0.021026	0.00661
Recharge Pond/Treatment Wetlands	0.00931	0.0196	0.023623	0.009047
Open Water	0.01089	0.02034	0.02622	0.011485
So. Cottonwood Willow Rip. Forest	0.00564	0.02043	0.022779	0.004764
So. Willow Scrub	0.00564	0.02043	0.022779	0.004764
Urban/Developed	0	0	0	0

Recharge Ponds/Treatment Wetlands

Mapping Unit Description

The Recharge Ponds/Treatment Wetlands habitat unit is a minor coverage class within the Prado Basin (Photo Point 1). This unit consists of a series of constructed wetland cells designed to facilitate the improvement of water quality by way of denitrification prior to entering a groundwater infiltration basin for basin recharge (Photo Point 2). Elevated water nitrate levels are effectively reduced by microbes associated with macrophytes such as cattails and bulrush. The optimal level of denitrifying microbial activity occurs when wetland cells have a macrophyte density of 50%. Periodic vegetation management is therefore required to maintain optimal levels of macrophyte density, which directly affects the efficiency of denitrifying microbial activity. Macrophyte density management is accomplished by a program that entails 1) draining a subset of wetland cells that support high densities of macrophytes; 2) allowing the substrate to partially dry; 3) crushing the vegetation into the soil with the use of heavy machinery (e.g. bulldozer, backhoe); and 4) refilling the cells. The conversion of live emergent macrophytes into submerged decaying biomass provides a cost effective source of organic carbon and favorable conditions for microbial denitrification. This macrophyte density management program is based on a rotating staggered schedule of treating approximately one third of the cells every third autumn.

Photo Point 1

Photo Point 2

Community Water Demand

Calculation for the highly managed *recharge basins/treatment wetlands* was determined in a unique manor. The vegetation within the approximate 50 created wetland cells are subject to regular maintenance to keep emergent vegetation at optimal densities for water denitrification (Walton and Jiannino 2005). The created wetlands are divided into types categorized by intended vegetation cover of 60, 40, and 0% of surface covered by emergent vegetation. The reduction of emergent vegetation is vital to maintaining optimal microbial and plant processes for nitrate reduction. On a three-year rotation, a subset of cells are drained and the dried emergent macrophyte biomass is knocked down with heavy equipment (bulldozers or excavators). Subsequent to vegetation treatment, the treated cells are refilled so the crushed vegetation will decompose making carbon available to the aquatic system (Walton 2002).

Due to the dynamic nature of the created wetlands, we calculated ET at 50% *open water* and 50% *freshwater marsh vegetation*, the average amount of total surface for all cells at any point in time. We arrived at this by considering 1/3 of the cells to be at an average of 20% covered (0-39%, range), 1/3 of the cells to be at an average of 50% covered (40-59%, range), 1/3 of the cells to be at an average of 80% covered (59-100%, range).

Evapotranspiration Calculations

Determination of ET has been accomplished as follows: ET values for constructed wetlands were calculated by averaging measured monthly ET values of *open water* and calculated ET values of *freshwater marsh*. See text in the both the *open water* and *freshwater marsh* accounts for details of the analyses. The calculated monthly ET for this community is illustrated in the figure below.

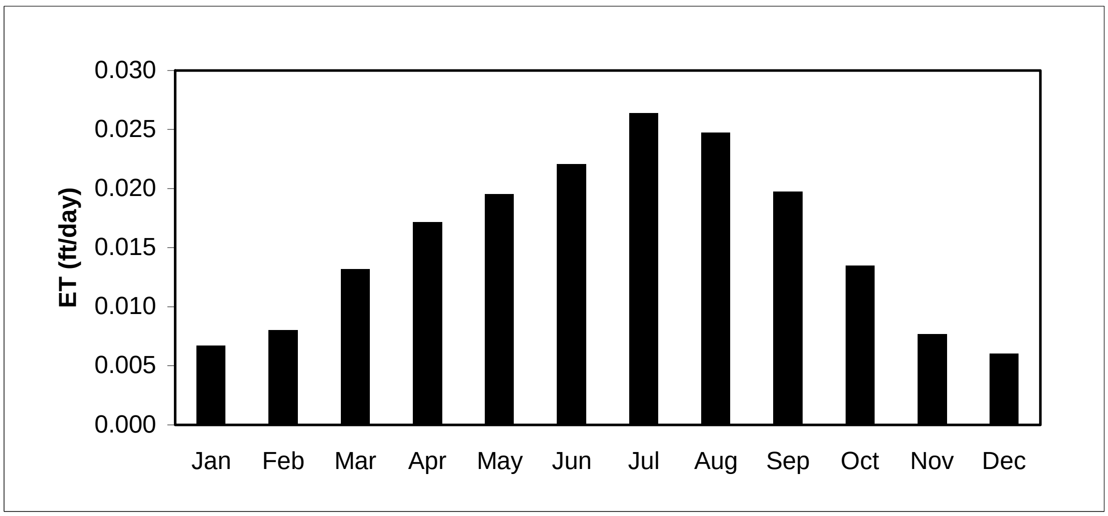

Monthly Evapotranspiration for Constructed Wetlands in Prado Basin

Disturbed Habitat

Mapping Unit Description

The *Disturbed Habitat* vegetation unit is not a dominant cover class within the Prado Basin (Photo Point 3). Areas that qualify as *Disturbed Habitat* either lack vegetation entirely or support less than 15% cover. These areas occur as the result of high levels of soil surface disturbance such as overgrazing, unimproved roads, and vehicle parking areas (Photo Point 4).

Disturbed Habitat supports a wide variety of sparsely growing opportunist plant species including pineapple weed (*Amblyopappus pusillus*), doveweed (*Croton setigerus*), telegraph weed (*Heterotheca grandiflora*), bicolor cudweed (*Pseudognaphalium biolettii*), tumble-mustard (*Sisymbrium altissimum*), Russian-thistle (*Salsola tragus*), and Indian sweetclover (*Melilotus indicus*). Dominant species of the habitat are identified below.

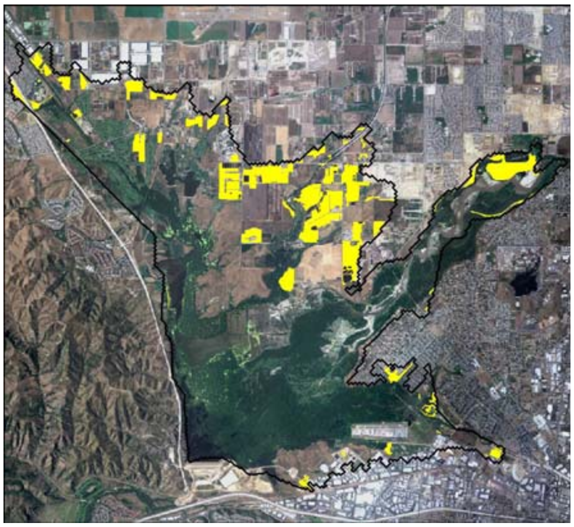

Photo Point 3

Photo Point 4

Disturbed Habitat Dominant Flora Species

Canopy Species	**Understory Species**
	Pineapple Weed (*Amblyopappus pusillus*)
	Doveweed (*Croton setigerus*)
	Telegraph Weed (*Heterotheca grandiflora*)
	Bicolor Cudweed (*Pseudognaphalium biolettii*)
	Tumble-Mustard (*Sisymbrium altissimum*)

Community Water Demand

Soil evaporation (E) rates are defined by a series of stages. Initially, the E rate is only limited by the amount of energy available to vaporize soil moisture in the upper layer of the soil. Once the water in the surface layer becomes depleted, hydraulic properties determine capillary action to bring water up to the surface layer. Beyond this point E rate becomes negligible due to soil physical and absorbing characteristics.

Evaporation Calculations

Determination of E has been accomplished as follows. Published monthly bare soil ET values for ET_o zones 6 and 9 were used to derive ET values for each month (ITRC 2003). The calculated monthly E for this community is illustrated in the figure below.

Calculated E Values for Landscape Coefficient (Kc)

Growing Season	Jun	Jul	Aug	Sep	Oct
ET (ft/day)	0.000069	0.000040	0.000309	0.001111	0.000860

Non-Growing Season	Nov	Dec	Jan	Feb	Mar	Apr	May
ET (ft/day)	0.003389	0.004167	0.004530	0.002039	0.000565	0.000417	0.000188

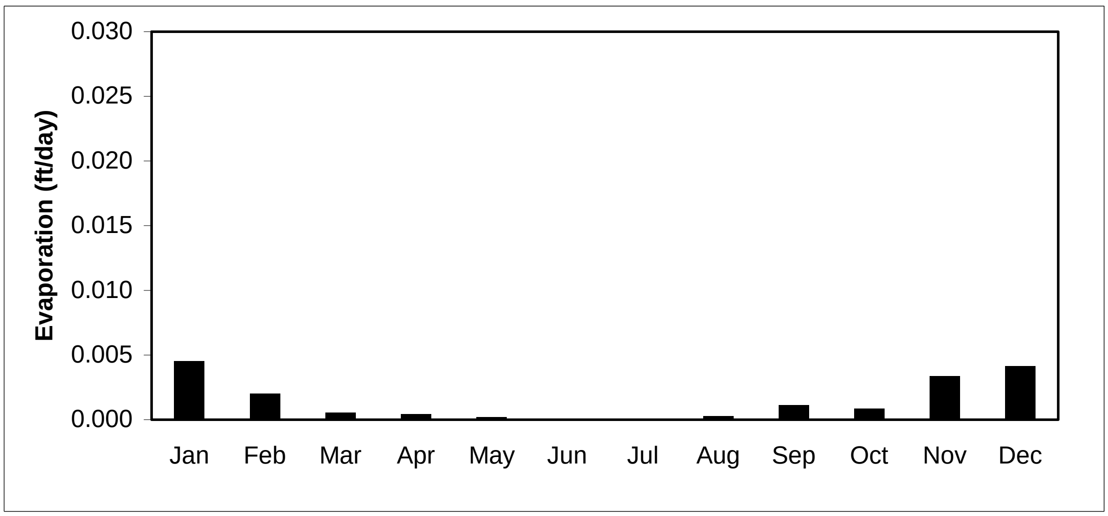

Monthly Evapotransipration for Disturbed Habitat in Prado Basin

Dryland-Agriculture (non-irrigated)

Mapping Unit Description

The *Dryland Agriculture (non-irrigated)* vegetation unit is a minor cover class within the Prado Basin (Photo Point 5). *Dryland Agriculture* is a single tiered monotypic community comprised of a single crop type, and to a much lesser extent, invading opportunistic weed species. Vegetation of Dryland Agriculture includes alfalfa (*Medicago sativa*) and seed and hay producing grasses that include cultivated barley (*Hordeum vulgare* var. *trifurcatum*), wild oat (*Avena fatua*), and cereal wheat (*Triticum aestivum*). These annual crops are typically planted in the fall and harvested in the spring, leading to a growth period that coincides with the normal rainfall season and removal of much of any remaining standing biomass upon harvest. Under ideal conditions, ample rainfall results in the production of solid stands forming 100 percent canopy at maturity.

The most common weeds in *Dryland Agriculture* include annual graminoids such as Italian ryegrass (*Lolium multiflorum*), ripgut grass (*Bromus diandrus*), foxtail fescue (*Vulpia myuros* var. *hirsuta*), foxtail barley (*Hordeum jubatum*), and hood canarygrass (*Phalaris paradoxa*). In the fall, broadleaf weeds such as wild radish (*Raphanus sativus*), rancher's fiddleneck (*Amsinckia menziesii* var. *intermedia*), short-pod mustard (*Hirschfeldia incana*), black mustard (*Brassica nigra*), London rocket (*Sisymbrium irio*), shepherd's-purse (*Capsella bursa-pastoris*), and prickly sow-thistle (*Sonchus asper*) may be common. Dominant species of the habitat are identified below.

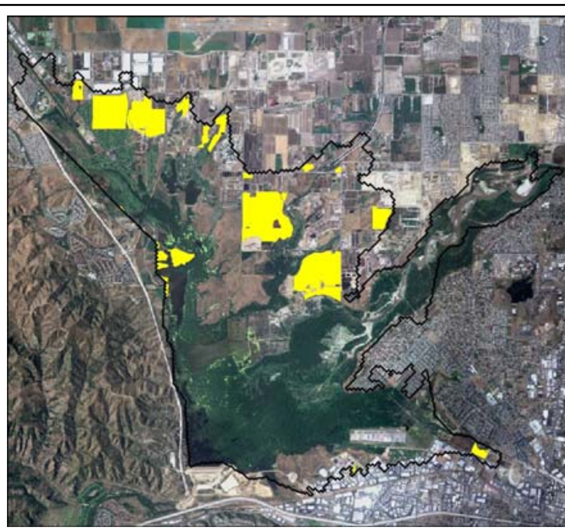

Photo Point 5

Photo Point 6

Dryland Agriculture Dominant Flora Species

Canopy Species	**Understory Species**
N/A	Alfalfa (*Medicago sativa*)
	Cereal Wheat (*Triticum aestivum*)
	Wild Oat (*Avena fatua*)
	Barley (*Hordeum vulgare* var. *trifurcatum*)

Community Water Demand

ET rates are correlated with wet soil resulting from rainfall.

Evapotranspiration Calculations

To derive ET values for each month of the growing season (June through October), published monthly alfalfa ET values for ET_o zones 6 and 9 were used (ITRC 2003). For the non-growing season (November through May), bare soil values were used in place of alfalfa values. The calculated monthly ET for this community is illustrated in the figure below.

Calculated ET Values for Landscape Coefficient (Kc)

Growing Season	Jun	Jul	Aug	Sep	Oct
ET (ft/day)	0.000069	0.000040	0.000309	0.001111	0.000860

Non-Growing Season	Nov	Dec	Jan	Feb	Mar	Apr	May
ET (ft/day)	0.005125	0.006344	0.004798	0.008393	0.010591	0.014236	0.016505

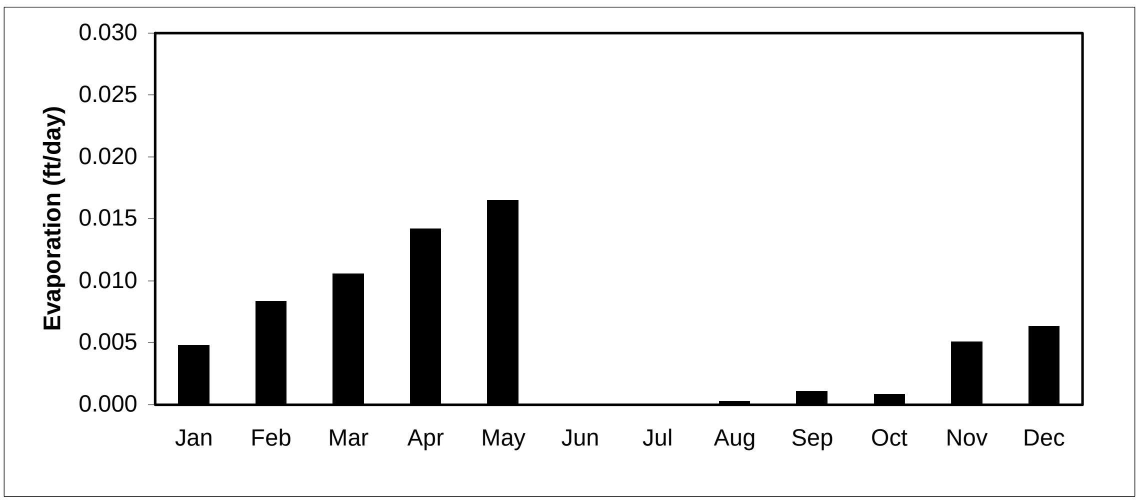

Monthly Evapotranspiration for Dryland Agriculture in Prado Basin

Emergent Wetland

Mapping Unit Description

The *Emergent Wetland* vegetation unit is a minor cover class within the Prado Basin (Photo Point 7) and exists as a result of extended periods of inundation and resulting anaerobic conditions in these areas. Dominant vegetation of the *Emergent Wetland* within Prado Basin includes typical perennial monocots adapted to oxidation-reduction potential (ORP) soils as well as several opportunistic, facultative species, which occur in less saturated areas. Species included in this vegetation unit are castor-bean (Ricinus communis), curly dock (Rumex crispus), tall flatsedge (Cyperus eragrostis), red-root flatsedge (C. erythrorhizos), toad rush (Juncus bufonius var. bufonius), Mexican rush (J. arcticus var. mexicanus), saltgrass (Distichlis spicata), bristly ox-tongue (Picris echioides), Dombey's spike-sedge (Eleocharis montevidensis), and African brass-buttons (Cotula coronopifolia) (Photo Point 8).

Photo Point 7

Photo Point 8

Emergent Wetland Dominant Flora Species

Canopy Species	**Understory Species**
N/A	Dombey's Spike-sedge (*Eleocharis montevidensis*)
	Saltgrass (*Distichlis spicata*)
	African Brass-buttons (*Cotula coronopifolia*)
	Castor-bean (*Ricinus communis*)
	Curly Dock (*Rumex crispus*)
	Bristly Ox-tongue (*Picris echioides*)
	Sedges (*Cyperus eragrostis*, *C. erythrorhizos*)
	Rushes (*Juncus bufonius*, *J. mexicanus*)

Community Water Demand

During the March – October growing season, *Emergent Wetland* vegetation has high water needs. This demand is reduced during the November – February non-growing season. Consequently, crop factors were calculated for both the growing and non-growing seasons.

Evapotranspiration Calculations

For the growing season, a high Species Factor (k_s) value was used to represent the high water demand of perennial, herbaceous flora and soils that are periodically saturated or flooded. A moderately high Density Factor (k_d) value was determined based on the sparse canopy cover and overall low density of vegetation. A moderately high Microclimate Factor (k_{mc}) value for was used to characterize the lack of shading that results in increased exposure to heat inputs.

Seasonal water demand during the non-growing is decreased due to the reduction of available moisture from soils, therefore resulting in a moderately low k_s value. A low k_d value relates to the absence of shading and a reduction of multiple tiers (i.e., vertical dimension). A moderately high k_{mc} value was again determined from the lack of shading of plant density and an increase in exposure to heat inputs. The calculated monthly ET for this community is illustrated in the figure below.

Factors for calculation of Landscape Coefficient (Kc)

Season	**Species Factor (k_s)**	**Density Factor (k_d)**	**Microclimate Factor (k_{mc})**	**Landscape Coefficient (K_c)**
Growing Season	**0.8**	**1.0**	**1.0**	**0.8**
Non-Growing Season	**0.3**	**0.5**	**1.0**	**0.15**

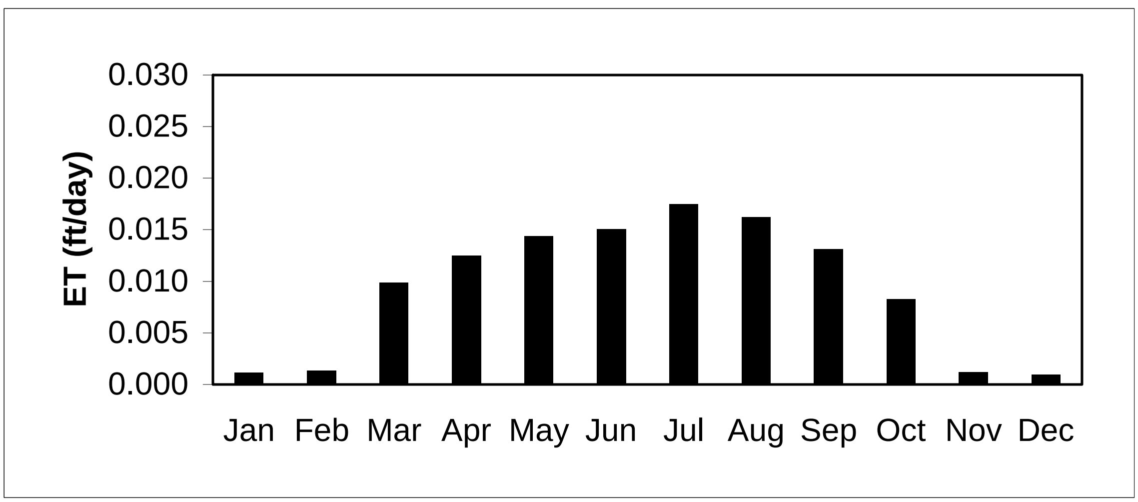

Monthly Evapotranspiration for Emergent Wetland in Prado Basin

Freshwater Marsh

Mapping Unit Description

The *Freshwater Marsh* vegetation unit is a minor coverage class within the Prado Basin (Photo Point 9). *Freshwater Marsh* is classified as areas having prolonged periods of inundation, which permits the accumulation of peaty soils and is dominated by perennial macrophytes (Photo Point 10). Areas mapped as *Freshwater Marsh* occur within the highly managed *Recharge Basins/Constructed Wetlands* vegetation unit previously discussed.

Photo Point 9

Photo Point 10

Freshwater Marsh Dominant Flora Species

Canopy Species	**Understory Species**
	Southern Cattail (*Typha domingensis*)
	Broad-leaved Cattail (*Typha latifolia*)
	Viscid Bulrush (*Schoenoplectus acutus* var. *occidentalis*)
	Olney's Bulrush (*S. americanus*)

Community Water Demand

During the March – October growing season, *Freshwater Marsh* vegetation has high water needs. This demand is reduced during the November – February non-growing season. Consequently, crop factors were calculated for both the growing and non-growing seasons.

Evapotranspiration Calculations

For the growing season, a high k_s value was used to represent the high water demand of perennial flora and soils that are saturated or flooded for prolonged periods. A moderately high k_d value was determined based on the tendency for the macrophytes to form dense stands of nearly complete canopy. A high k_{mc} value was used to represent the high exposure of the leaves to solar radiation and wind.

Seasonal water demand during the non-growing is decreased due to the lower angle of the sun and cooler temperatures, resulting in a moderate ks value. A moderately high k_d value relates to the tendency for the macrophytes to form dense stands of nearly complete canopy. A high k_{mc} value was used to represent the high exposure of the leaves to solar radiation and wind. The calculated monthly ET for this community is illustrated in the figure below.

Factors for calculation of Landscape Coefficient (Kc)

Season	Species Factor (k_s)	Density Factor (k_d)	Microclimate Factor (k_{mc})	Landscape Coefficient (K_c)
Growing Season	0.9	1.0	1.2	1.08
Non-Growing Season	0.5	1.0	1.2	0.6

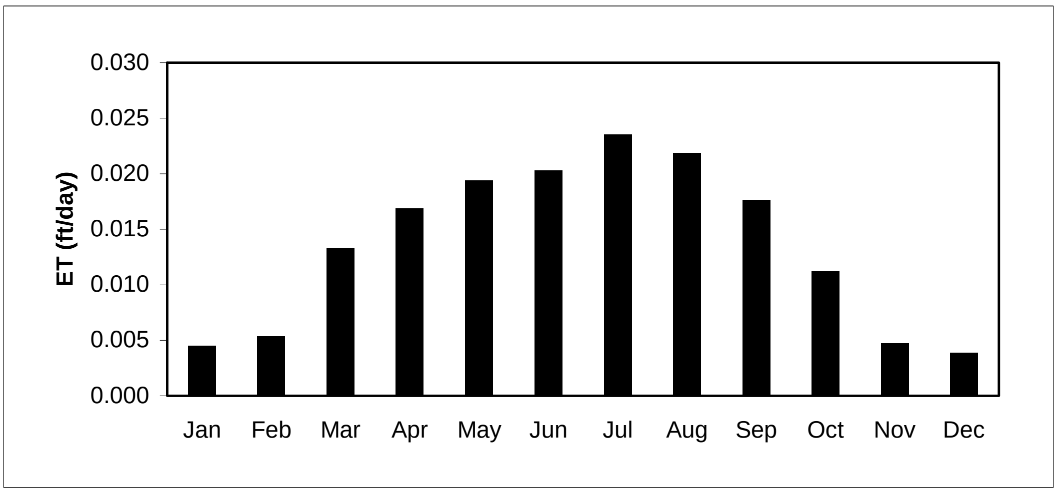

Monthly evapotranspiration for Freshwater Marsh in Prado Basin

Irrigated Agriculture

Mapping Unit Description

The *Irrigated Agriculture* vegetation unit is a minor cover class within the Prado Basin (Photo Point 11). Irrigated Agriculture within the Prado Basin includes grain and seed crops (Photo Point 12). These crops can include either perennials (i.e., alfalfa fields) or annuals such as grass or hay fields and/or beans and are typically planted in the fall and harvested in the spring. This period of planting and growing coincides with the highest solar radiation and warmest temperatures. Dominant species of the habitat are identified in the table below.

Photo Point 11

Photo Point 12

Irrigated Agriculture Dominant Flora Species

Canopy Species	**Understory Species**
	Alfalfa (*Medicago sativa*)
	Dry Beans - various types
	Wheat (*Triticum* spp.)
	Oats (*Avena fatua*)
	Barley (*Hordeum vulgare*)

Irrigated Agriculture as a vegetation unit was excluded from the ET analysis because its water usage is accounted for in imported water calculations. Areas of *Irrigated Agriculture*, however, were mapped to show the relative area and distribution in relation to other vegetation units.

Non-native Grassland

Mapping Unit Description

The *Non-native Grassland* vegetation unit is a relatively large cover class within the Prado Basin (Photo Point 13). Seasonal emergence and growth of this annual community is dependent upon rainfall that is typically received during the period from November through April. During the dry season, annual grasses quickly die out and form a dense thatch to sparse coverage of degraded plant duff. The *Non-native Grassland* vegetation community is comprised almost entirely of species of the genus *Avena*, *Bromus*, and *Hordeum* (Photo Point 14). These species are highly opportunistic and have the ability to readily establish after soil disturbance activities such as overgrazing, off-road vehicle activity, and native vegetation clearing by mechanical means. Additional herbaceous species include filaree (*Erodium* spp.), tocalote (*Centaurea melitensis*), black mustard (*Brassica nigra*), radish (*Raphanus sativus*), and Russian thistle (*Salsola tragus*). Dominant species of the habitat are identified below.

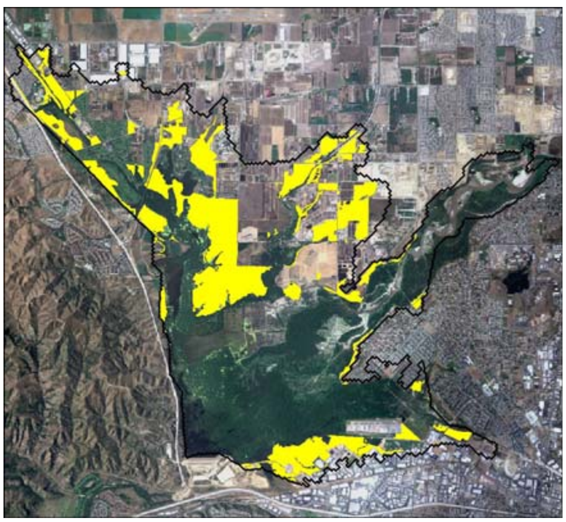

Photo Point 13

Photo Point 14

Non-native Grassland Dominant Flora Species

Canopy Species	**Understory Species**
	Oat Grasses (*Avena* spp.)
	Brome Grasses (Bromus spp.)
	Barley Grasses (*Hordeum* spp.)
	Black Mustard (*Brassica nigra*)
	Radish (*Raphanus sativus*)
	Filaree (*Erodium* spp.)
	Tecalote (*Centaurea melitensis*)
	Doveweed (*Eremocarous setigerus*)
	Fiddleneck (*Amsinckia menziesii*)
	Shepherd’s Purse (*Capsella bursa-pastoris*)

Community Water Demand

Water demand for this habitat varies by season due to its dependence on rainfall normally received from November through May. For species adapted to the arid climate, fog, mist, and morning dew are important sources of moisture during drought years and between infrequent rainfall events.

Evapotranspiration Calculations

Published monthly alfalfa ET values for reference evaporation (ET_o) zones 6 and 9 were used to derive ET values for each month of the growing season (June through October) (ITRC 2003). For the non-growing season (November through May), bare soil values were used in place of alfalfa values. The calculated monthly ET for this community is illustrated in below.

Calculated E Values for Landscape Coefficient (Kc)

Growing Season	Jun	Jul	Aug	Sep	Oct
ET (ft/day)	0.000069	0.000040	0.000309	0.001111	0.000860

Non-Growing Season	Nov	Dec	Jan	Feb	Mar	Apr	May
ET (ft/day)	0.005125	0.006344	0.004798	0.008393	0.010591	0.014236	0.016505

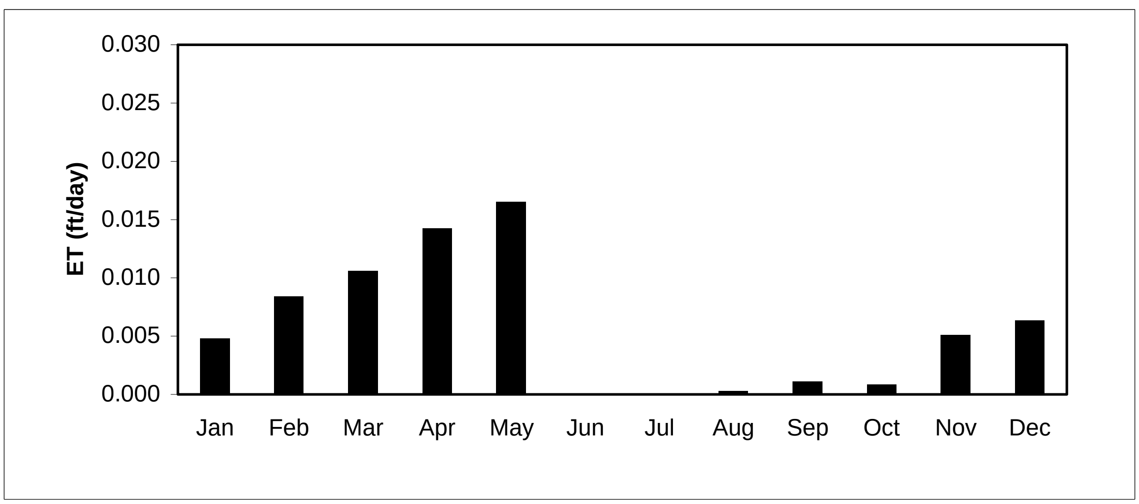

Monthly Evapotranspiration for Non-native Grassland in Prado Basin

Non-native Trees

Mapping Unit Description

The *Non-native Trees* vegetation unit is a minor cover class within the Prado Basin (Photo Point 15). Non-native trees are typically planted to provide shade, serve as windbreaks, and for aesthetic enhancement in suburban and urban areas. Increasingly, escaped ornamentals are also found in non-desirable locations such as native areas as stand-alone trees as well as in clusters of various sizes (Photo Point 16). Evergreen species include various eucalyptus (*Eucalyptus spp*.), Brazilian pepper tree (*Schinus terebinthifolius*), Mexican fan palm (*Washingtonia robusta*), Canary Island date palm (*Phoenix canariensis*), as well as deciduous species such as tree of heaven (*Ailanthus altissima*), and velvet ash (*Fraxinus velutina*). Also present but less common, are various pine (*Pinus spp*.), Peruvian pepper tree (*Schinus molle*), ngaio (*Myoporum laetum*), and acacia (*Acacia spp*.). Dominant species of the habitat are identified below.

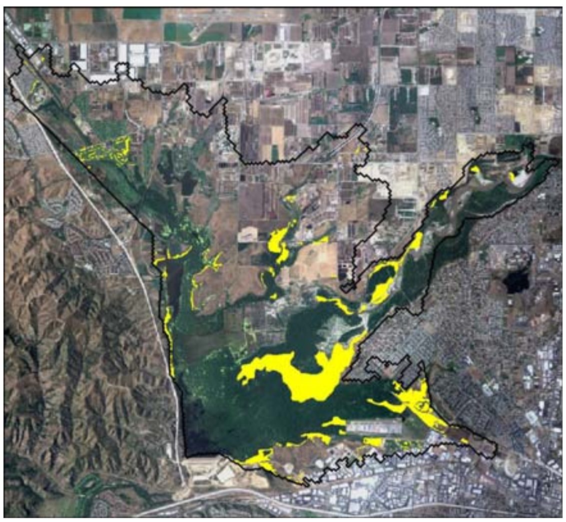

Photo Point 15

Photo Point 16

Non-native Trees Dominant Flora Species

Canopy Species	**Understory Species**
Eucalyptus (*Eucalyptus* spp.)	
Brazilian Pepper Tree (*Schinus terebinthifolius*)	
Mexican Fan Palm (*Washingtonia robusta*)	
Canary Island Date Palm (*Phoenix canariensis*)	
Tree of Heaven (*Ailanthus altissima*)	

Non-native Trees as a vegetation unit was excluded from ET analysis because its water usage is principally accounted for in imported water calculations. Areas of *Non-native Trees*, however, were mapped to show the relative area and distribution in relation to other vegetation units.

Olive Grove

Mapping Unit Description

The *Olive Grove* vegetation unit is a minor cover class within the Prado Basin comprised of mature, evenly spaced mission olive trees (*Olea europea*) that form a partial canopy (Photo Points 17 and 18). The grove is currently fallow, and water input is provided only by rain. Areas between the rows of mission olive trees support an herbaceous understory comprised of non-native grasses and broad-leafed herbaceous species. Dominant species of the habitat are identified below.

Photo Point 17

Photo Point 18

Olive Grove Dominant Flora Species

Canopy Species	Understory Species
Mission Olive (*Olea europea*)	

Community Water Demand

The mission olive tree is a drought tolerant evergreen species with low water needs. Olive groves have a significant canopy water storage capacity that delays the drying out of the canopy when the rainy season ends. Non-native grasses comprise only a small percentage of the total area; thus, ET has been calculated using only characteristics of the mission olive trees.

Evapotranspiration Calculations

ET was calculated using a constant landscape coefficient value of 0.80 from Snyder (2007). The calculated monthly ET for this community is illustrated in the figure below.

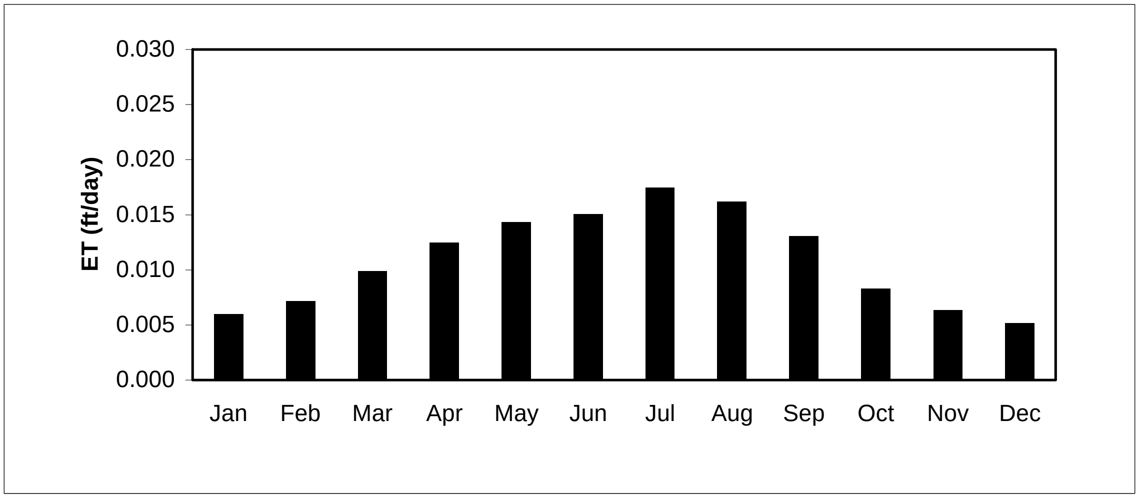

Monthly Evapotranspiration for Olive Grove in Prado Basin

Open Water

Mapping Unit Description

The *Open Water* mapping unit is a moderate cover within the Prado Basin, representing the exposed surfaces of lotic and lentic water bodies (Photo Points 19 and 20). Vegetation within this category is sparse and typically includes species with floating leaves. The areas of *Open Water* support a wide variety of hydrophytes including duckweed (*Lemna sp*.), water cress (*Rorippa nasturtium-aquaticum*), water primrose (*Ludwigia peploides ssp. peploides*), Pacific mosquito fern (*Azolla filiculoides*), and hairy clover fern (*Marsilea vestita ssp. vestita*). Dominant species of the habitat are identified below.

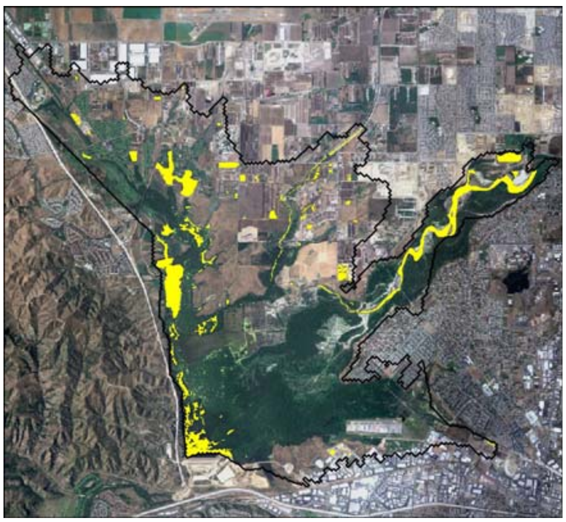

Photo Point 19

Photo Point 20

Open Water Dominant Flora Species

Canopy Species	**Understory Species**
Duckweed (*Lemna* sp.)	
Water Cress (*Rorippa nasturtium-aquaticum*)	
Water Primrose (*Ludwigia peploides* ssp. *peploides*)	
Pacific mosquito fern (*Azolla filiculoides*)	
Hairy Clover Fern (*Marsilea vestita* ssp. *vestita*)	

Community Water Demand

This community is unique because E occurs as free water and is exposed to elements such as solar radiation and wind. Only to a minor degree is water transferred into the atmosphere by the process of ET from vegetation. Consequently, water loss to the atmosphere is calculated by E only.

Evapotranspiration Calculations

Calculation of E has been accomplished as follows. Standard pan E was used to determine E rates for the Open Water habitat unit. Daily pan E rates were measured at the Chino weather station. Pans are installed above ground to control radiation on the sidewalls and heat exchanges with the pan material that increase the evaporation totals. In addition, pan water level readings are adjusted for precipitation. It is generally recommended that pan evaporation rates be scaled by a factor of 0.70 to 0.80 in order to simulate naturally existing surfaces such as shallow lakes, wet soil or other moist natural surfaces that are altered in evaporative properties as a result of scale driven ambient humidity. For this project we used an intermediate factor of 0.75 in the scaling process. The calculated monthly E for this community is illustrated below.

Factors for calculation of Landscape Coefficient (Kc)

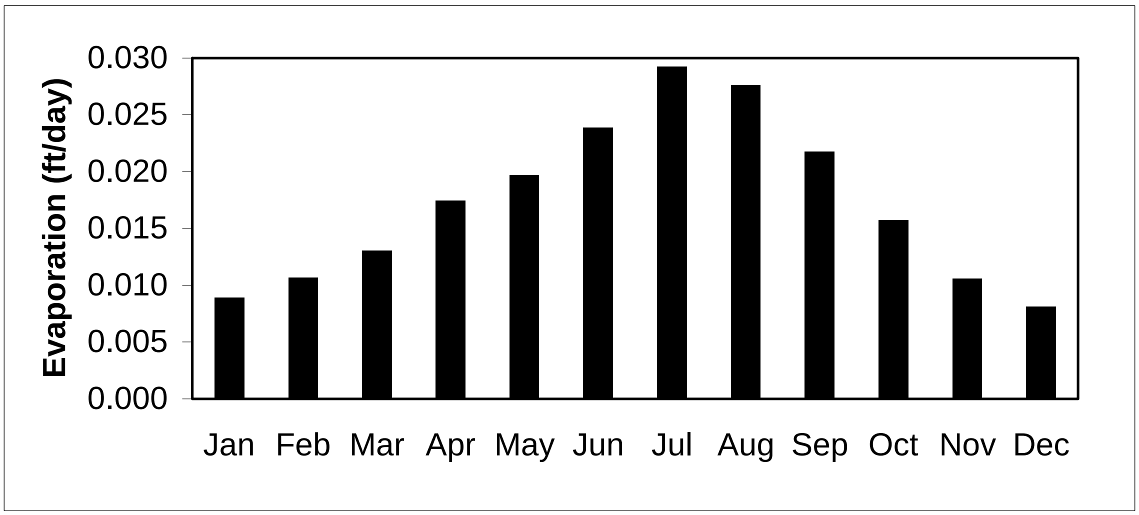

Monthly Evaporation for Open Water in Prado Basin

Southern Cottonwood Willow Riparian Forest

<u>Mapping Unit Description</u>

Southern Cottonwood Willow Riparian Forest (Riparian Forest) is the dominant cover class within the Prado Basin (Photo Point 21). Throughout the basin, *Riparian Forest* exists predominantly as a mature forest with a solid canopy of mature deciduous trees, averaging 20-30 feet tall (Photo Point 22). The canopy is dominated by willows, sycamores, and Fremont's cottonwood trees, while the patchy understory is comprised of lower stature species resulting from scouring created by periodic natural and anthropogenic activities such as river channel maintenance. The understory includes a mix of non-deciduous, deciduous, and drought deciduous species.

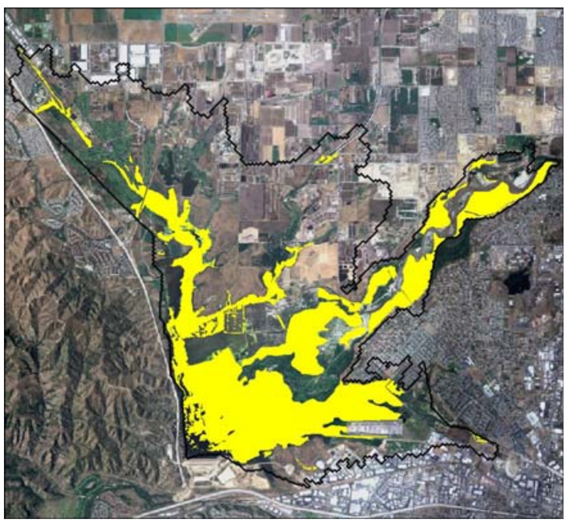

Photo Point 21

Photo Point 22

As a result of yearly seasonal cycling between physiologically active and dormant stages, this vegetation community has been divided between two temporal periods, which represent the growing (March to October) and non-growing (November to February) seasons. During the growing season, formation of the tree canopy results in nearly complete shading of the ground. During the non-growing season when deciduous trees have lost their leaves and become dormant, solar radiation penetrates down to the lower tiers and allows the herbaceous understory vegetation to thrive.

Dominant species include arroyo willow (*Salix lasiolepis*), Fremont cottonwood (*Populus fremontii*), Goodding's black willow (*Salix gooddingii*), sycamore (*Platanus racemosa*), western false-indigo (*Amorpha fruticosa*), blue elderberry (*Sambucus mexicana*), giant reed (*Arundo donex*), and tamarisk (*Tamarisk aphylla*). Additional species that occur in this area include non-natives such as lemon-scented gum (*Eucalyptus maculata*), red gum (*Eucalyptus rostrata*), Brazilian pepper (*Schinus molle*), Mexican fan palm (*Washingtonia robusta*), and Canary Island palm (*Phoenix canariensis*). The non-native species giant reed and tamarisk are categorically similar to the major constituents of *Riparian Forest*, with relatively high evapotranspiration rates and dormancy during the cooler months. As a result, many interspersed non-native tree species are grouped into the *Riparian Forest* unit. Dominant species of the habitat are identified below.

The constituent species of the herbaceous layer include mugwort (*Artemisia douglasiana*), arrow weed (*Pluchea sericea*), caster-bean (*Ricinus communis*), wild rose (*Rosa californica*), wild grape (*Vitis girdiana*), cocklebur (*Xanthium strumarium*), stinging nettle (*Urtica holosericea*), and California blackberry (*Rubus ursinus*).

Southern Cottonwood Willow Riparian Forest Dominant Flora Species

Canopy Species	**Understory Species**
Goodding's Willow (*Salix gooddingii*)	Douglas' Mugwort (*Artemisia douglasiana*)
Arroyo Willow (*Salix lasiolepis*)	Arrow Weed (*Pluchea sericea*)
Giant Reed (*Arundo donax*)	Caster-bean (*Ricinus communis*)
Fremont cottonwood (*Populus fremontii*)	Wild Rose (*Rosa californica*)
Sycamore (*Platanus racemosa*)	Wild Grape (*Vitis girdiana*)

Community Water Demand

Water demand for this habitat varies by season due to the winter deciduous nature of both the canopy trees and several of the understory shrubs. Dormancy of the canopy does not translate directly to dormancy of the entire system because substantial growth of herbaceous understory plants during the winter months can lead to water loss.

Evapotranspiration Calculations

Factors used for calculation of both growing and non-growing season landscape coefficients are listed below. A high landscape coefficient K_c was computed for the growing season and a low value was determined for the non-growing season. During the growing season (March – October) the *Riparian Forest* has high water needs. A high species factor (k_s) value was obtained from the willows category listed in the WUCOLS III Species Evaluation List (Costello and Jones 2000). An almost complete canopy cover and the presence of multiple tiers during the growing season resulted in a high-density factor (k_d). The growing season microclimate factor (k_{mc}) was determined by taking into account both high exposure zones existing around the perimeter of the *Riparian Forest* communities and the resulting protection that the perimeter vegetation provides to the adjacent interior region. Although the trees on the perimeter of this vegetation community are exposed to the drying elements of heat and wind, they act as a buffer to the interior core. The two effects are thought to largely offset one another, resulting in a moderately high microclimate (k_{mc}) value.

During the non-growing season (November – February) the *Riparian Forest* has a reduced water demand resulting in a moderately low species factor (k_s) value. Deciduous tree species are considered dormant during the non-growing season. As a result (k_d) was considered to be low. Despite only partial shading of vegetation, a lower sun angle and cooler temperature resulted in a moderately high microclimate (k_{mc}) value for the non-growing season. The calculated monthly ET for this community is illustrated below.

Calculated E Values for Landscape Coefficient (Kc)

Season	Species Factor (k_{sp})	Density Factor (k_d)	Microclimate Factor (k_{mc})	Landscape Coefficient (K_c)
Growing	0.9	1.3	1.0	1.17
Non-Growing	0.3	0.5	1.0	0.15

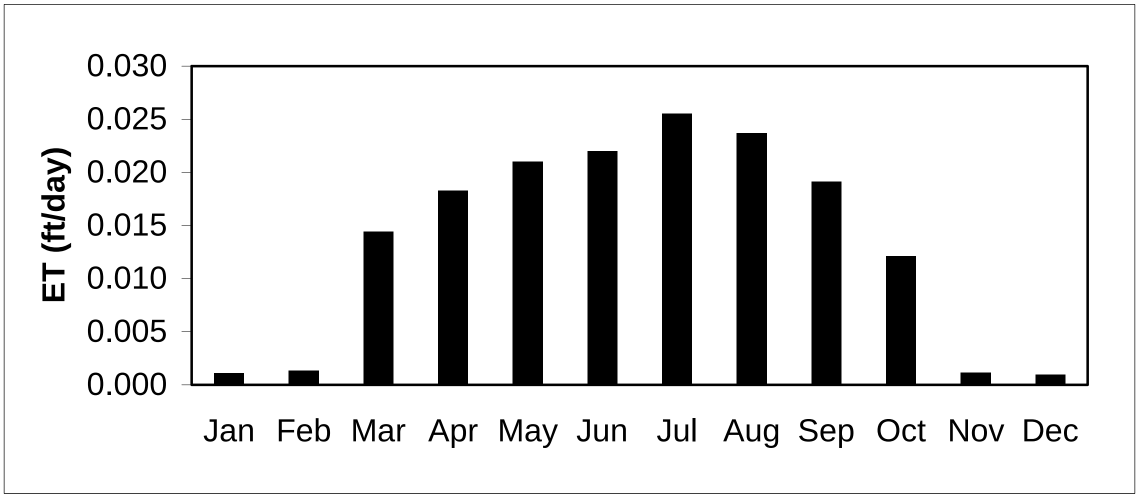

Monthly Evapotranspiration for Southern Cottonwood Willow Riparian Woodland in Prado Basin

Southern Willow Scrub

<u>Mapping Unit Description</u>

Southern Willow Scrub vegetation unit is a minor cover class within Prado Basin (Photo Points 23 and 24). *Southern Willow Scrub* is often found in very dense thickets adjacent to creeks and ponded areas. It is typically associated with areas of loose, sandy alluvium, developed by frequent flooding or scouring that prevents succession to a riparian forest of larger trees species. The great majority of the flora within this category consists of deciduous shrubs and annuals. Dominant species include sandbar willow (*Salix hindsiana*), arroyo willow (*Salix lasiolepis*), tamarisk (*Tamarisk aphylla*), Douglas' mugwort (*Artemisia douglasiana*), arrow weed (*Pluchea sericea*), and cocklebur (*Xanthium strumarium*). Dominant species of the habitat are identified below.

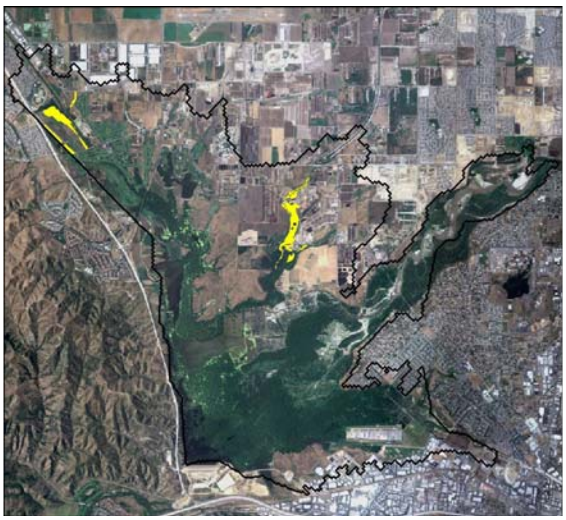

Photo Point 23

Photo Point 24

Southern Willow Scrub Dominant Flora Species

Canopy Species	**Understory Species**
Sandbar Willow (*Salix hindsiana*)	Douglas' Mugwort (*Artemisia douglasiana*)
Arroyo Willow (*Salix lasiolepis*)	Arrow Weed (*Pluchea sericea*)
Tamarisk (*Tamarisk aphylla*)	Cocklebur (*Xanthium strumarium*)

<u>Community Water Demand</u>

Water demand for this habitat varies by season due to the deciduous nature of both the taller shrubs and several of the understory species. Foliage loss by the dominant canopy species does not translate to dormancy of the entire plant community, because growth of perennials during the winter months can lead to some water loss. Therefore, a high landscape coefficient (K_c) was computed for the growing season and a low value was determined for the non-growing season. The factors used for calculation of both growing and non-growing season landscape coefficients are listed below.

<u>Evapotranspiration Calculations</u>

Determination of ET has been accomplished as follows. During the growing season (March – October) the *Southern Willow Scrub* community vegetation unit has a relatively high water need. A high species factor (k_s) value was obtained for the willows category as listed in the

WUCOLS III Species Evaluation List (Costello and Jones, 2000). Multiple tiers during the growing season resulted in a high density factor (k_d). A moderately high microclimate (k_{mc}) value was determined due to the high exposure of the vegetation.

During the non-growing season, (November – February) the *Southern Willow Scrub* vegetation unit has a reduced water demand because it occurs on the upper banks of drainages and washes with high seasonal flows resulting in a moderately low species factor (k_s) value. Deciduous tree species are considered dormant during the non-growing season, and although some understory vegetation is growing, canopy cover is largely incomplete and the community lacks multiple tiers (i.e. vertical dimension). As a result (k_d) was considered moderately low. Despite only partial shading of vegetation, a lower sun angle and cooler temperatures resulted in a moderately high microclimate (k_{mc}) value for the non-growing season. The calculated monthly ET for this community is illustrated below.

Factors for calculation of Landscape Coefficient (Kc)

Season	**Species Factor (k_{sp})**	**Density Factor (k_d)**	**Microclimate Factor (k_{mc})**	**Landscape Coefficient (K_c)**
Growing Season	0.9	1.3	1.0	1.17
Non-Growing Season	0.3	0.5	1.0	0.15

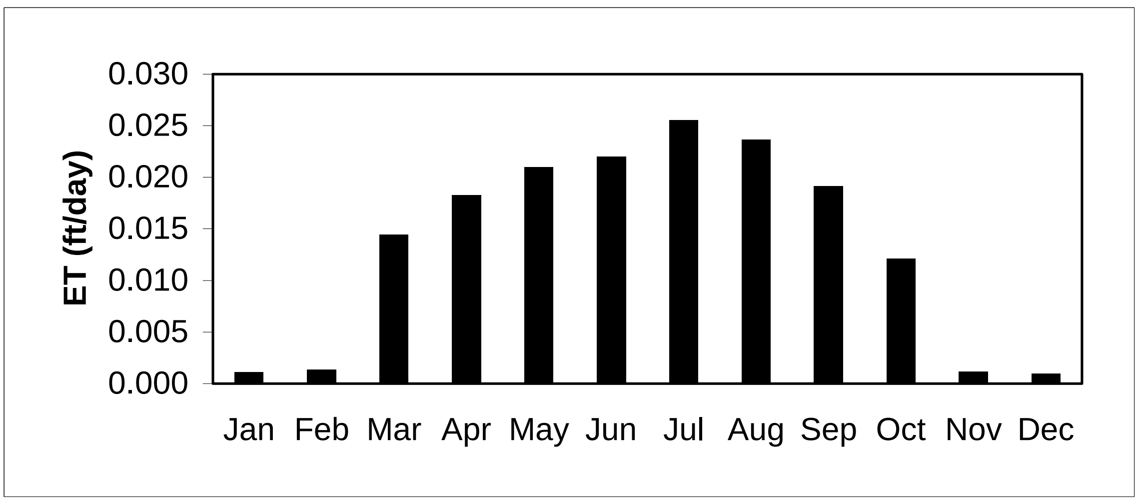

Monthly Evapotranspiration for Southern Willow Scrub in Prado Basin

Unvegetated/Sparsely-vegetated Sandbar

Mapping Unit Description

The *Unvegetated/Sparsely-vegetated Sandbar* vegetation unit is a minor cover class within the Prado Basin. This category is associated with larger drainages within Prado Basin such as the Santa Ana River and Temescal Wash (Photo Points 25 and 26). Sandbars are dynamic in nature because they are formed and maintained during seasonal periods of high flow. The *Unvegetated/Sparsely-vegetated Sandbar* unit occurs in a patchwork pattern along the drainage channels and is comprised primarily of depositional alluvial sands and gravels that become exposed during periods of low flow. These areas support a wide variety of sparsely distributed herbaceous species including curly dock (*Rumex crispus*), common calyptridium (*Calyptridium monandrum*), purslane (*Portulaca oleracea*), fluellin (*Kicksia elatine*), common groundsel (*Senecio vulgaris*), wild heliotrope (*Heliotropium curassavicum*), windmill pink (*Silene gallica*), rattlesnake weed (*Euphorbia albomarginata*), yellow sweet clover (*Melilotus indicus*), and lovegrass (*Eragrostis pilosa*). Due to the sparseness of the herbaceous vegetation that colonizes the sandbars, they are treated as bare soil in our analysis. Dominant species of the habitat are identified below.

Photo Point 25

Photo Point 26

Unvegetated/Sparsely Vegetated Sandbar Dominant Flora Species

Canopy Species	Understory Species
	Curly Dock (*Rumex crispus*)
	Common Calyptridium (*Calyptridium monandrum*)
	Purslane (*Portulaca oleracea*)
	Fluellin (*Kicksia elatine*)
	Common Groundsel (*Senecio vulgaris*)

Community Water Demand

Soil evaporation (E) follows a series of stages. Initially, the E rate is only limited by the amount of energy available to vaporize soil moisture in the upper layer of the soil. Once the water in the surface layer becomes depleted, hydraulic properties determine capillary action to bring water up to the surface layer. Beyond this point, E rate becomes negligible due to soil physical and adsorbing characteristics.

Evaporation Calculations

To calculate E values for each month for the Prado Basin study area, we used published monthly E values for bare soil from reference evapotranspiration zones 6 and 9 (ITRC 2003). The calculated monthly E rates for Prado Basin for bare soil were used to determine E for the Unvegetated/Sparsely -vegetated Sandbar category. The calculated monthly E for this community is illustrated below.

Calculated E Values for Landscape Coefficient (Kc)

Growing Season	Jun	Jul	Aug	Sep	Oct
Evaporation (ft/day)	0.000069	0.000040	0.000309	0.001111	0.000860

Non-Growing Season	Nov	Dec	Jan	Feb	Mar	Apr	May
Evaporation (ft/day)	0.003389	0.004167	0.004530	0.002039	0.000565	0.000417	0.000188

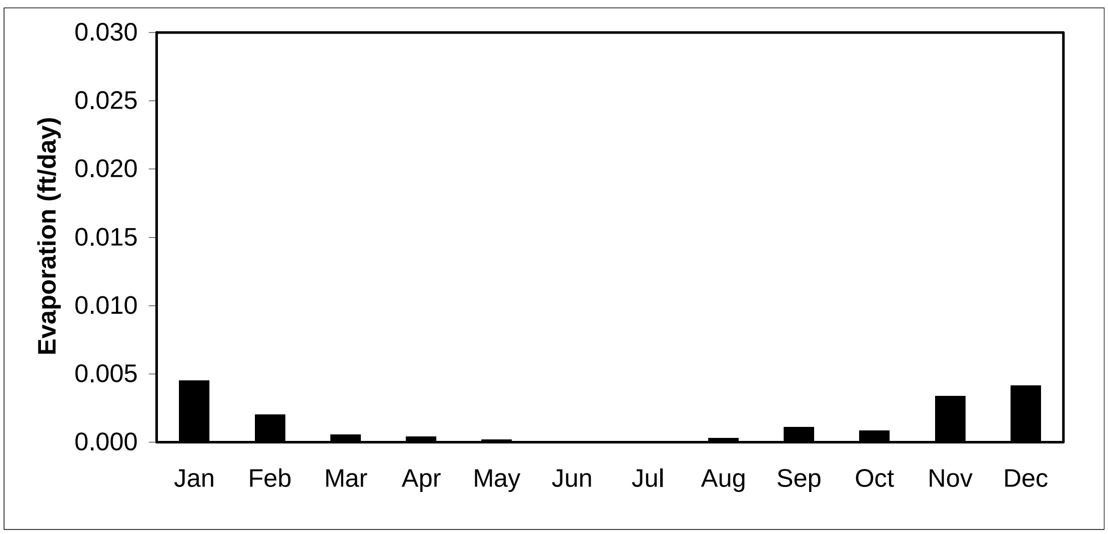

Monthly Evaporation for Unvegetated/Sparsely Vegetated Sandbar in Prado Basin

Turf Irrigated

Mapping Unit Description

The *Turf Irrigated* vegetation unit is a minor cover class within the Prado Basin created to encompass golf course greens of different grass species of the semi-arid southwest varieties (Photo Points 27 and 28). They are similar in their physiological requirements and adaptations to high heat, wind, sunlight, shade, and salt. As actively managed vegetation, *Turf Irrigated* areas are regularly mowed to maintain heights typically between 1 to 3 inches. *Turf Irrigated* is the most structurally uniform of all the vegetative units included in this report. Turf grasses grow in the higher range of soil moisture compared to other non-wetland vegetation communities, and under optimal conditions they are maintained in 4 to 6 inches of damp soil. Dominant species of the habitat are identified below.

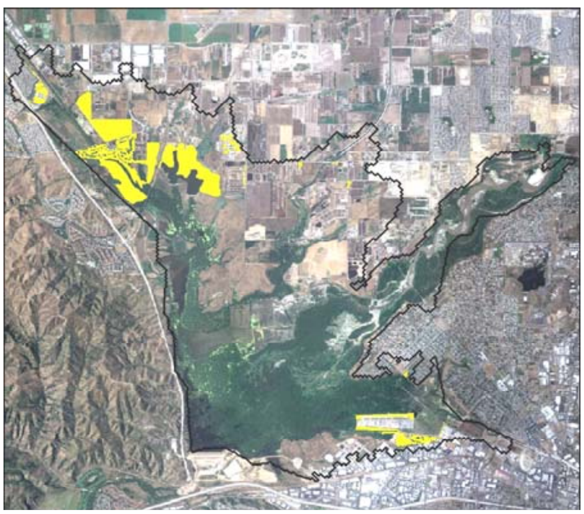

Photo Point 27

Photo Point 28

Turf Irrigated Dominant Flora Species

Canopy Species	**Understory Species**
	St. Augustine Grass (*Stenotaphrum secundatum*)
	Common Bermuda Grass (*Cynodon dactylon*)
	Dandelion (*Taraxacum officinale*) –as weed
	Plantain (*Plantago* spp.) – as weed
	Clover (*Orthocarpus* spp.) - as weed

Turf Irrigated as a vegetation unit was excluded from ET analysis because its water usage is accounted for in imported water calculations. Areas of *Turf Irrigated*, however, were mapped to graphically represent its relative area, locations, and distribution, in relation to the other vegetation units.

Urban Developed

Mapping Unit Description

Urban/Developed as a 'vegetation' unit is a minor cover class within the Prado Basin (Photo Point 29). The *Urban/Developed* category is unique in that this cover class does not represent a collection of vegetation but is characterized by impervious cover associated with developed landscape, paved roads, parking lots (Photo Point 30). These impervious surfaces significantly alter the natural cycling of water from rainfall, evapotranspiration, runoff, and groundwater recharge. For example, as the percent of impervious surfaces increase, there is an increase in rainfall runoff, and concomitantly a reduction in ET and infiltration into the ground.

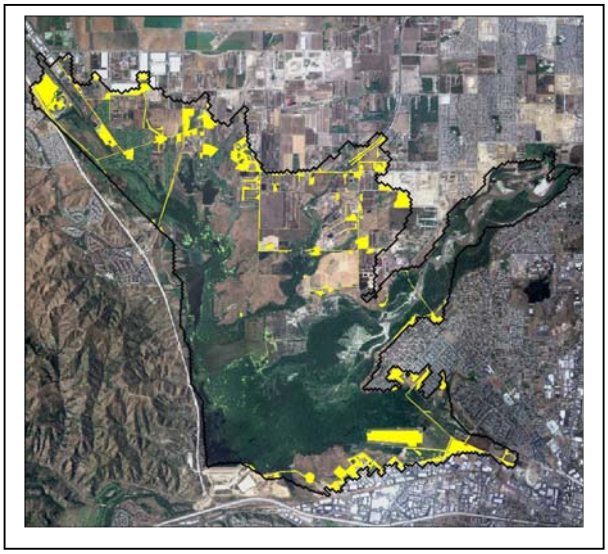

Photo Point 29

Photo Point 30

The *Urban/Developed* catagory was excluded from ET analysis because its water usage is acounted for in imported water calculations. Areas of *Urban/Developed* land, however, were mapped to graphically represent its relative area, location, and distribution in relation to the other vegetation units.

ANALYSIS AND RESULTS

As discussed above, habitat classes were digitized from aerial photographs dated 1974, 1984, and 2006. From this, historic vegetation shapefiles were created for each year. A shapefile of even 60 by 60 meter grid cells for the entire study area was provided by Wildermuth Environmental Inc. to correlate with the grid system employed for the basin water modeling. The model grid was intersected with each of the vegetation shapefiles, resulting in the creation of three (1974, 1984, 2006) new vegetation shapefiles containing the vegetation polygons divided into model grid cells. The area of each polygon was calculated in acres, and this value was multiplied by the appropriate ET_c (ft/day) for each water quarter resulting in four values for each polygon (acre ft/day) for each of the three modeled years. Finally, these values were summed within each cell and the final product was a cell shapefile containing ET_c (acre ft/day) for each cell for each water quarter.

The results of the modeling effort are graphically illustrated as ET (acre ft/day) by model cell for 1974 (Figure10), 1984 (Figure11), and 2006 (Figure12). The summation of the grid cell water demands yields a cumulative demand on a daily basis during the water quarters. When summed across days in each water quarter, the WQ demand in (acre ft) can be derived. The sum of demand for all WQs yields the annual ET demand in (acre ft). These calculated values are shown in Table 2 based on the mean ETo for the Corona RAWS weather station.

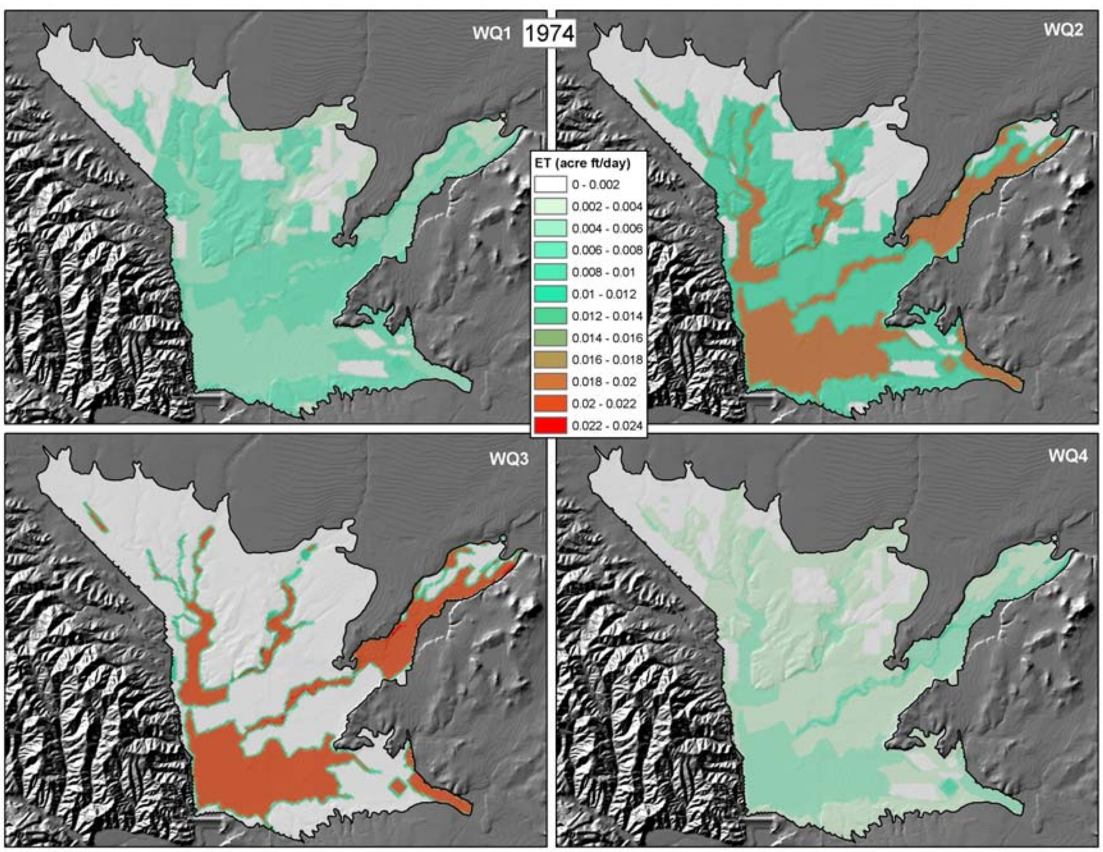

Figure 10. Modeled Evapotranspiration Rates by Water Quarter for 1974 Habitat Conditions.

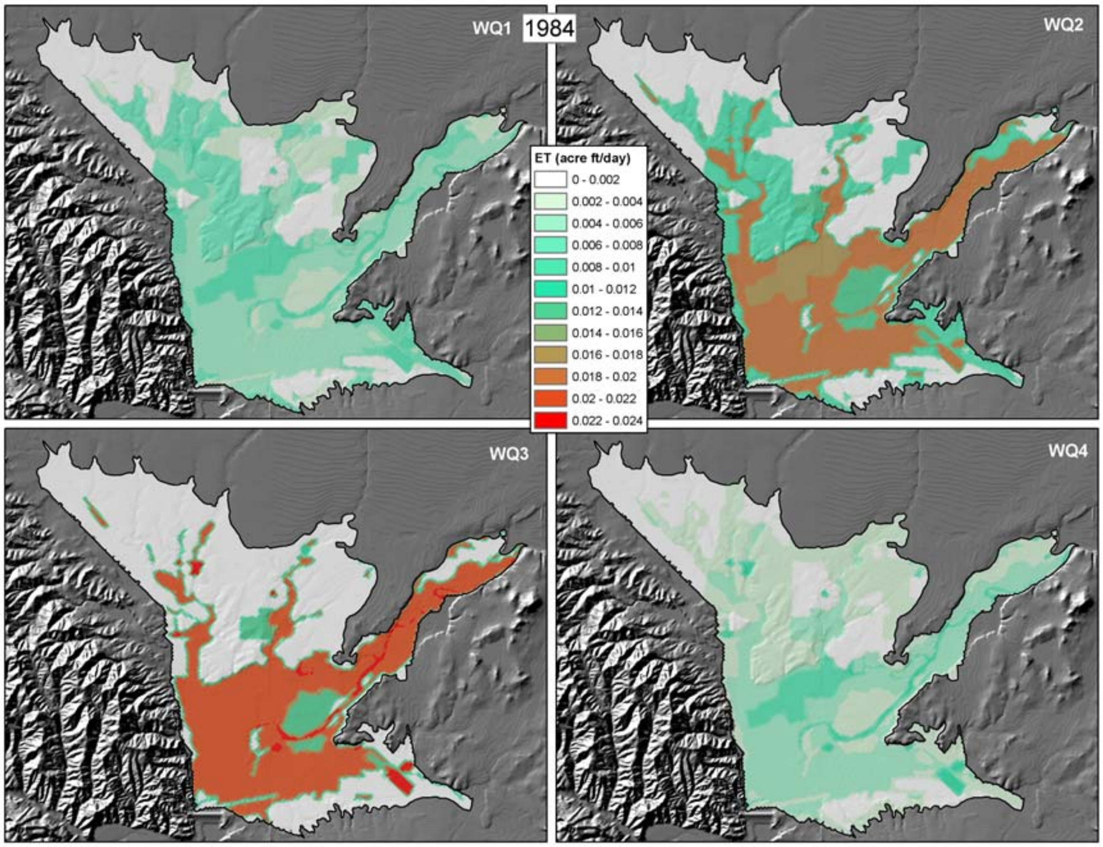

Figure 11. Modeled Evapotranspiration Rates by Water Quarter for 1984 Habitat Conditions.

Table 2. Evapotranspiration for the Prado Basin by Water Quarter (acre feet) Based on Corona RAWS Station Monthly Mean Reference ET 2001-2007.

Year	WQ1		WQ2		WQ3		WQ4		Total
	(per day)	(per WQ)	(per day)	(per WQ)	(per day)	(per WQ)	(per day)	(per WQ)	(per Year)
1974	52	4,710	103	9,358	71	6,491	35	3,196	23,755
1984	48	4,331	109	9,960	101	9,296	38	3,452	27,038
2006	56	5,073	120	10,961	108	9,949	44	4,002	29,985

As a check of the magnitude of variation that may be encountered from year to year, however, the same analyses were conducted using ET_o for the maximum and minimum monthly extremes that were encountered in the station records. This does not suggest that these conditions were all encountered within a given maximum or minimum year, but rather the values are composites of the highest and lowest ET_o conditions encountered for any calendar month of record. The values for the maximum and minimum conditions are illustrated in Table 3.

Table 3. Evapotranspiration for the Prado Basin by Water Quarter (acre feet) Based on Corona RAWS Station Monthly Mean Reference ET 2001-2007.

Year	WQ1		WQ2		WQ3		WQ4		Total
	(per day)	(per WQ)	(per day)	(per WQ)	(per day)	(per WQ)	(per day)	(per WQ)	(per Year)
2006(Min)	26	2,386	78	7,081	92	8,422	28	2,588	20,478
2006(Max)	63	5,695	141	12,830	120	11,063	51	4,696	34,285

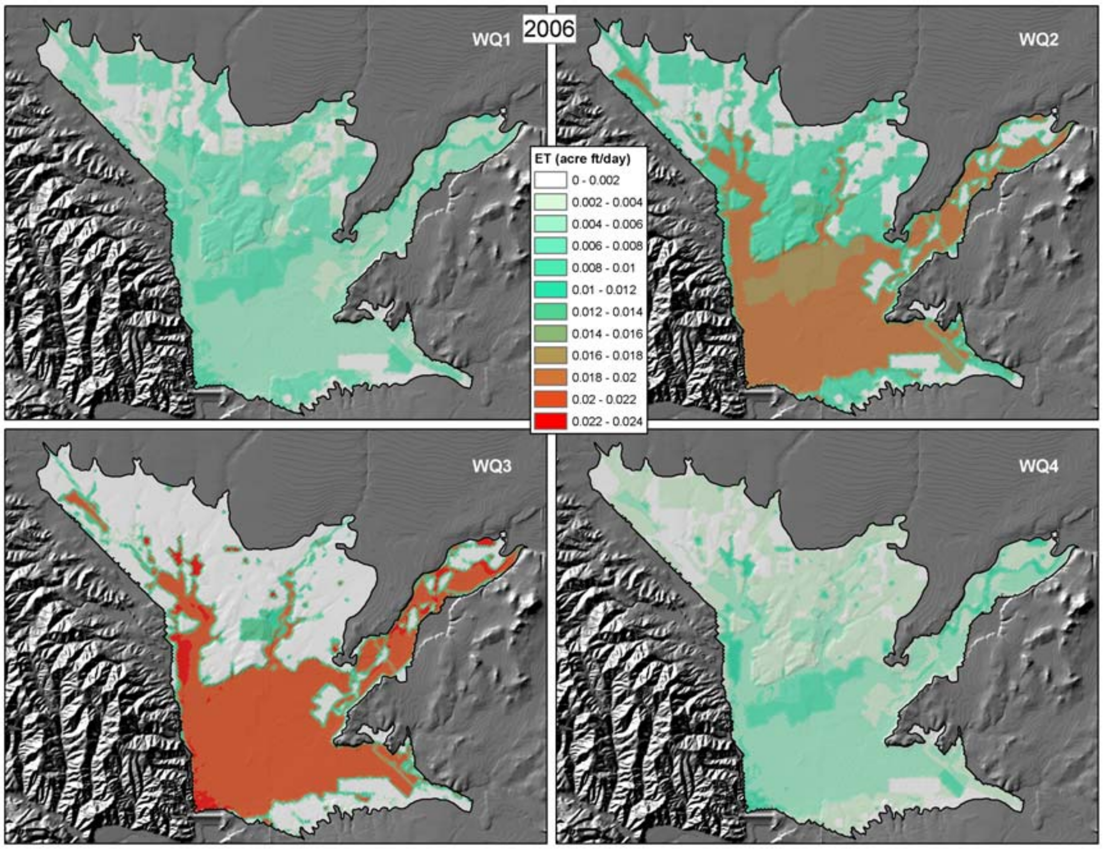

Figure 12. Modeled Evapotranspiration Rates by Water Quarter for 1984 Habitat Conditions.

The sensitivity testing of the maximum and minimum monthly values indicate that under extreme conditions represented by the cumulatively most extreme monthly conditions measured in the past 6 years, evapotranspiration may vary significantly, inspite of static habitat conditions. Elevated evapotranspiration from Prado Basin may exceed by as much as 4,300 acre-feet or 14% per year above the mean. Depressed evapotranspiration rates (minimum) may be as much as 9507 acre-feet or 32% per year below the average.

Digital data has been provided for the grid modeling effort to Wildermuth Environmental, Inc. These data include grid based summary data by water quarter for calculated evapotranspiration rates and values.

REFERENCES

Allen, R.G., Walter, I.A., Elliott, R.L., Howell, T.A., Itenfisu, D., Jensen, M.E., Snyder, R.L. 2005. The ASCE Standardized Reference Evapotranspiration Equation. Reston, Virginia: American Society of Civil Engineers. 59 p. with six appendices.

Costello, L.R., and K.S. Jones, 2000. WUCOLS III (Water Use Classification of Landscape Species); In: A Guide to Estimating Irrigation Water Needs of Landscape Plantings in California. University of California Cooperative Extension, California Department of Water Resources, pp. 150.

Costello, L.R., N.P. Matheny, and J.R. Clark, 2000. The Landscape Coefficient Method); In: A Guide to Estimating Irrigation Water Needs of Landscape Plantings in California. University of California Cooperative Extension, California Department of Water Resources, pp. 44.

Irrigation Training and Research Center (ITRC). 2003. California Crop and Soil Evapotranspiration. ITRC, California Polytechnic State University, San Luis Obispo, California, USA, pp. 65.

Snyder, R.L., 2007. KcMM Crop Coefficient Multiple Model. LAWR, University of California, Davis, CA.

Snyder, R.L., B.J. Lanini, D.A. Shaw, and W.O. Pruitt, 1989. Using Reference Evapotranspiration (ETo) and Crop Coefficients to Estimate Crop Evapotranspiration (ETc) for Agronomic Crops, Grasses, and Vegetable Crops. Cooperative Extension University of California, Division of Agriculture and Natural Resources, Leaflet 21427.

Walton, W. E. 2002. Multipurpose Constructed Treatment Wetlands in the Arid Southwestern United States: Are The Benefits Worth the Risks? In: “Treatment Wetlands for Water Quality Improvement: Quebec 2000 Conference Proceedings (Selected Papers).” (J. Pries, ed.). CH2M Hill Canada Limited, Pandora Press, Waterloo, ON. (Invited paper). pp. 115-123.

Walton, W. E. and J. A. Jiannino. 2005. Vegetation Management to Stimulate Denitrification Increases Mosquito Abundance in Multipurpose Constructed Wetlands. J. Am. Mosq. Control Assoc. 21: 22-27.

Appendix D

Simulated and Measured Water Levels in the Calibration Wells, 1960-2006

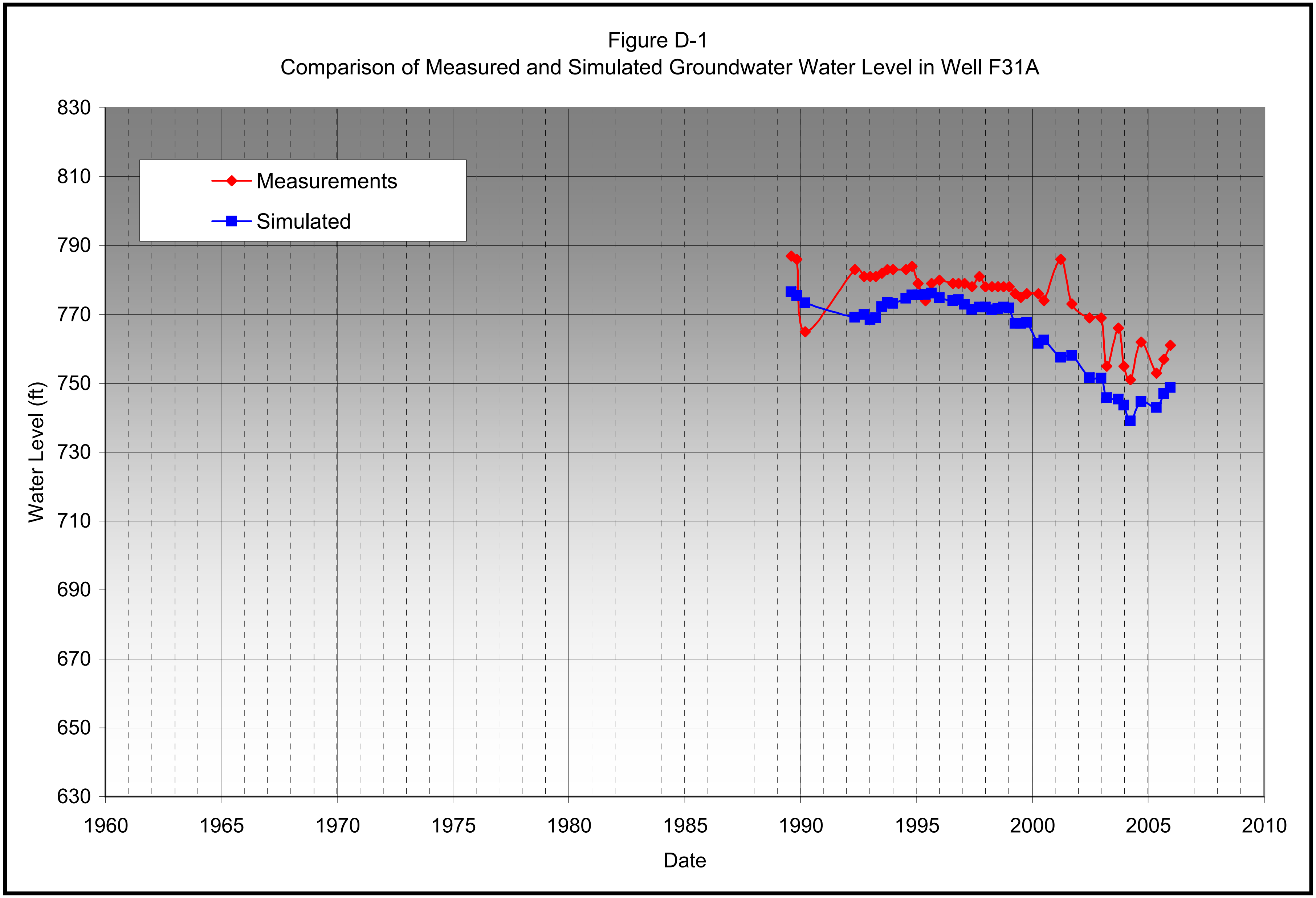

WILDERMUTH™ ENVIRONMENTAL INC.

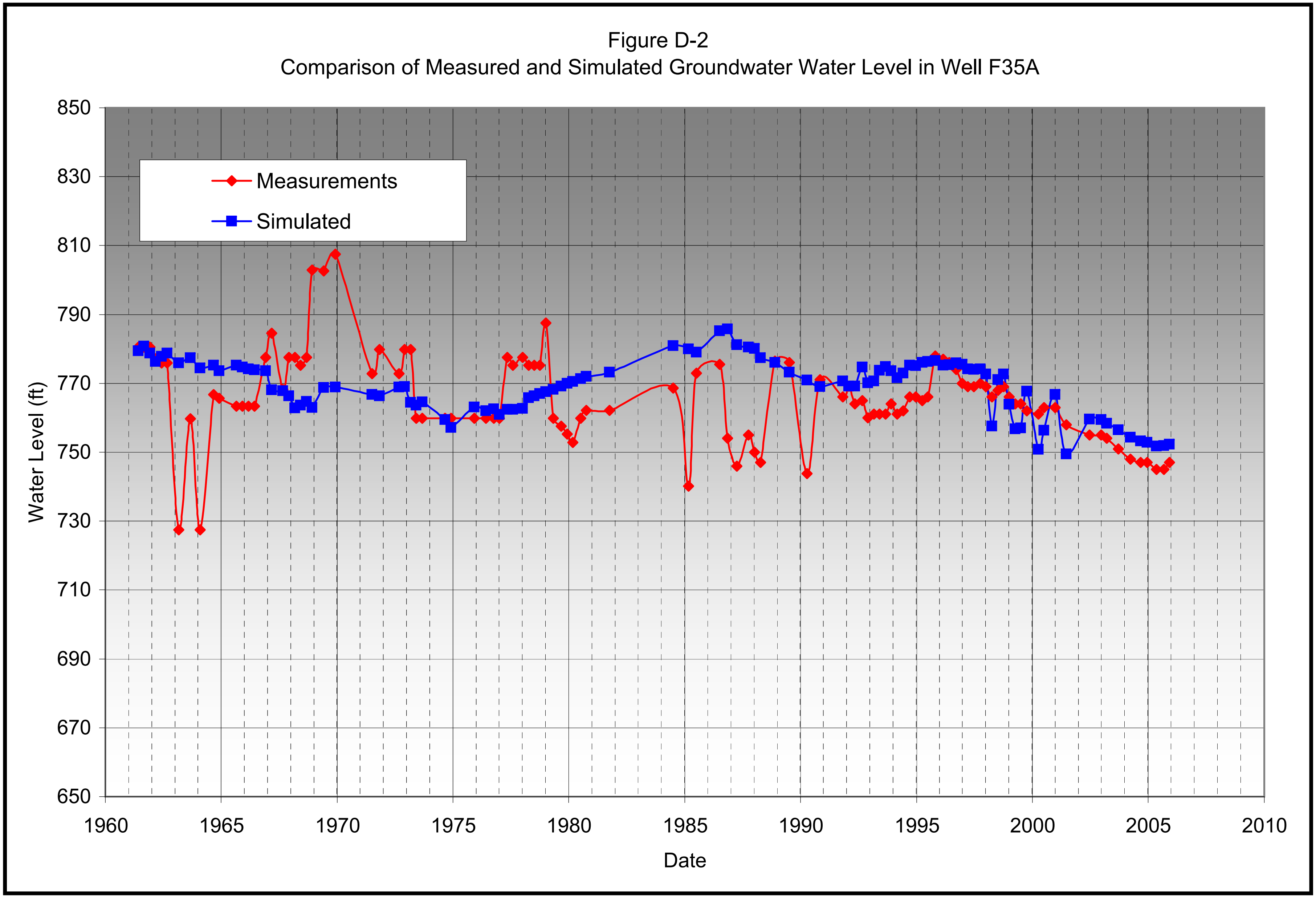

WILDERMUTH™ ENVIRONMENTAL INC.

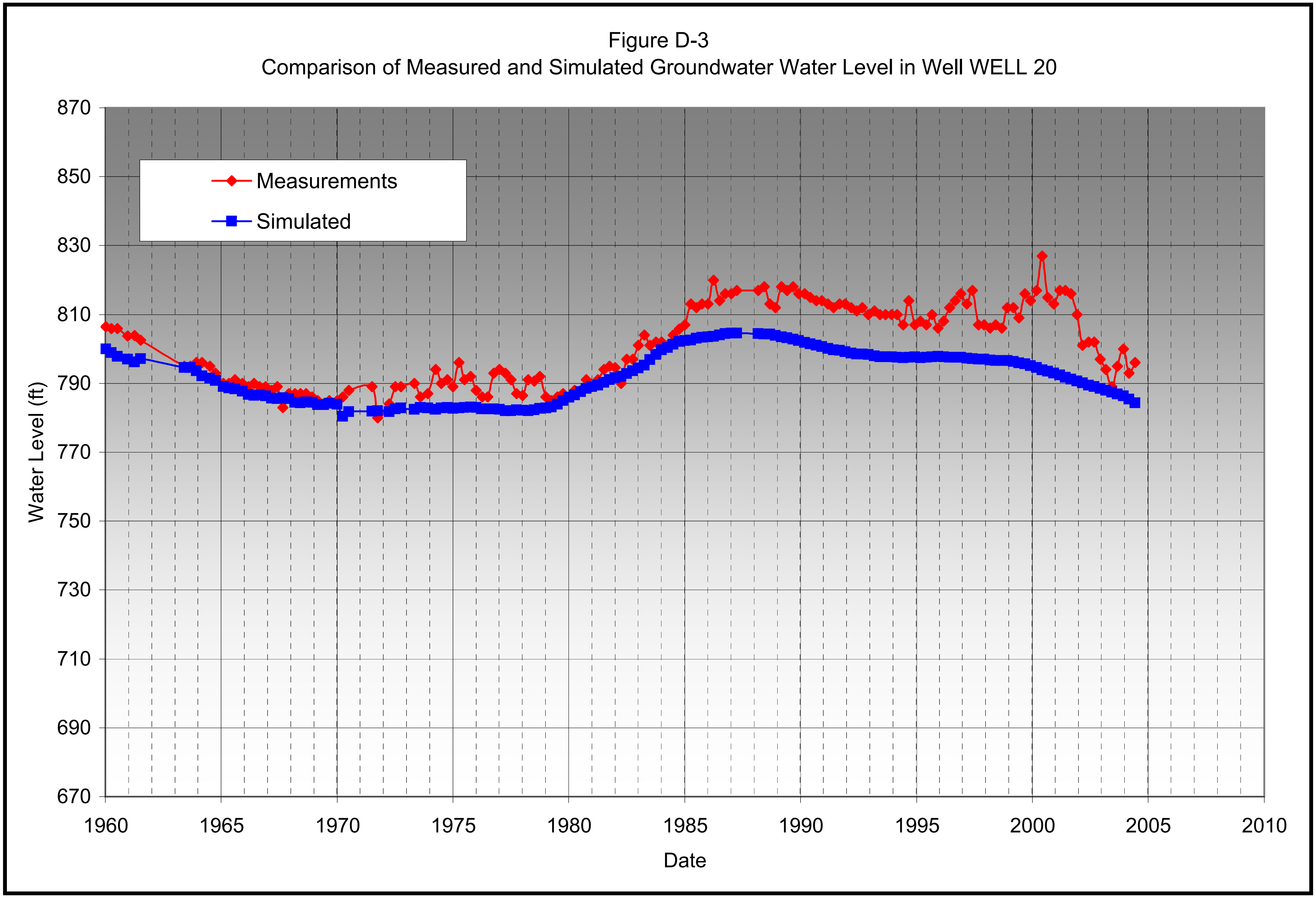

WILDERMUTH™ ENVIRONMENTAL INC.

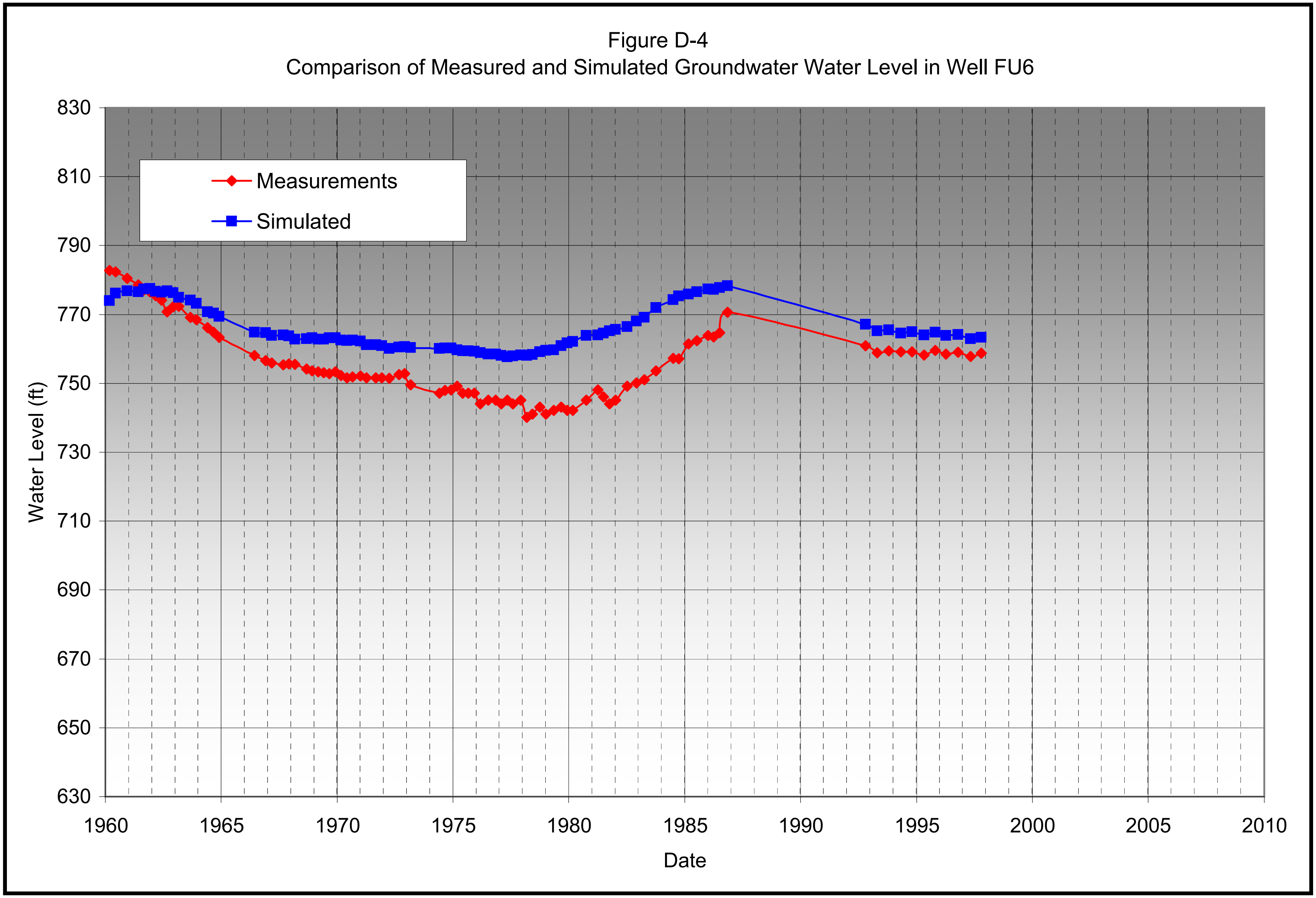

Figure D-4
Comparison of Measured and Simulated Groundwater Water Level in Well FU6
Measurements
Simulated
Water Level (ft)
830
810
790
770
750
730
710
690
670
650
630
1960
1965
1970
1975
1980
1985
1990
1995
2000
2005
2010
Date

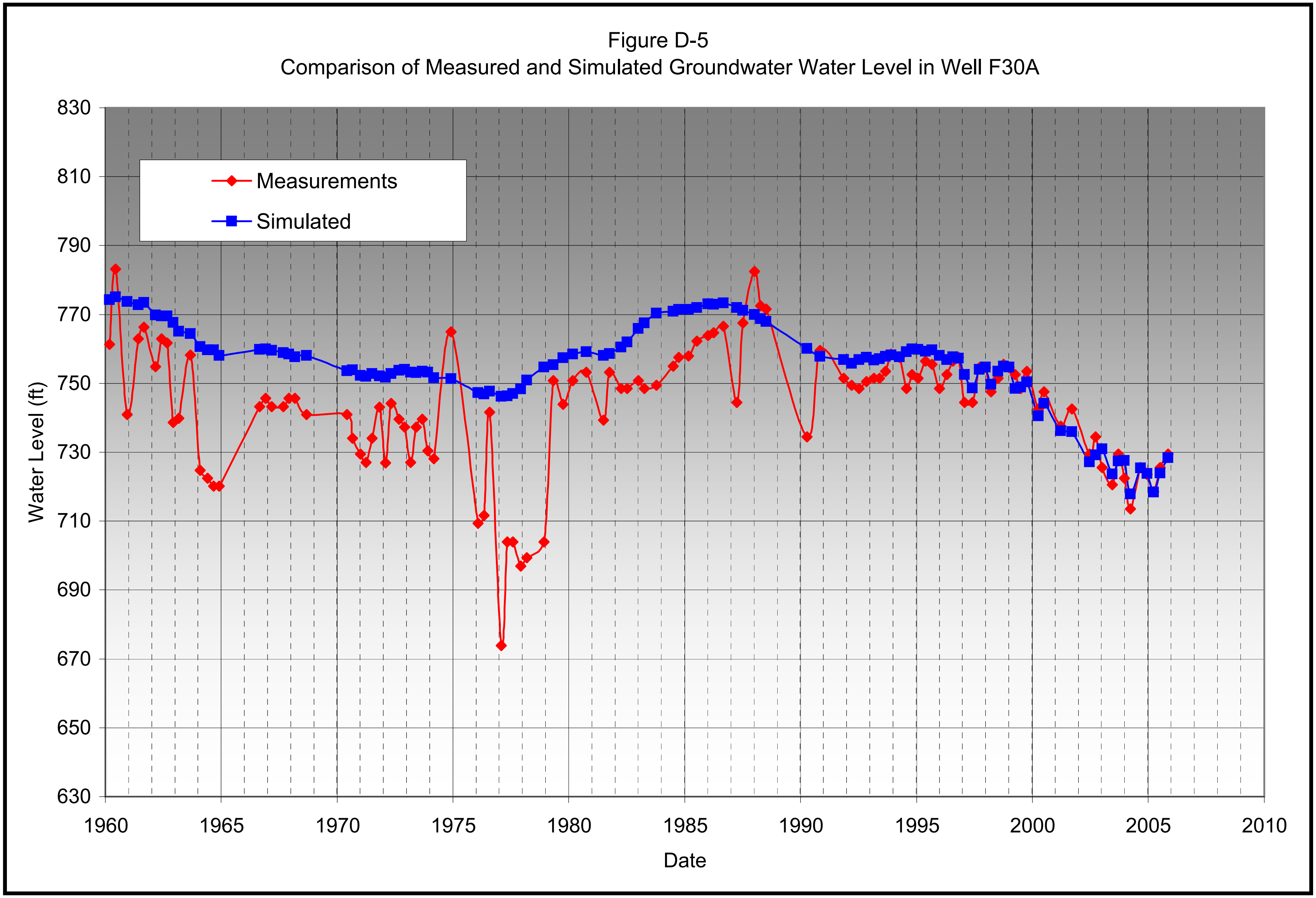

Figure D-5
Comparison of Measured and Simulated Groundwater Water Level in Well F30A
Measurements
Simulated
Water Level (ft)
830
810
790
770
750
730
710
690
670
650
630
1960
1965
1970
1975
1980
1985
1990
1995
2000
2005
2010
Date

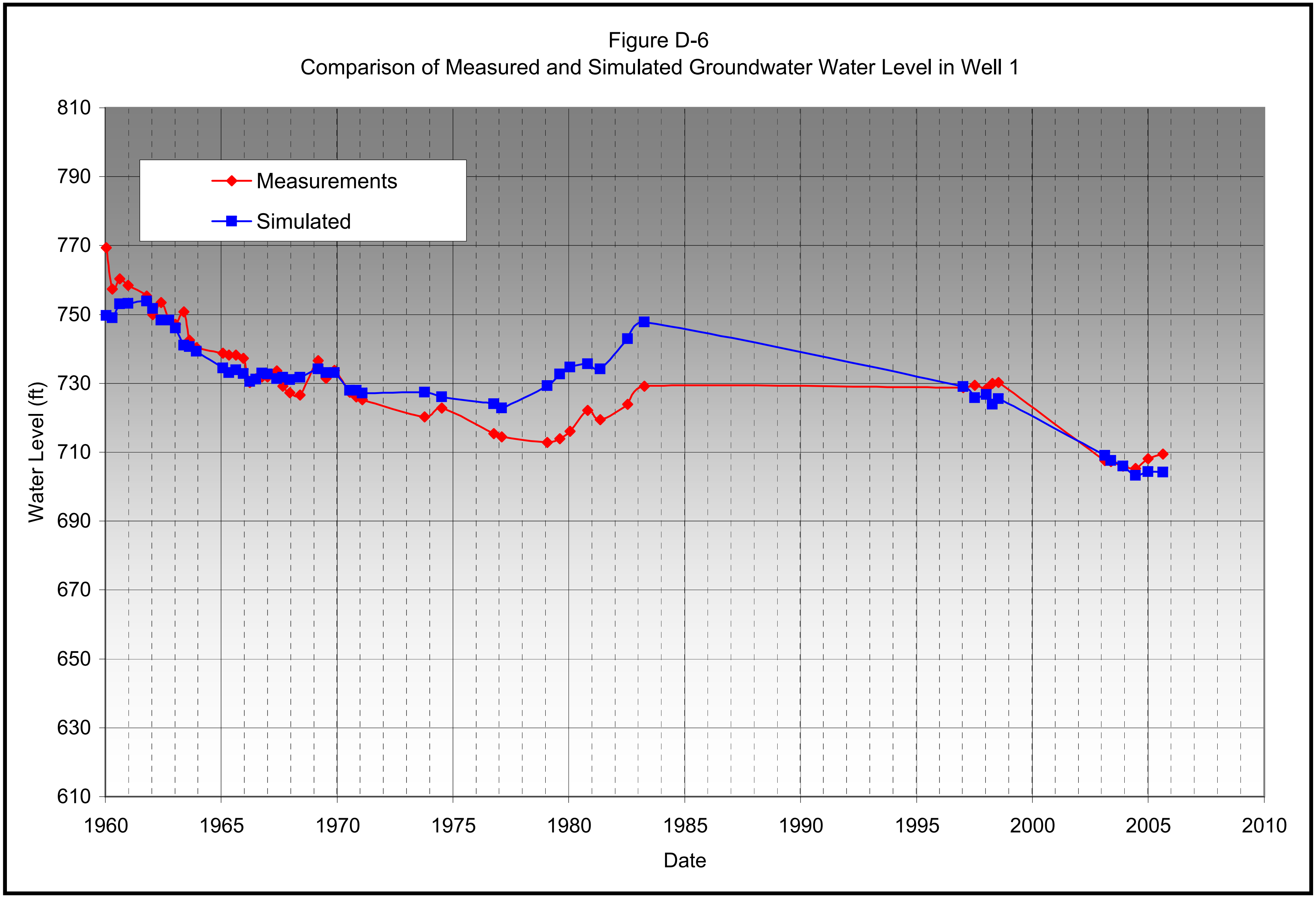

WILDERMUTH ENVIRONMENTAL INC.

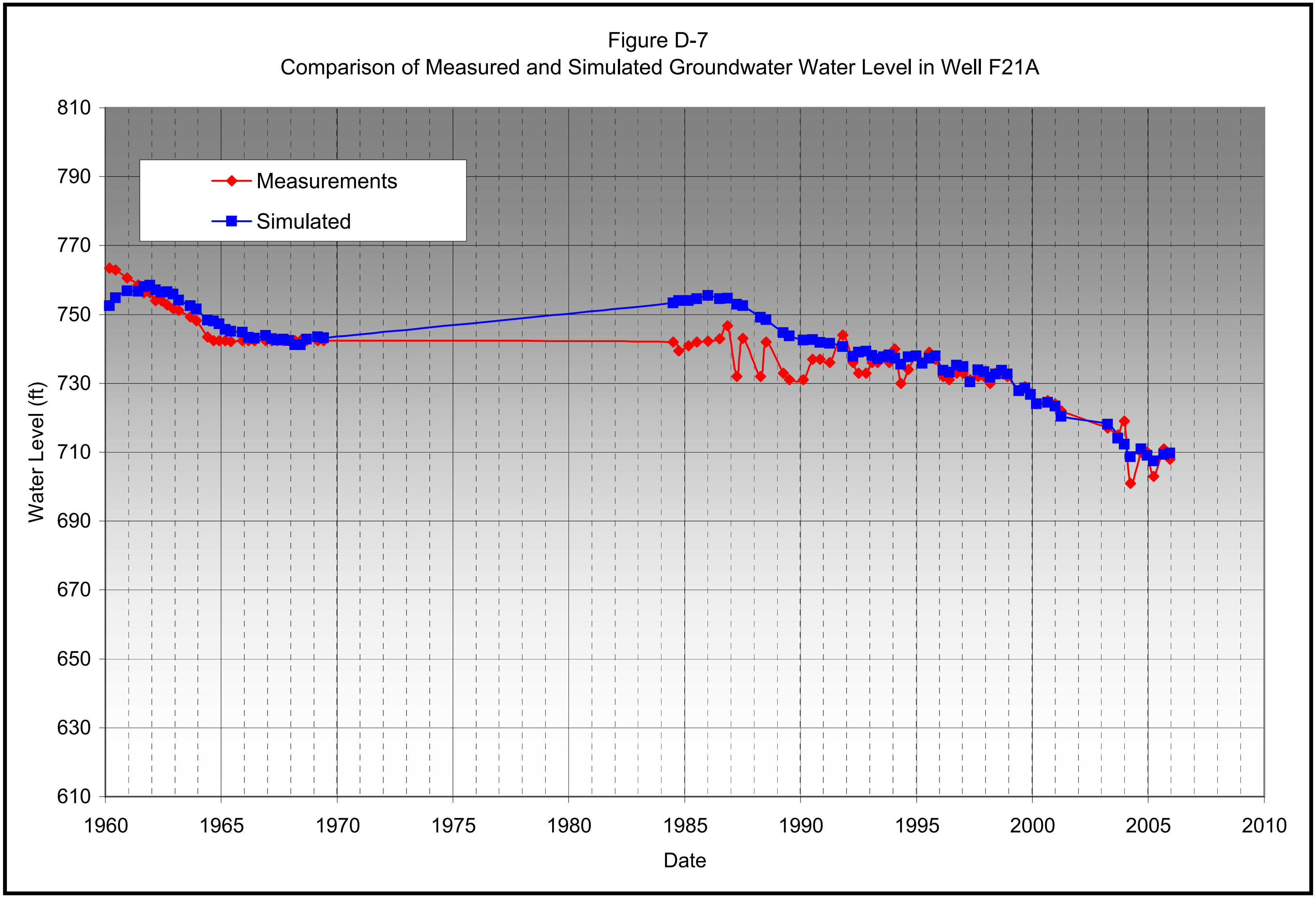

WILDERMUTH™ ENVIRONMENTAL INC.

Figure D-8
Comparison of Measured and Simulated Groundwater Water Level in Well 31

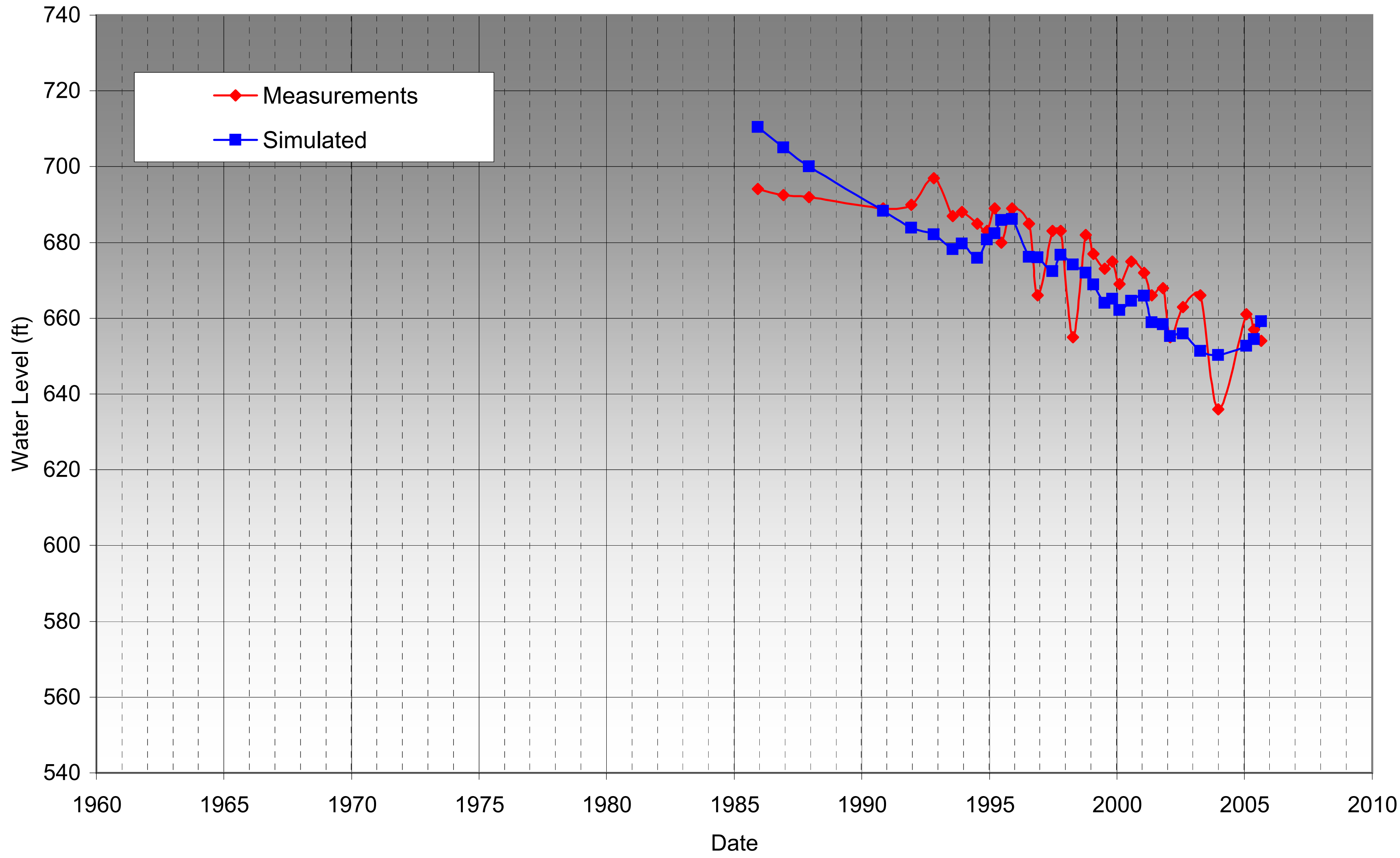

Appendix D Calibration Plots.xls

WILDERMUTH™ ENVIRONMENTAL INC.

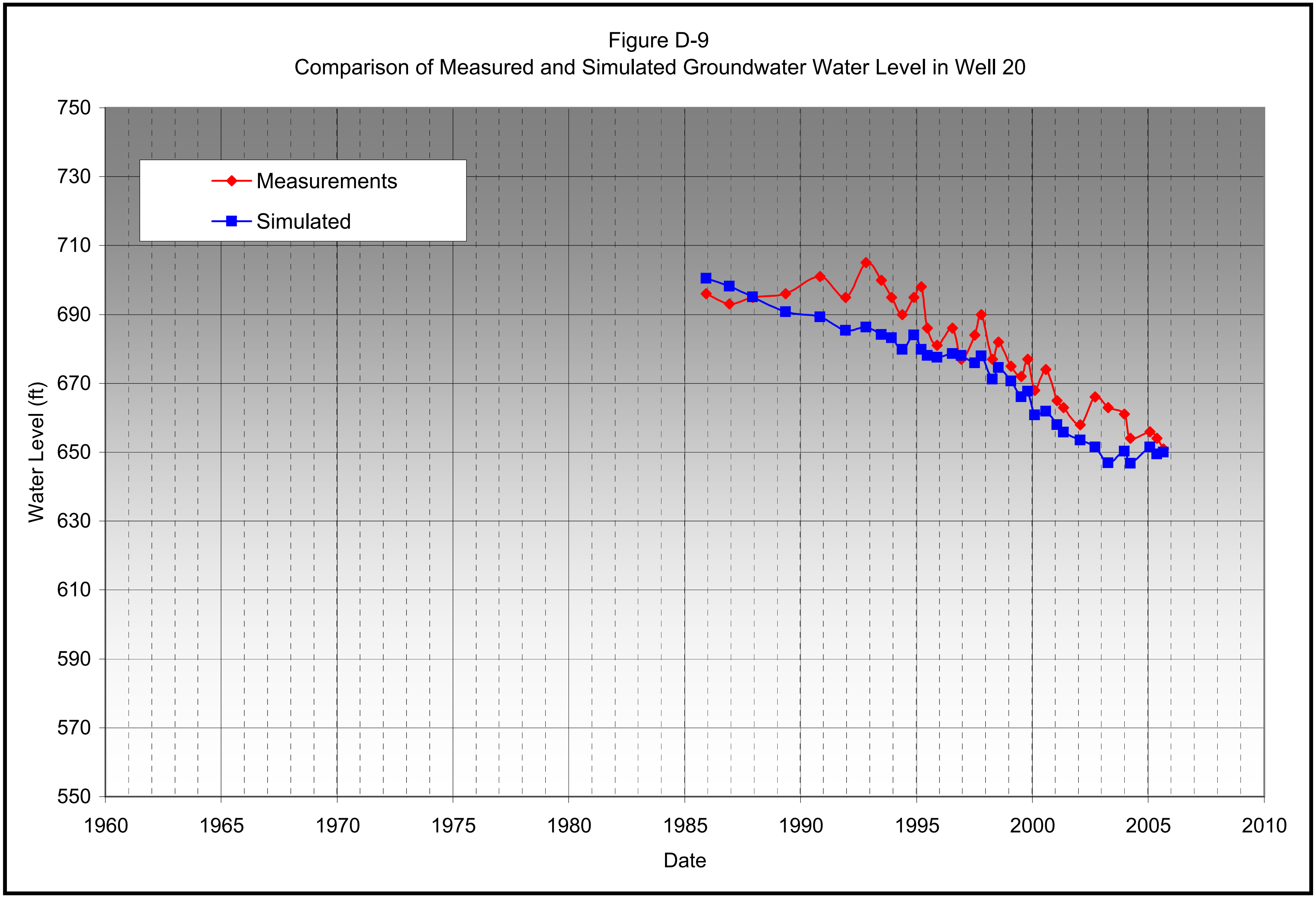

Figure D-9
Comparison of Measured and Simulated Groundwater Water Level in Well 20
Measurements
Simulated
Water Level (ft)
750
730
710
690
670
650
630
610
590
570
550
1960
1965
1970
1975
1980
1985
1990
1995
2000
2005
2010
Date

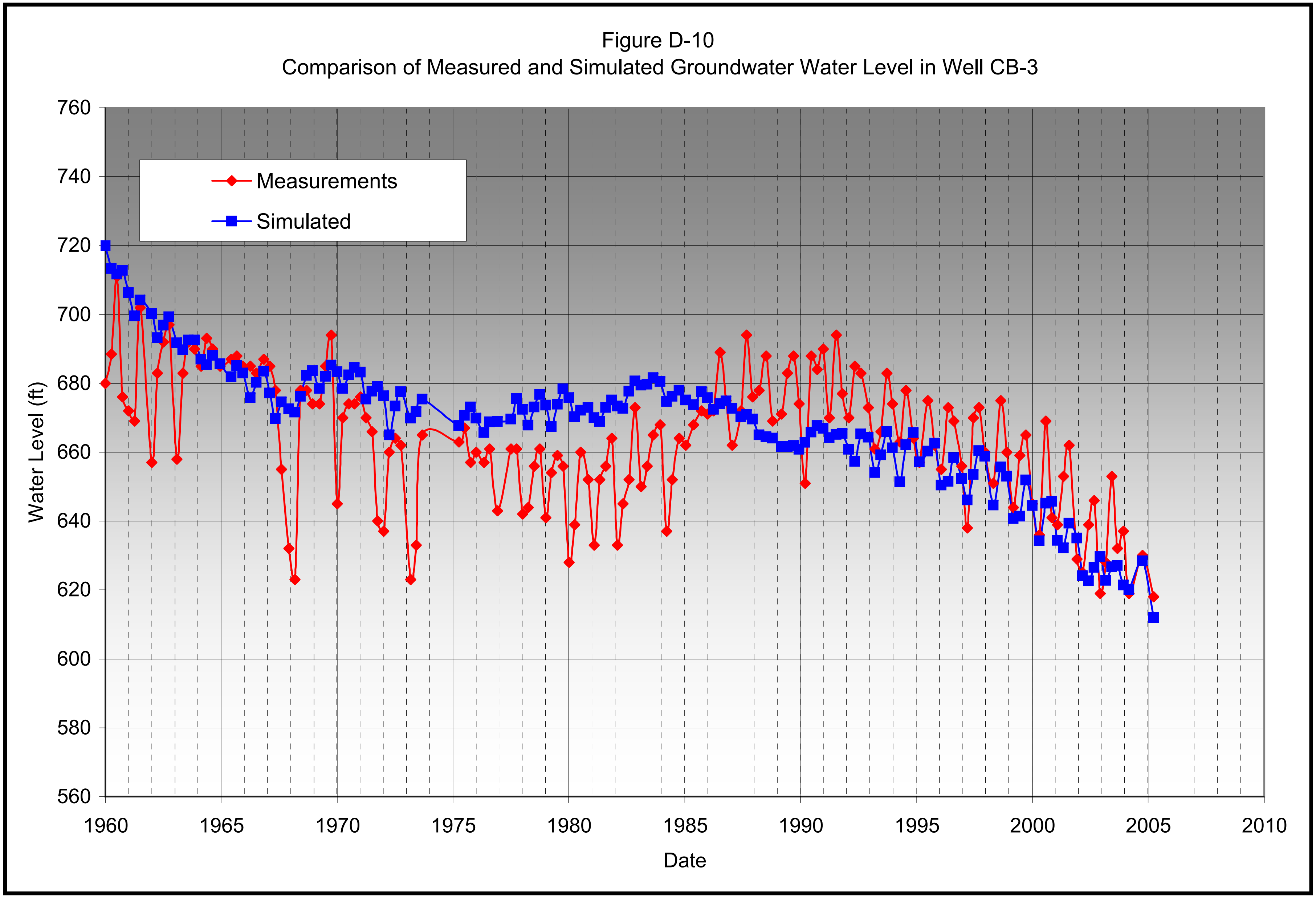

WILDERMUTH™ ENVIRONMENTAL INC.

Figure D-11
Comparison of Measured and Simulated Groundwater Water Level in Well Ontario09

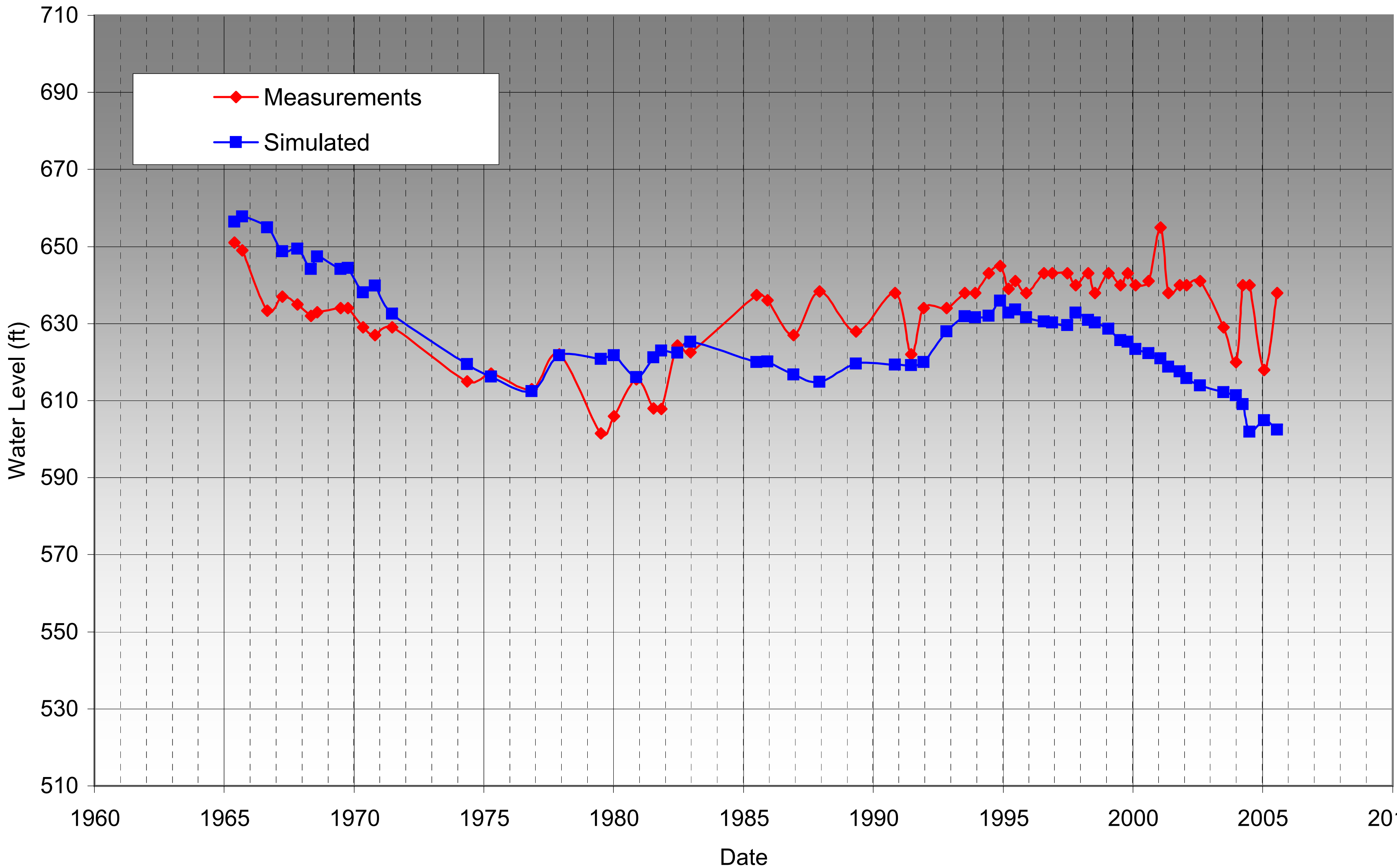

Appendix D Calibration Plots.xls

WILDERMUTH™ ENVIRONMENTAL INC.

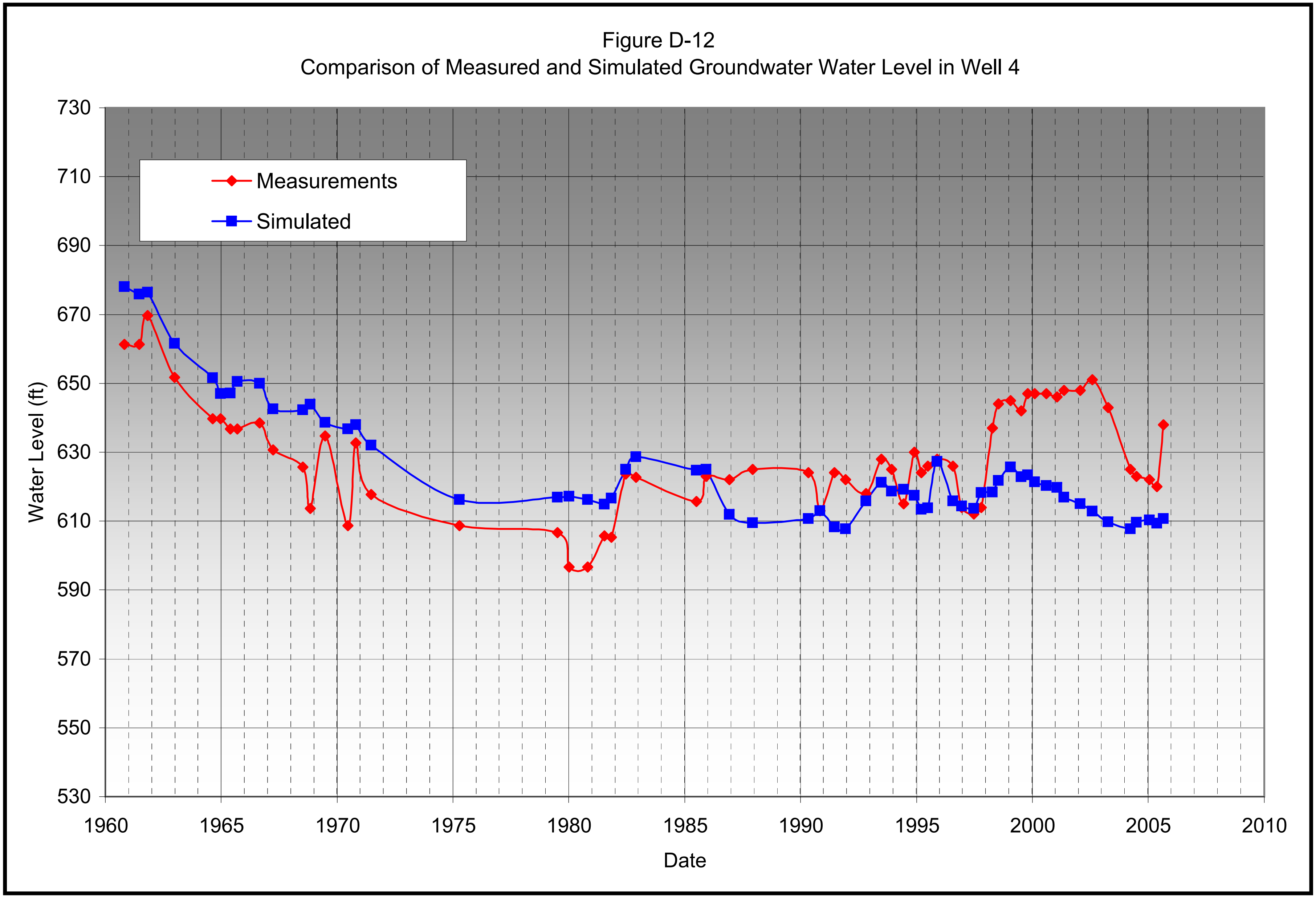
Figure D-12
Comparison of Measured and Simulated Groundwater Water Level in Well 4
Measurements
Simulated
Water Level (ft)
730
710
690
670
650
630
610
590
570
550
530
1960
1965
1970
1975
1980
1985
1990
1995
2000
2005
2010
Date

Figure D-13
Comparison of Measured and Simulated Groundwater Water Level in Well Ontario07

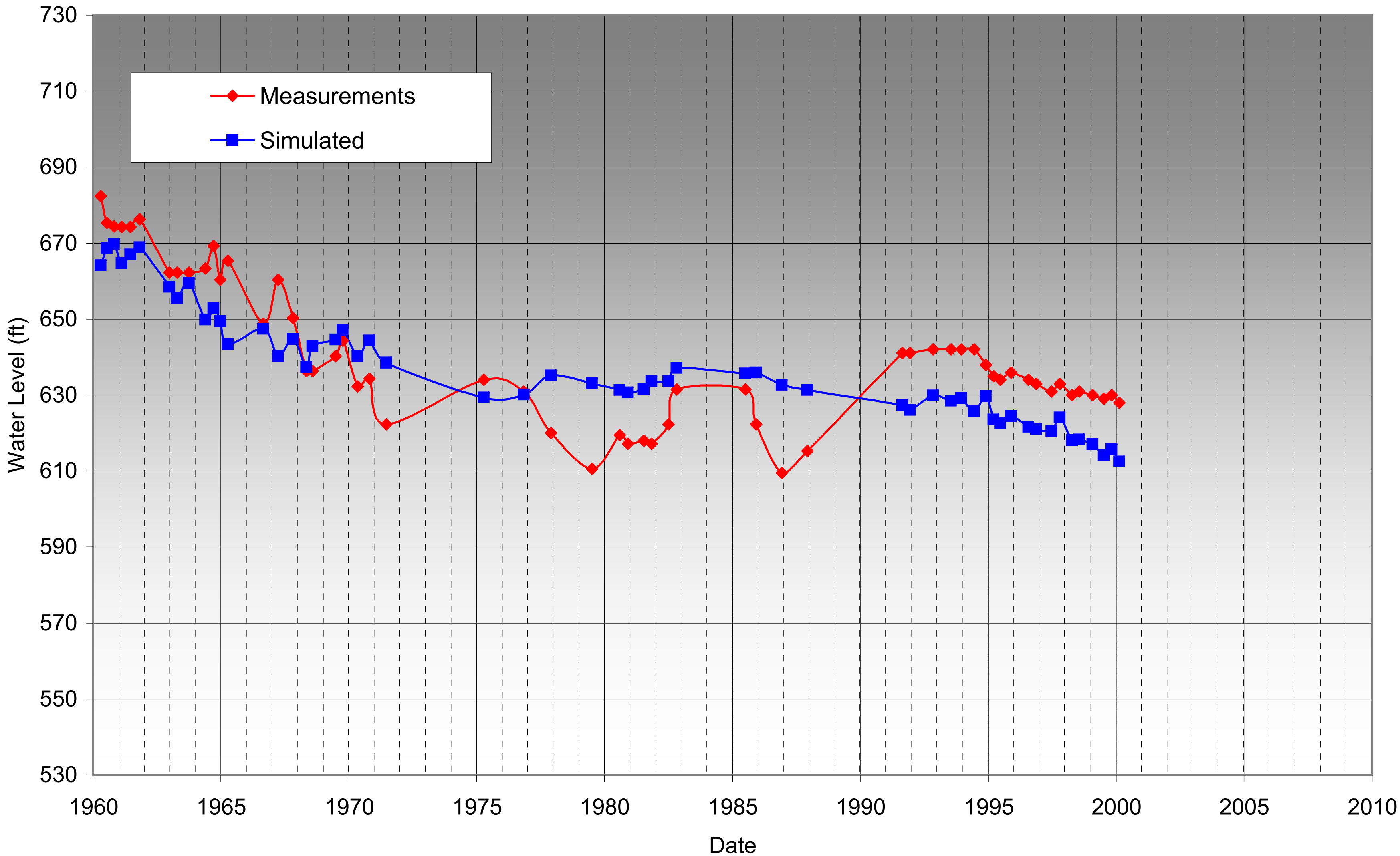

WILDERMUTH™ ENVIRONMENTAL INC.

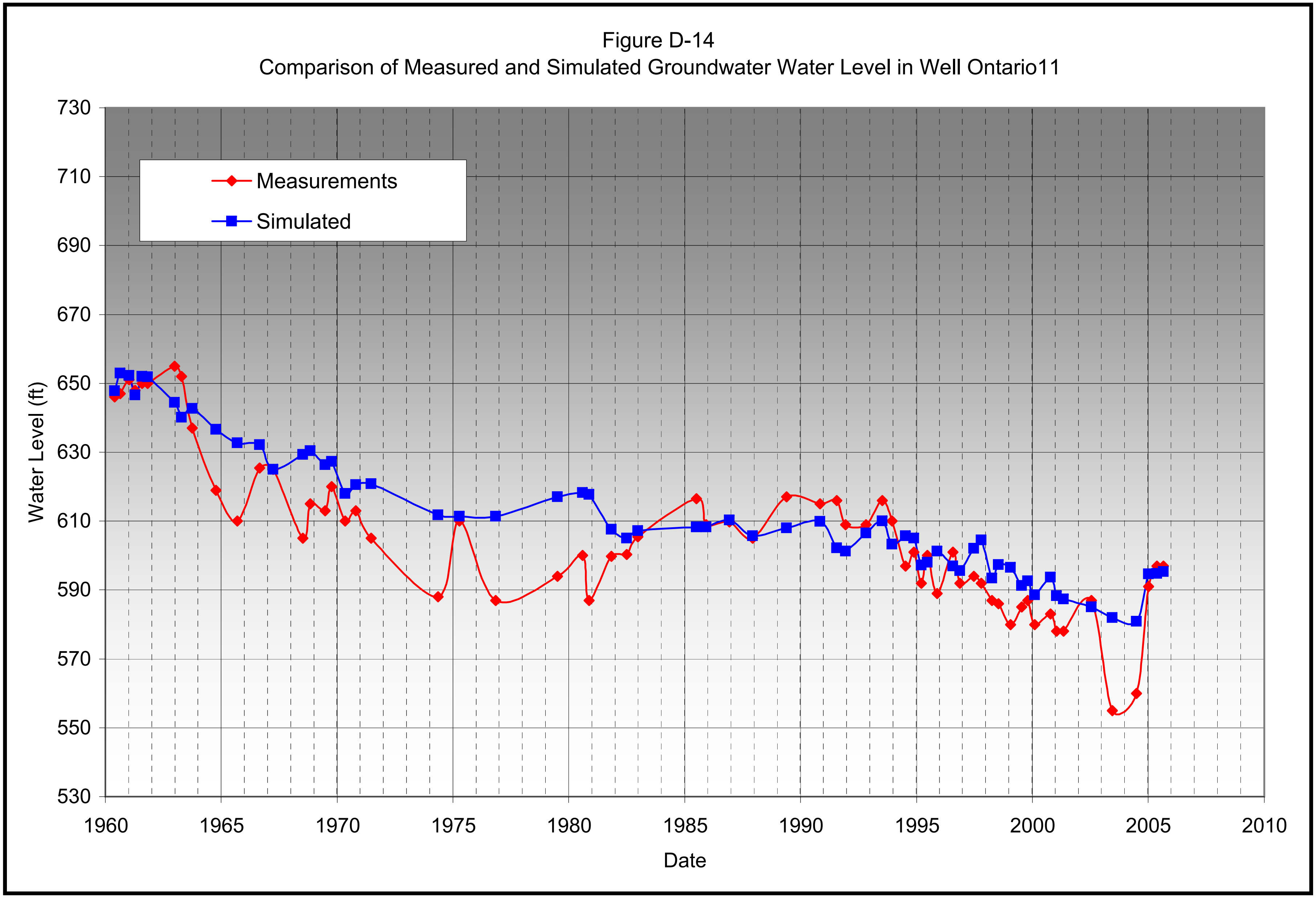
Figure D-14
Comparison of Measured and Simulated Groundwater Water Level in Well Ontario11
Measurements
Simulated
Water Level (ft)
730
710
690
670
650
630
610
590
570
550
530
1960
1965
1970
1975
1980
1985
1990
1995
2000
2005
2010
Date

Figure D-15
Comparison of Measured and Simulated Groundwater Water Level in Well Ontario08

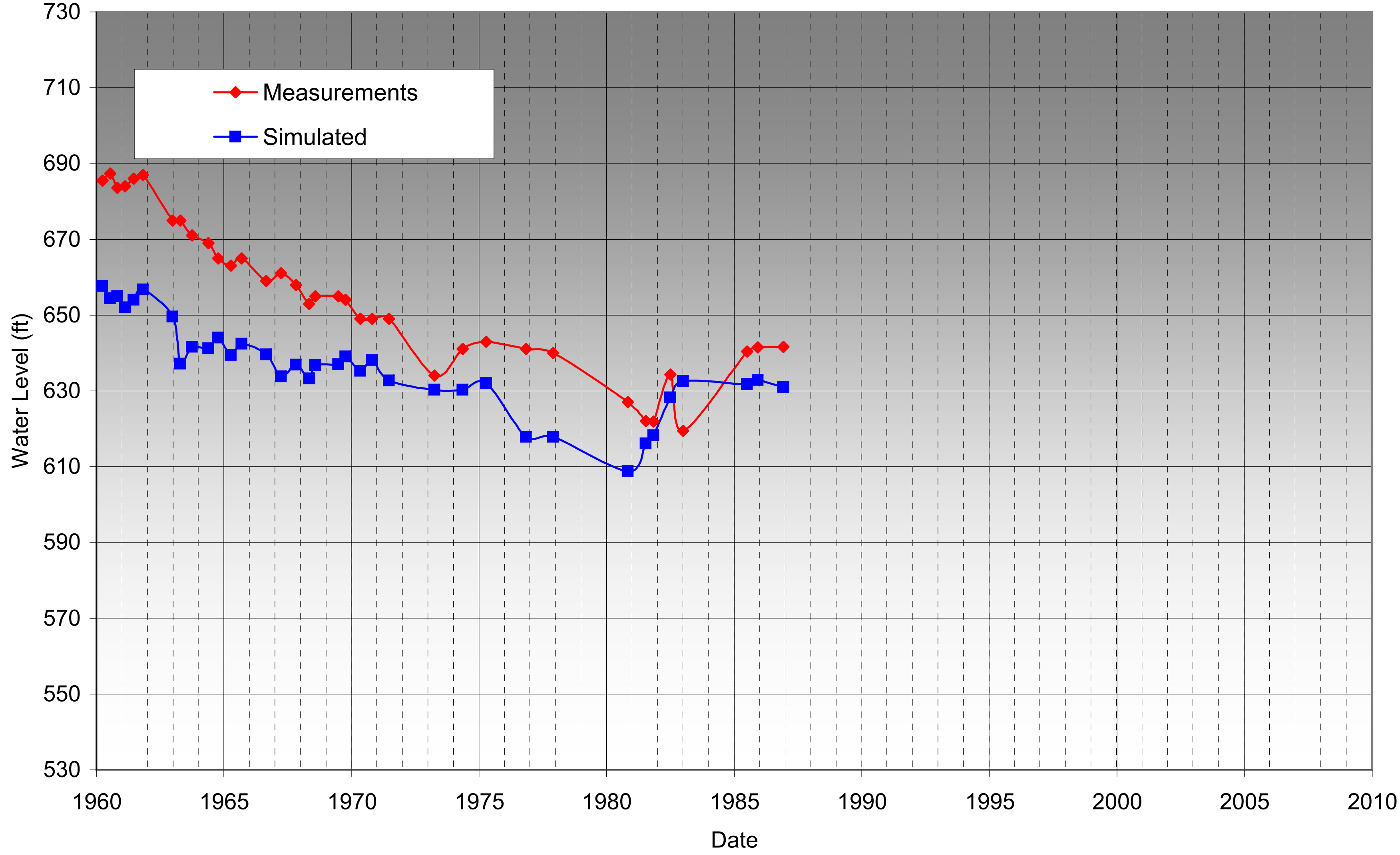

WILDERMUTH™ ENVIRONMENTAL INC.

Figure D-16
Comparison of Measured and Simulated Groundwater Water Level in Well 36

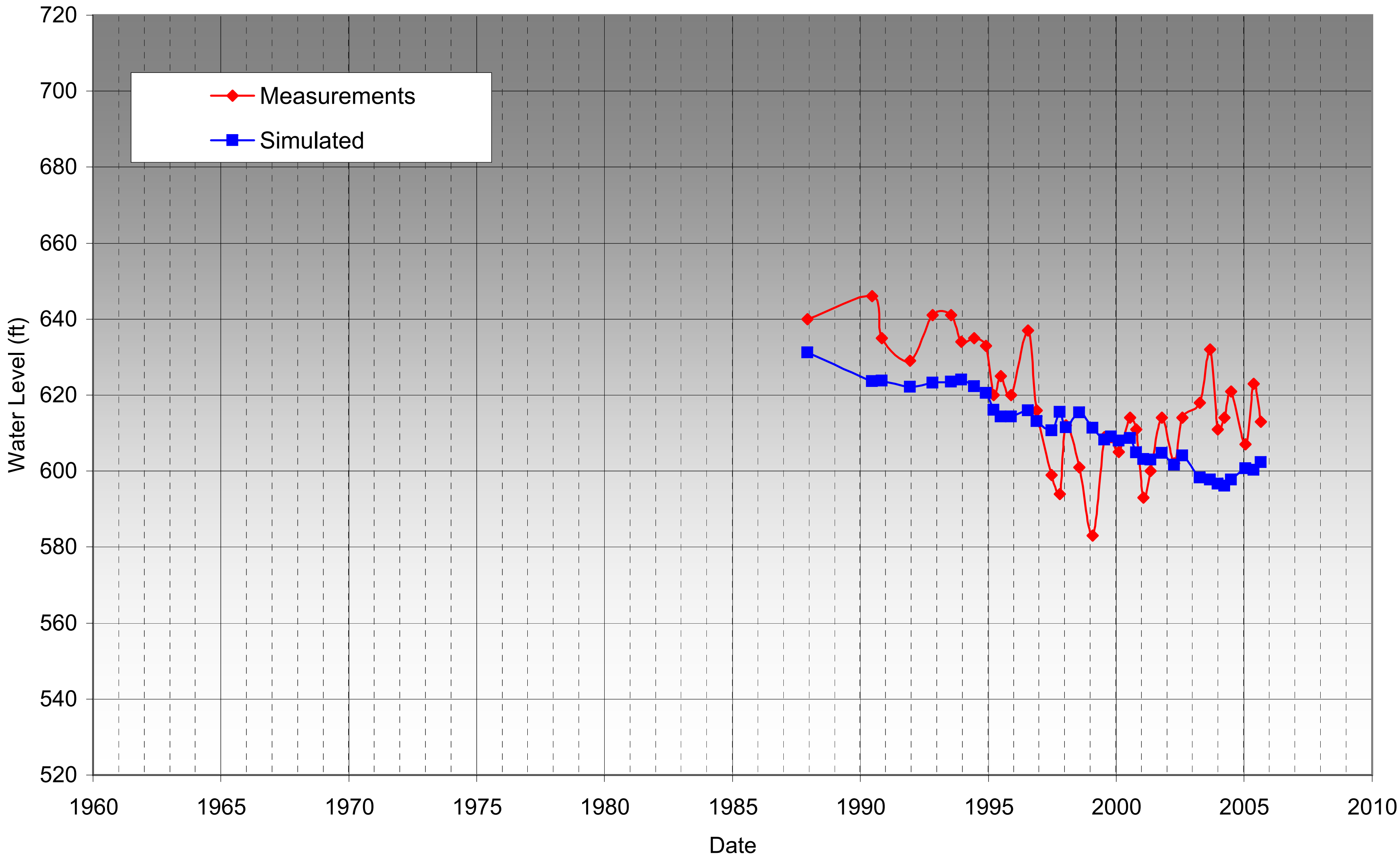

Appendix D Calibration Plots.xls

WILDERMUTH™ ENVIRONMENTAL INC.

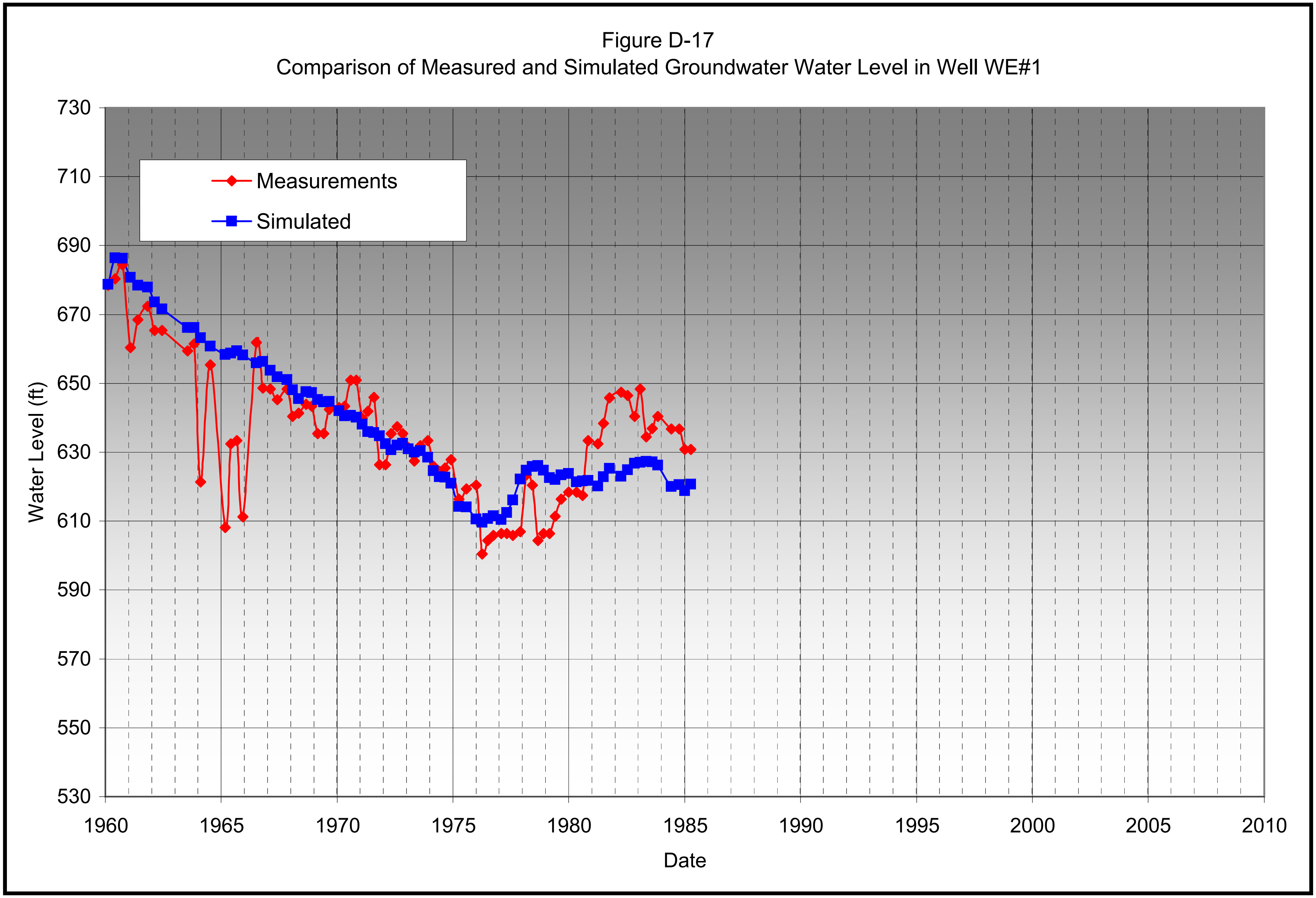

WILDERMUTH™ ENVIRONMENTAL INC.

Figure D-18
Comparison of Measured and Simulated Groundwater Water Level in Well 32G1

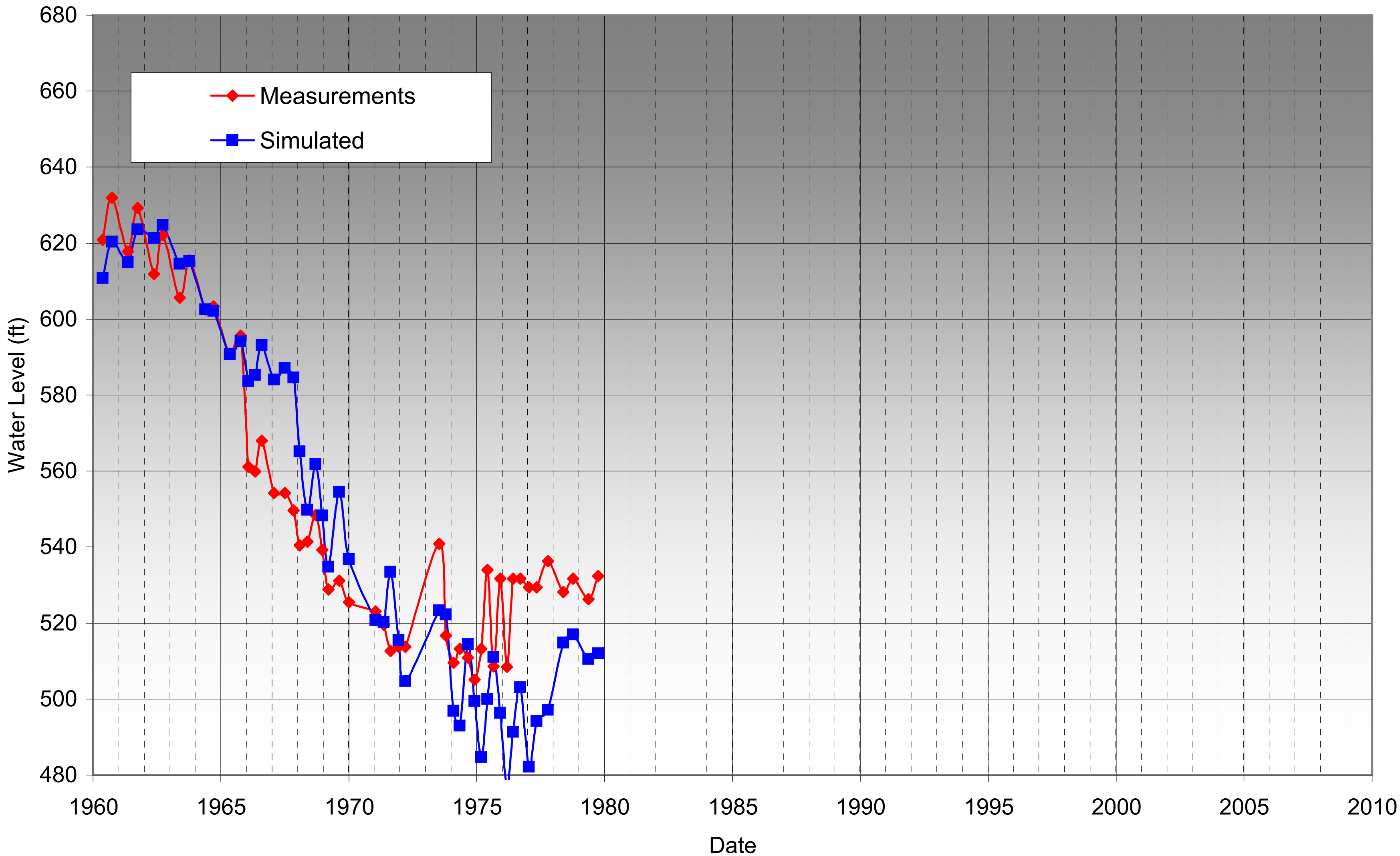

Appendix D Calibration Plots.xls

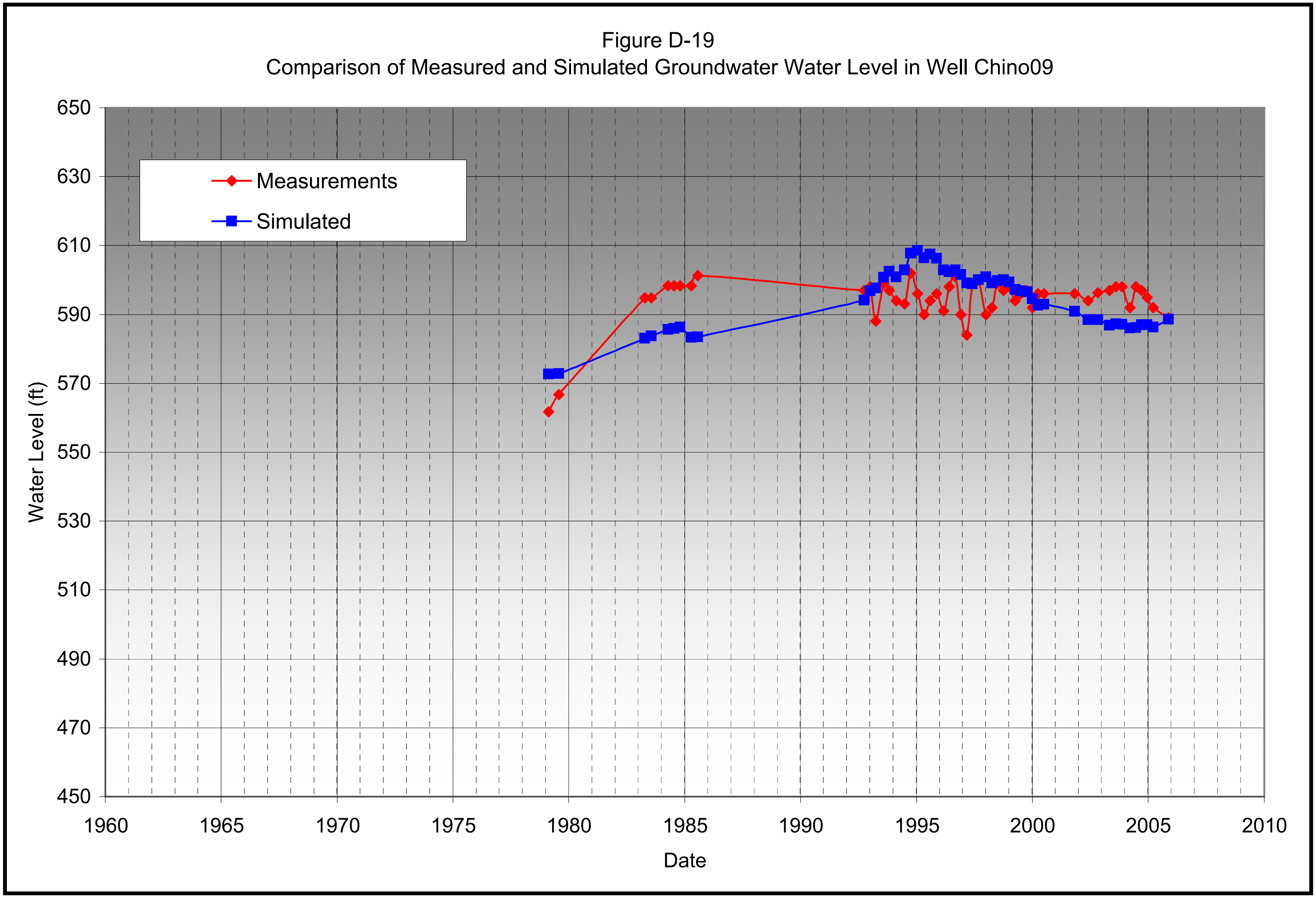

WILDERMUTH™ ENVIRONMENTAL INC.

Figure D-20
Comparison of Measured and Simulated Groundwater Water Level in Well 16

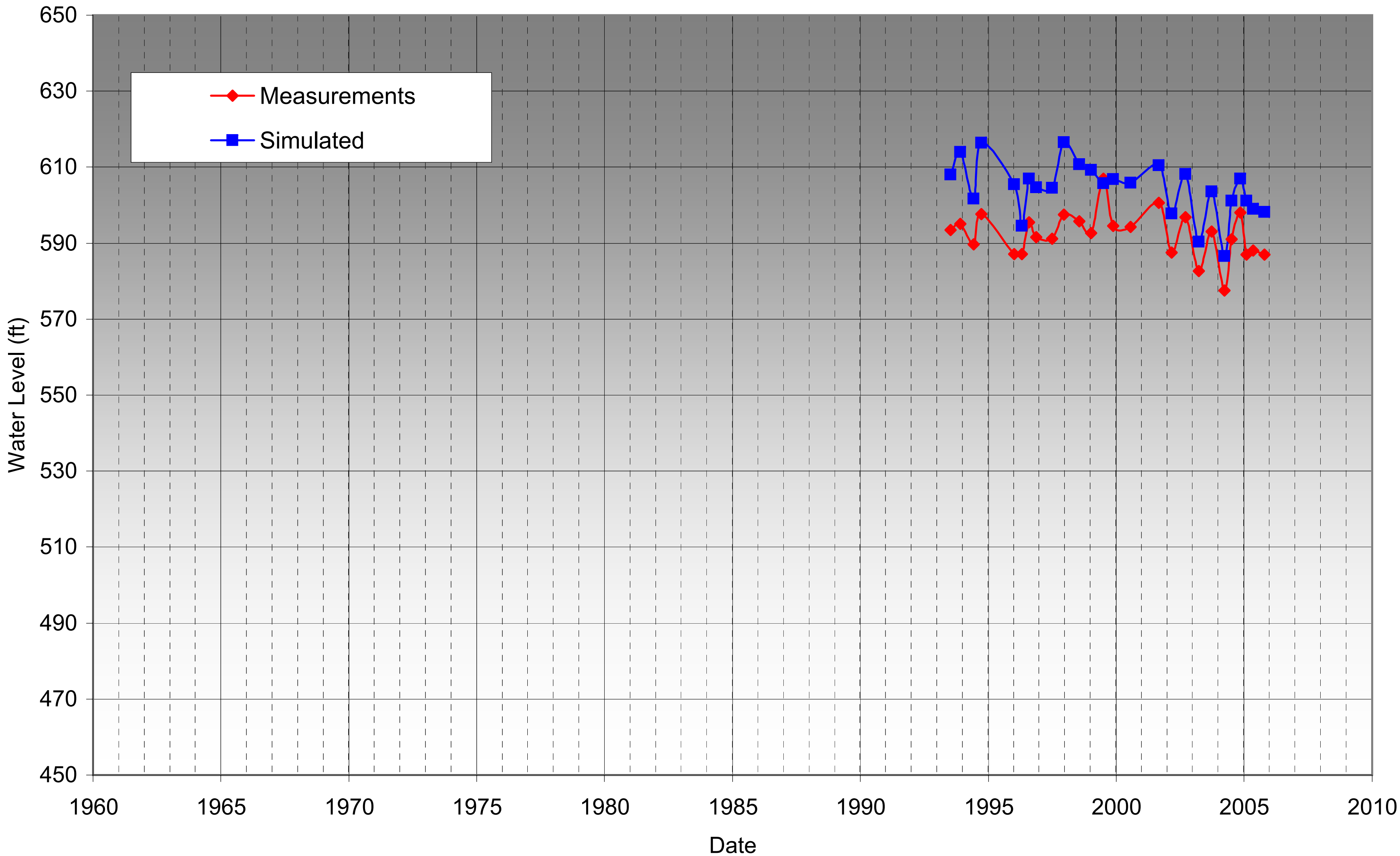

WILDERMUTH ENVIRONMENTAL INC.

Figure D-21
Comparison of Measured and Simulated Groundwater Water Level in Well Norco11

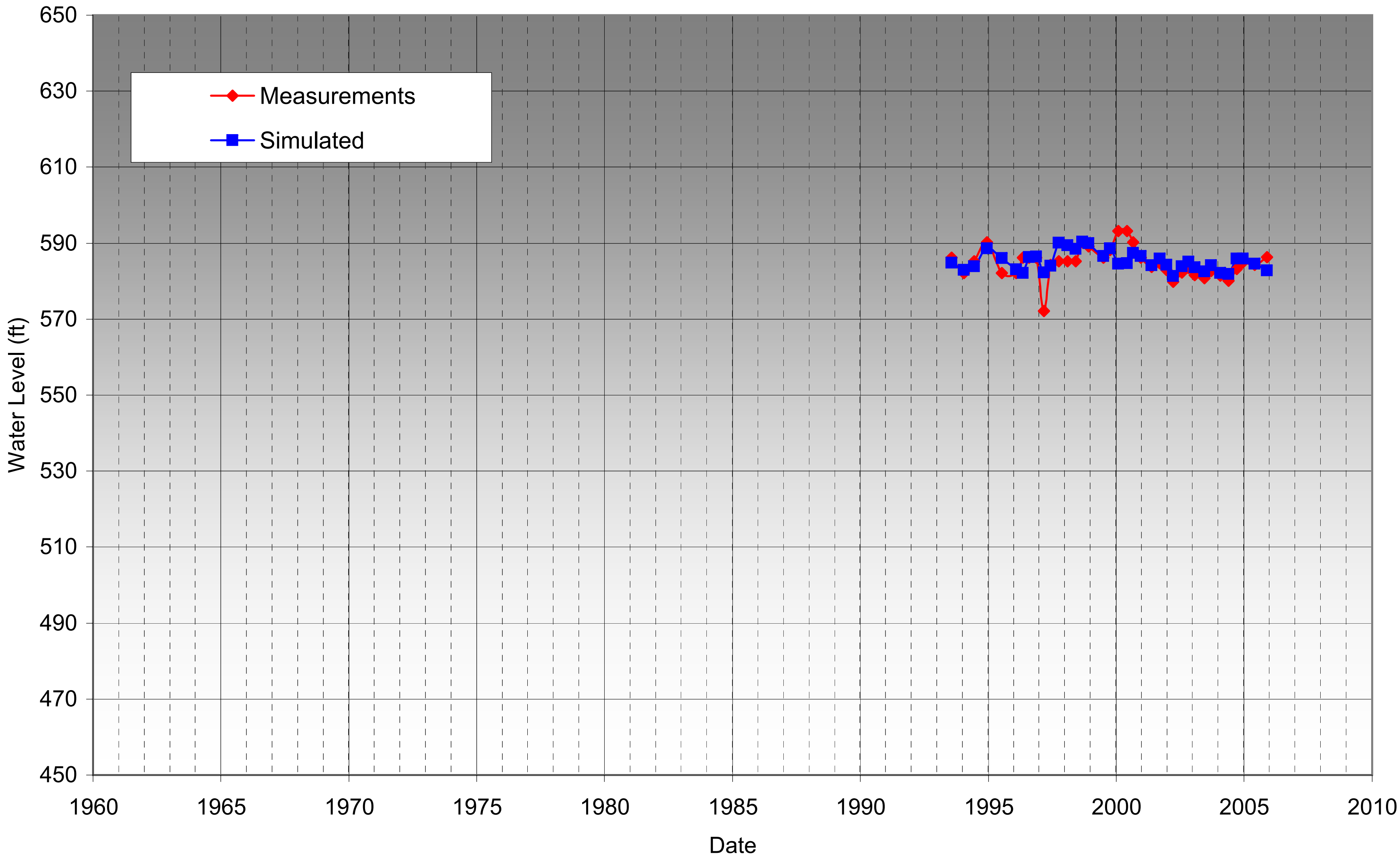

Figure D-22
Comparison of Measured and Simulated Groundwater Water Level in Well SARWC07

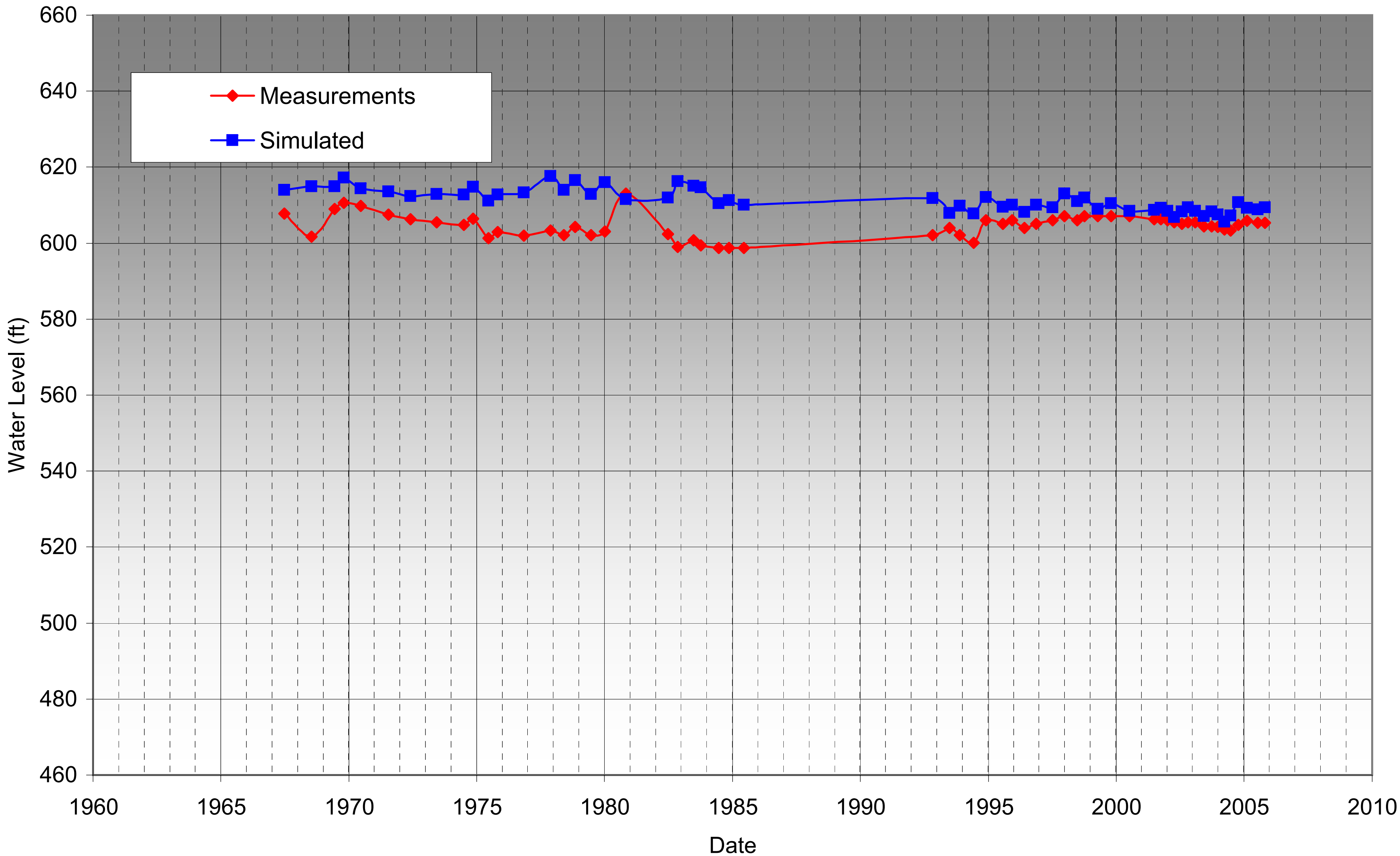

WILDERMUTH™ ENVIRONMENTAL INC.

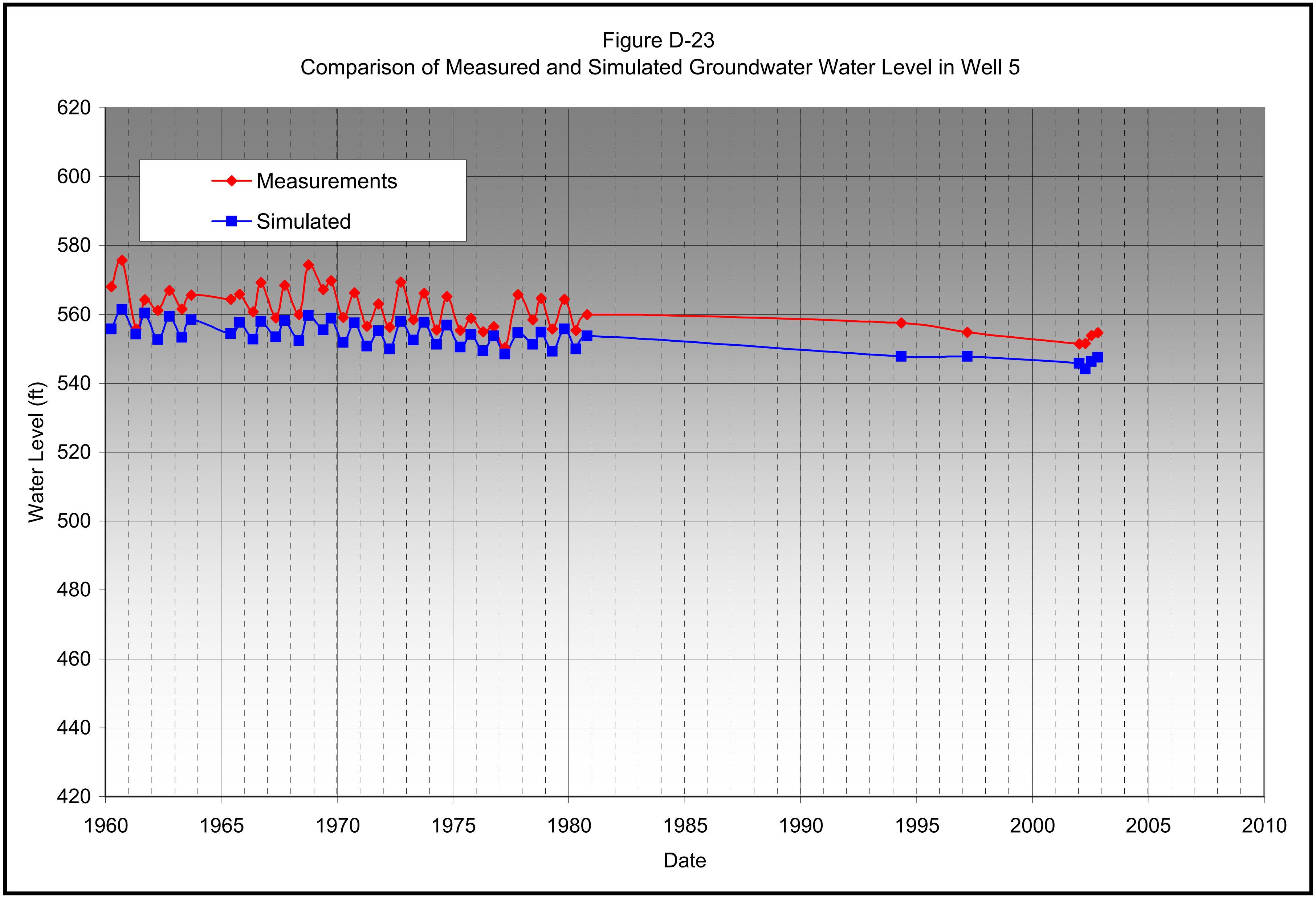

WILDERMUTH™ ENVIRONMENTAL INC.

Figure D-24
Comparison of Measured and Simulated Groundwater Water Level in Well 17

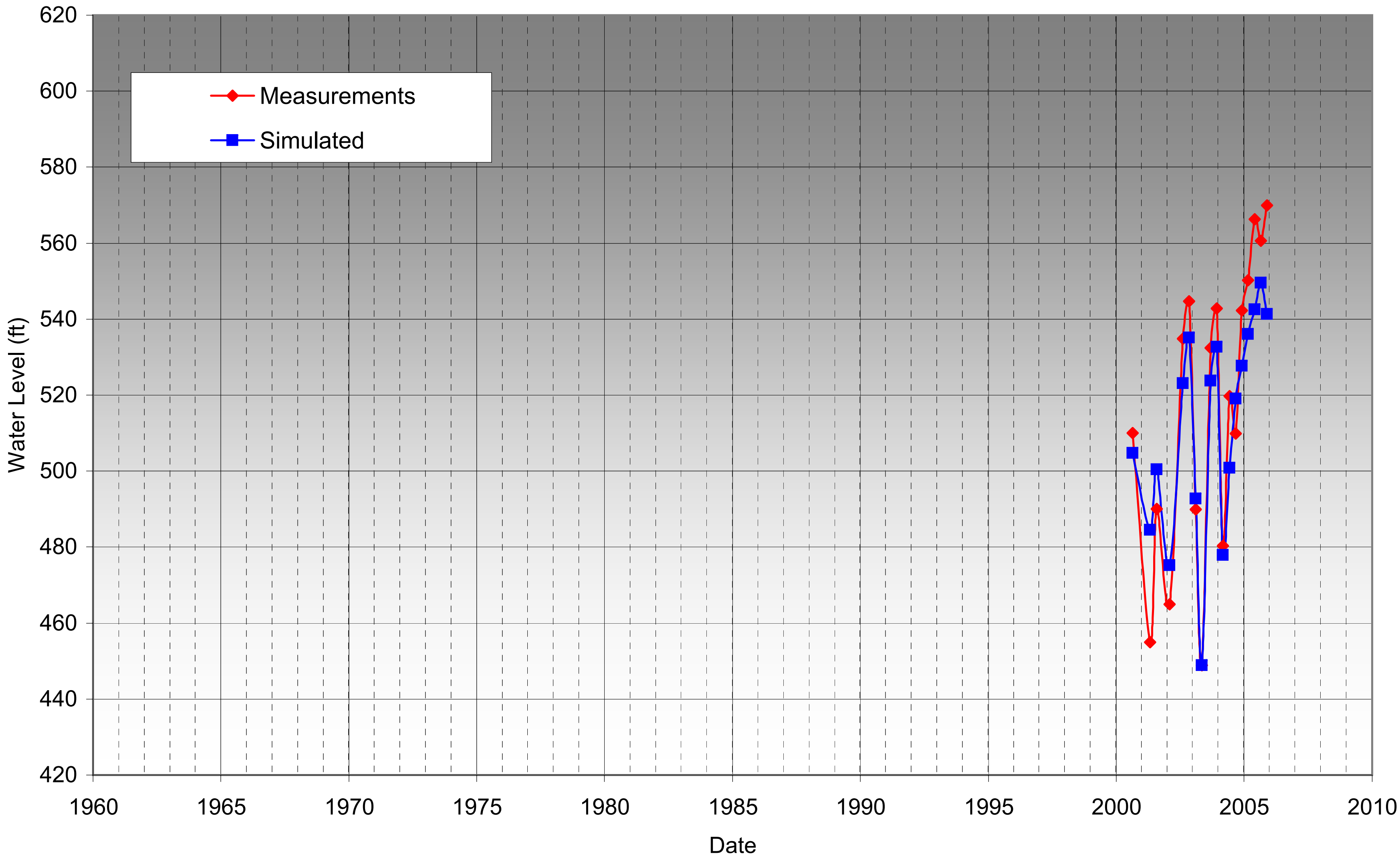

WILDERMUTH™ ENVIRONMENTAL INC.

Figure D-25
Comparison of Measured and Simulated Groundwater Water Level in Well Chino13

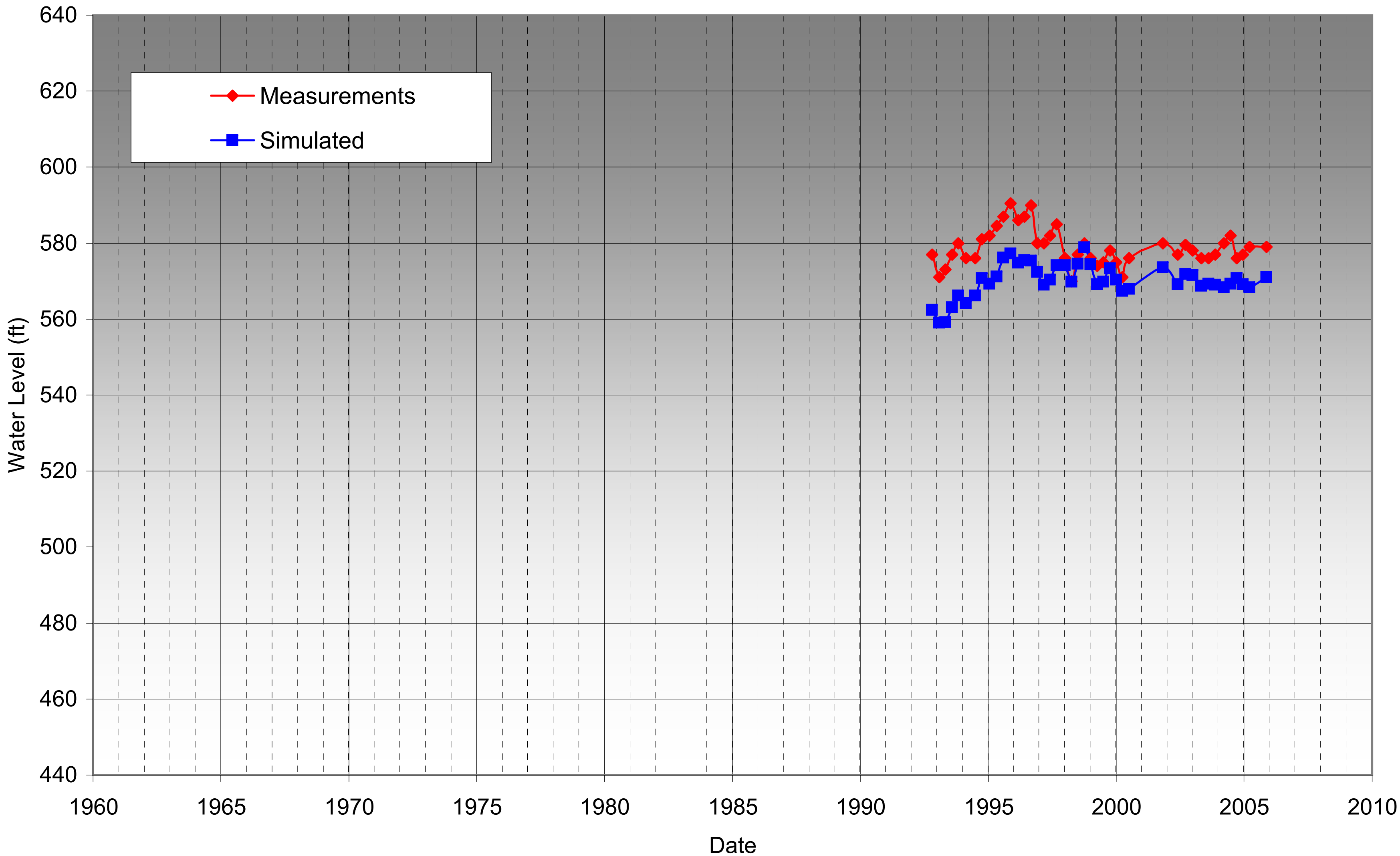

WILDERMUTH ENVIRONMENTAL INC.

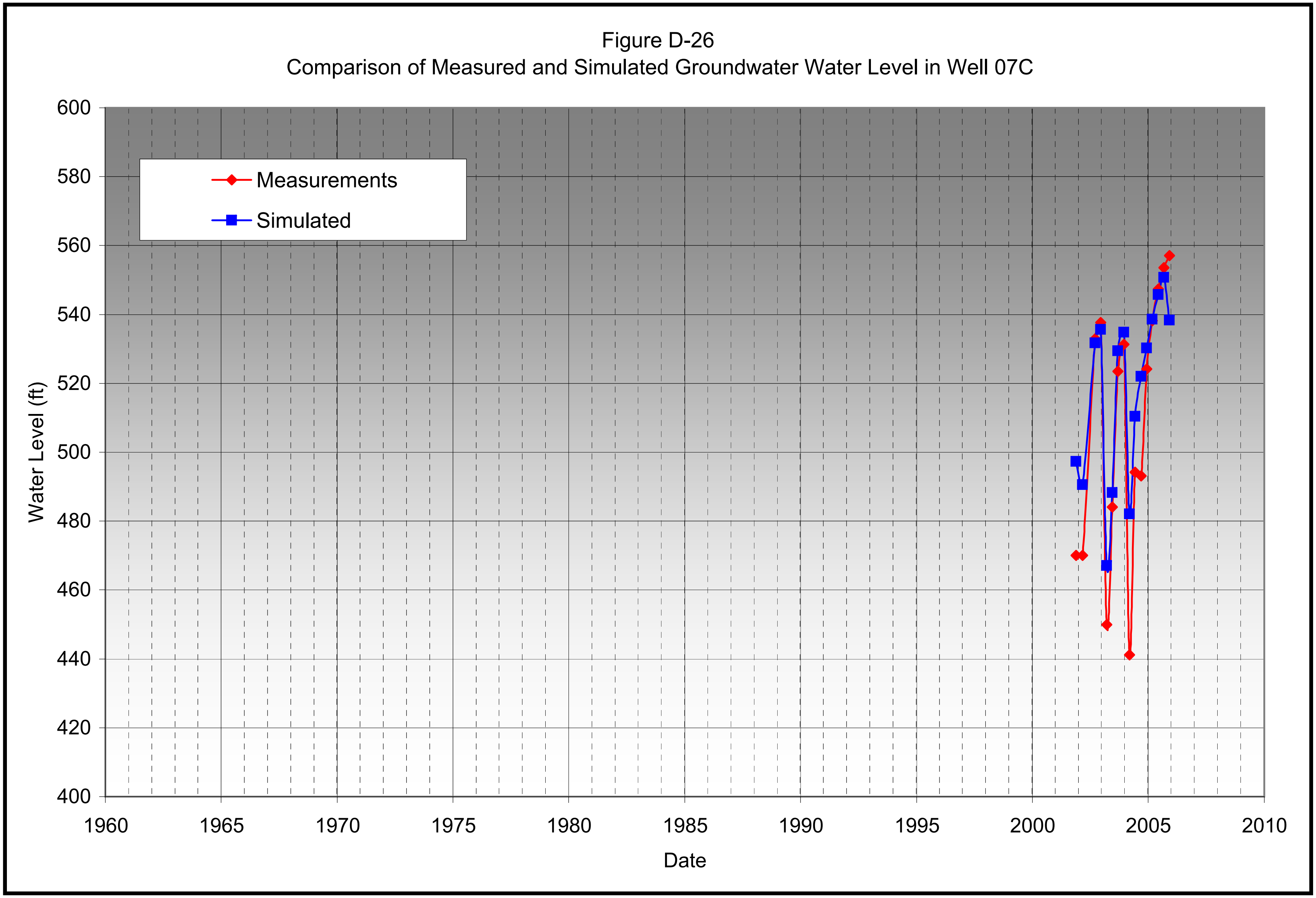

WILDERMUTH™ ENVIRONMENTAL INC.

Figure D-27
Comparison of Measured and Simulated Groundwater Water Level in Well 9

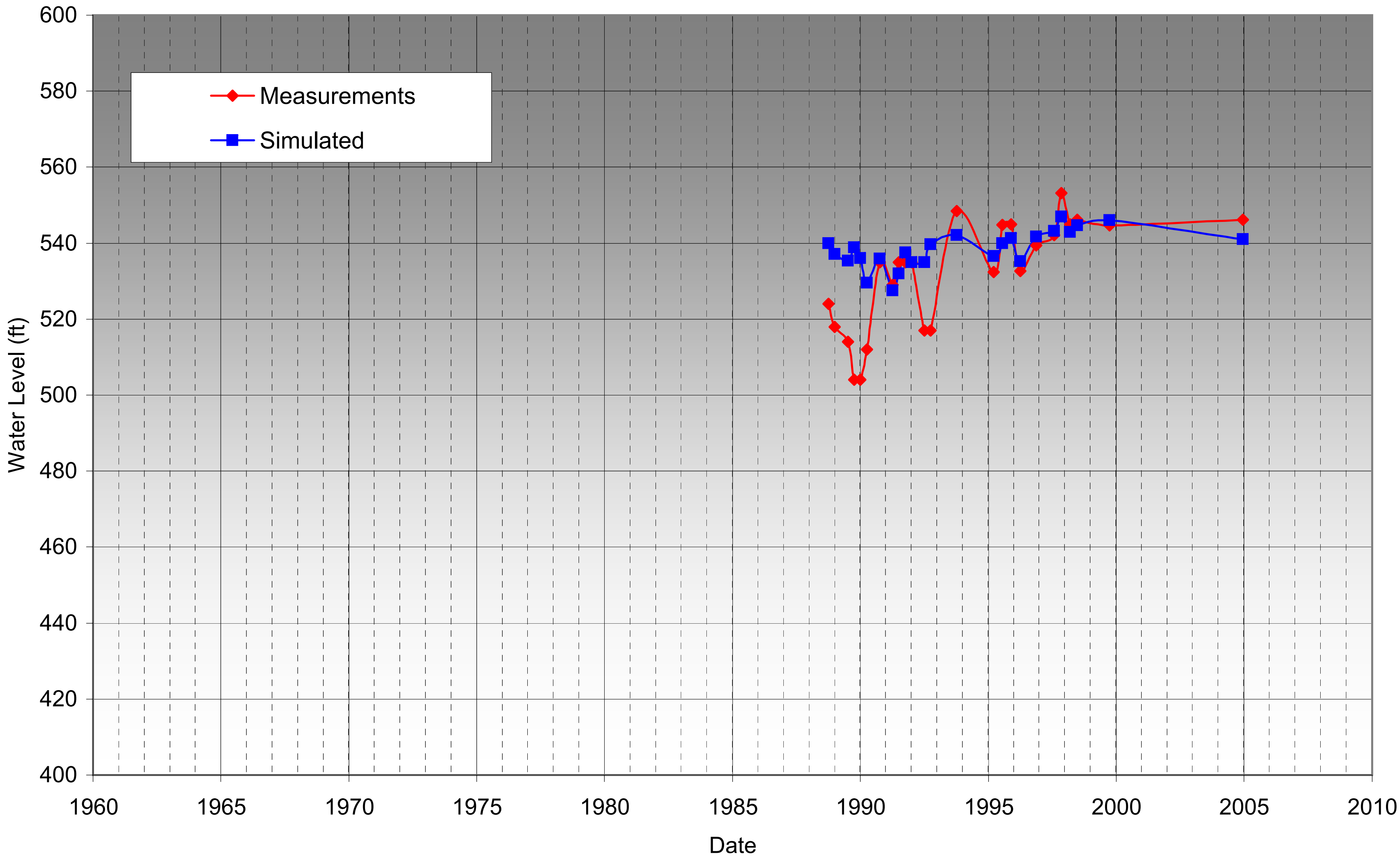

WILDERMUTH™ ENVIRONMENTAL INC.

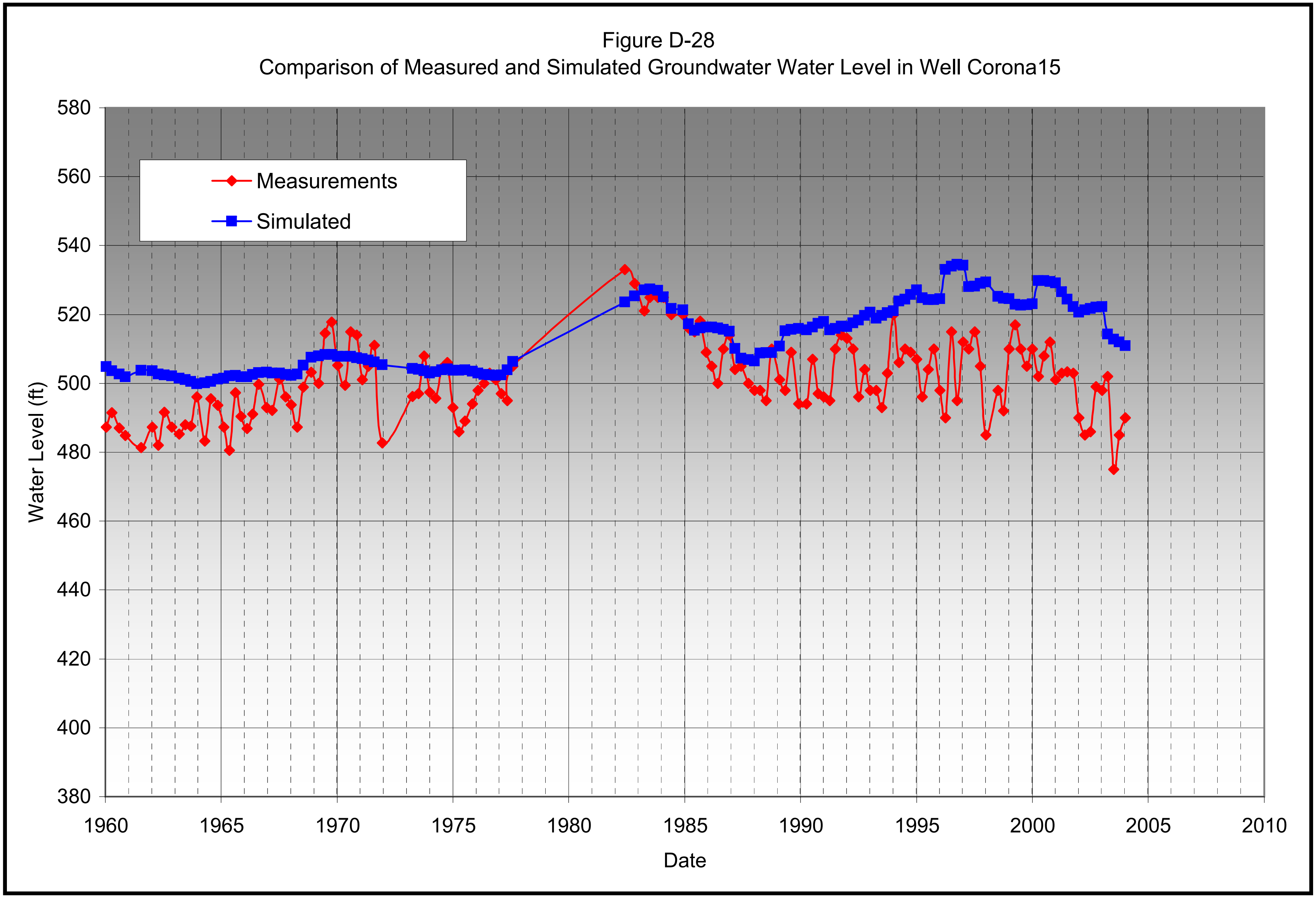
Figure D-28
Comparison of Measured and Simulated Groundwater Water Level in Well Corona15
Measurements
Simulated
Water Level (ft)
580
560
540
520
500
480
460
440
420
400
380
1960
1965
1970
1975
1980
1985
1990
1995
2000
2005
2010
Date

Figure D-29
Comparison of Measured and Simulated Groundwater Water Level in Well Corona14

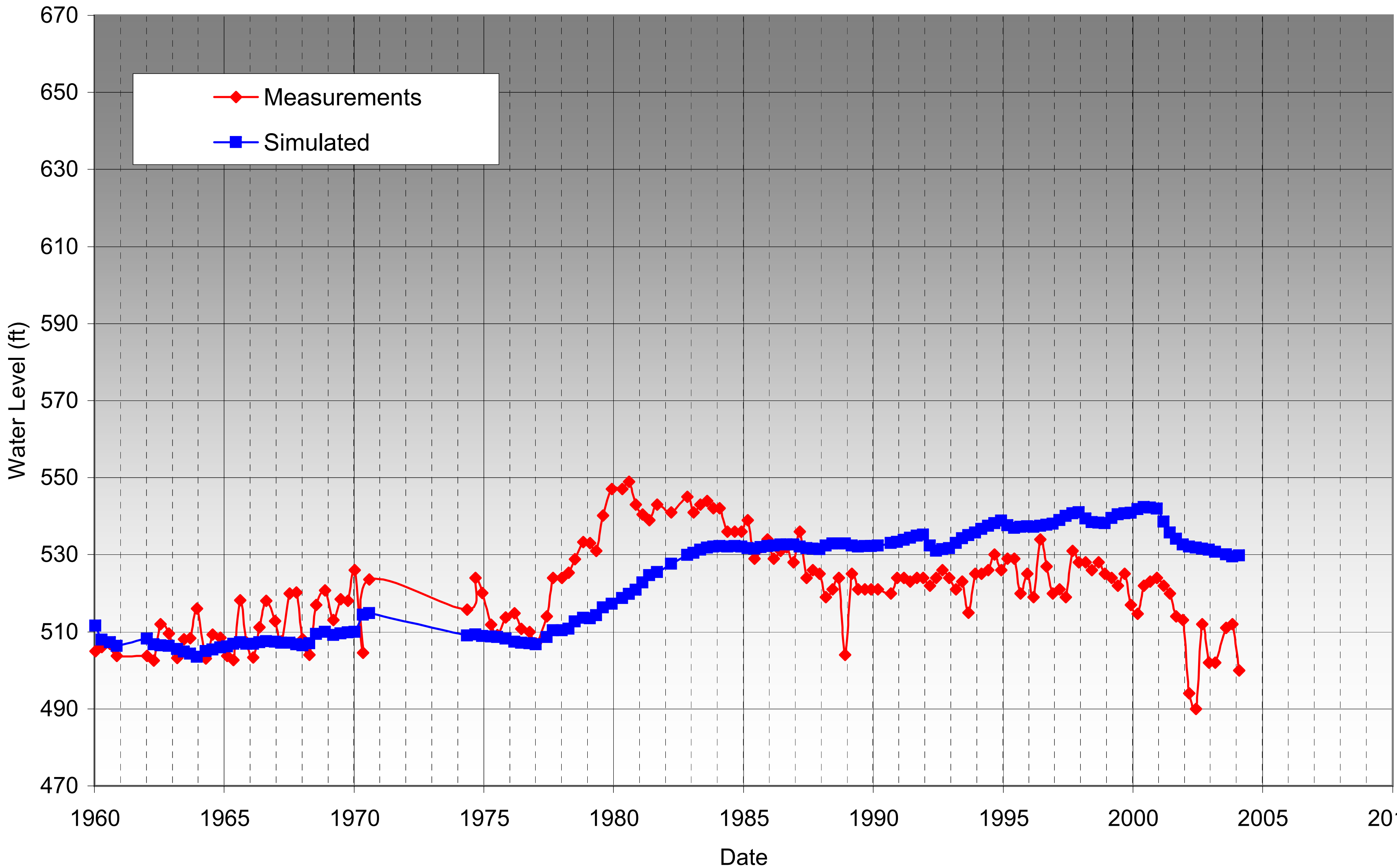

WILDERMUTH™ ENVIRONMENTAL INC.

Figure D-30
Comparison of Measured and Simulated Groundwater Water Level in Well M-3

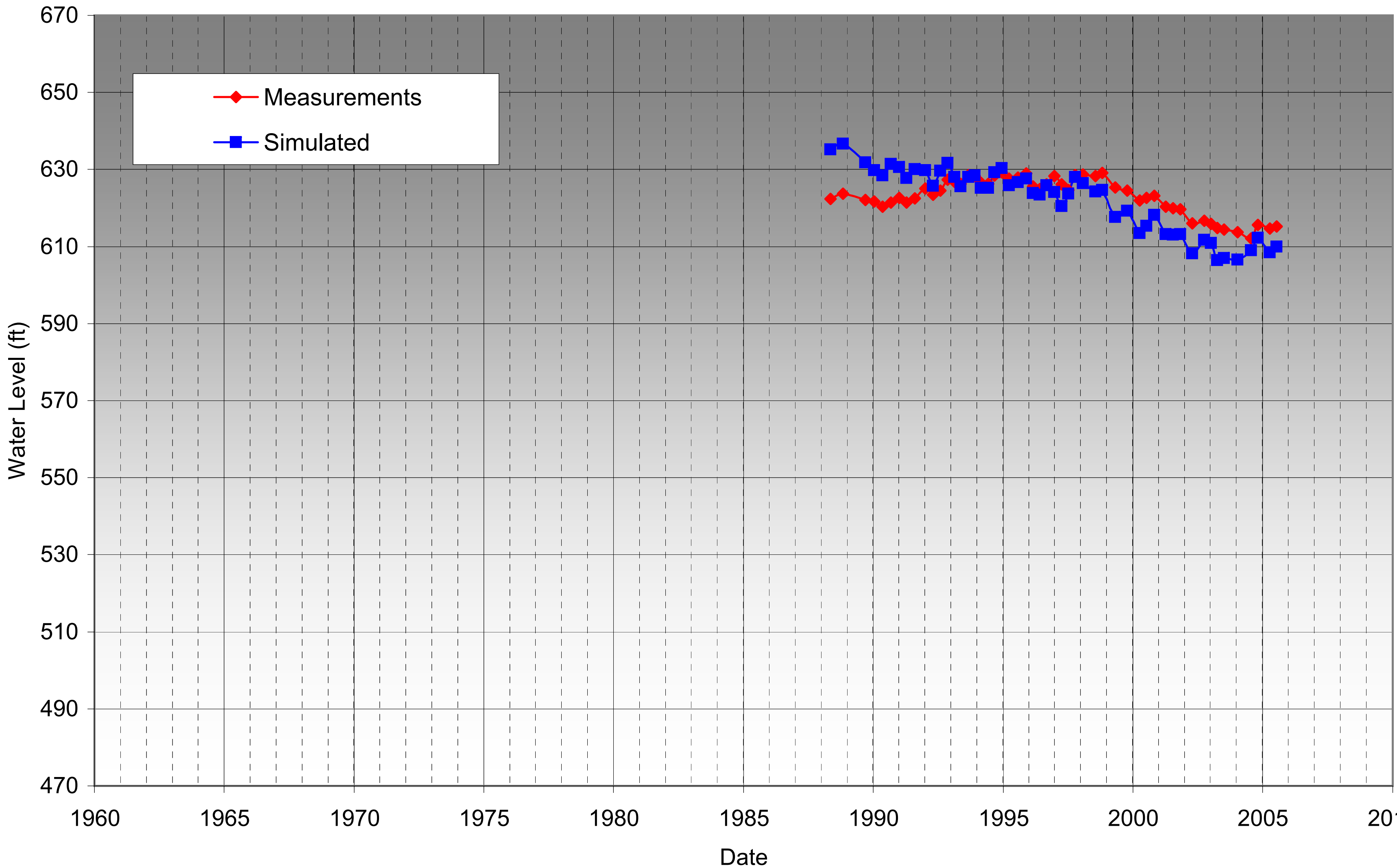

WILDERMUTH ENVIRONMENTAL INC.

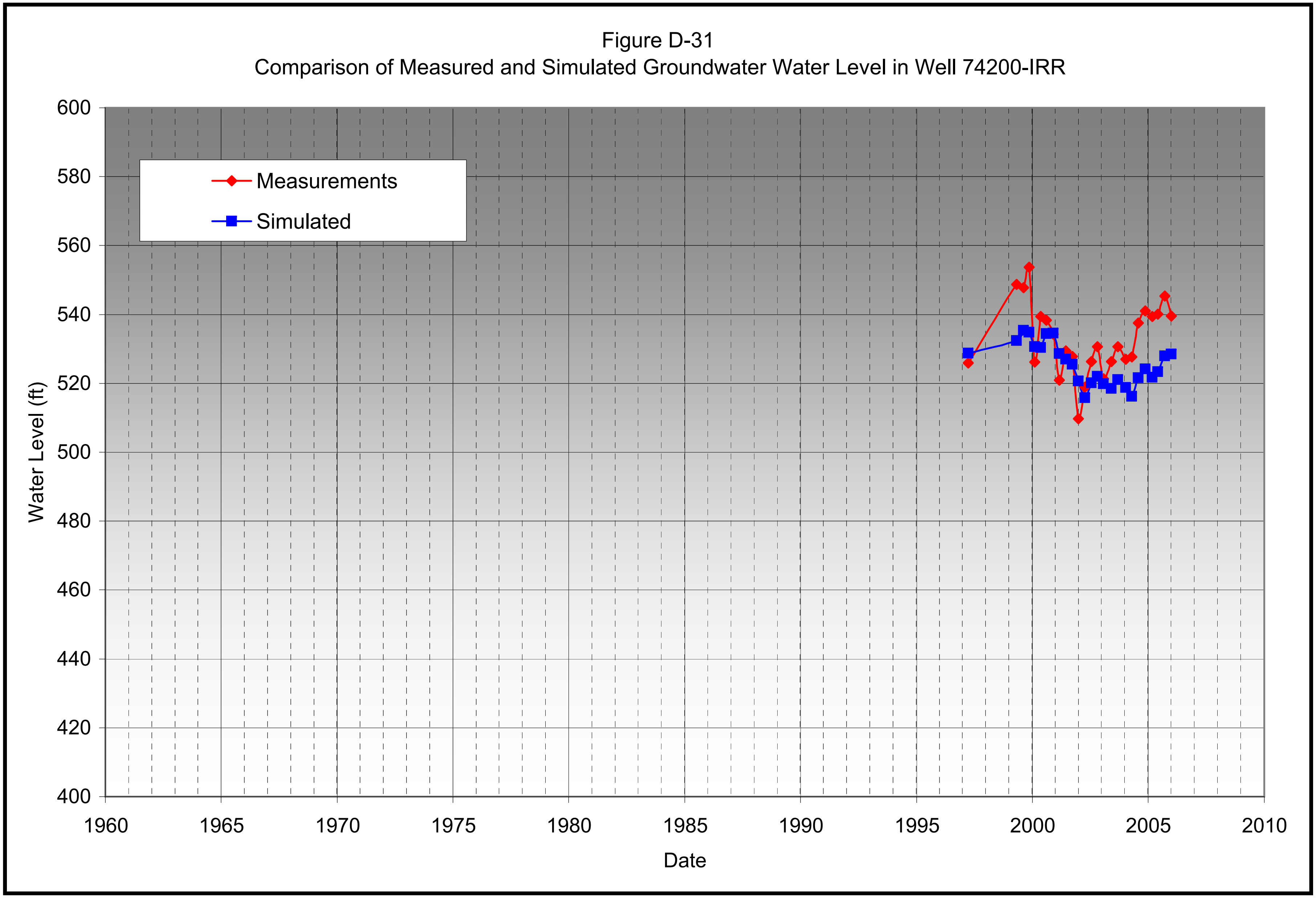

WILDERMUTH™ ENVIRONMENTAL INC.

Figure D-32
Comparison of Measured and Simulated Groundwater Water Level in Well P-29

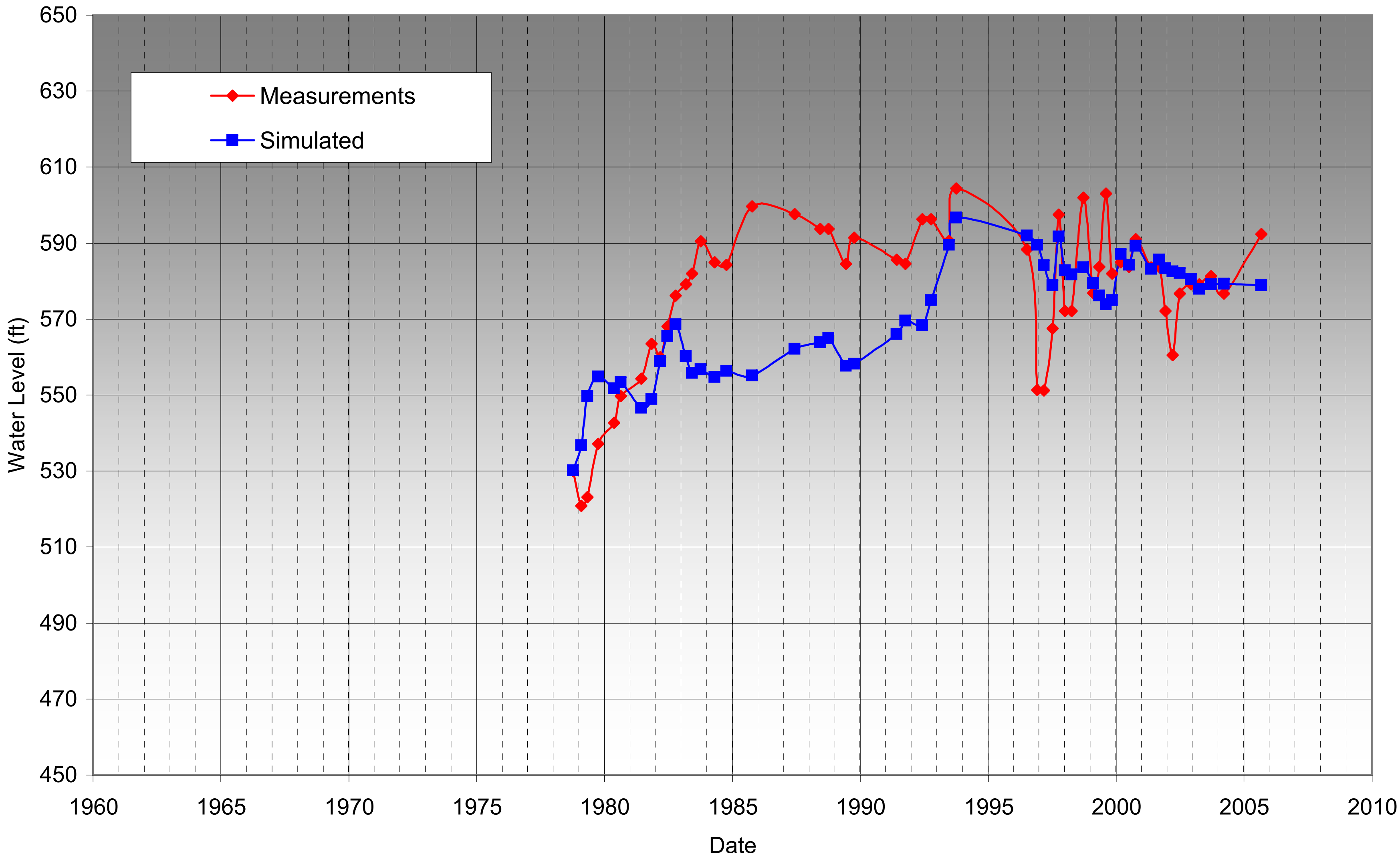

Figure D-33
Comparison of Measured and Simulated Groundwater Water Level in Well 18A

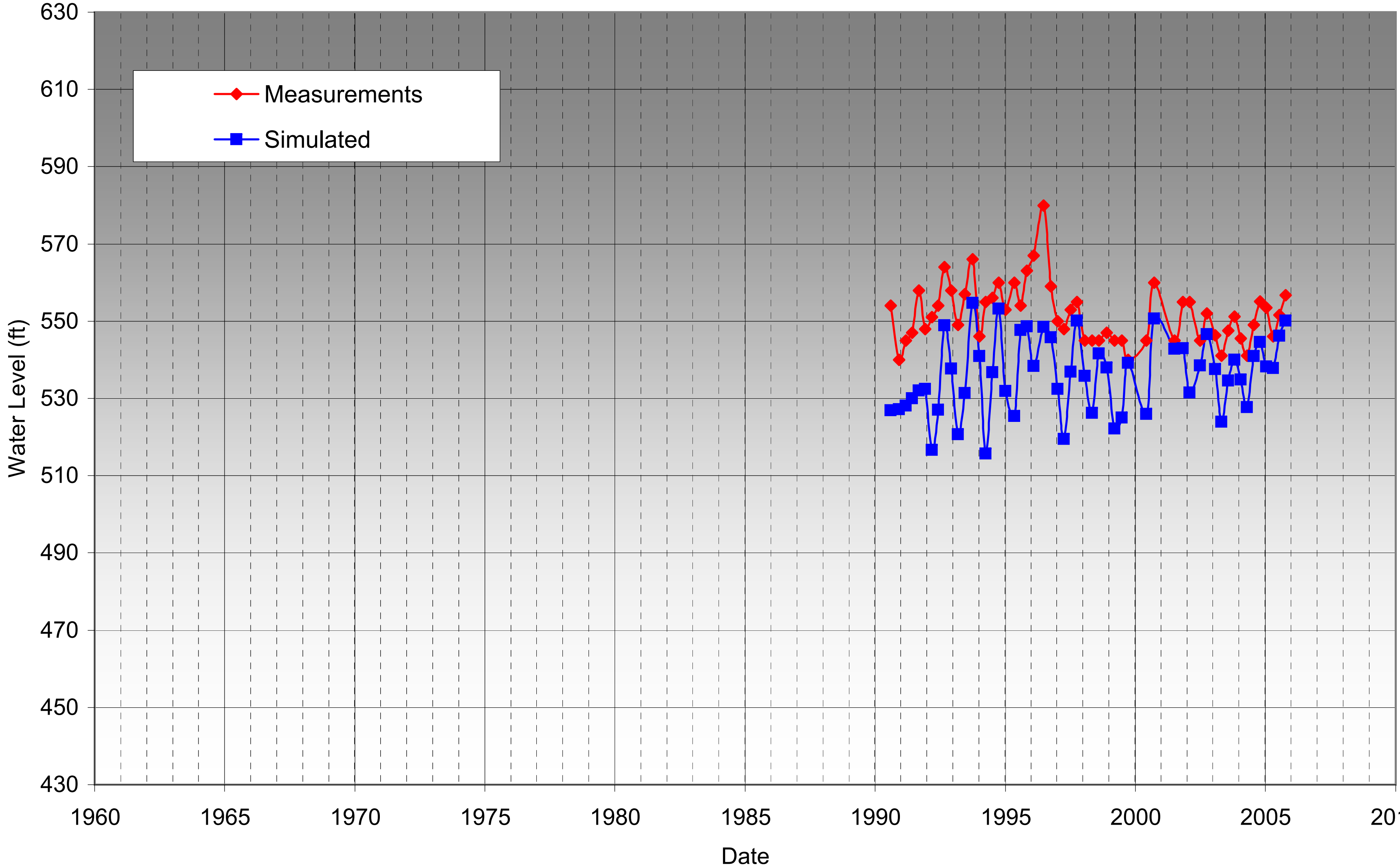

WILDERMUTH™ ENVIRONMENTAL INC.

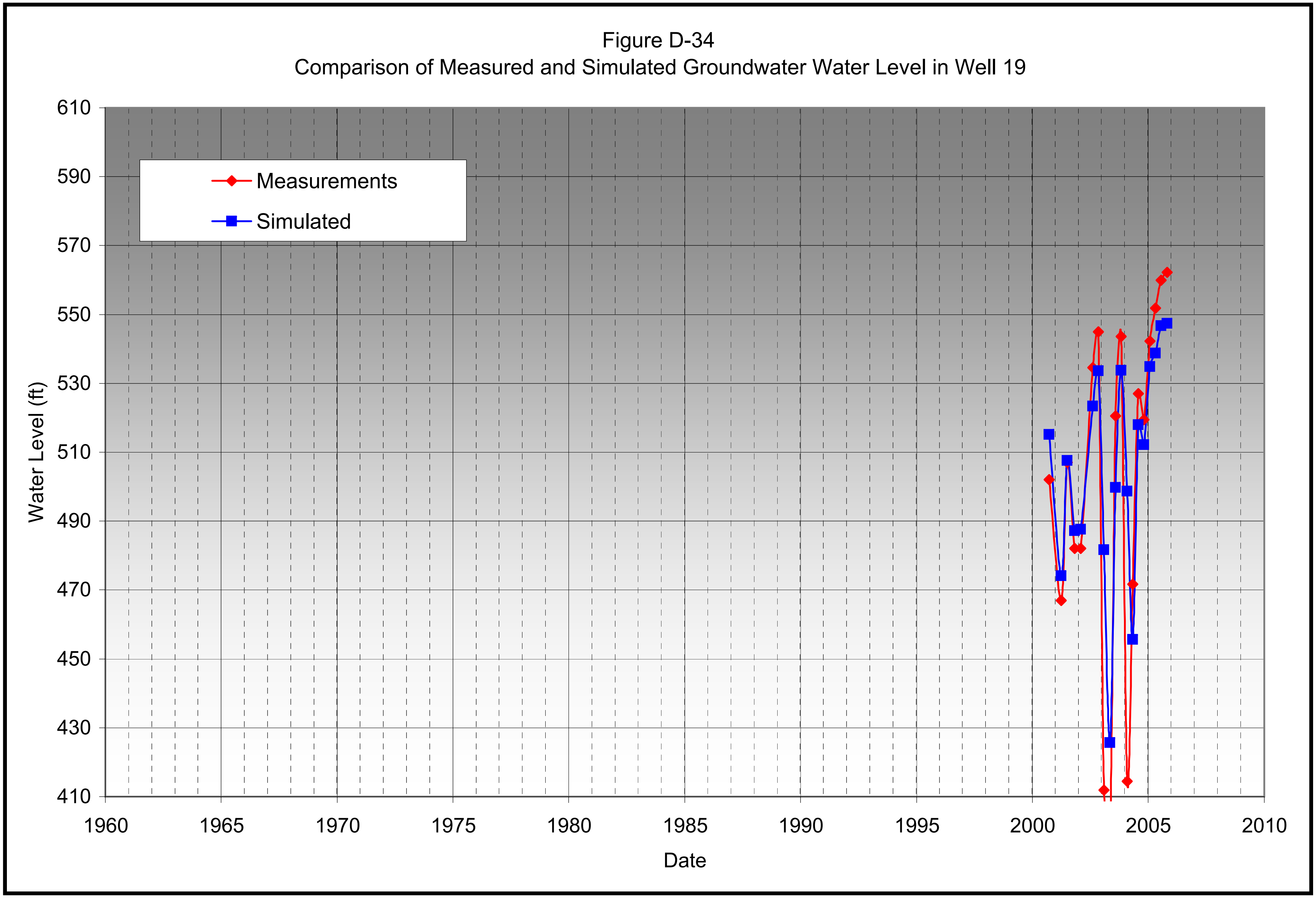

WILDERMUTH™ ENVIRONMENTAL INC.

Figure D-35
Comparison of Measured and Simulated Groundwater Water Level in Well 15B

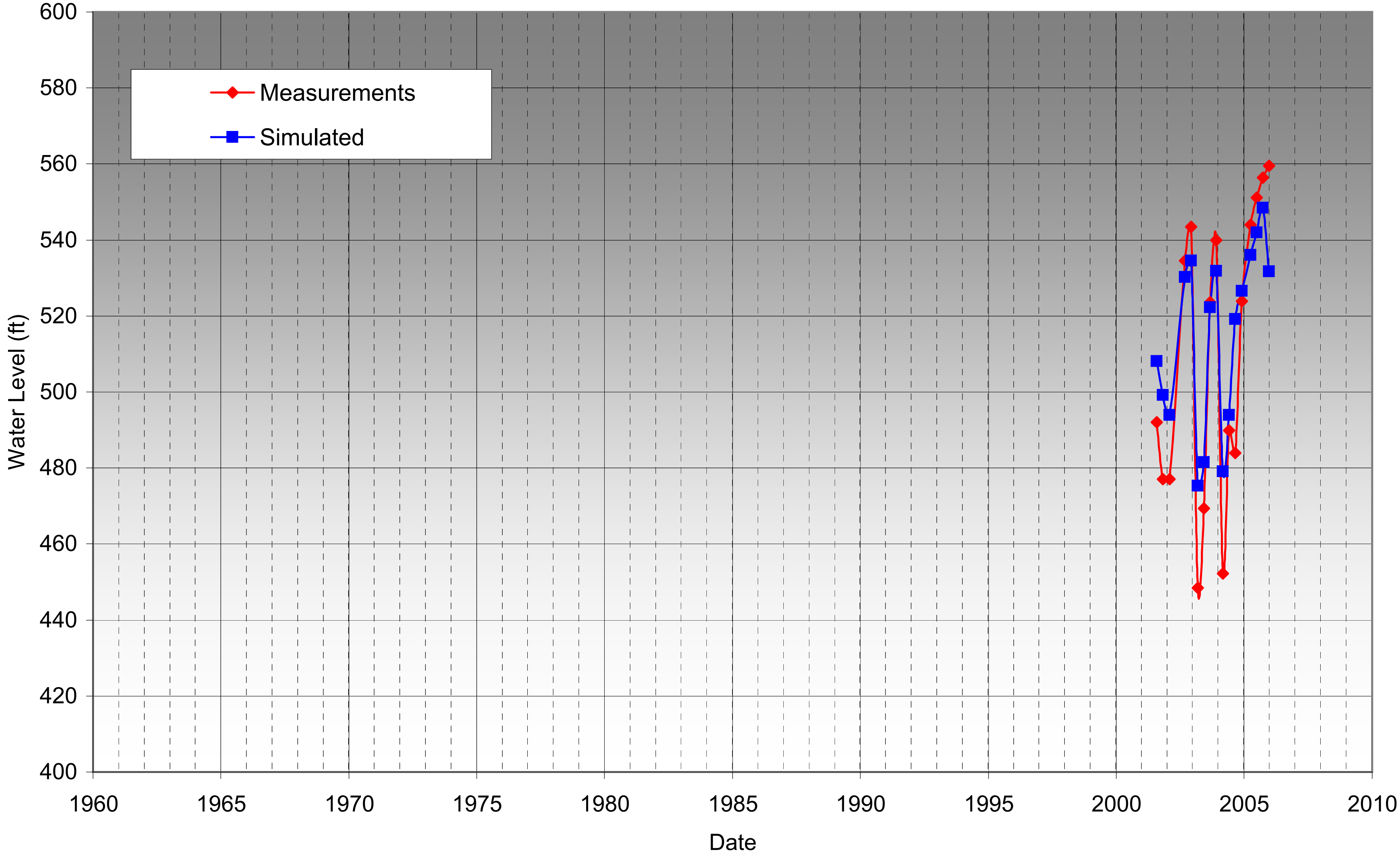

WILDERMUTH™ ENVIRONMENTAL INC.

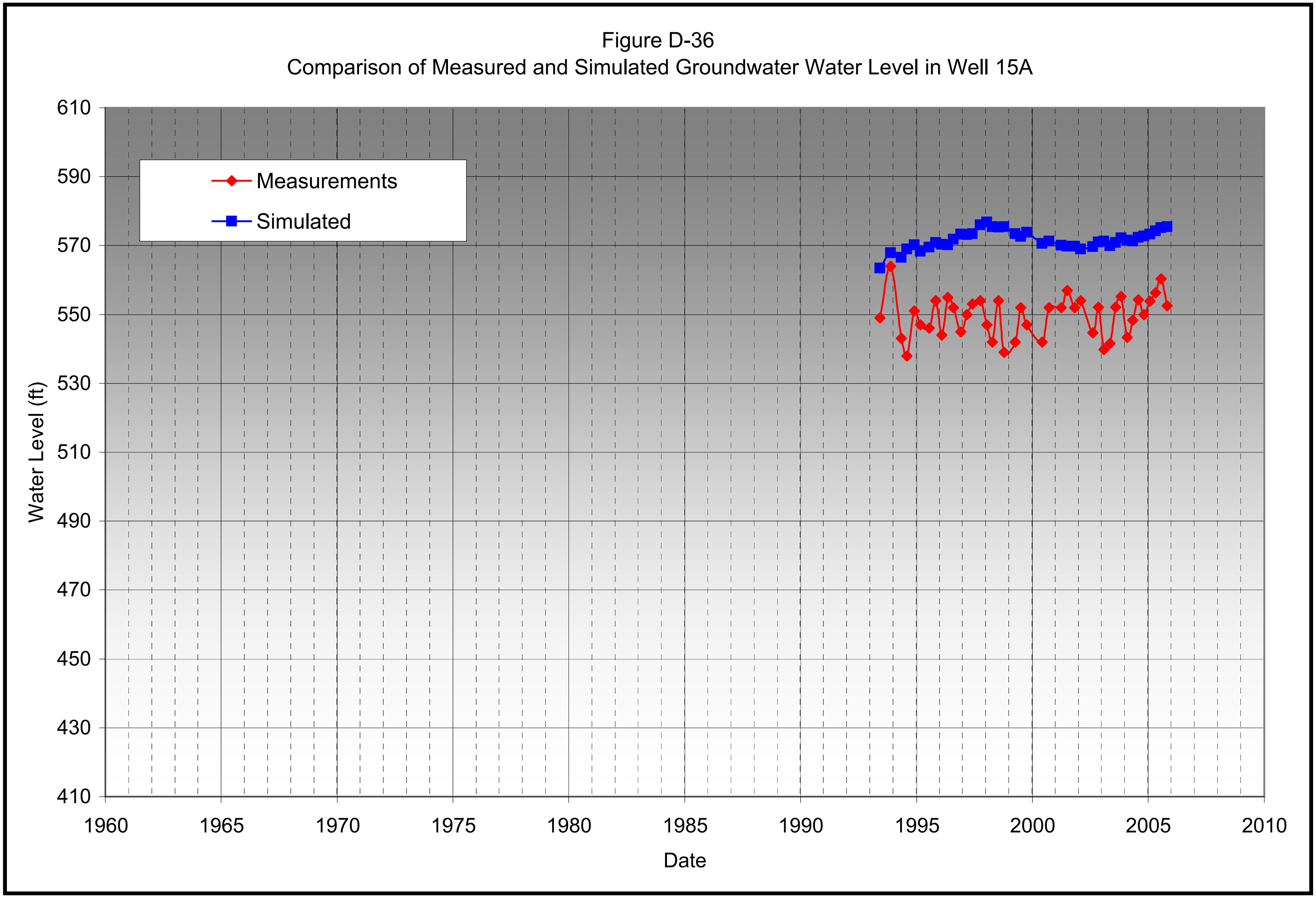

WILDERMUTH™ ENVIRONMENTAL INC.

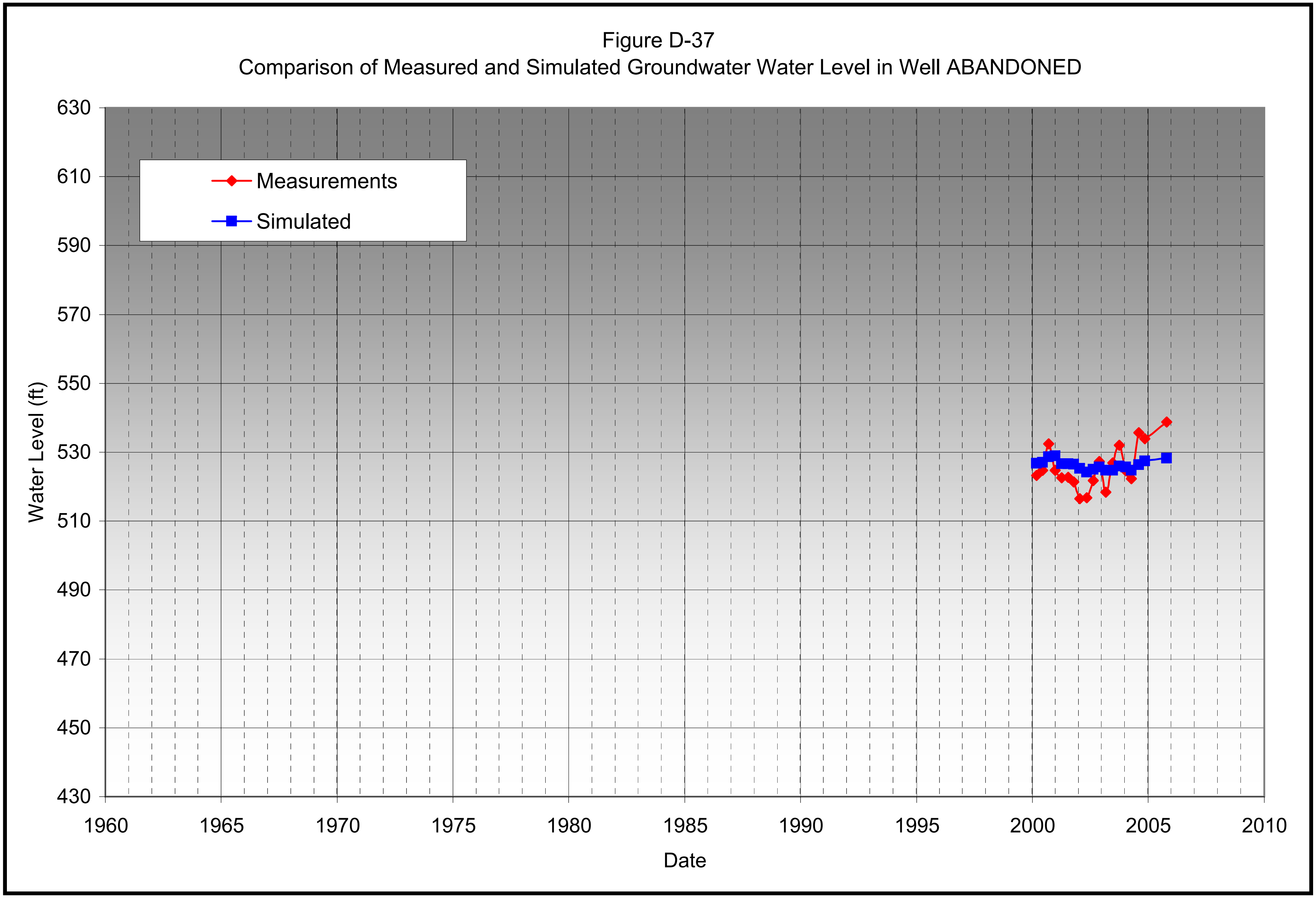

WILDERMUTH ENVIRONMENTAL INC.

Figure D-38
Comparison of Measured and Simulated Groundwater Water Level in Well Dairy-Dom

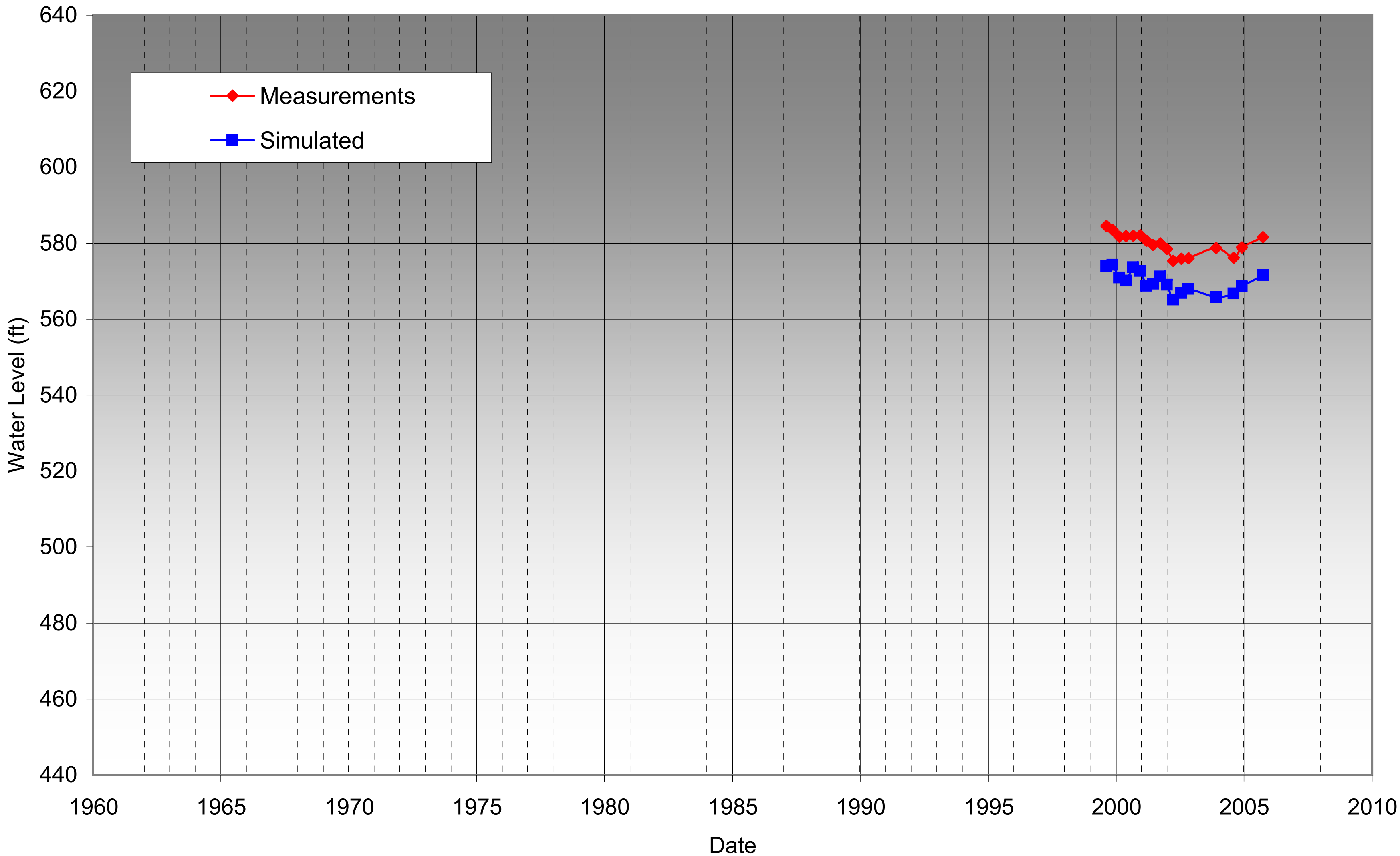

WILDERMUTH ENVIRONMENTAL INC.

Figure D-39
Comparison of Measured and Simulated Groundwater Water Level in Well Dom

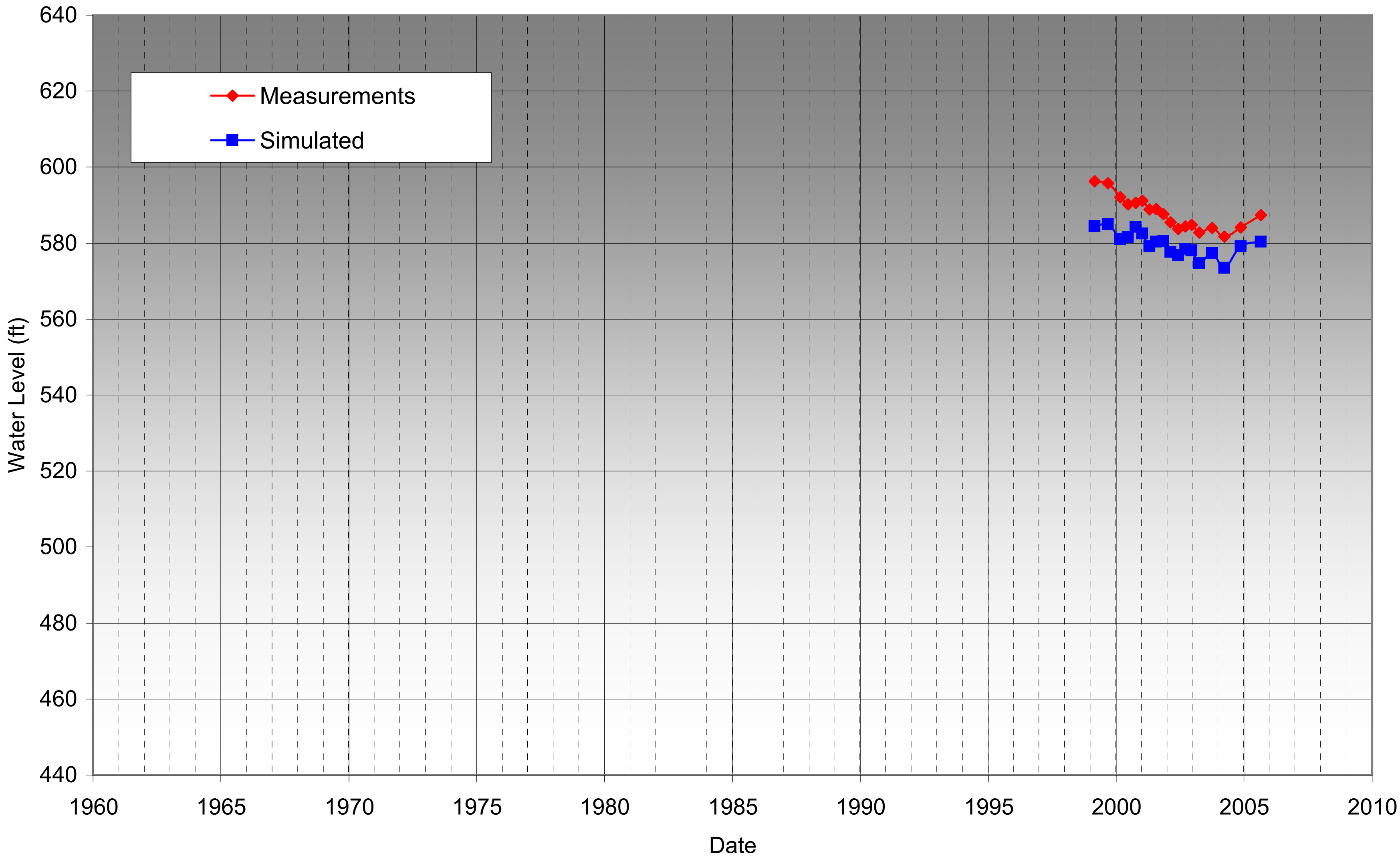

Appendix D Calibration Plots.xls

WILDERMUTH ENVIRONMENTAL INC.

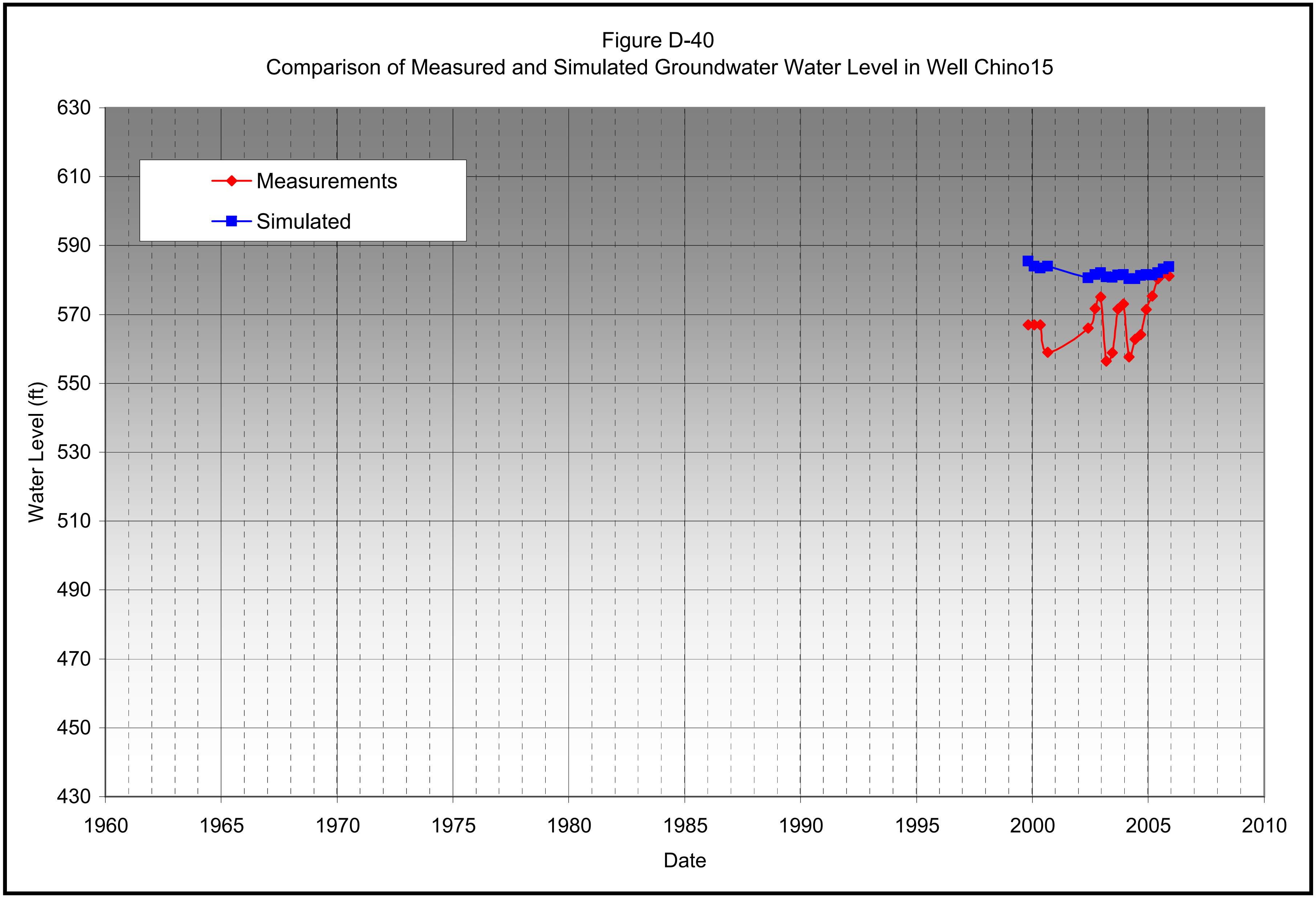

WILDERMUTH™ ENVIRONMENTAL INC.

Figure D-41
Comparison of Measured and Simulated Groundwater Water Level in Well I-10

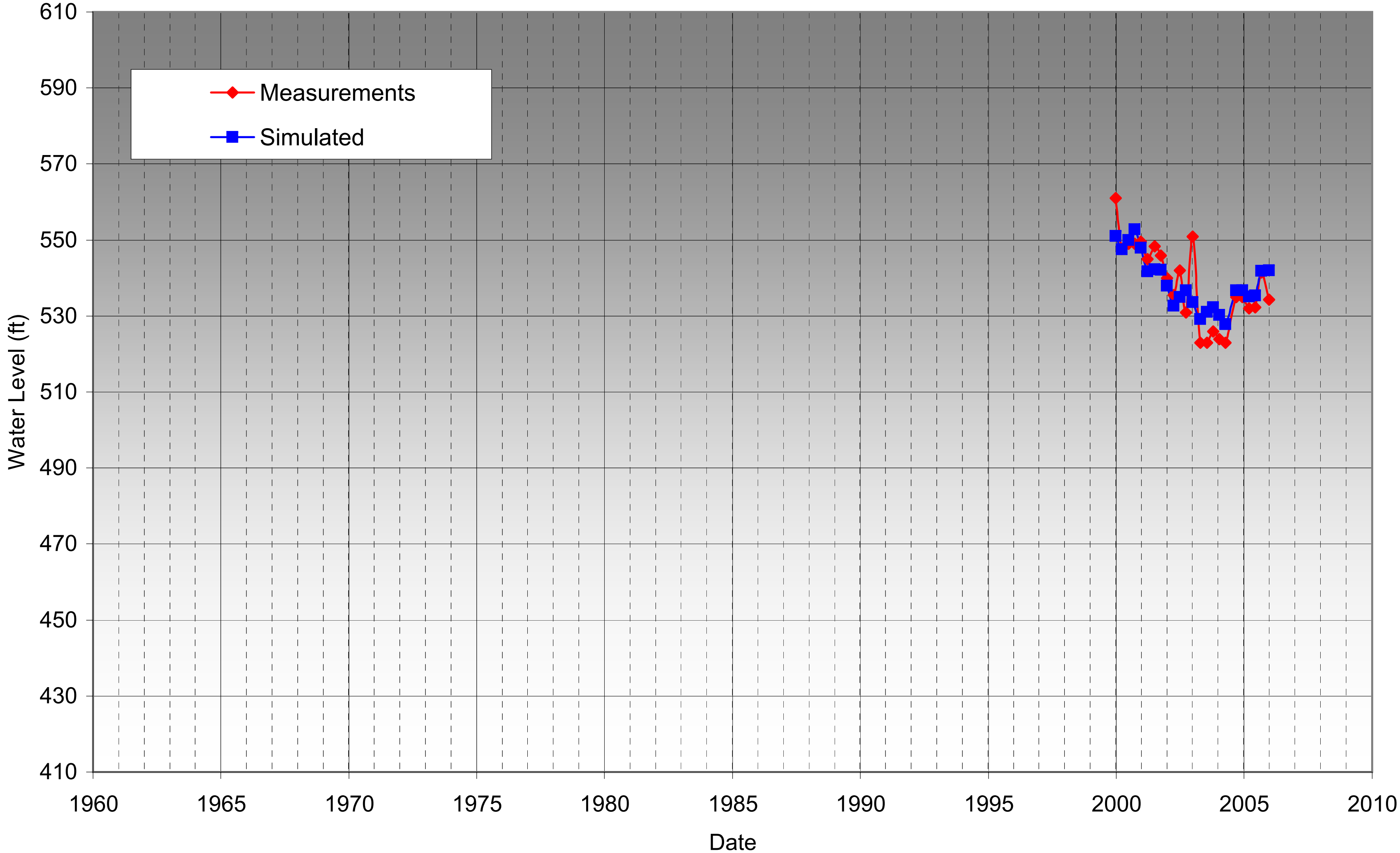

WILDERMUTH ENVIRONMENTAL INC.

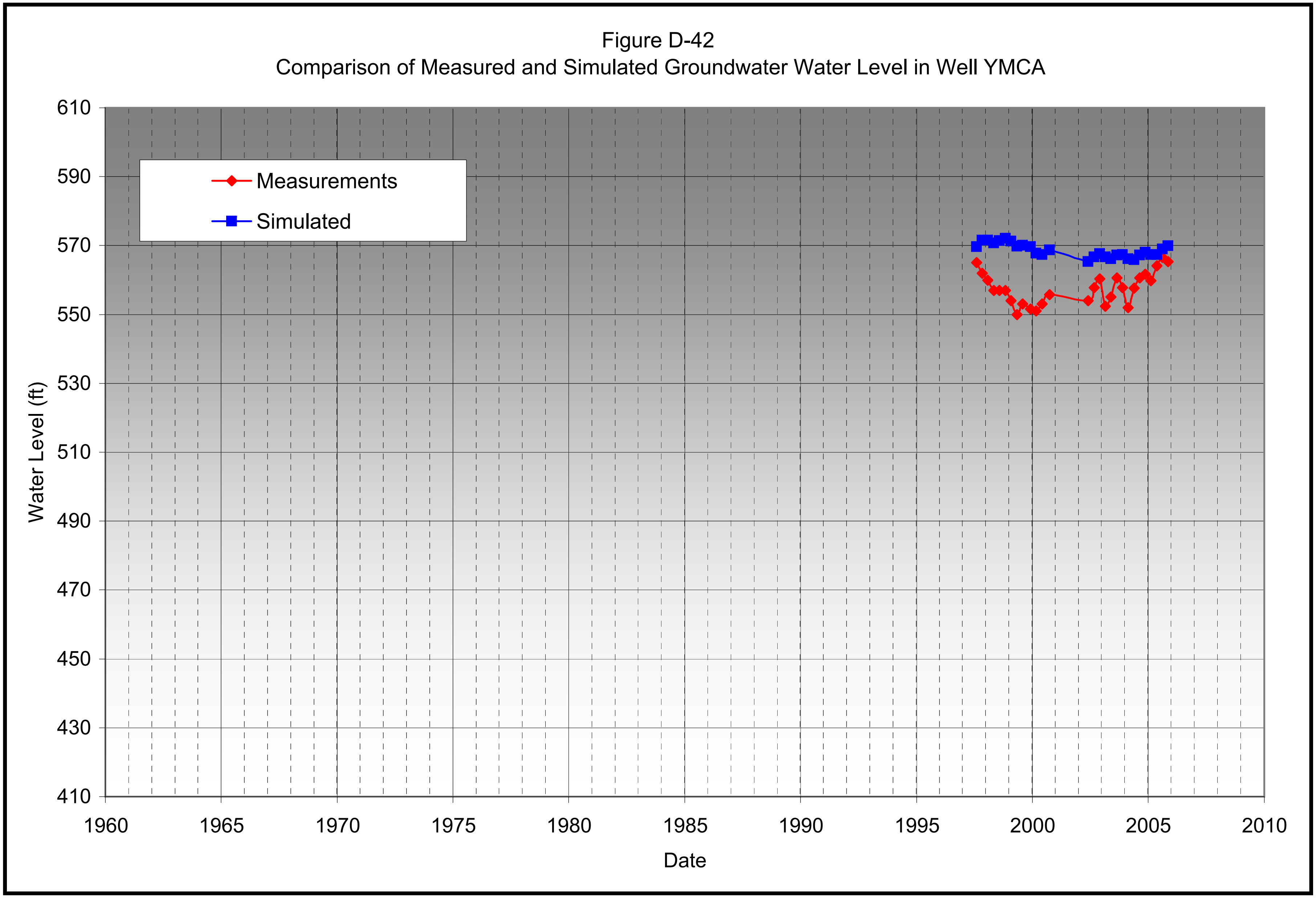

WILDERMUTH™ ENVIRONMENTAL INC.

Figure D-43
Comparison of Measured and Simulated Groundwater Water Level in Well MW-24I

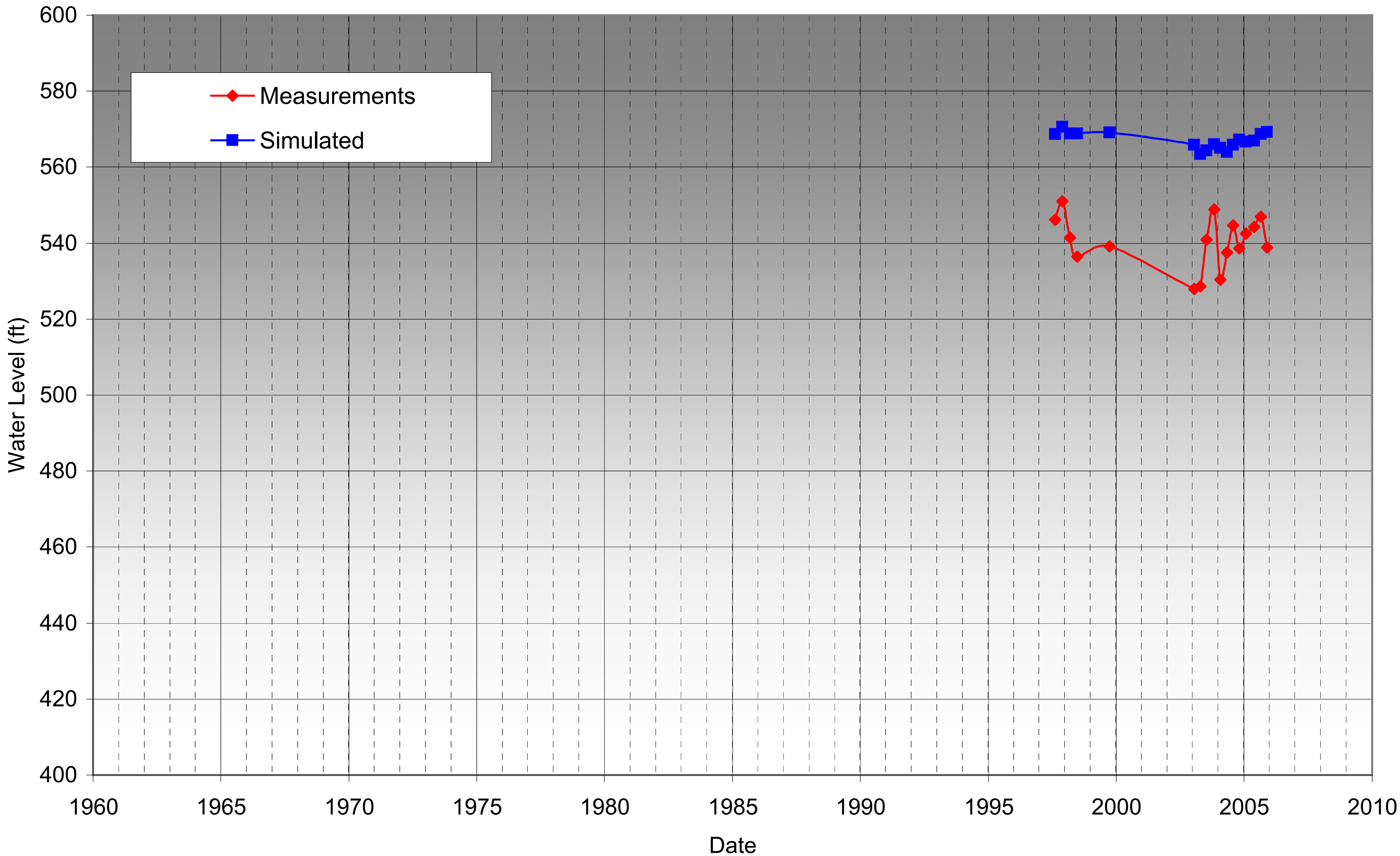

WILDERMUTH™ ENVIRONMENTAL INC.

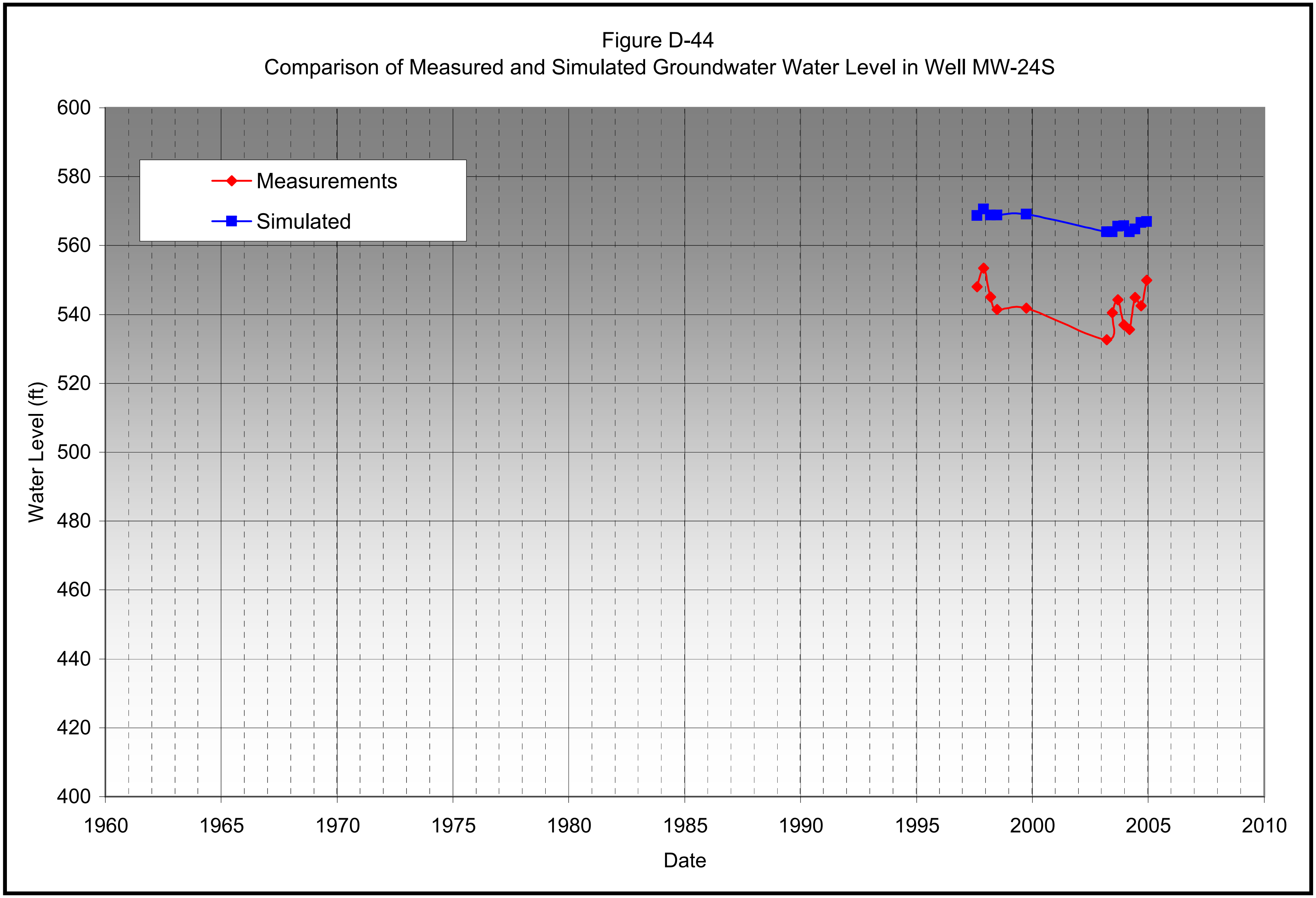

WILDERMUTH ENVIRONMENTAL INC.

Figure D-45
Comparison of Measured and Simulated Groundwater Water Level in Well AP-PA-7

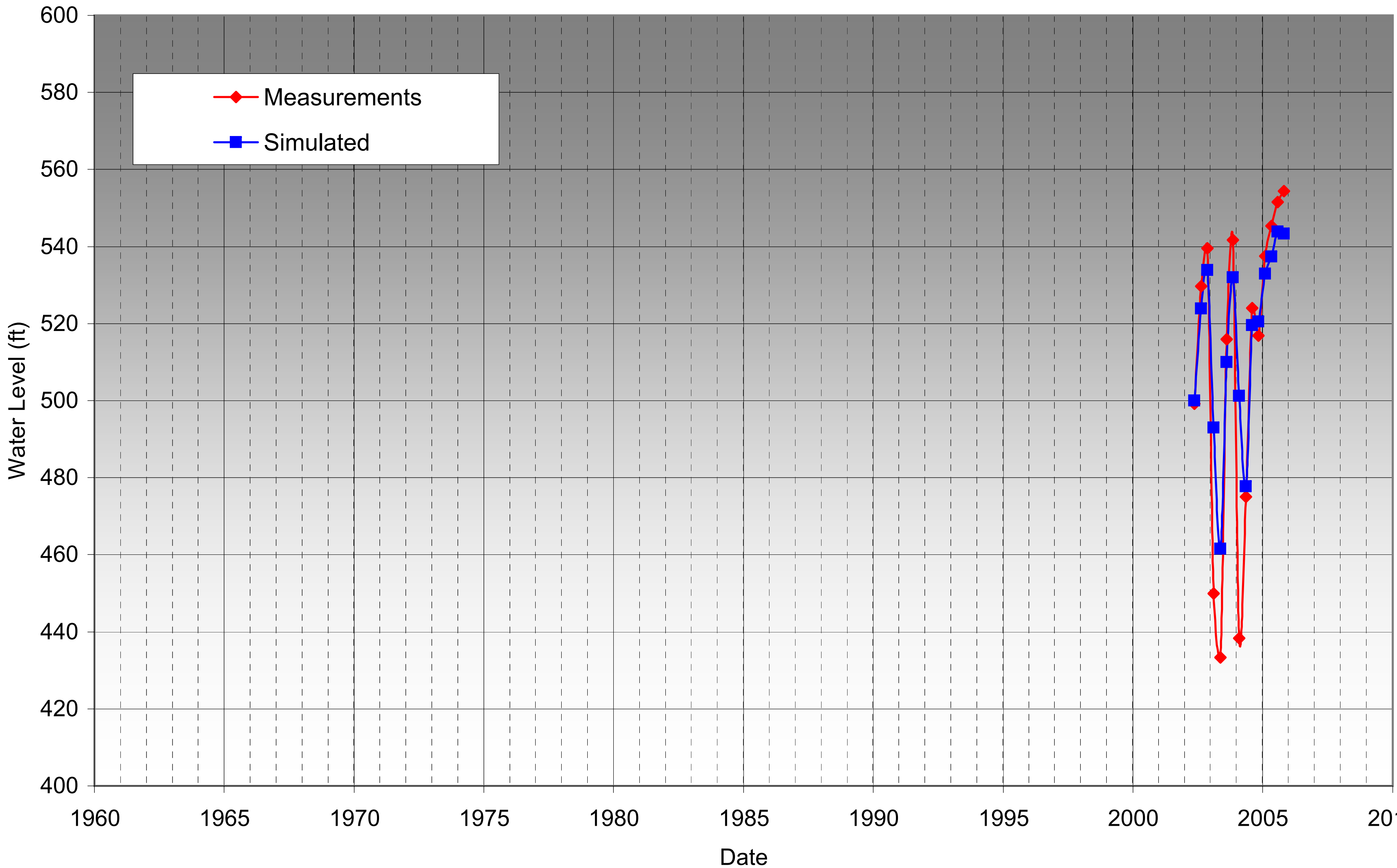

WILDERMUTH™ ENVIRONMENTAL INC.

Figure D-46
Comparison of Measured and Simulated Groundwater Water Level in Well AP-PA-10

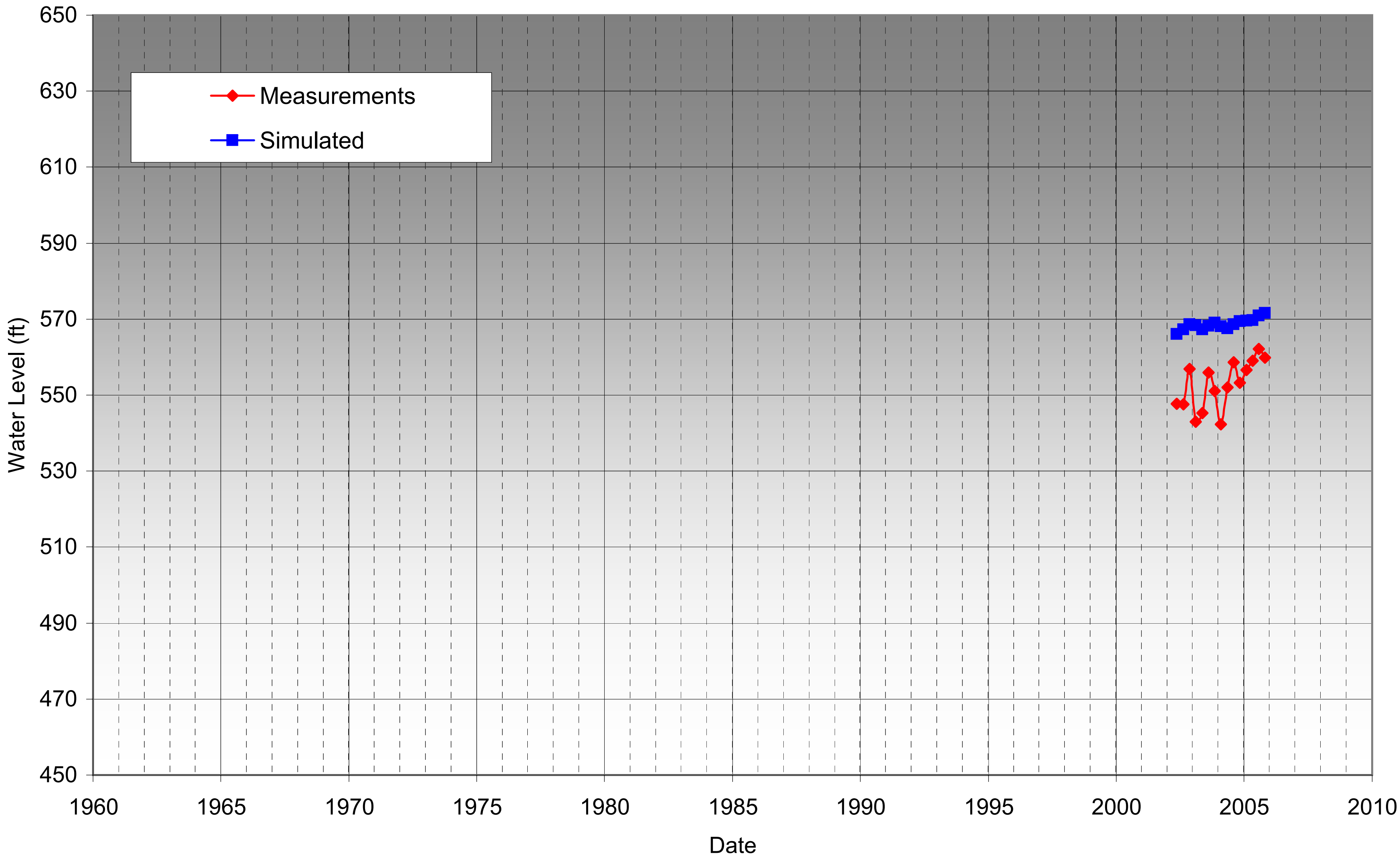

WILDERMUTH™ ENVIRONMENTAL INC.

Figure D-47
Comparison of Measured and Simulated Groundwater Water Level in Well MW-11

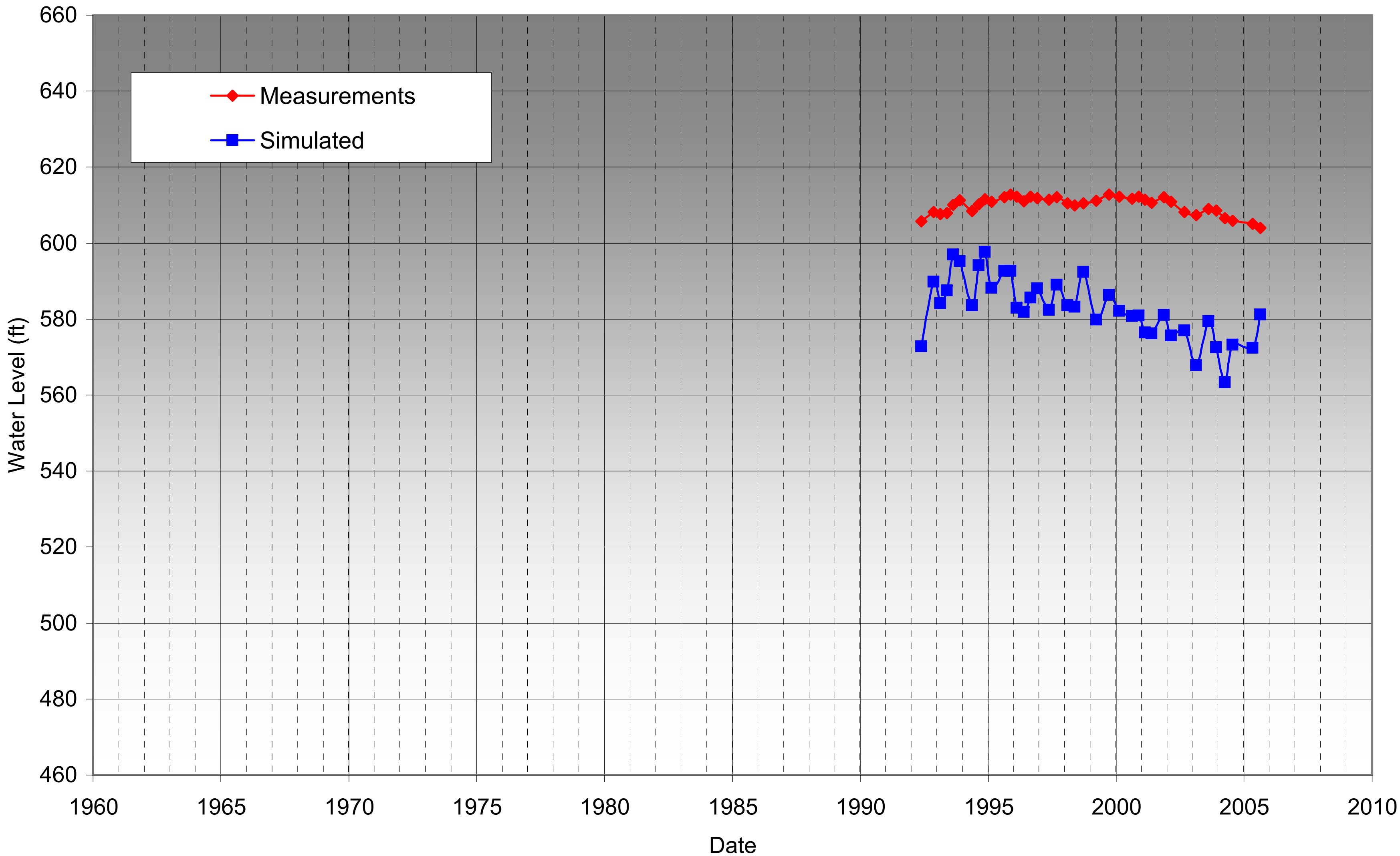

Appendix E

Groundwater Elevations and Elevation Change Maps for the Planning Alternatives

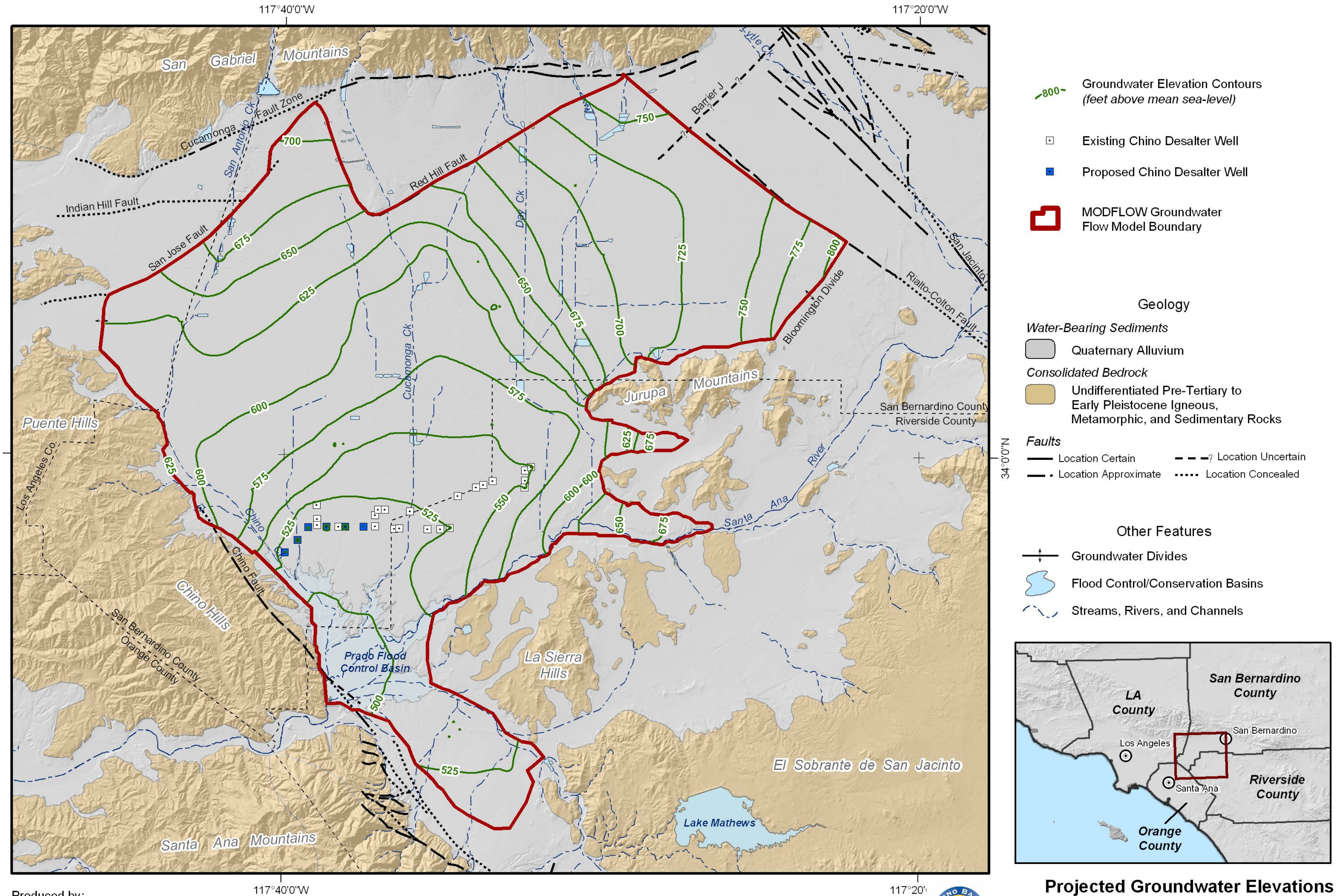

Produced by:

WILDERMUTH ENVIRONMENTAL INC.

23692 Birtcher Drive
Lake Forest, CA 92630
949.420.3030
www.wildermuthenvironmental.com

Author: MJC
Date: 20071030
File: Figure_E-1.mxd

2007 CBWM Groundwater Model Documentation and Evaluation of the Peace II Project Description
Groundwater Elevation Maps

Projected Groundwater Elevations for Layer 1
Baseline Alternative in 2023

Figure E-1

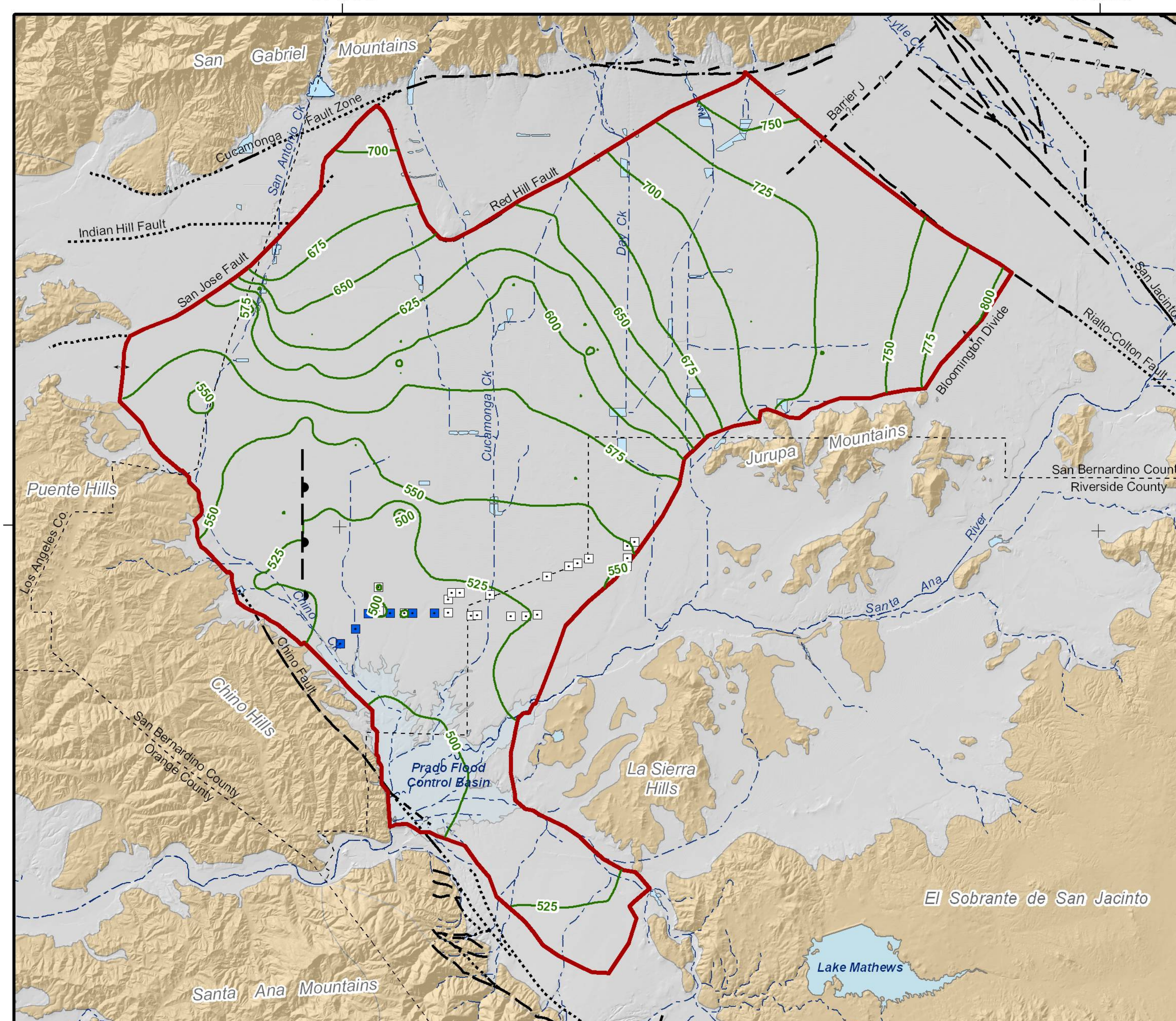

Groundwater Elevation Contours (feet above mean sea-level)

Existing Chino Desalter Well

Proposed Chino Desalter Well

MODFLOW Groundwater Flow Model Boundary

Geology

Water-Bearing Sediments

Quaternary Alluvium

Consolidated Bedrock

Undifferentiated Pre-Tertiary to Early Pleistocene Igneous, Metamorphic, and Sedimentary Rocks

Faults

Location Certain

Location Approximate

Location Concealed

Location Uncertain

Approximate Location of Groundwater Barrier

Other Features

Groundwater Divides

Flood Control/Conservation Basins

Streams, Rivers, and Channels

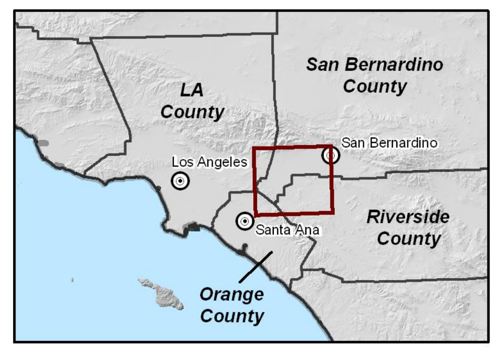

Produced by:

WILDERMUTH ENVIRONMENTAL INC.

23692 Birtcher Drive
Lake Forest, CA 92630
949.420.3030
www.wildermuthenvironmental.com

Author: MJC

Date: 20071030

File: Figure_E-2.mxd

0 1 2 3 4 Miles

0 2 4 6 KM

2007 CBWM Groundwater Model Documentation and Evaluation of the Peace II Project Description

Groundwater Elevation Maps

Projected Groundwater Elevations for Layer 2

Baseline Alternative in 2023

Figure E-2

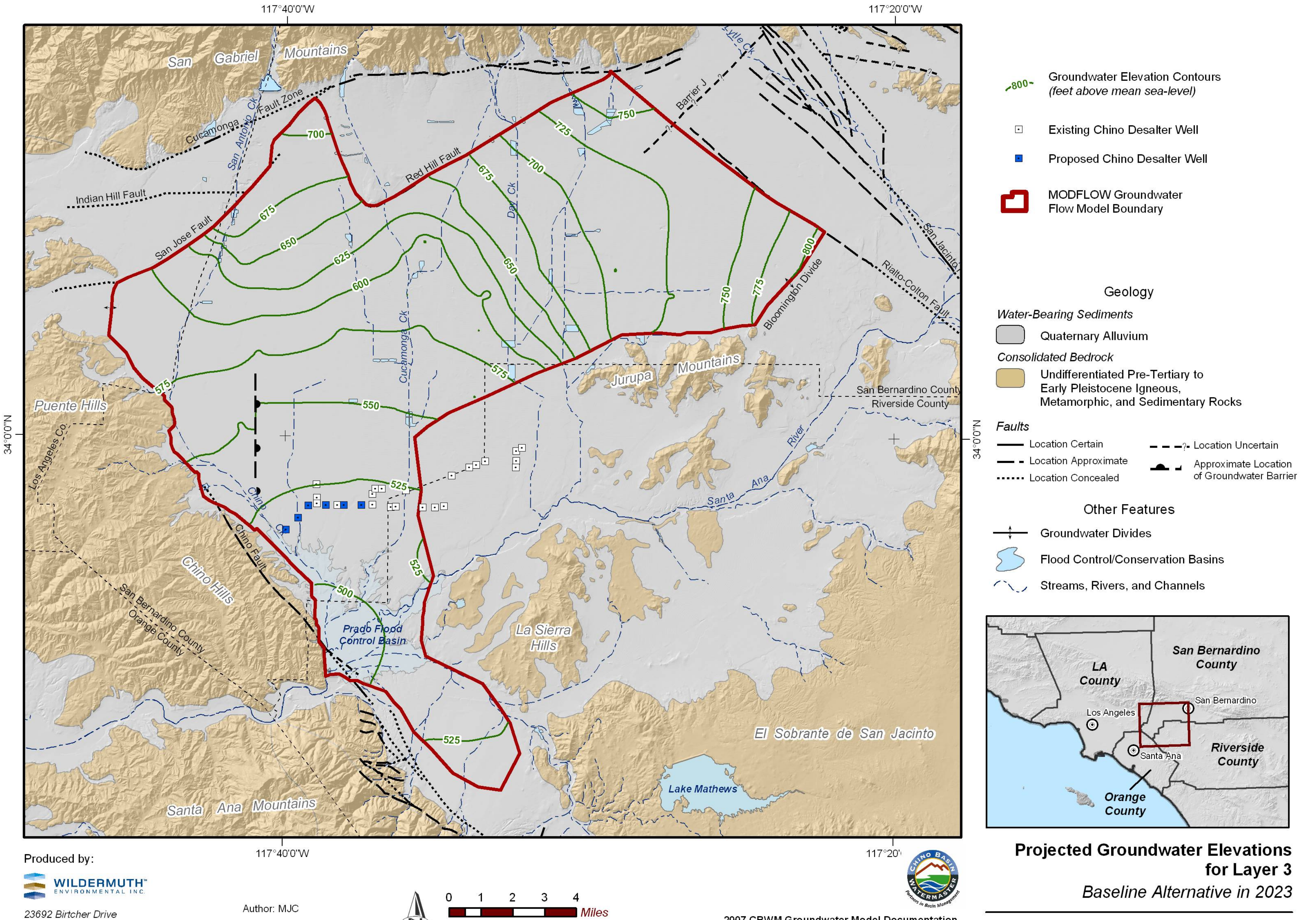

Produced by:

WILDERMUTH ENVIRONMENTAL INC.

23692 Birtcher Drive
Lake Forest, CA 92630
949.420.3030
www.wildermuthenvironmental.com

Author: MJC
Date: 20071030
File: Figure_E-3.mxd

2007 CBWM Groundwater Model Documentation and Evaluation of the Peace II Project Description
Groundwater Elevation Maps

Projected Groundwater Elevations for Layer 3
Baseline Alternative in 2023

Figure E-3

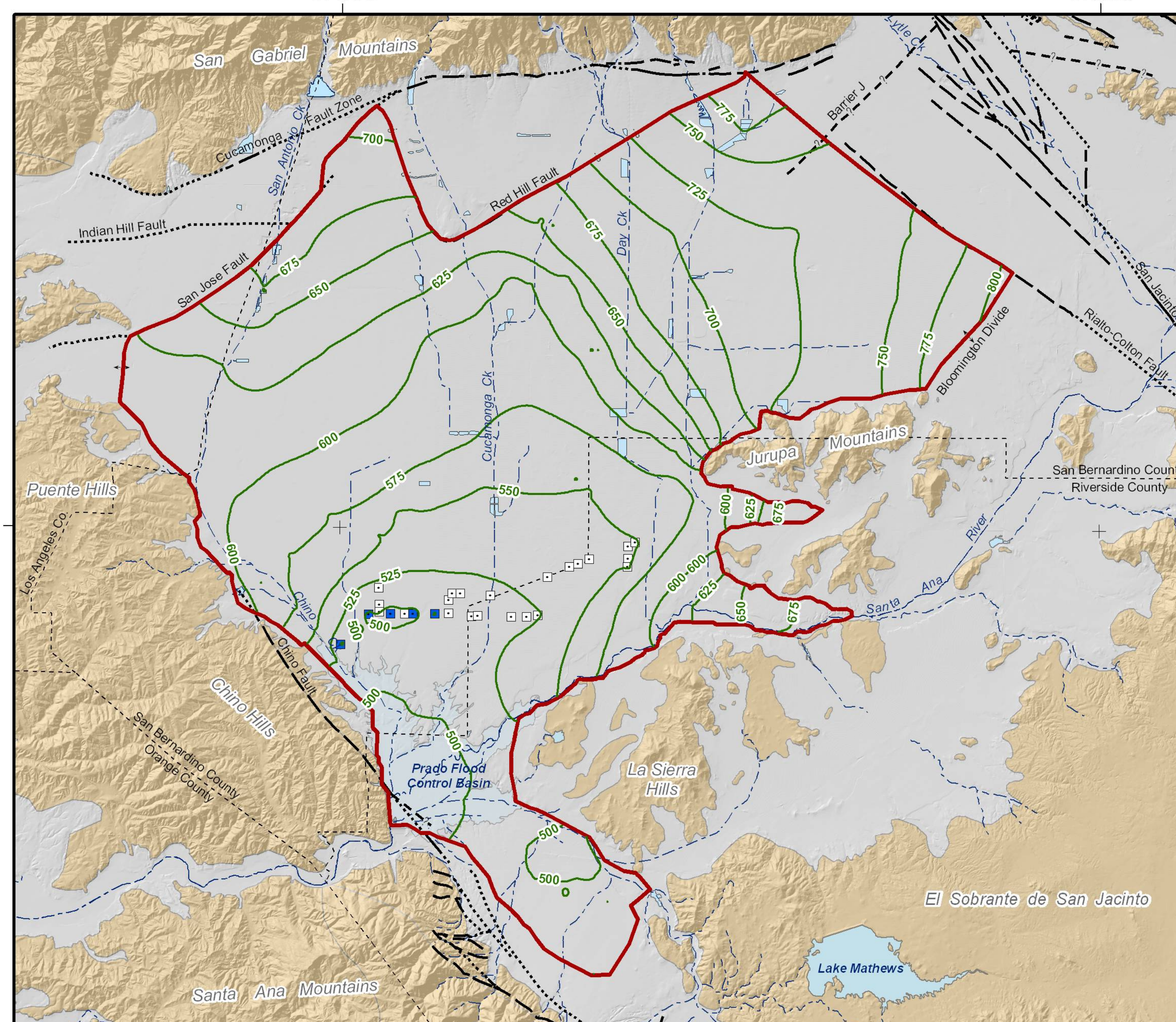

Groundwater Elevation Contours (feet above mean sea-level)

Existing Chino Desalter Well

Proposed Chino Desalter Well

MODFLOW Groundwater Flow Model Boundary

Geology

Water-Bearing Sediments

Quaternary Alluvium

Consolidated Bedrock

Undifferentiated Pre-Tertiary to Early Pleistocene Igneous, Metamorphic, and Sedimentary Rocks

Faults

Location Certain
Location Approximate
Location Uncertain
Location Concealed

Other Features

Groundwater Divides

Flood Control/Conservation Basins

Streams, Rivers, and Channels

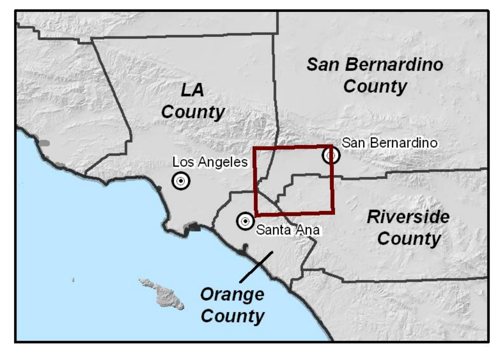

Produced by:

WILDERMUTH ENVIRONMENTAL INC.
23692 Birtcher Drive
Lake Forest, CA 92630
949.420.3030
www.wildermuthenvironmental.com

Author: MJC
Date: 20071030
File: Figure_E-4.mxd

0 1 2 3 4 Miles
0 2 4 6 KM

2007 CBWM Groundwater Model Documentation and Evaluation of the Peace II Project Description
Groundwater Elevation Maps

Projected Groundwater Elevations for Layer 1

Baseline Alternative in 2053

Figure E-4

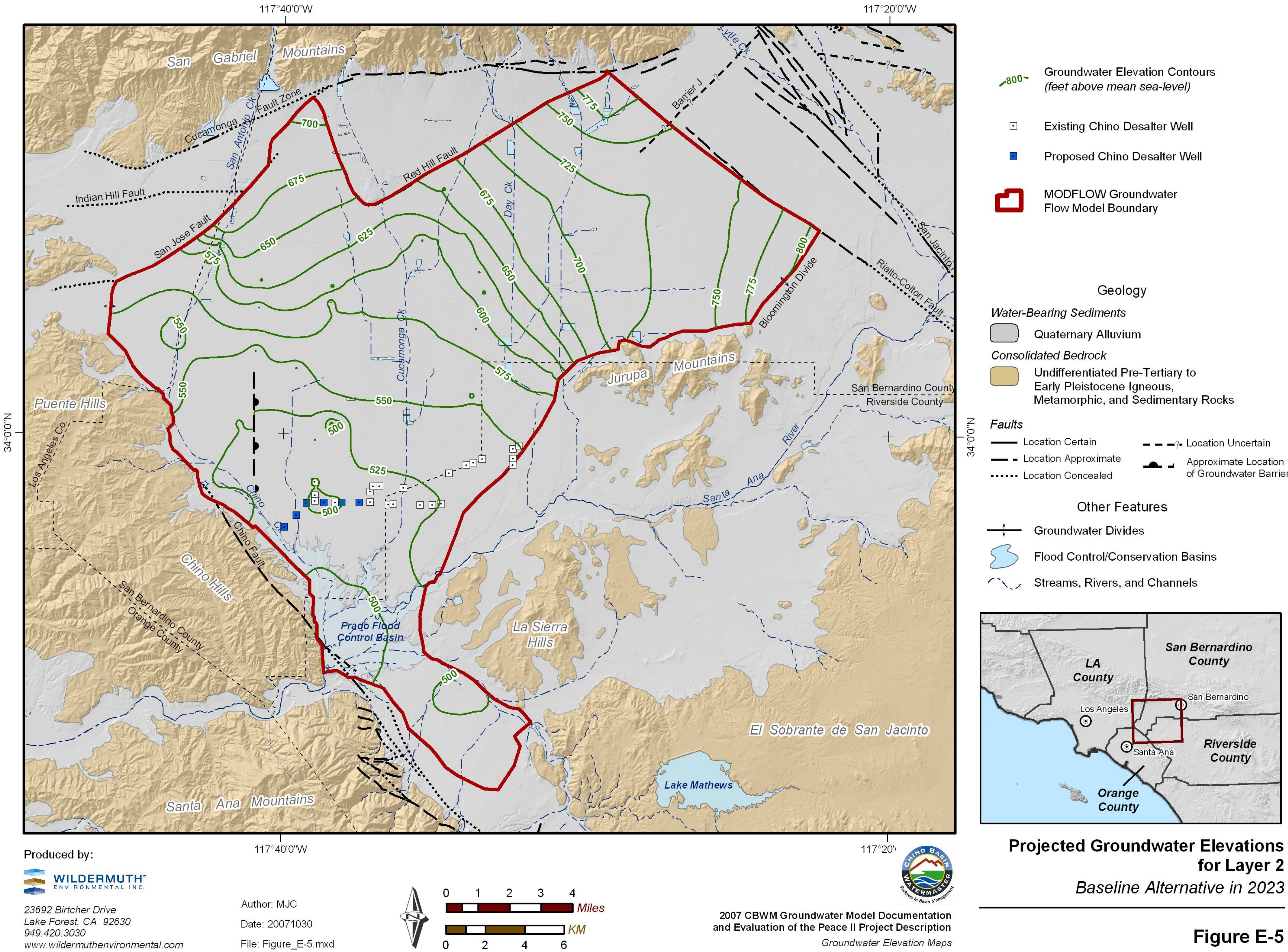

Produced by:

WILDERMUTH ENVIRONMENTAL INC.

23692 Birtcher Drive
Lake Forest, CA 92630
949.420.3030
www.wildermuthenvironmental.com

Author: MJC

Date: 20071030

File: Figure_E-5.mxd

2007 CBWM Groundwater Model Documentation and Evaluation of the Peace II Project Description

Groundwater Elevation Maps

Projected Groundwater Elevations for Layer 2

Baseline Alternative in 2023

Figure E-5

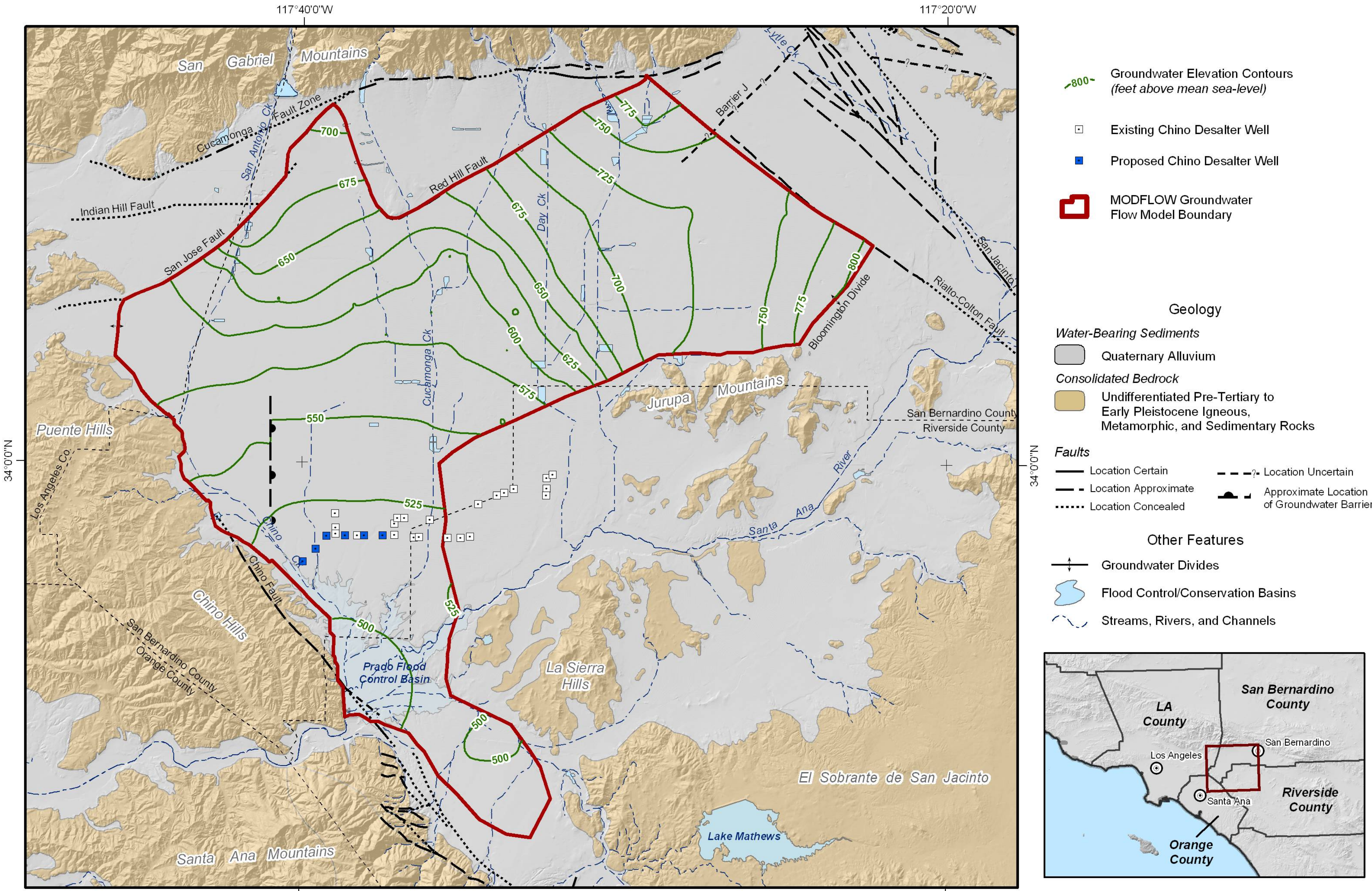

Produced by:

WILDERMUTH ENVIRONMENTAL INC.

23692 Birtcher Drive
Lake Forest, CA 92630
949.420.3030
www.wildermuthenvironmental.com

Author: MJC
Date: 20071030
File: Figure_E-6.mxd

2007 CBWM Groundwater Model Documentation and Evaluation of the Peace II Project Description
Groundwater Elevation Maps

Projected Groundwater Elevations for Layer 3

Baseline Alternative in 2053

Figure E-6

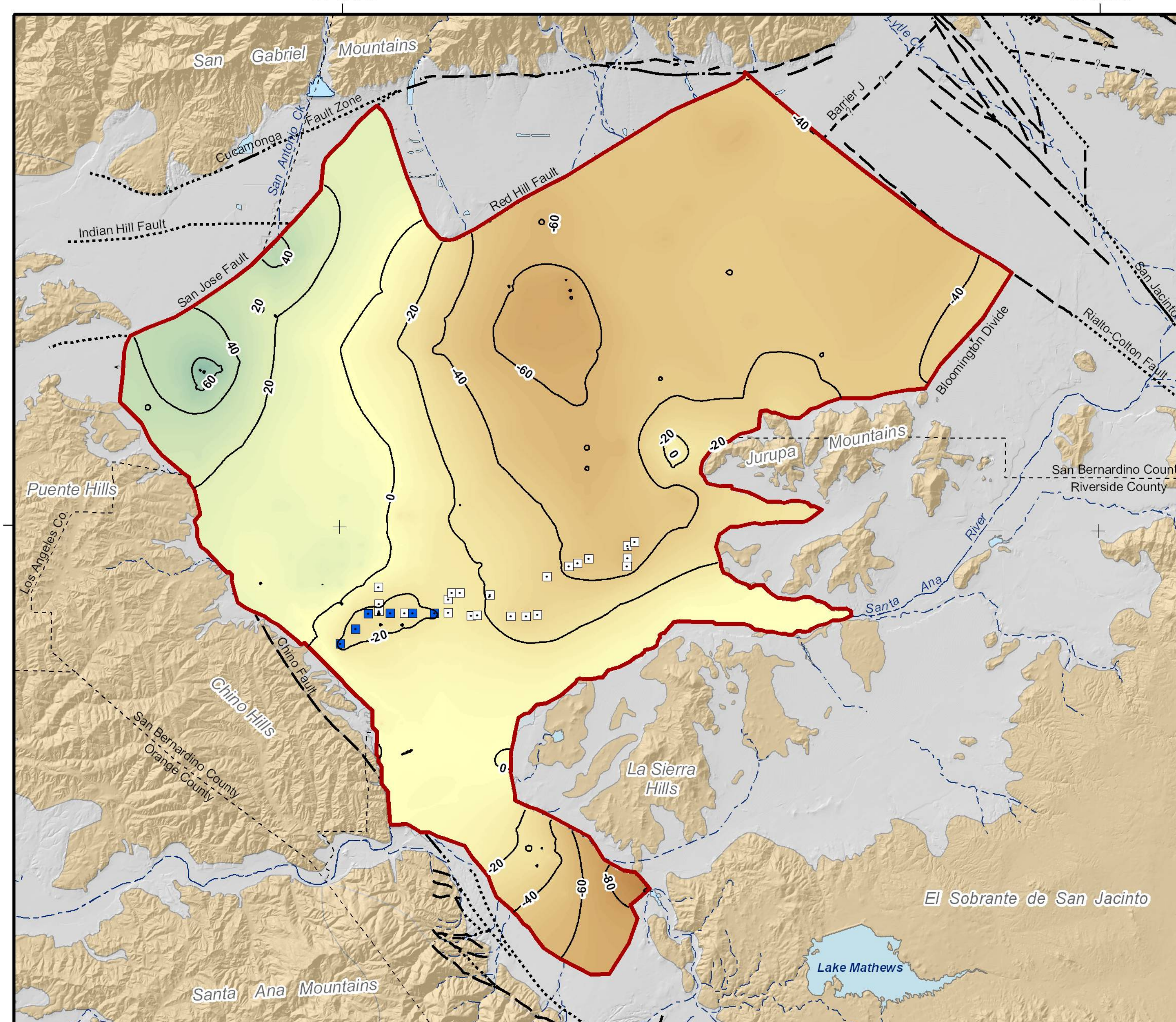

Grid of Change in Groundwater-Level *(ft-msl)*

150

-150

Existing Chino Desalter Well

Proposed Chino Desalter Well

MODFLOW Groundwater Flow Model Boundary

Geology

Water-Bearing Sediments

Quaternary Alluvium

Consolidated Bedrock

Undifferentiated Pre-Tertiary to Early Pleistocene Igneous, Metamorphic, and Sedimentary Rocks

Faults

Location Certain

Location Approximate

Location Uncertain

Location Concealed

Other Features

Groundwater Divides

Flood Control/Conservation Basins

Streams, Rivers, and Channels

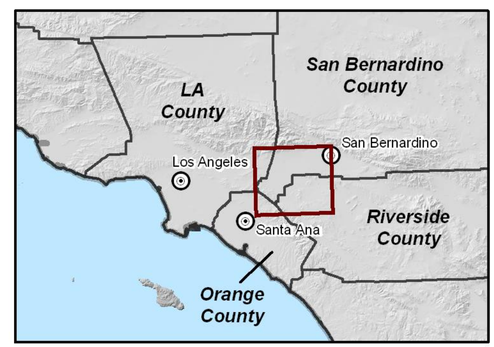

Produced by:

WILDERMUTH ENVIRONMENTAL INC.

23692 Birtcher Drive
Lake Forest, CA 92630
949.420.3030
www.wildermuthenvironmental.com

Author: MJC

Date: 20071030

File: Figure_E-7.mxd

0 1 2 3 4 Miles

0 2 4 6 KM

2007 CBWM Groundwater Model Documentation and Evaluation of the Peace II Project Description

Groundwater Elevation Maps

Change in Groundwater Elevations for Layer 1

Baseline Alternative 2005 - 2023

Figure E-7

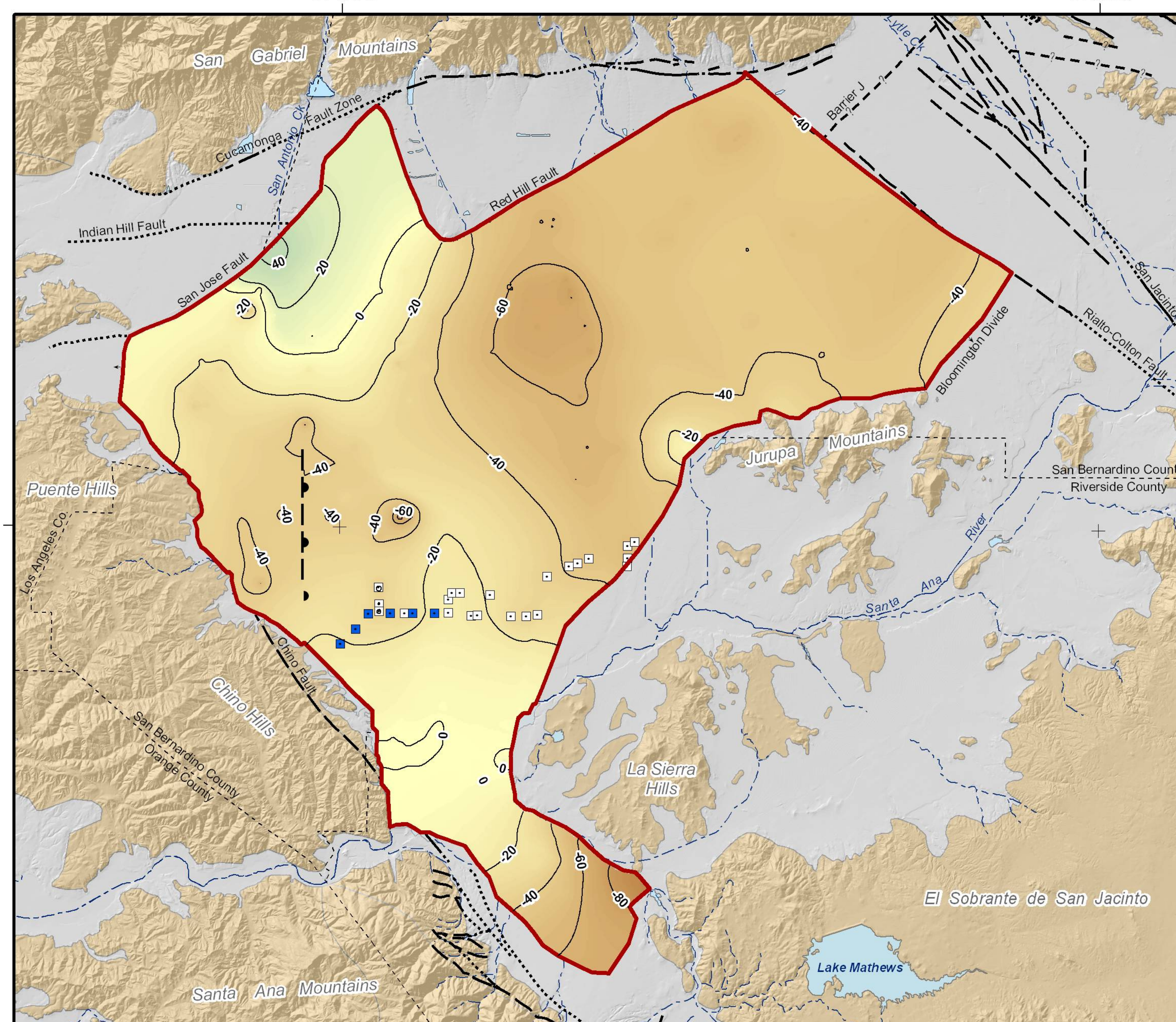

150

Grid of Change in Groundwater-Level *(ft-msl)*

-150

Existing Chino Desalter Well

Proposed Chino Desalter Well

MODFLOW Groundwater Flow Model Boundary

Geology

Water-Bearing Sediments

Quaternary Alluvium

Consolidated Bedrock

Undifferentiated Pre-Tertiary to Early Pleistocene Igneous, Metamorphic, and Sedimentary Rocks

Faults

Location Certain

Location Approximate

Location Concealed

Location Uncertain

Approximate Location of Groundwater Barrier

Other Features

Groundwater Divides

Flood Control/Conservation Basins

Streams, Rivers, and Channels

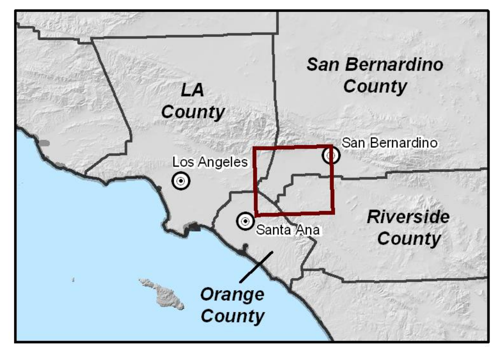

Produced by:

WILDERMUTH ENVIRONMENTAL INC.

23692 Birtcher Drive
Lake Forest, CA 92630
949.420.3030
www.wildermuthenvironmental.com

Author: MJC

Date: 20071030

File: Figure_E-8.mxd

0 1 2 3 4 Miles

0 2 4 6 KM

2007 CBWM Groundwater Model Documentation and Evaluation of the Peace II Project Description

Groundwater Elevation Maps

Change in Groundwater Elevations for Layer 2

Baseline Alternative 2005 - 2023

Figure E-8

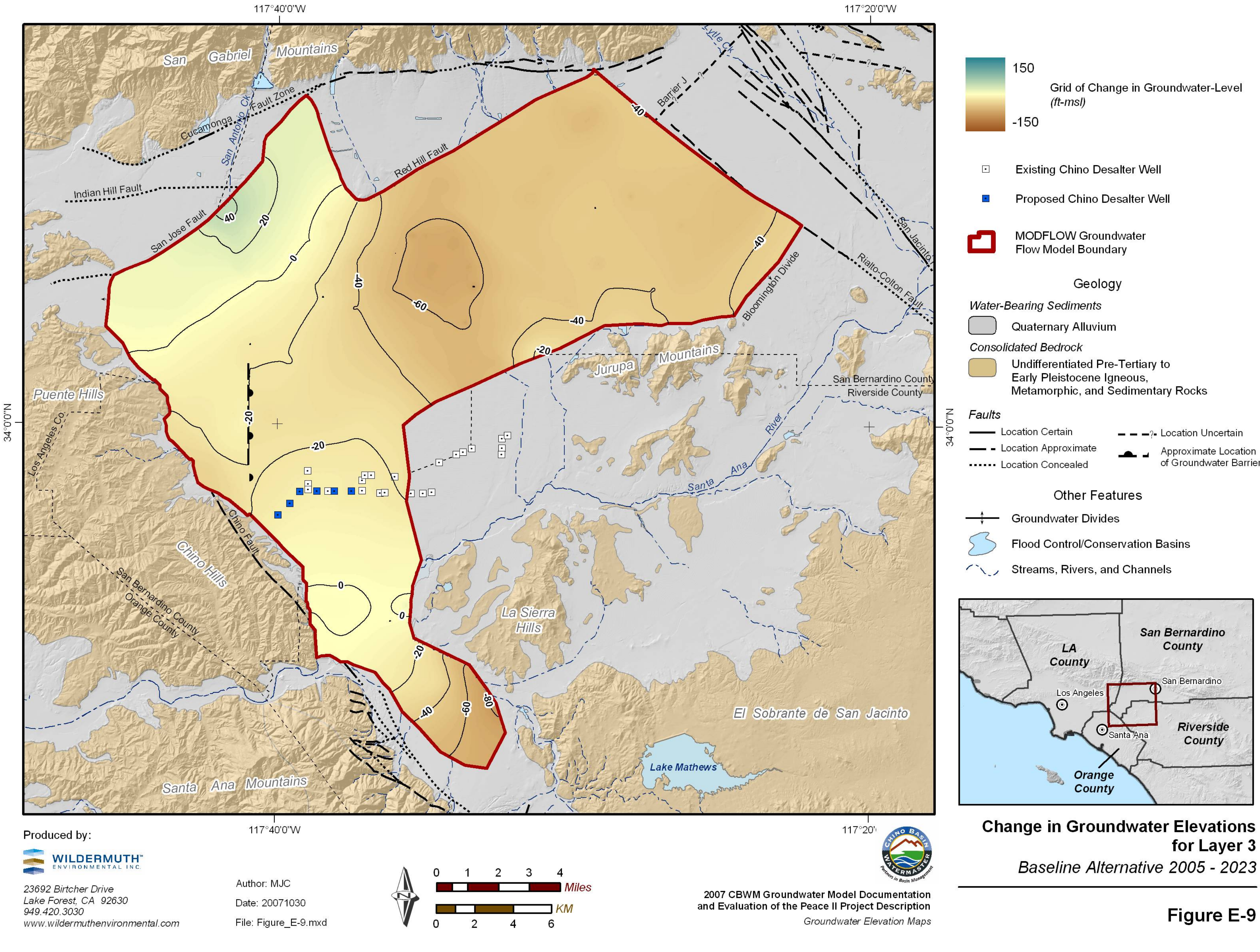

Produced by:

WILDERMUTH ENVIRONMENTAL INC.

23692 Birtcher Drive
Lake Forest, CA 92630
949.420.3030
www.wildermuthenvironmental.com

Author: MJC
Date: 20071030
File: Figure_E-9.mxd

2007 CBWM Groundwater Model Documentation and Evaluation of the Peace II Project Description
Groundwater Elevation Maps

Change in Groundwater Elevations for Layer 3
Baseline Alternative 2005 - 2023

Figure E-9

117°40'0"W 117°20'0"W

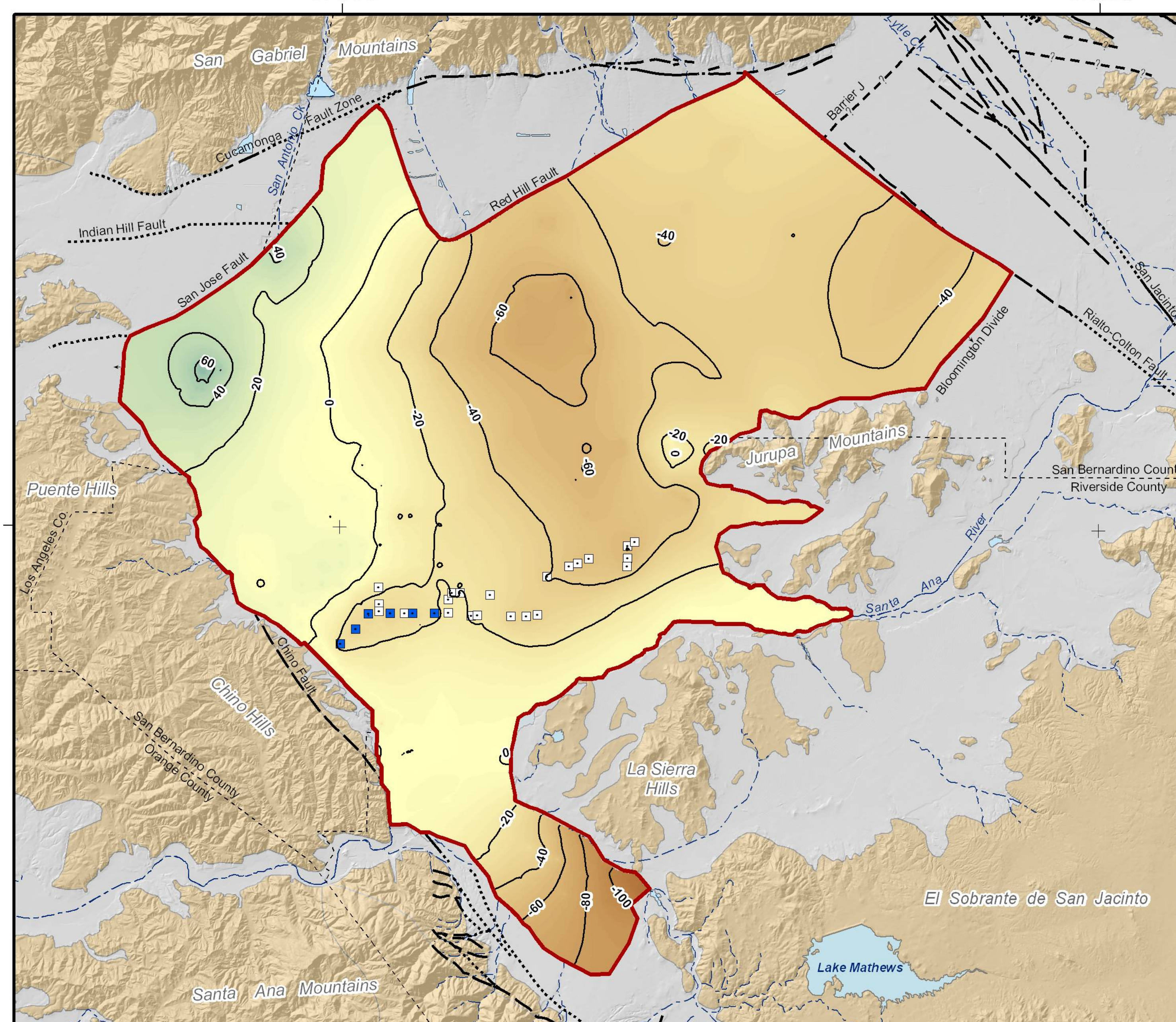

34°0'0"N

117°40'0"W 117°20'

150

-150

Grid of Change in Groundwater-Level *(ft-msl)*

Existing Chino Desalter Well

Proposed Chino Desalter Well

MODFLOW Groundwater Flow Model Boundary

Geology

Water-Bearing Sediments

Quaternary Alluvium

Consolidated Bedrock

Undifferentiated Pre-Tertiary to Early Pleistocene Igneous, Metamorphic, and Sedimentary Rocks

Faults

Location Certain

Location Approximate

Location Uncertain

Location Concealed

Other Features

Groundwater Divides

Flood Control/Conservation Basins

Streams, Rivers, and Channels

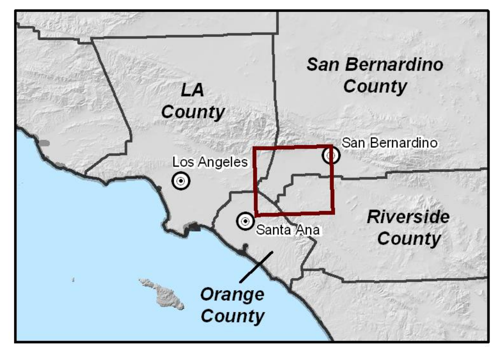

Produced by:

WILDERMUTH ENVIRONMENTAL INC.

23692 Birtcher Drive
Lake Forest, CA 92630
949.420.3030
www.wildermuthenvironmental.com

Author: MJC

Date: 20071030

File: Figure_E-10.mxd

0 1 2 3 4 Miles

0 2 4 6 KM

2007 CBWM Groundwater Model Documentation and Evaluation of the Peace II Project Description

Groundwater Elevation Maps

Change in Groundwater Elevations for Layer 1

Baseline Alternative 2005 - 2053

Figure E-10

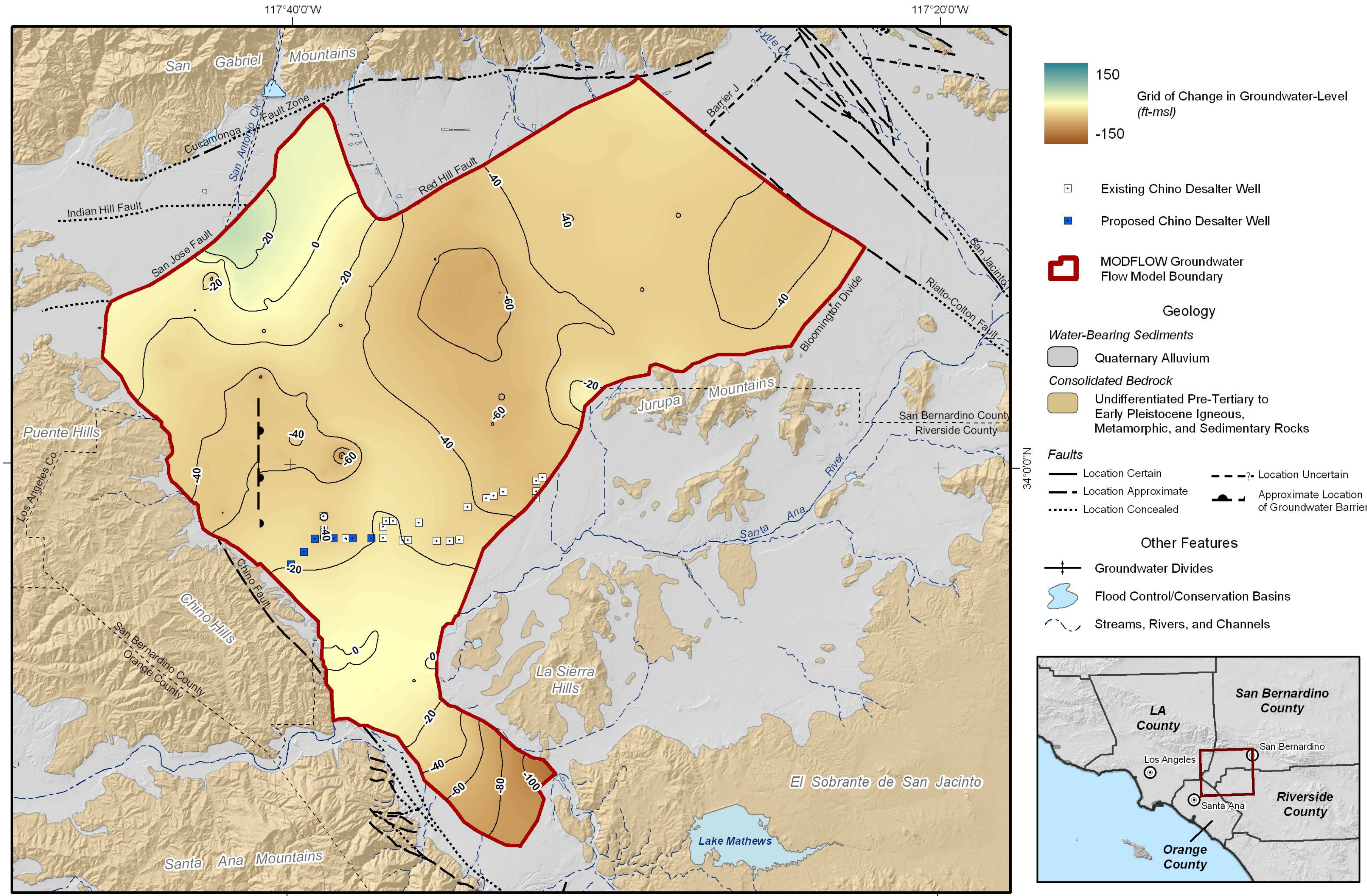

Produced by:

WILDERMUTH ENVIRONMENTAL INC.

23692 Birtcher Drive
Lake Forest, CA 92630
949.420.3030
www.wildermuthenvironmental.com

Author: MJC
Date: 20071030
File: Figure_E-11.mxd

2007 CBWM Groundwater Model Documentation and Evaluation of the Peace II Project Description
Groundwater Elevation Maps

Change in Groundwater Elevations for Layer 2
Baseline Alternative 2005 - 2053

Figure E-11

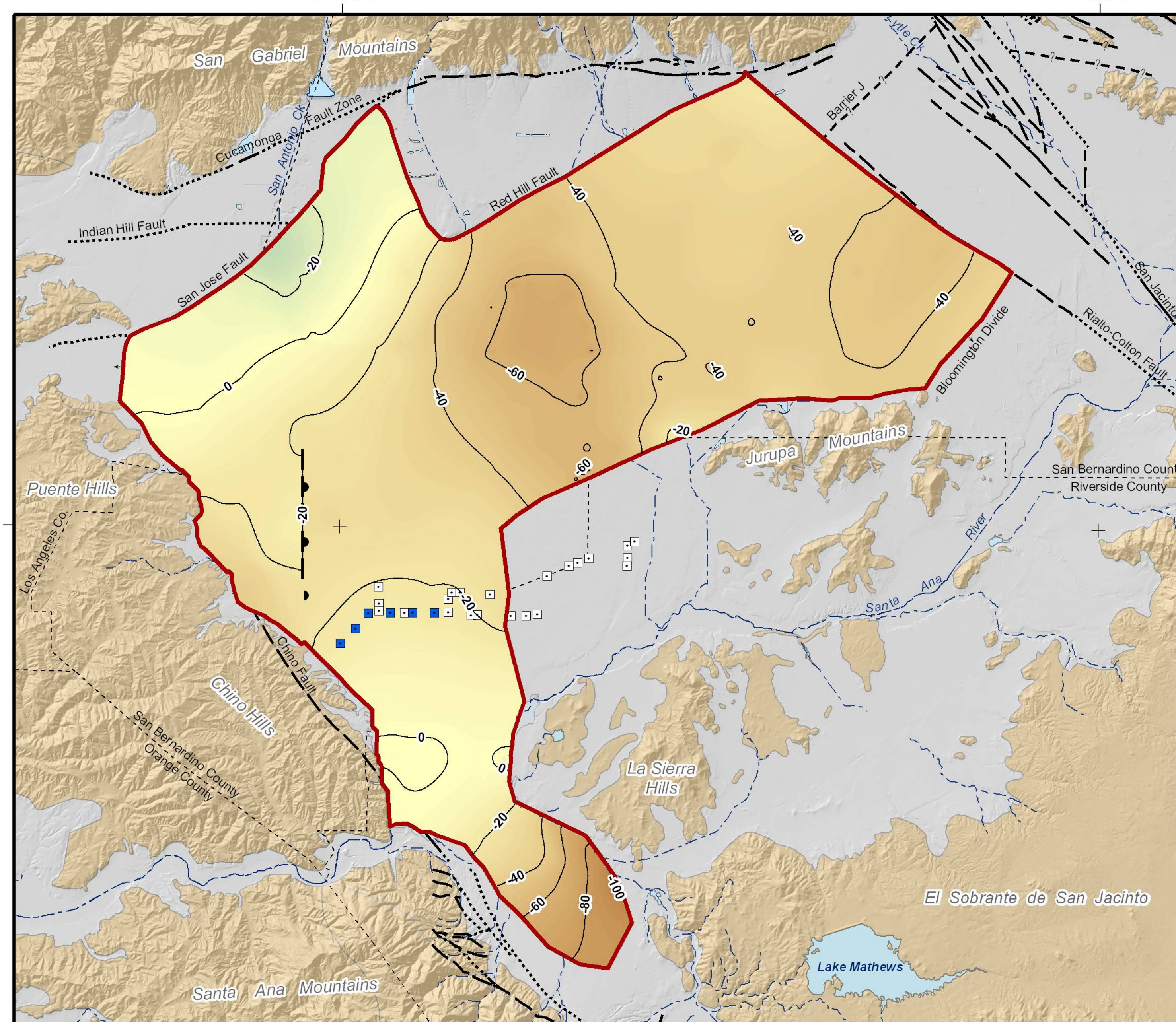

150

-150

Grid of Change in Groundwater-Level *(ft-msl)*

Existing Chino Desalter Well

Proposed Chino Desalter Well

MODFLOW Groundwater Flow Model Boundary

Geology

Water-Bearing Sediments

Quaternary Alluvium

Consolidated Bedrock

Undifferentiated Pre-Tertiary to Early Pleistocene Igneous, Metamorphic, and Sedimentary Rocks

Faults

Location Certain

Location Approximate

Location Concealed

Location Uncertain

Approximate Location of Groundwater Barrier

Other Features

Groundwater Divides

Flood Control/Conservation Basins

Streams, Rivers, and Channels

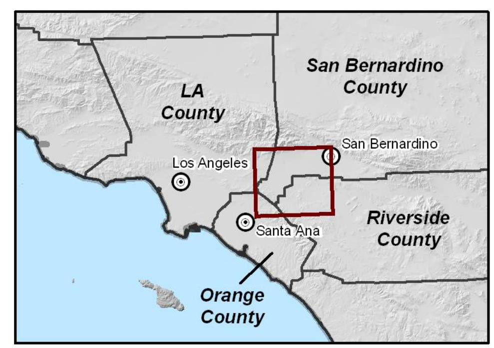

Produced by:

WILDERMUTH ENVIRONMENTAL INC.

23692 Birtcher Drive
Lake Forest, CA 92630
949.420.3030
www.wildermuthenvironmental.com

Author: MJC

Date: 20071030

File: Figure_E-12.mxd

0 1 2 3 4 Miles

0 2 4 6 KM

2007 CBWM Groundwater Model Documentation and Evaluation of the Peace II Project Description

Groundwater Elevation Maps

Change in Groundwater Elevations for Layer 3

Baseline Alternative 2005 - 2053

Figure E-12

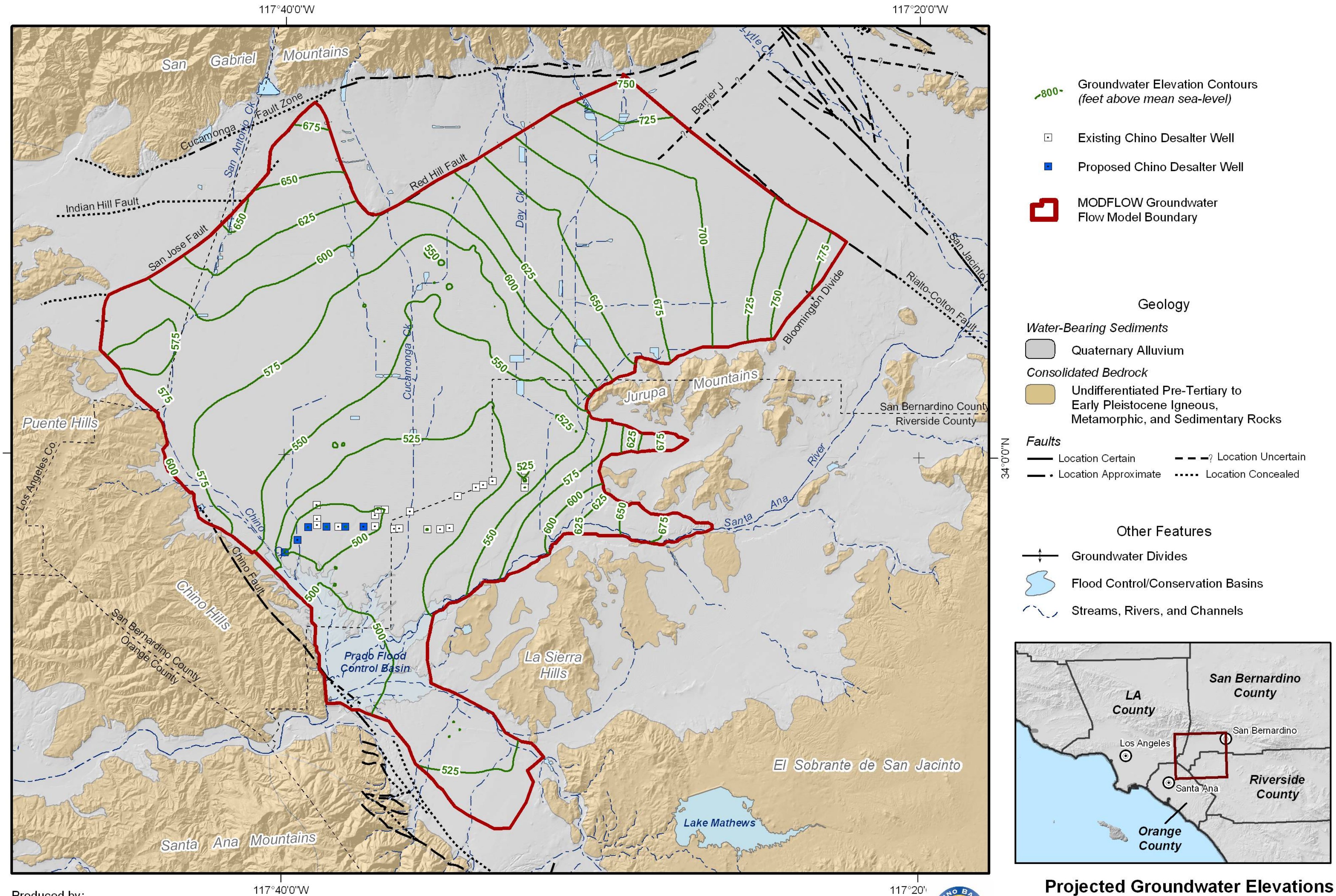

Produced by:

WILDERMUTH ENVIRONMENTAL INC.

23692 Birtcher Drive
Lake Forest, CA 92630
949.420.3030
www.wildermuthenvironmental.com

Author: MJC
Date: 20071030
File: Figure_E-13.mxd

2007 CBWM Groundwater Model Documentation and Evaluation of the Peace II Project Description
Groundwater Elevation Maps

Projected Groundwater Elevations for Layer 1
Alternative 1A in 2023

Figure E-13

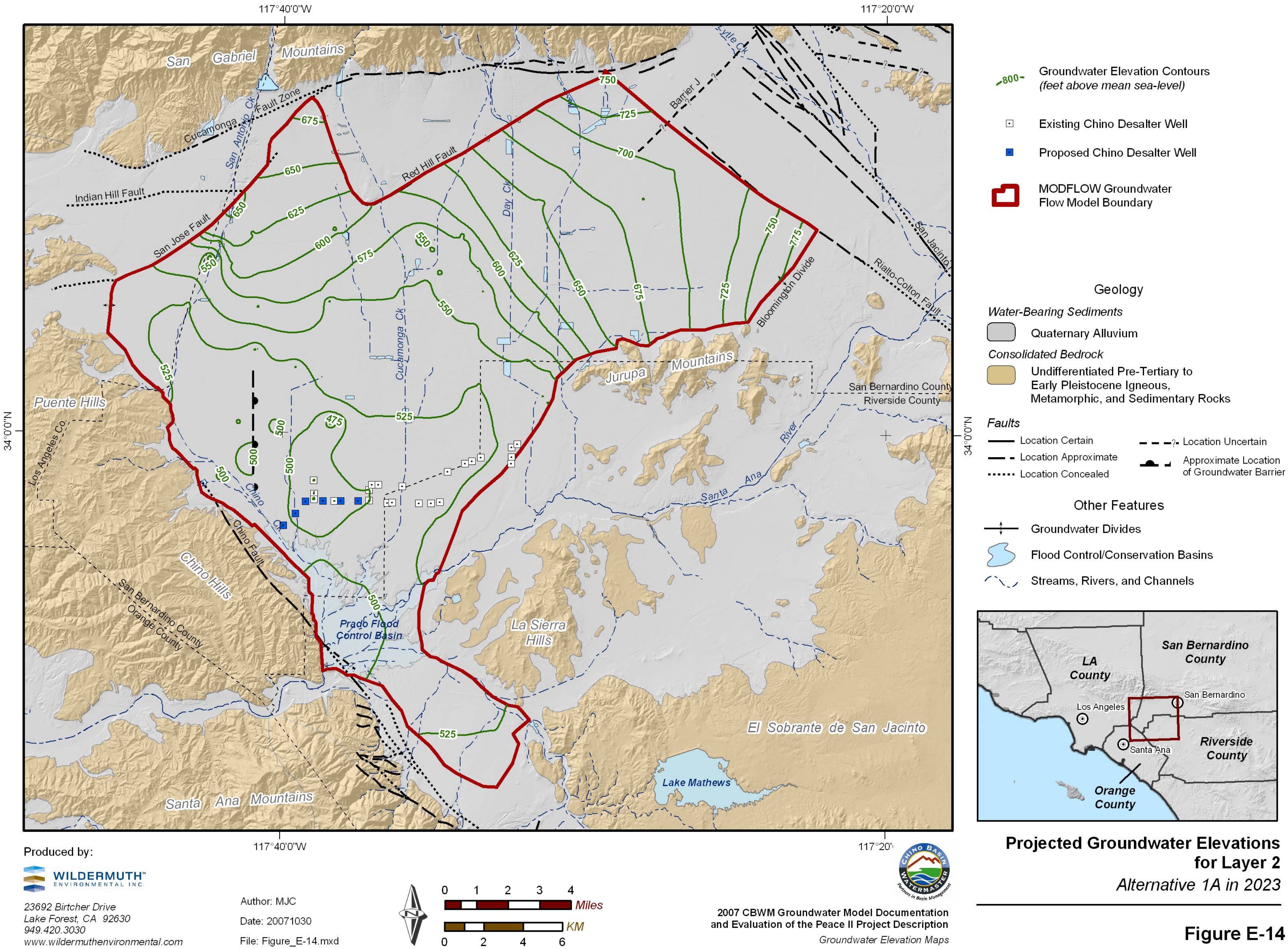

Produced by:

WILDERMUTH ENVIRONMENTAL INC.

23692 Birtcher Drive
Lake Forest, CA 92630
949.420.3030
www.wildermuthenvironmental.com

Author: MJC
Date: 20071030
File: Figure_E-14.mxd

2007 CBWM Groundwater Model Documentation and Evaluation of the Peace II Project Description
Groundwater Elevation Maps

Projected Groundwater Elevations for Layer 2
Alternative 1A in 2023

Figure E-14

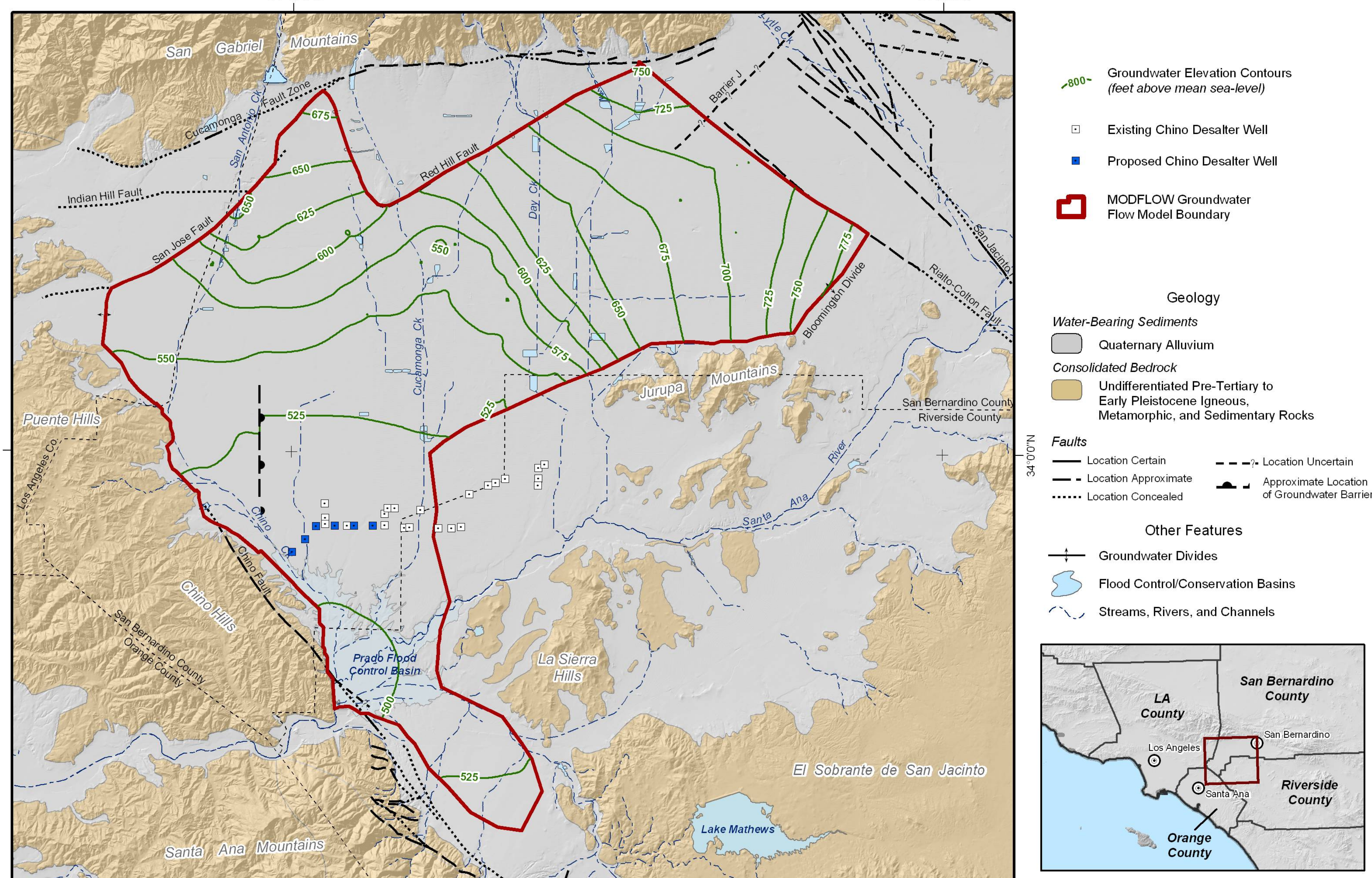

Produced by:
WILDERMUTH ENVIRONMENTAL INC.
23692 Birtcher Drive
Lake Forest, CA 92630
949.420.3030
www.wildermuthenvironmental.com

Author: MJC
Date: 20071030
File: Figure_E-15.mxd

2007 CBWM Groundwater Model Documentation and Evaluation of the Peace II Project Description
Groundwater Elevation Maps

Projected Groundwater Elevations for Layer 3
Alternative 1A in 2023

Figure E-15

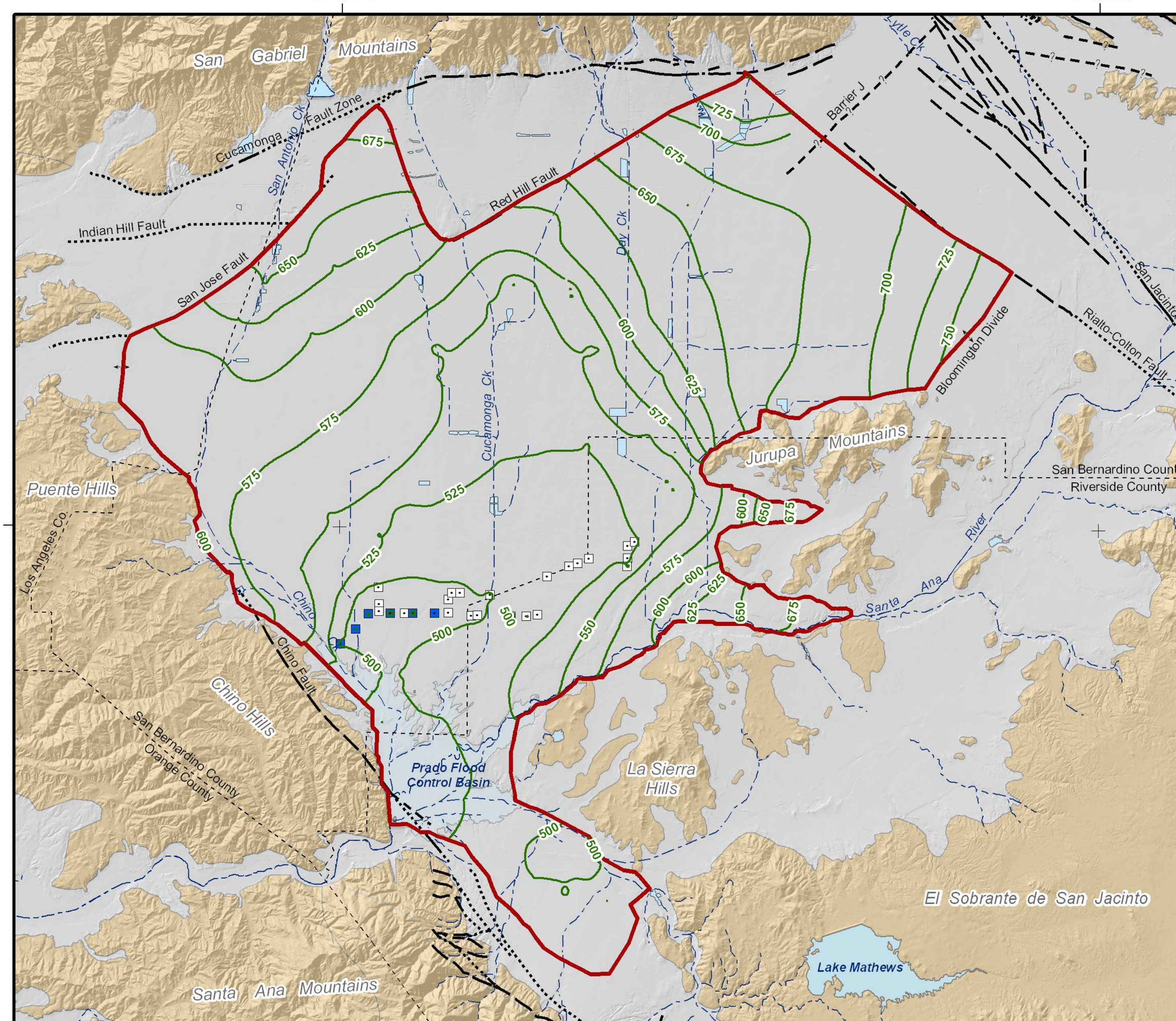

Groundwater Elevation Contours *(feet above mean sea-level)*

Existing Chino Desalter Well

Proposed Chino Desalter Well

MODFLOW Groundwater Flow Model Boundary

Geology

Water-Bearing Sediments

Quaternary Alluvium

Consolidated Bedrock

Undifferentiated Pre-Tertiary to Early Pleistocene Igneous, Metamorphic, and Sedimentary Rocks

Faults

Location Certain

Location Approximate

Location Uncertain

Location Concealed

Other Features

Groundwater Divides

Flood Control/Conservation Basins

Streams, Rivers, and Channels

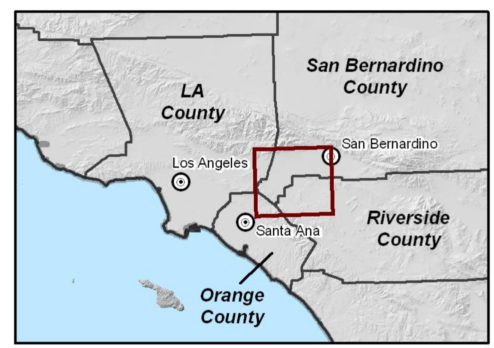

Projected Groundwater Elevations for Layer 1

Alternative 1A in 2053

Produced by:

WILDERMUTH ENVIRONMENTAL INC.

23692 Birtcher Drive
Lake Forest, CA 92630
949.420.3030
www.wildermuthenvironmental.com

Author: MJC

Date: 20071030

File: Figure_E-16.mxd

0 1 2 3 4 Miles

0 2 4 6 KM

CHINO BASIN WATERMASTER — Partners in Basin Management

2007 CBWM Groundwater Model Documentation and Evaluation of the Peace II Project Description

Groundwater Elevation Maps

Figure E-16

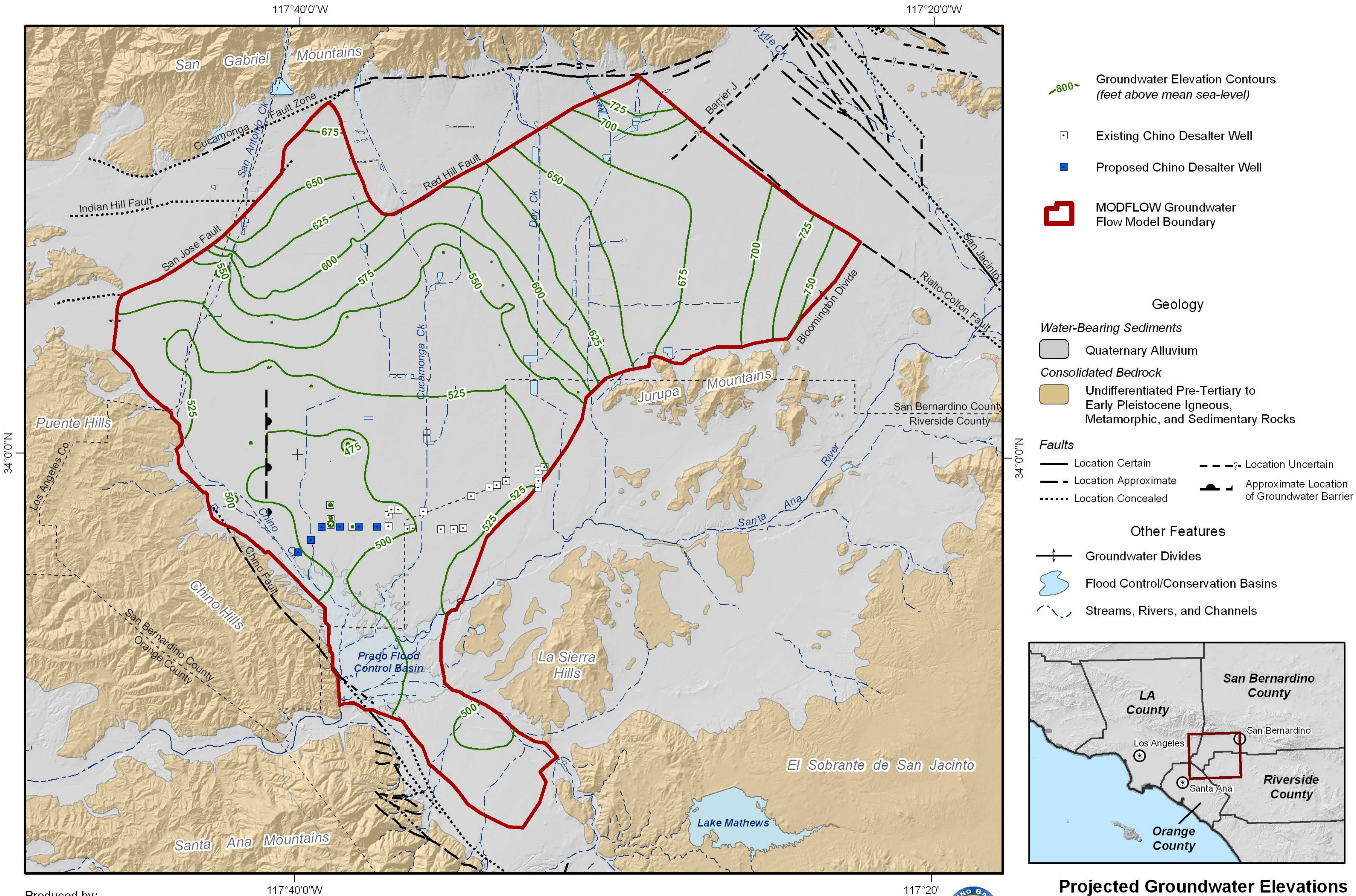

Produced by:

WILDERMUTH ENVIRONMENTAL INC.

23692 Birtcher Drive
Lake Forest, CA 92630
949.420.3030
www.wildermuthenvironmental.com

Author: MJC

Date: 20071030

File: Figure_E-17.mxd

2007 CBWM Groundwater Model Documentation and Evaluation of the Peace II Project Description

Groundwater Elevation Maps

Projected Groundwater Elevations for Layer 2

Alternative 1A in 2053

Figure E-17

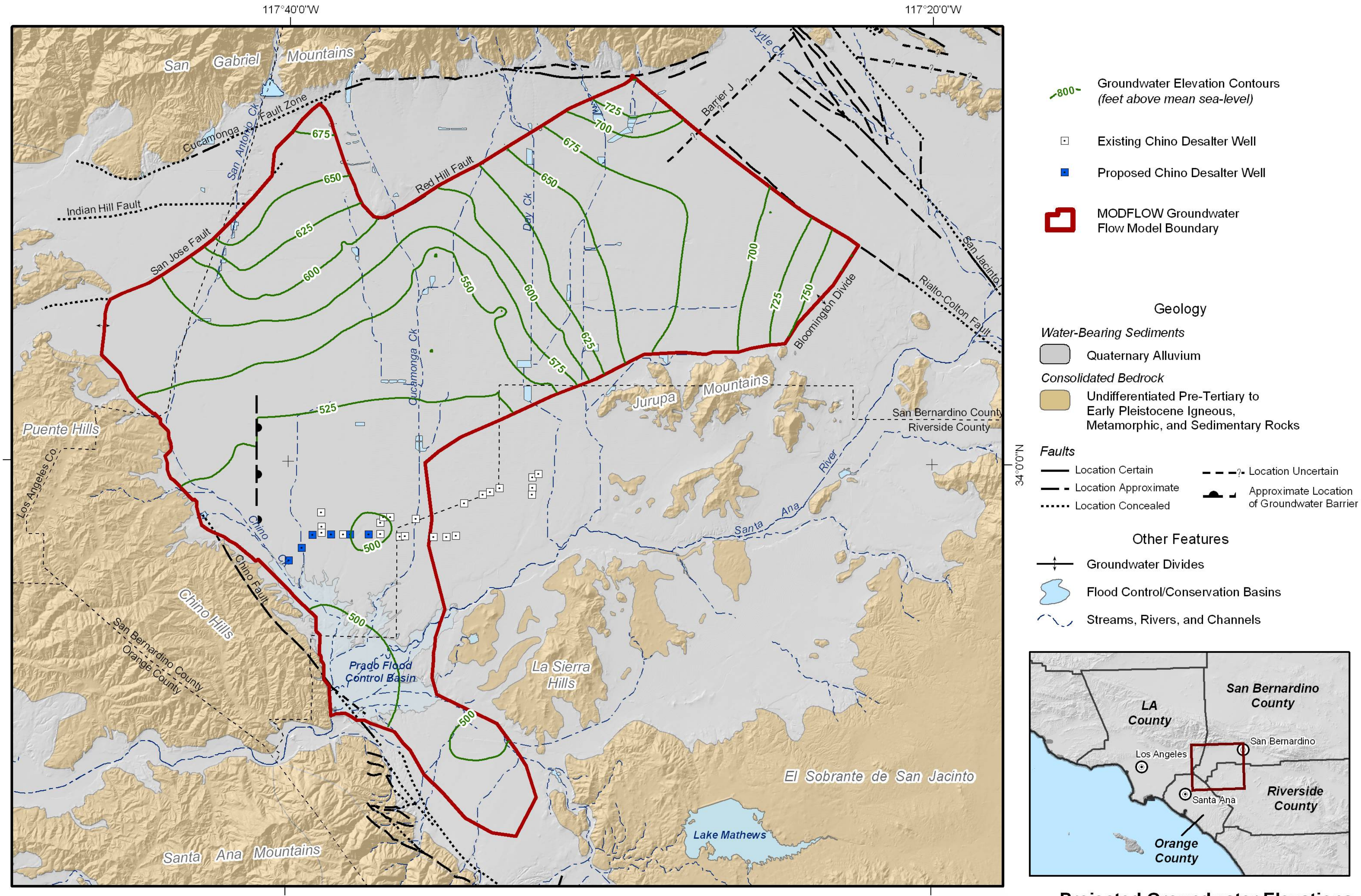

Produced by:

WILDERMUTH ENVIRONMENTAL INC.

23692 Birtcher Drive
Lake Forest, CA 92630
949.420.3030
www.wildermuthenvironmental.com

Author: MJC
Date: 20071030
File: Figure_E-18.mxd

2007 CBWM Groundwater Model Documentation and Evaluation of the Peace II Project Description
Groundwater Elevation Maps

Projected Groundwater Elevations for Layer 3

Alternative 1A in 2053

Figure E-18

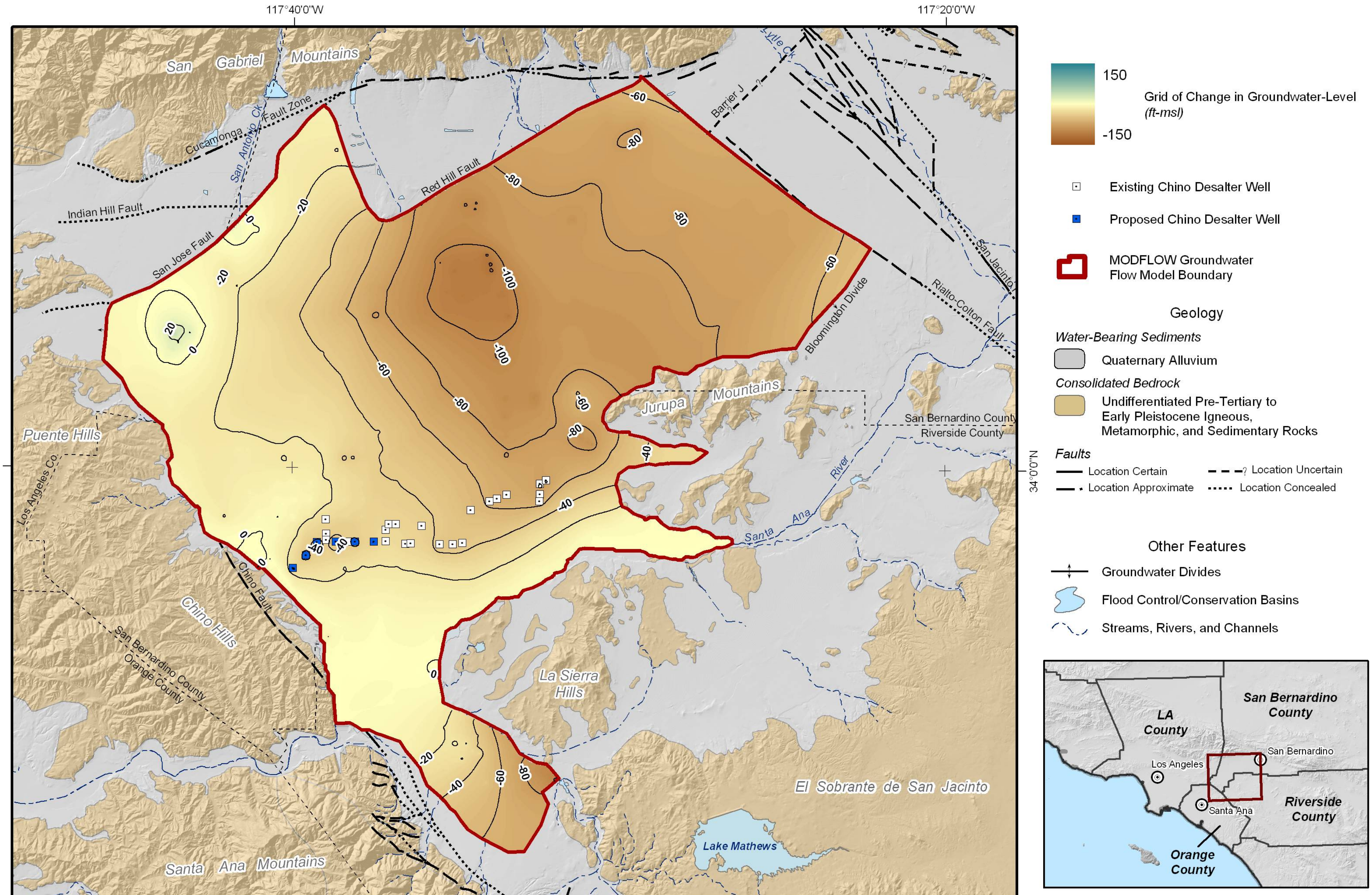

Produced by:

WILDERMUTH ENVIRONMENTAL INC.

23692 Birtcher Drive
Lake Forest, CA 92630
949.420.3030
www.wildermuthenvironmental.com

Author: MJC
Date: 20071030
File: Figure_E-19.mxd

2007 CBWM Groundwater Model Documentation and Evaluation of the Peace II Project Description
Groundwater Elevation Maps

Change in Groundwater Elevations for Layer 1
Alternative 1A 2005 - 2023

Figure E-19

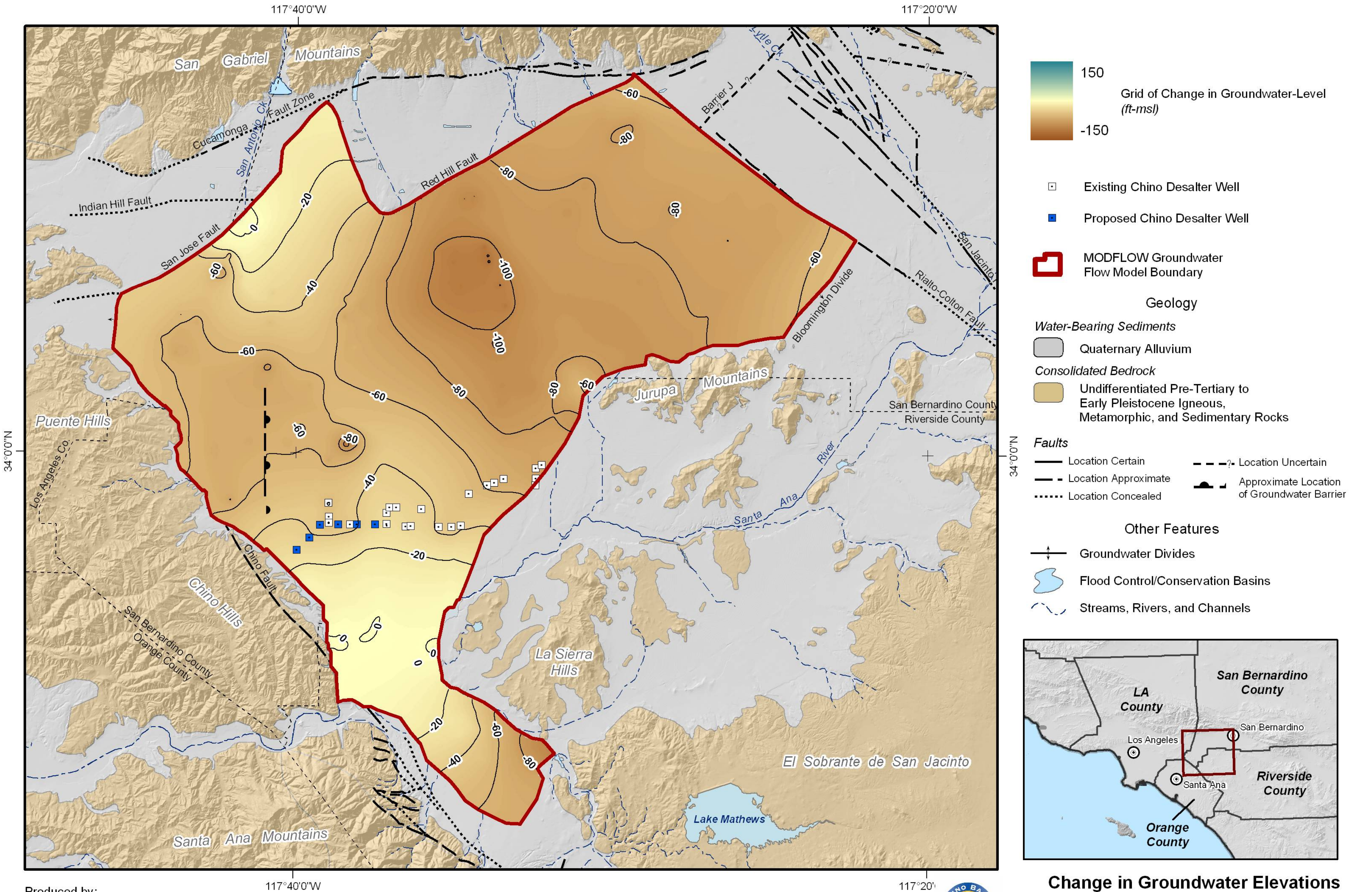

Produced by:

WILDERMUTH ENVIRONMENTAL INC.

23692 Birtcher Drive
Lake Forest, CA 92630
949.420.3030
www.wildermuthenvironmental.com

Author: MJC
Date: 20071030
File: Figure_E-20.mxd

2007 CBWM Groundwater Model Documentation and Evaluation of the Peace II Project Description
Groundwater Elevation Maps

Change in Groundwater Elevations for Layer 2
Alternative 1A 2005 - 2023

Figure E-20

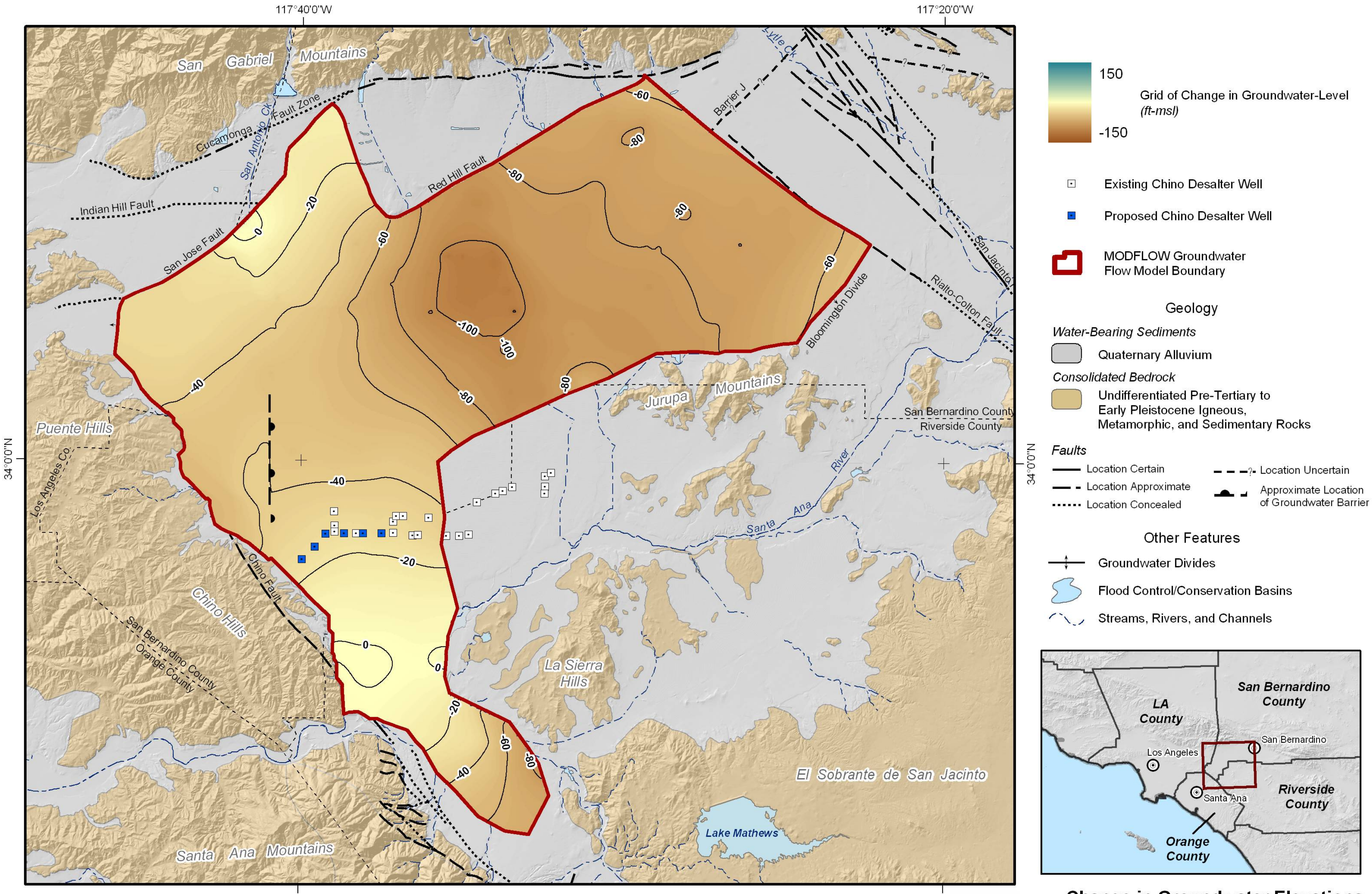

Produced by:

WILDERMUTH ENVIRONMENTAL INC.

23692 Birtcher Drive
Lake Forest, CA 92630
949.420.3030
www.wildermuthenvironmental.com

Author: MJC
Date: 20071030
File: Figure_E-21.mxd

2007 CBWM Groundwater Model Documentation and Evaluation of the Peace II Project Description
Groundwater Elevation Maps

Change in Groundwater Elevations for Layer 3
Alternative 1A 2005 - 2023

Figure E-21

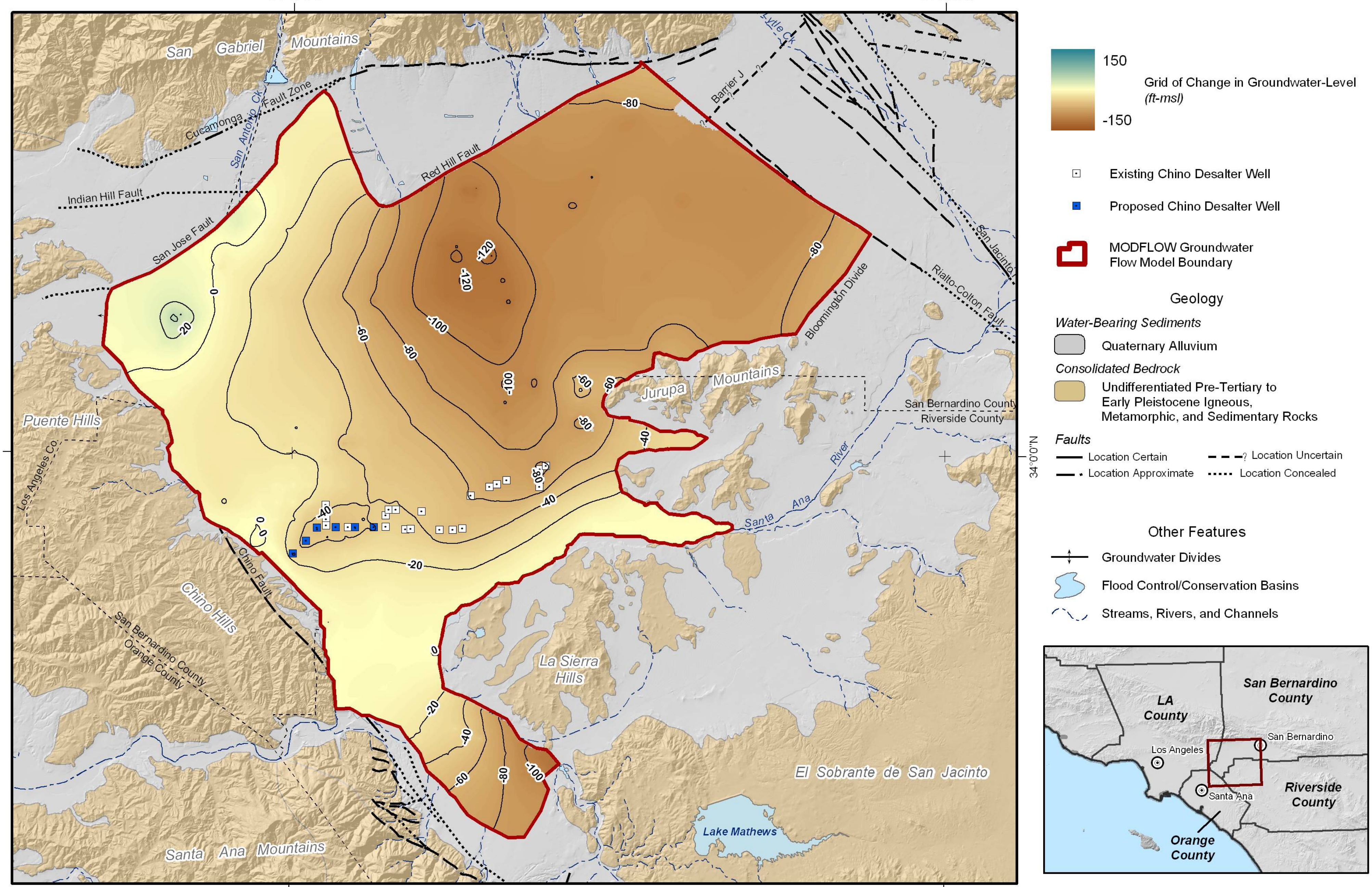

Produced by:

WILDERMUTH ENVIRONMENTAL INC.

23692 Birtcher Drive
Lake Forest, CA 92630
949.420.3030
www.wildermuthenvironmental.com

Author: MJC
Date: 20071030
File: Figure_E-22.mxd

2007 CBWM Groundwater Model Documentation and Evaluation of the Peace II Project Description
Groundwater Elevation Maps

Change in Groundwater Elevations for Layer 1
Alternative 1A 2005 - 2053

Figure E-22

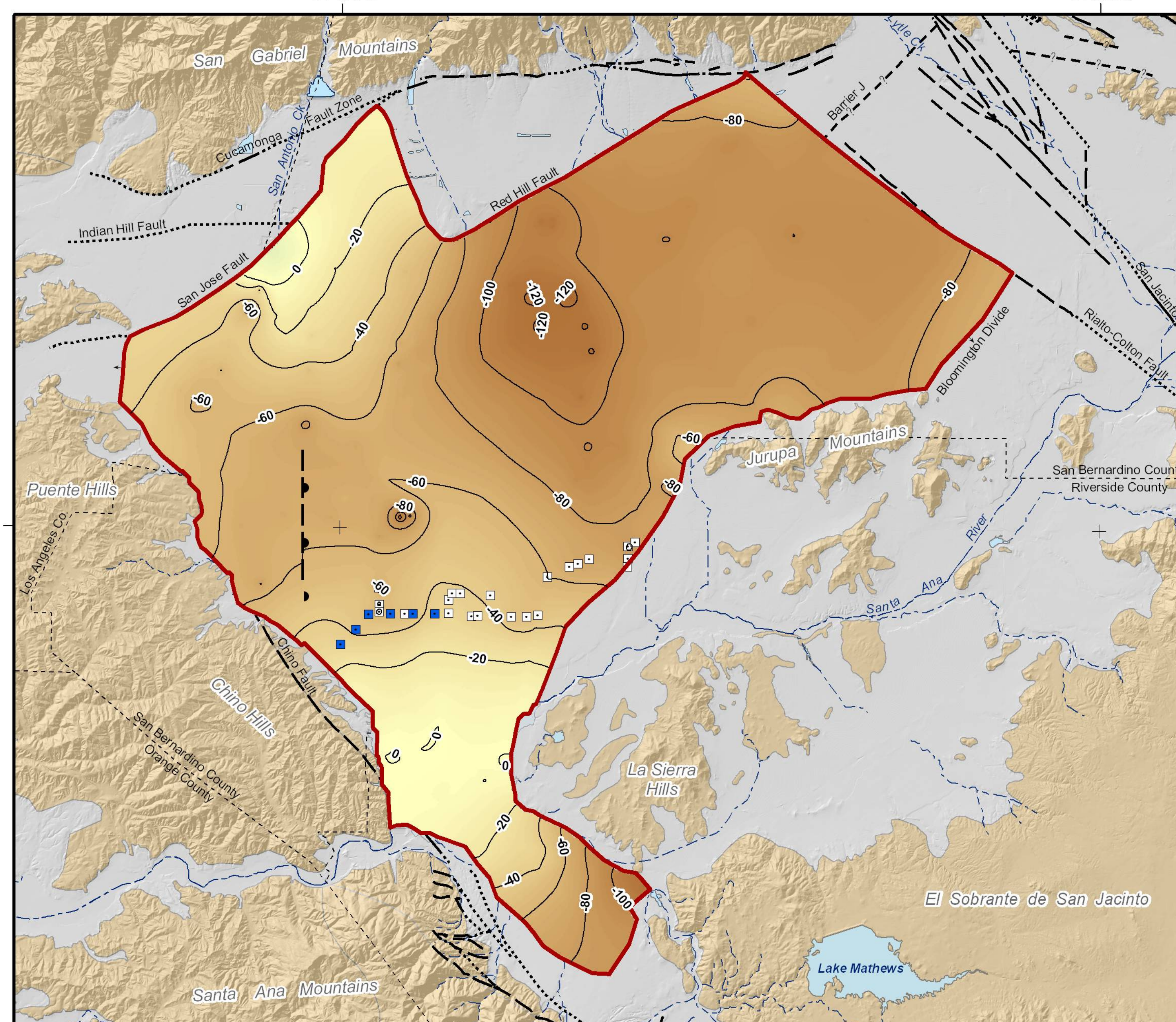

150
-150
Grid of Change in Groundwater-Level *(ft-msl)*

Existing Chino Desalter Well

Proposed Chino Desalter Well

MODFLOW Groundwater Flow Model Boundary

Geology

Water-Bearing Sediments

Quaternary Alluvium

Consolidated Bedrock

Undifferentiated Pre-Tertiary to Early Pleistocene Igneous, Metamorphic, and Sedimentary Rocks

Faults

Location Certain

Location Approximate

Location Concealed

Location Uncertain

Approximate Location of Groundwater Barrier

Other Features

Groundwater Divides

Flood Control/Conservation Basins

Streams, Rivers, and Channels

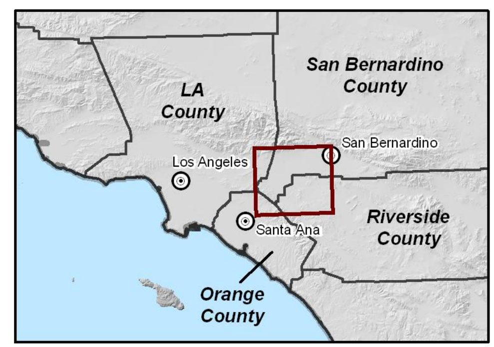

Produced by:

WILDERMUTH ENVIRONMENTAL INC.

23692 Birtcher Drive
Lake Forest, CA 92630
949.420.3030
www.wildermuthenvironmental.com

Author: MJC

Date: 20071030

File: Figure_E-23.mxd

0 1 2 3 4 *Miles*

0 2 4 6 *KM*

2007 CBWM Groundwater Model Documentation and Evaluation of the Peace II Project Description

Groundwater Elevation Maps

Change in Groundwater Elevations for Layer 2

Alternative 1A 2005 - 2053

Figure E-23

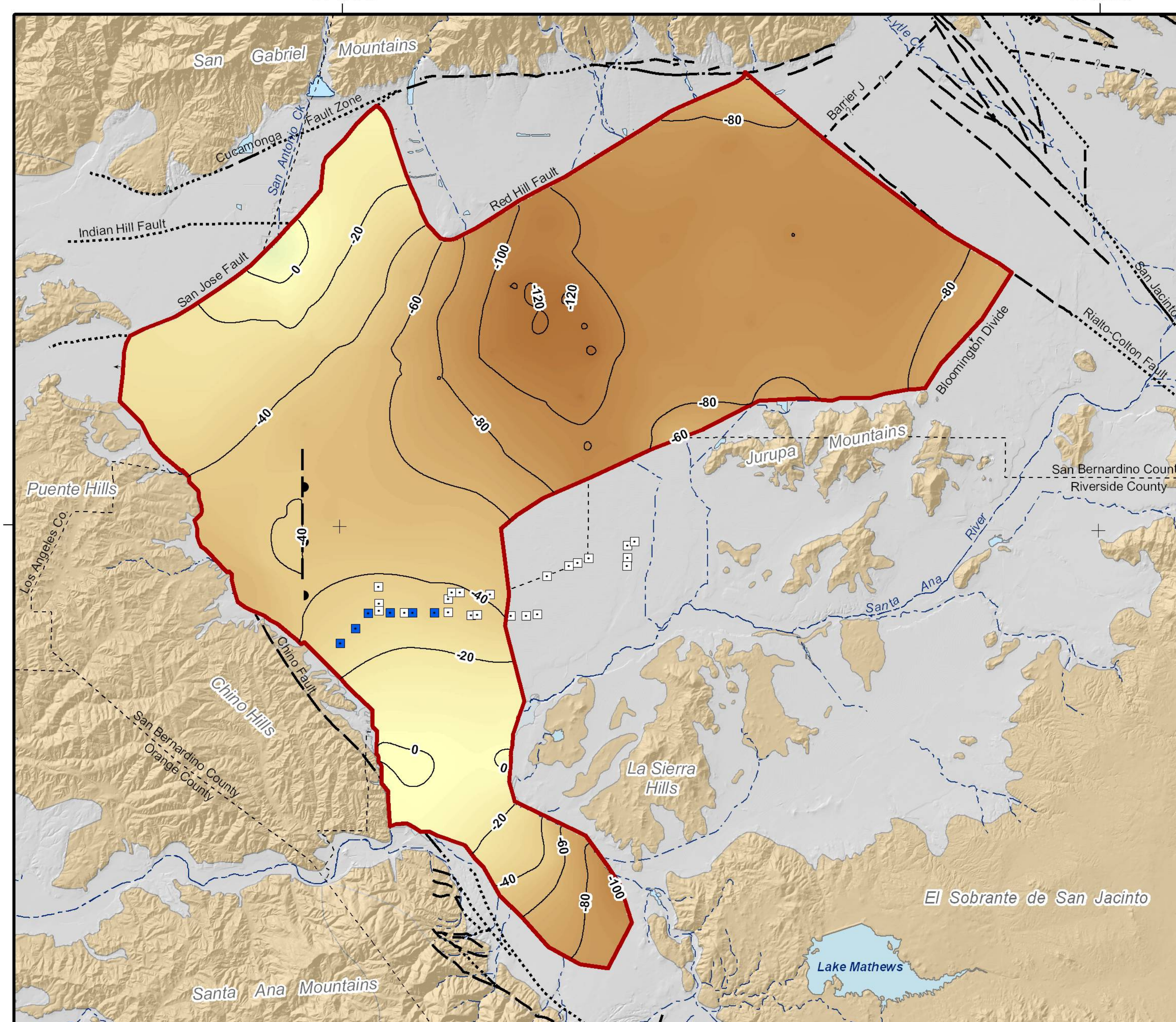

150

Grid of Change in Groundwater-Level *(ft-msl)*

-150

Existing Chino Desalter Well

Proposed Chino Desalter Well

MODFLOW Groundwater Flow Model Boundary

Geology

Water-Bearing Sediments

Quaternary Alluvium

Consolidated Bedrock

Undifferentiated Pre-Tertiary to Early Pleistocene Igneous, Metamorphic, and Sedimentary Rocks

Faults

Location Certain

Location Approximate

Location Concealed

Location Uncertain

Approximate Location of Groundwater Barrier

Other Features

Groundwater Divides

Flood Control/Conservation Basins

Streams, Rivers, and Channels

Produced by:

WILDERMUTH ENVIRONMENTAL INC.

23692 Birtcher Drive
Lake Forest, CA 92630
949.420.3030
www.wildermuthenvironmental.com

Author: MJC

Date: 20071030

File: Figure_E-24.mxd

0 1 2 3 4 Miles

0 2 4 6 KM

2007 CBWM Groundwater Model Documentation and Evaluation of the Peace II Project Description

Groundwater Elevation Maps

Change in Groundwater Elevations for Layer 3

Alternative 1A 2005 - 2053

Figure E-24

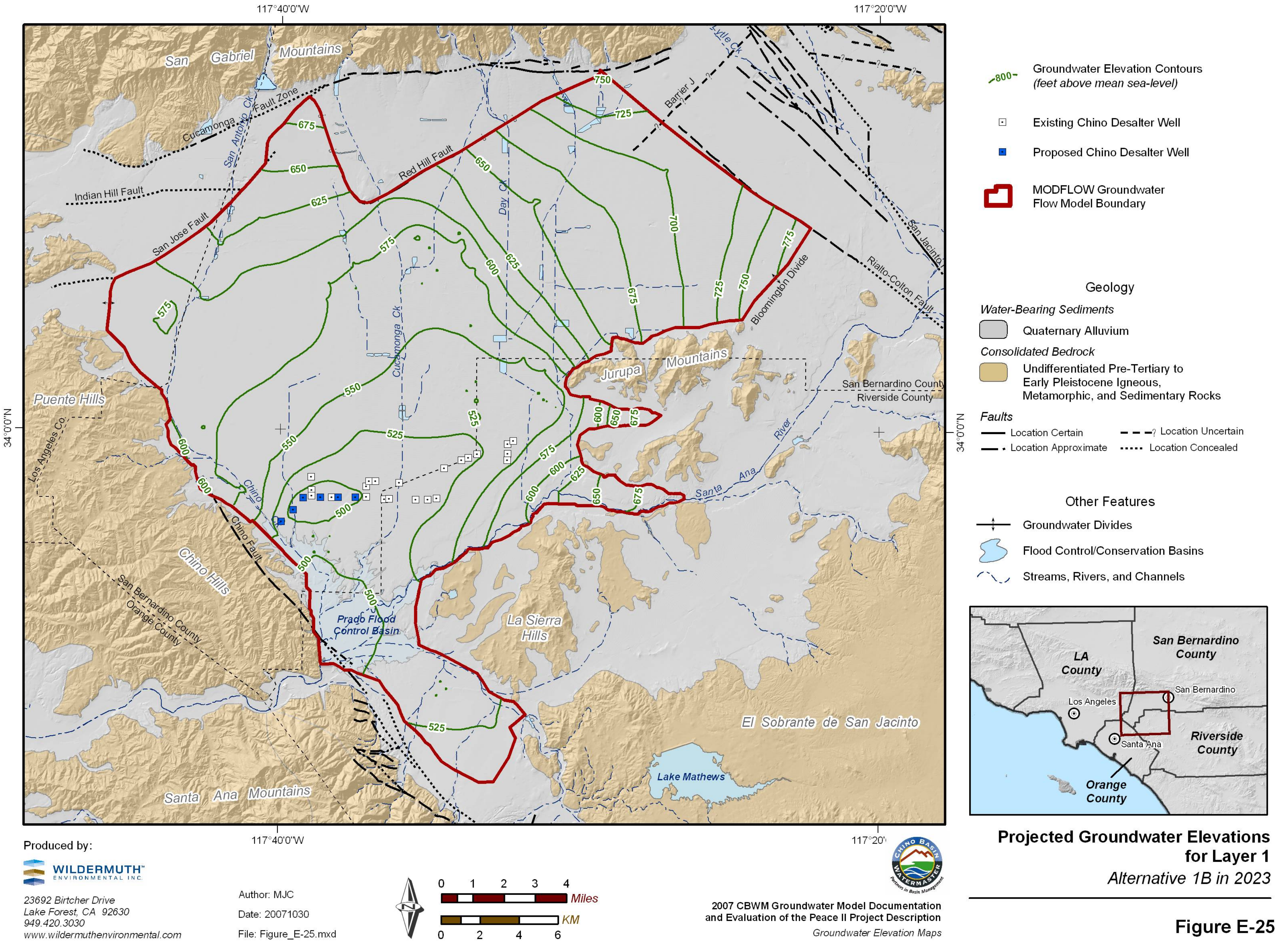

Produced by:

WILDERMUTH ENVIRONMENTAL INC.

23692 Birtcher Drive
Lake Forest, CA 92630
949.420.3030
www.wildermuthenvironmental.com

Author: MJC
Date: 20071030
File: Figure_E-25.mxd

2007 CBWM Groundwater Model Documentation and Evaluation of the Peace II Project Description
Groundwater Elevation Maps

Projected Groundwater Elevations for Layer 1
Alternative 1B in 2023

Figure E-25

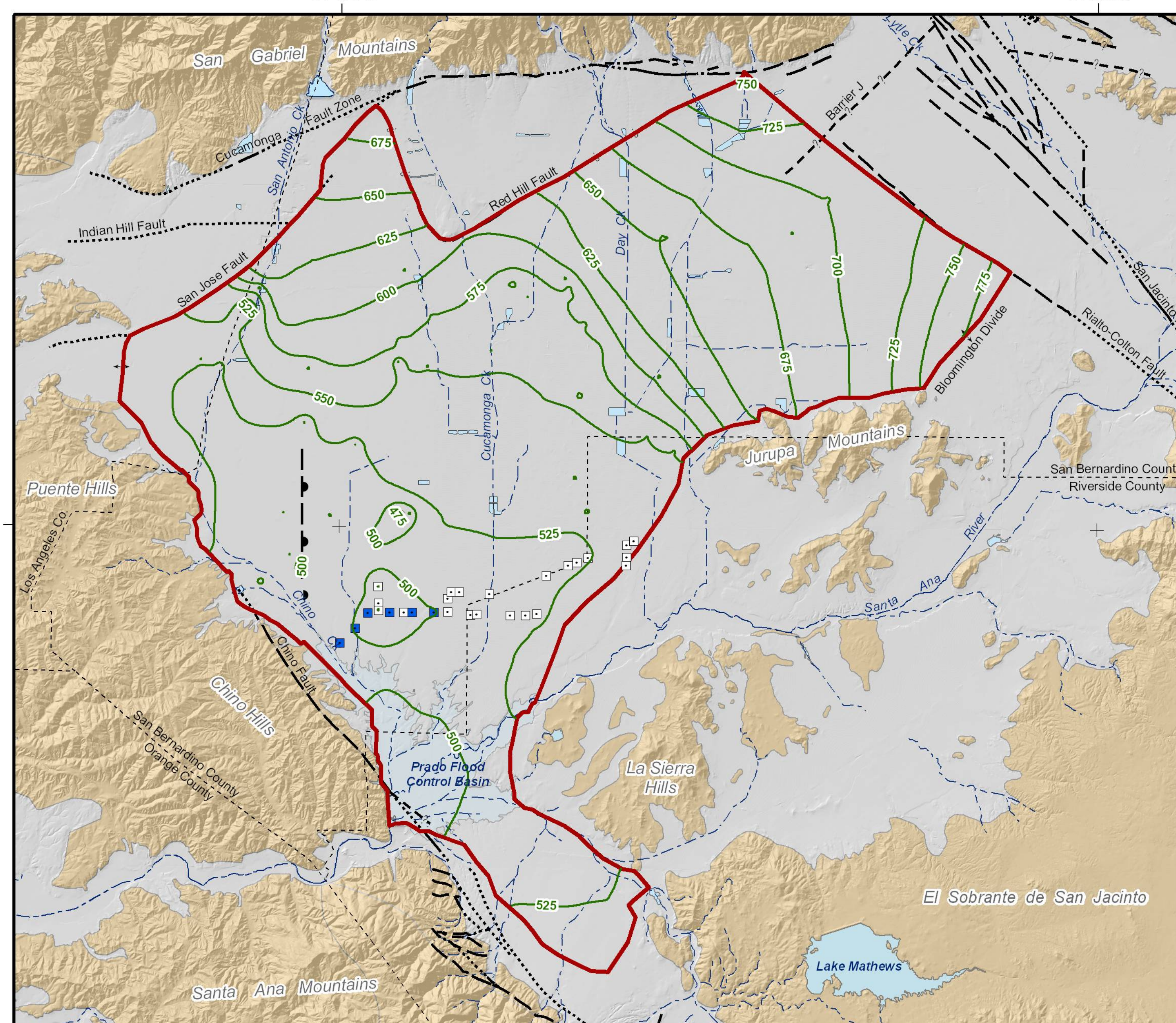

Groundwater Elevation Contours (feet above mean sea-level)

Existing Chino Desalter Well

Proposed Chino Desalter Well

MODFLOW Groundwater Flow Model Boundary

Geology

Water-Bearing Sediments

Quaternary Alluvium

Consolidated Bedrock

Undifferentiated Pre-Tertiary to Early Pleistocene Igneous, Metamorphic, and Sedimentary Rocks

Faults

Location Certain

Location Approximate

Location Concealed

Location Uncertain

Approximate Location of Groundwater Barrier

Other Features

Groundwater Divides

Flood Control/Conservation Basins

Streams, Rivers, and Channels

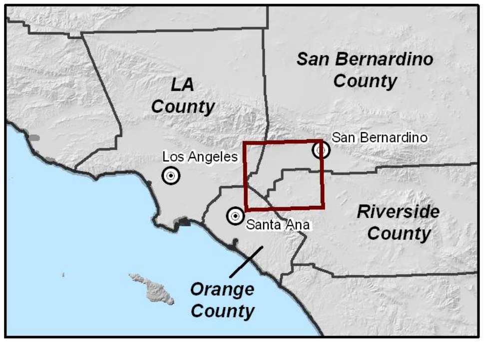

Produced by:

WILDERMUTH ENVIRONMENTAL INC.

23692 Birtcher Drive
Lake Forest, CA 92630
949.420.3030
www.wildermuthenvironmental.com

Author: MJC

Date: 20071030

File: Figure_E-26.mxd

0 1 2 3 4 Miles

0 2 4 6 KM

2007 CBWM Groundwater Model Documentation and Evaluation of the Peace II Project Description

Groundwater Elevation Maps

Projected Groundwater Elevations for Layer 2

Alternative 1B in 2023

Figure E-26

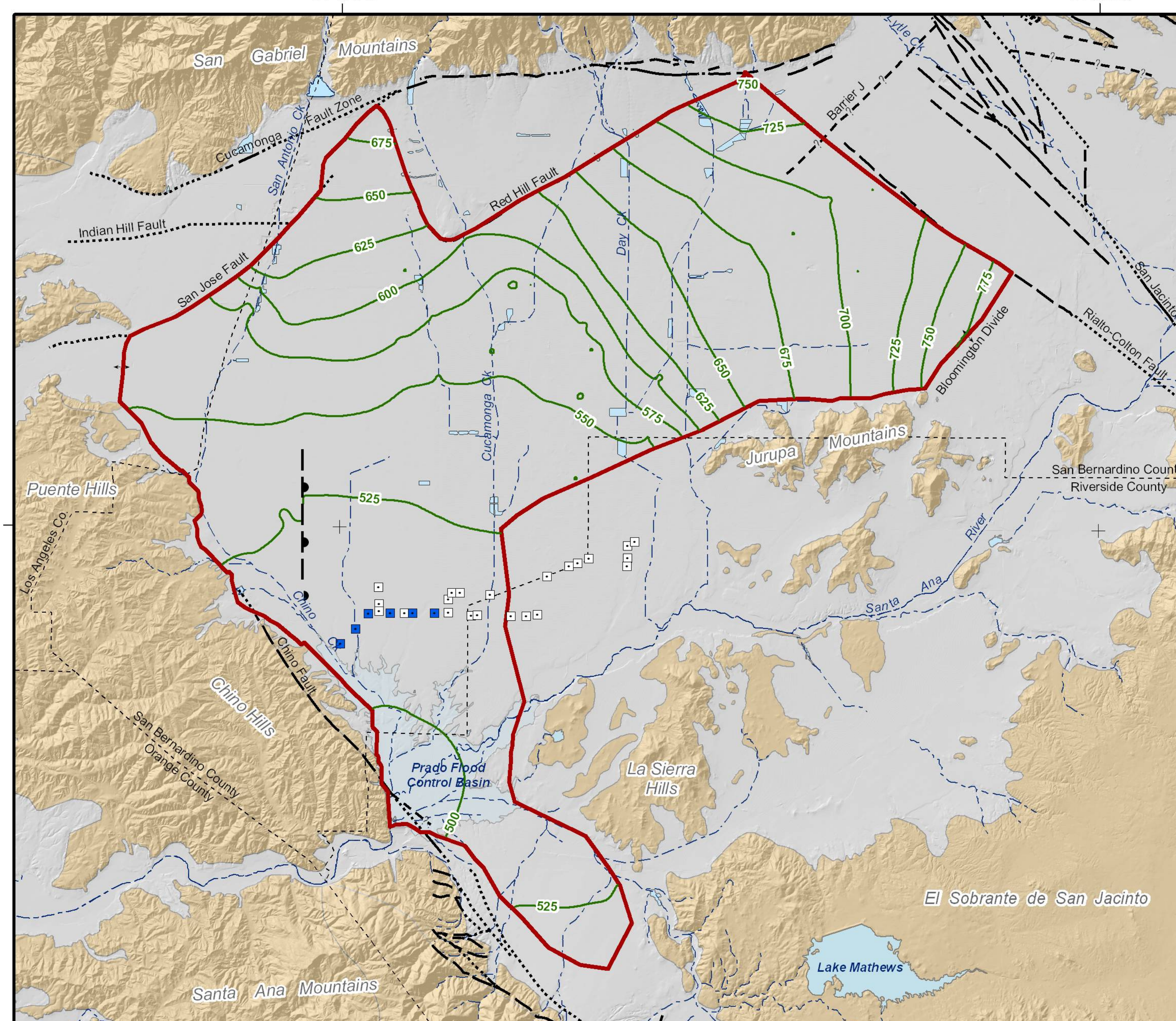

Groundwater Elevation Contours (feet above mean sea-level)

Existing Chino Desalter Well

Proposed Chino Desalter Well

MODFLOW Groundwater Flow Model Boundary

Geology

Water-Bearing Sediments

Quaternary Alluvium

Consolidated Bedrock

Undifferentiated Pre-Tertiary to Early Pleistocene Igneous, Metamorphic, and Sedimentary Rocks

Faults

- Location Certain
- Location Approximate
- Location Concealed
- Location Uncertain
- Approximate Location of Groundwater Barrier

Other Features

- Groundwater Divides
- Flood Control/Conservation Basins
- Streams, Rivers, and Channels

Produced by:

WILDERMUTH ENVIRONMENTAL INC.
23692 Birtcher Drive
Lake Forest, CA 92630
949.420.3030
www.wildermuthenvironmental.com

Author: MJC
Date: 20071030
File: Figure_E-27.mxd

0 1 2 3 4 Miles
0 2 4 6 KM

2007 CBWM Groundwater Model Documentation and Evaluation of the Peace II Project Description
Groundwater Elevation Maps

Projected Groundwater Elevations for Layer 3

Alternative 1B in 2023

Figure E-27

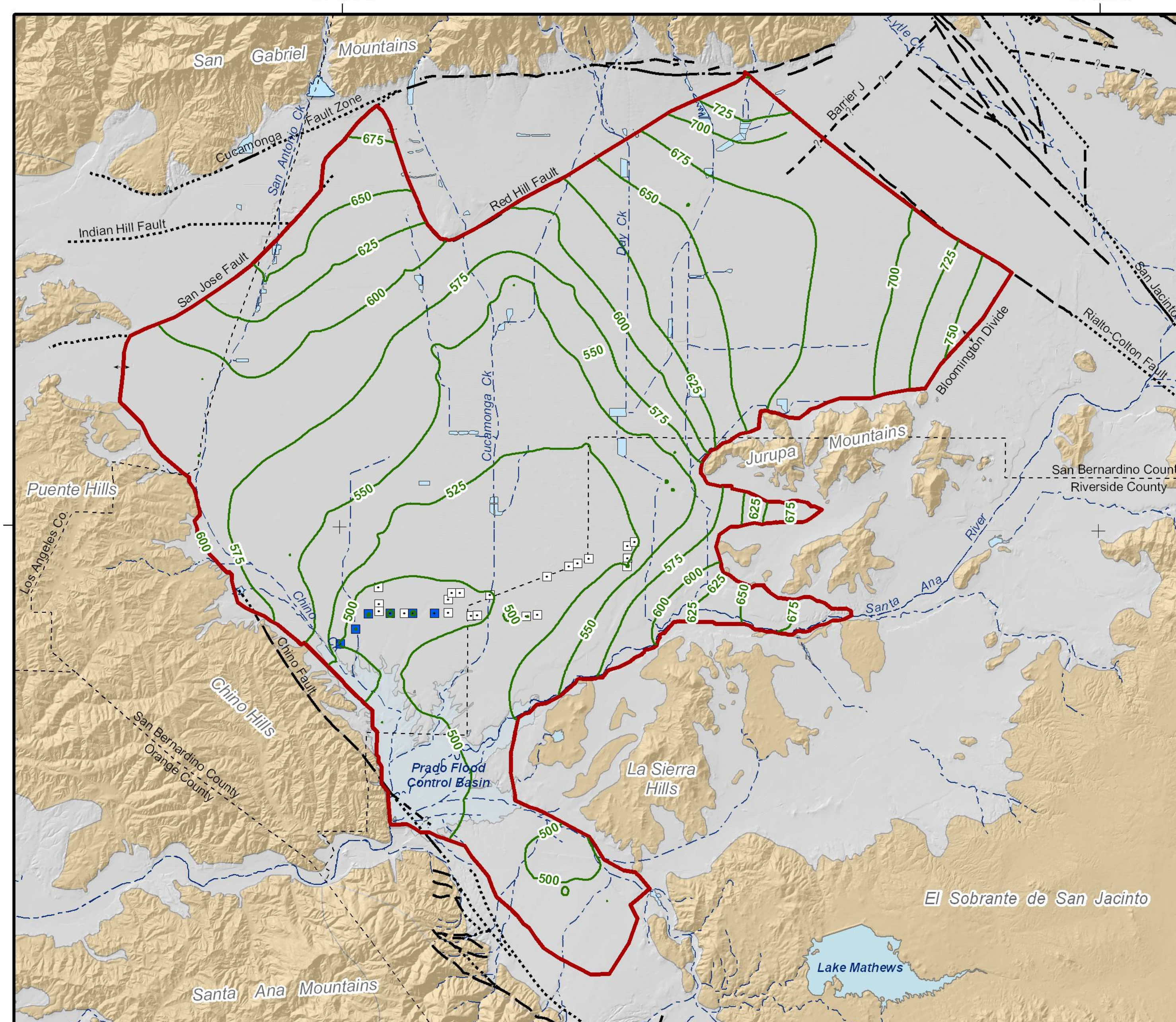

- 800 Groundwater Elevation Contours *(feet above mean sea-level)*
- Existing Chino Desalter Well
- Proposed Chino Desalter Well
- MODFLOW Groundwater Flow Model Boundary

Geology

Water-Bearing Sediments

- Quaternary Alluvium

Consolidated Bedrock

- Undifferentiated Pre-Tertiary to Early Pleistocene Igneous, Metamorphic, and Sedimentary Rocks

Faults

- Location Certain
- Location Approximate
- ? Location Uncertain
- Location Concealed

Other Features

- Groundwater Divides
- Flood Control/Conservation Basins
- Streams, Rivers, and Channels

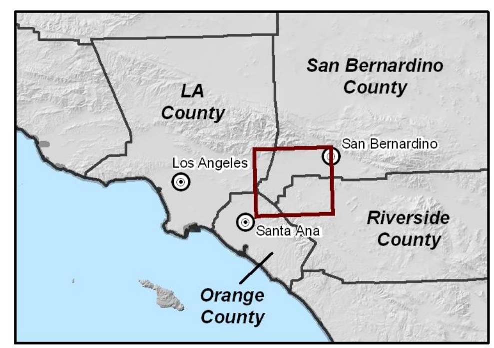

Scale: 0 1 2 3 4 Miles; 0 2 4 6 KM

Produced by:

WILDERMUTH ENVIRONMENTAL INC.

23692 Birtcher Drive
Lake Forest, CA 92630
949.420.3030
www.wildermuthenvironmental.com

Author: MJC

Date: 20071030

File: Figure_E-28.mxd

2007 CBWM Groundwater Model Documentation and Evaluation of the Peace II Project Description

Groundwater Elevation Maps

Projected Groundwater Elevations for Layer 1

Alternative 1B in 2053

Figure E-28

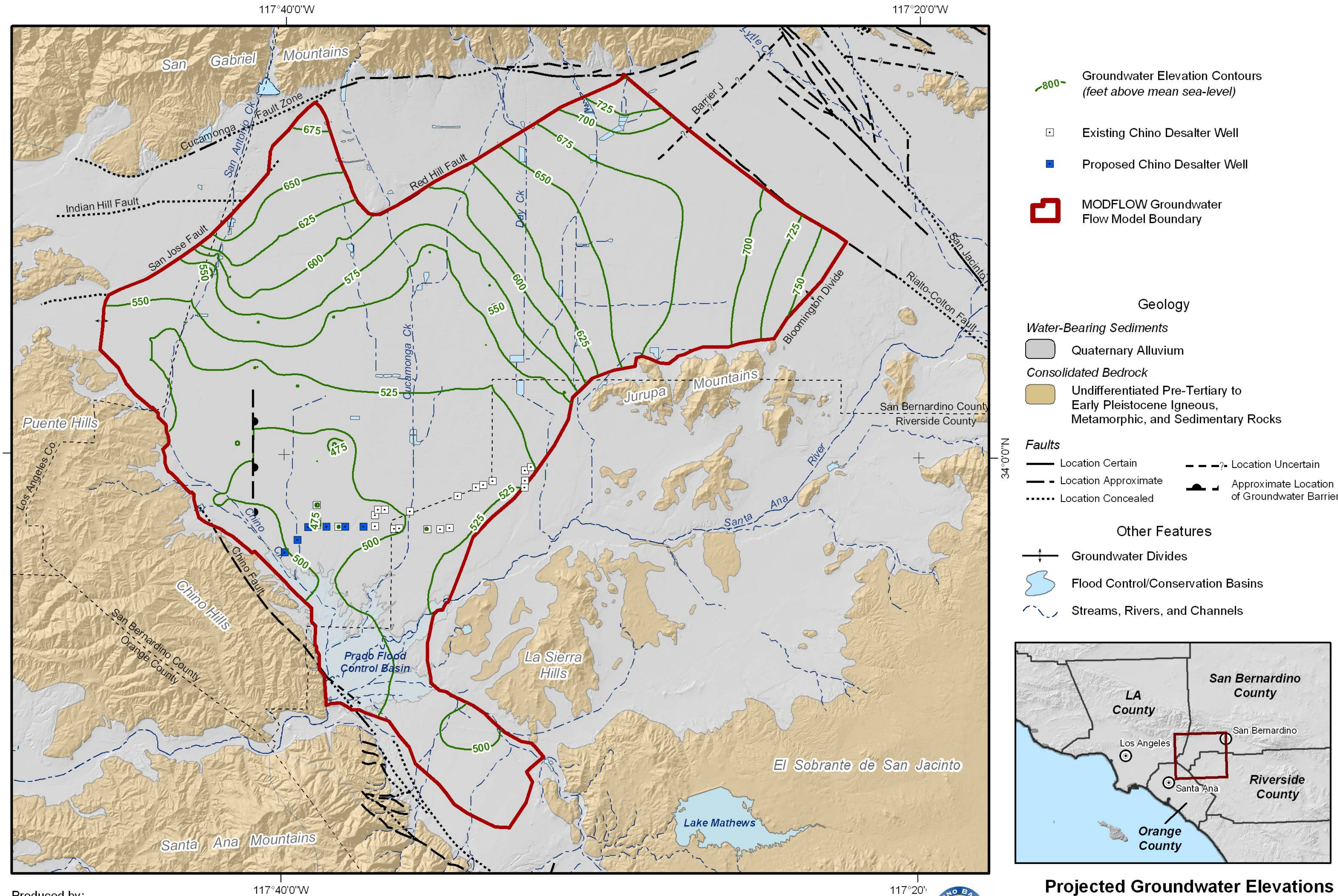

Produced by:

WILDERMUTH ENVIRONMENTAL INC.

23692 Birtcher Drive
Lake Forest, CA 92630
949.420.3030
www.wildermuthenvironmental.com

Author: MJC

Date: 20071030

File: Figure_E-29.mxd

2007 CBWM Groundwater Model Documentation and Evaluation of the Peace II Project Description

Groundwater Elevation Maps

Projected Groundwater Elevations for Layer 2

Alternative 1B in 2053

Figure E-29

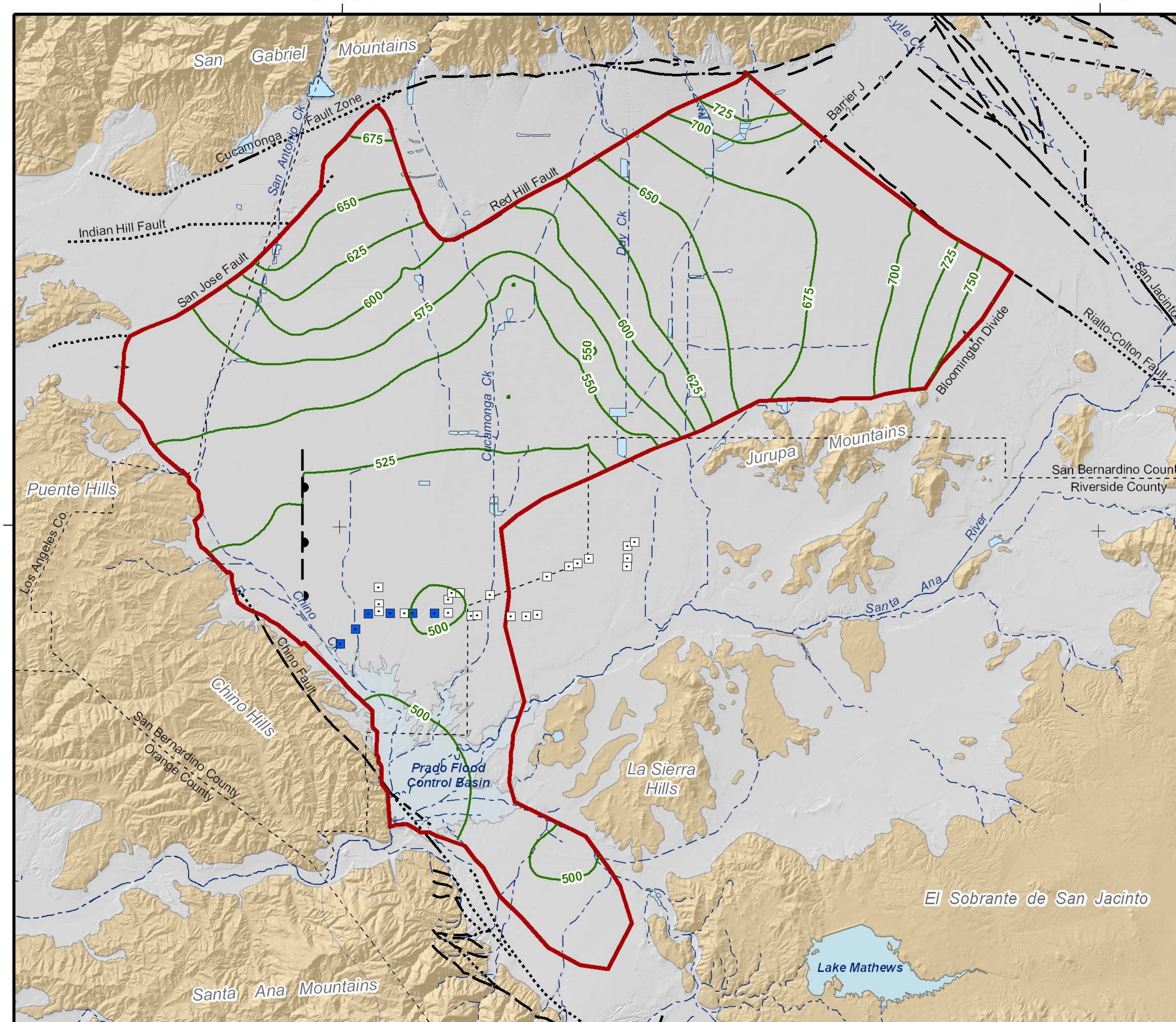

- Groundwater Elevation Contours (*feet above mean sea-level*)
- Existing Chino Desalter Well
- Proposed Chino Desalter Well
- MODFLOW Groundwater Flow Model Boundary

Geology

Water-Bearing Sediments

- Quaternary Alluvium

Consolidated Bedrock

- Undifferentiated Pre-Tertiary to Early Pleistocene Igneous, Metamorphic, and Sedimentary Rocks

Faults

- Location Certain
- Location Approximate
- Location Concealed
- Location Uncertain
- Approximate Location of Groundwater Barrier

Other Features

- Groundwater Divides
- Flood Control/Conservation Basins
- Streams, Rivers, and Channels

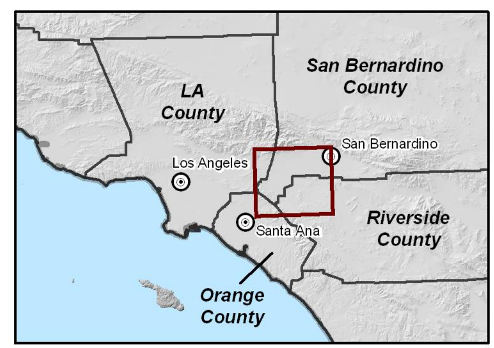

0 1 2 3 4 Miles
0 2 4 6 KM

Produced by:
WILDERMUTH ENVIRONMENTAL INC.
23692 Birtcher Drive
Lake Forest, CA 92630
949.420.3030
www.wildermuthenvironmental.com

Author: MJC
Date: 20071030
File: Figure_E-30.mxd

2007 CBWM Groundwater Model Documentation and Evaluation of the Peace II Project Description
Groundwater Elevation Maps

Projected Groundwater Elevations for Layer 3
Alternative 1B in 2053

Figure E-30

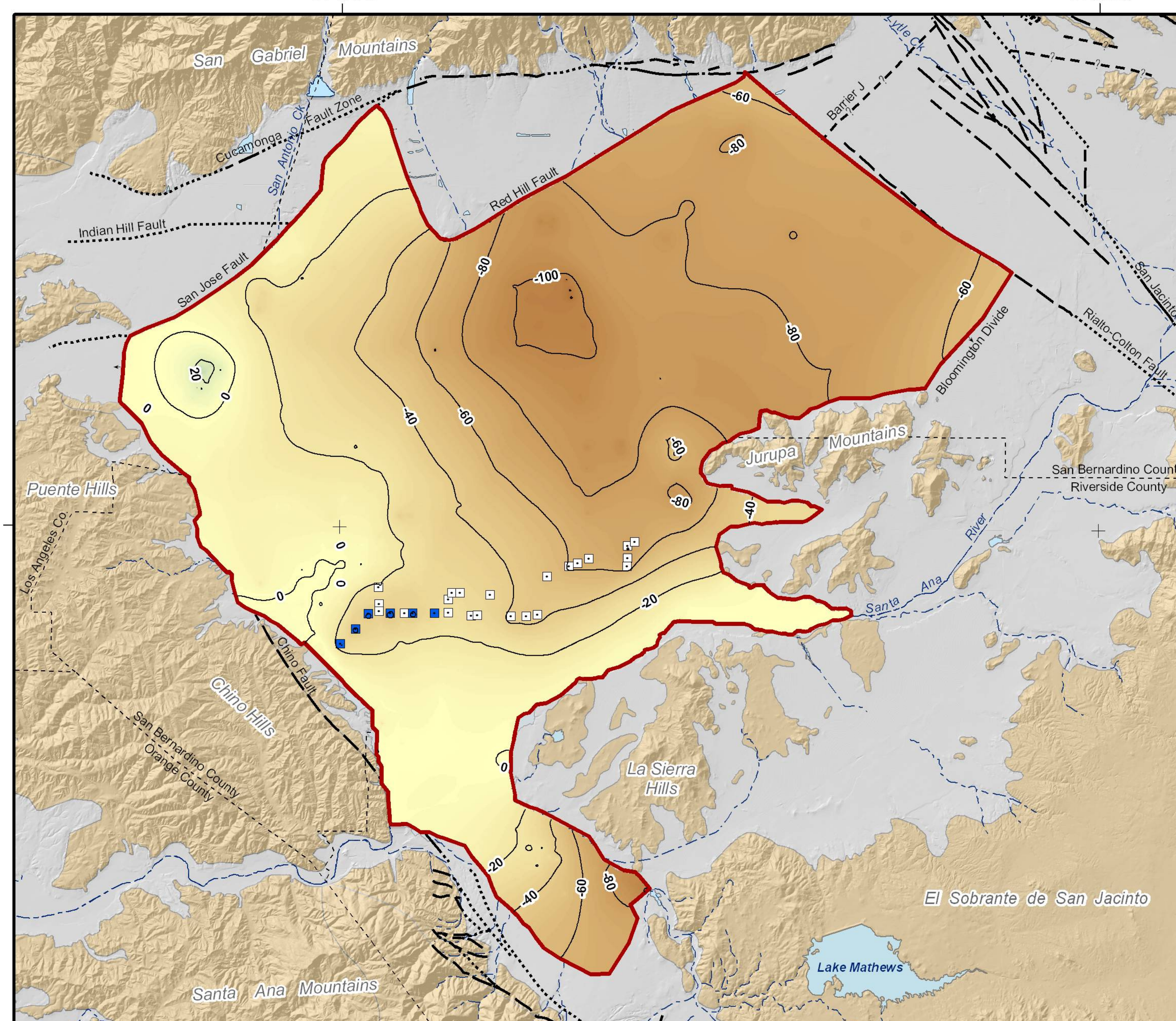

150

Grid of Change in Groundwater-Level *(ft-msl)*

-150

Existing Chino Desalter Well

Proposed Chino Desalter Well

MODFLOW Groundwater Flow Model Boundary

Geology

Water-Bearing Sediments

Quaternary Alluvium

Consolidated Bedrock

Undifferentiated Pre-Tertiary to Early Pleistocene Igneous, Metamorphic, and Sedimentary Rocks

Faults

Location Certain

Location Approximate

Location Uncertain

Location Concealed

Other Features

Groundwater Divides

Flood Control/Conservation Basins

Streams, Rivers, and Channels

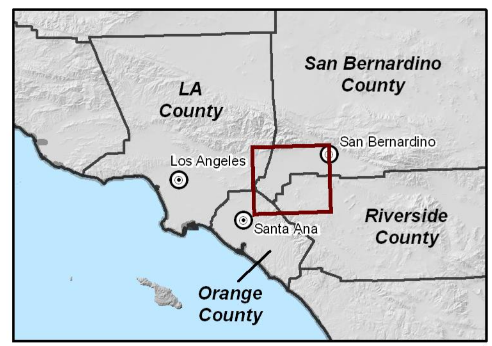

Produced by:

WILDERMUTH ENVIRONMENTAL INC.

23692 Birtcher Drive
Lake Forest, CA 92630
949.420.3030
www.wildermuthenvironmental.com

Author: MJC

Date: 20071030

File: Figure_E-31.mxd

0 1 2 3 4 Miles

0 2 4 6 KM

2007 CBWM Groundwater Model Documentation and Evaluation of the Peace II Project Description

Groundwater Elevation Maps

Change in Groundwater Elevations for Layer 1

Alternative 1B 2005 - 2023

Figure E-31

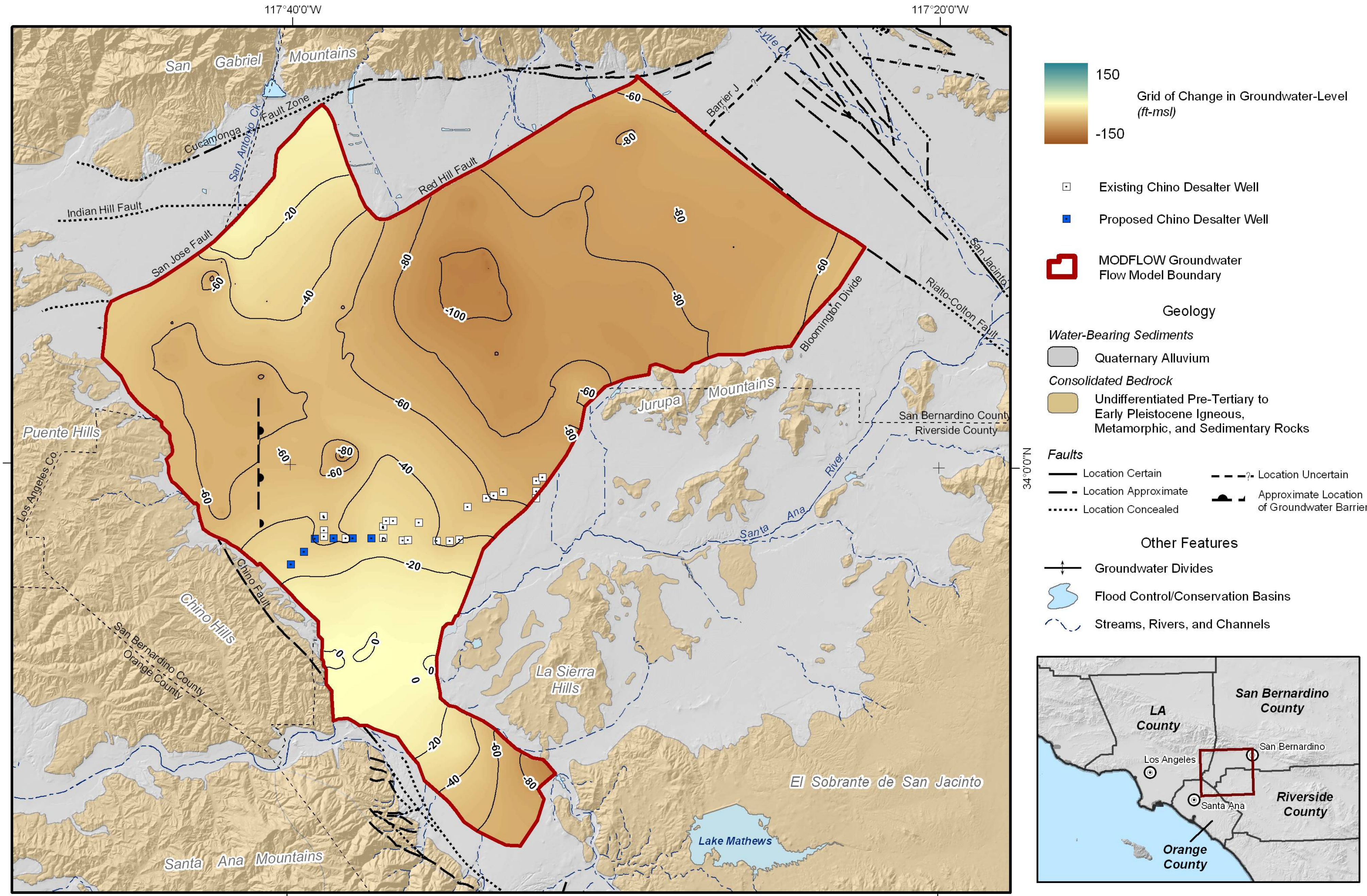

Produced by:

WILDERMUTH ENVIRONMENTAL INC.

23692 Birtcher Drive
Lake Forest, CA 92630
949.420.3030
www.wildermuthenvironmental.com

Author: MJC

Date: 20071030

File: Figure_E-32.mxd

2007 CBWM Groundwater Model Documentation and Evaluation of the Peace II Project Description

Groundwater Elevation Maps

Change in Groundwater Elevations for Layer 2

Alternative 1B 2005 - 2023

Figure E-32

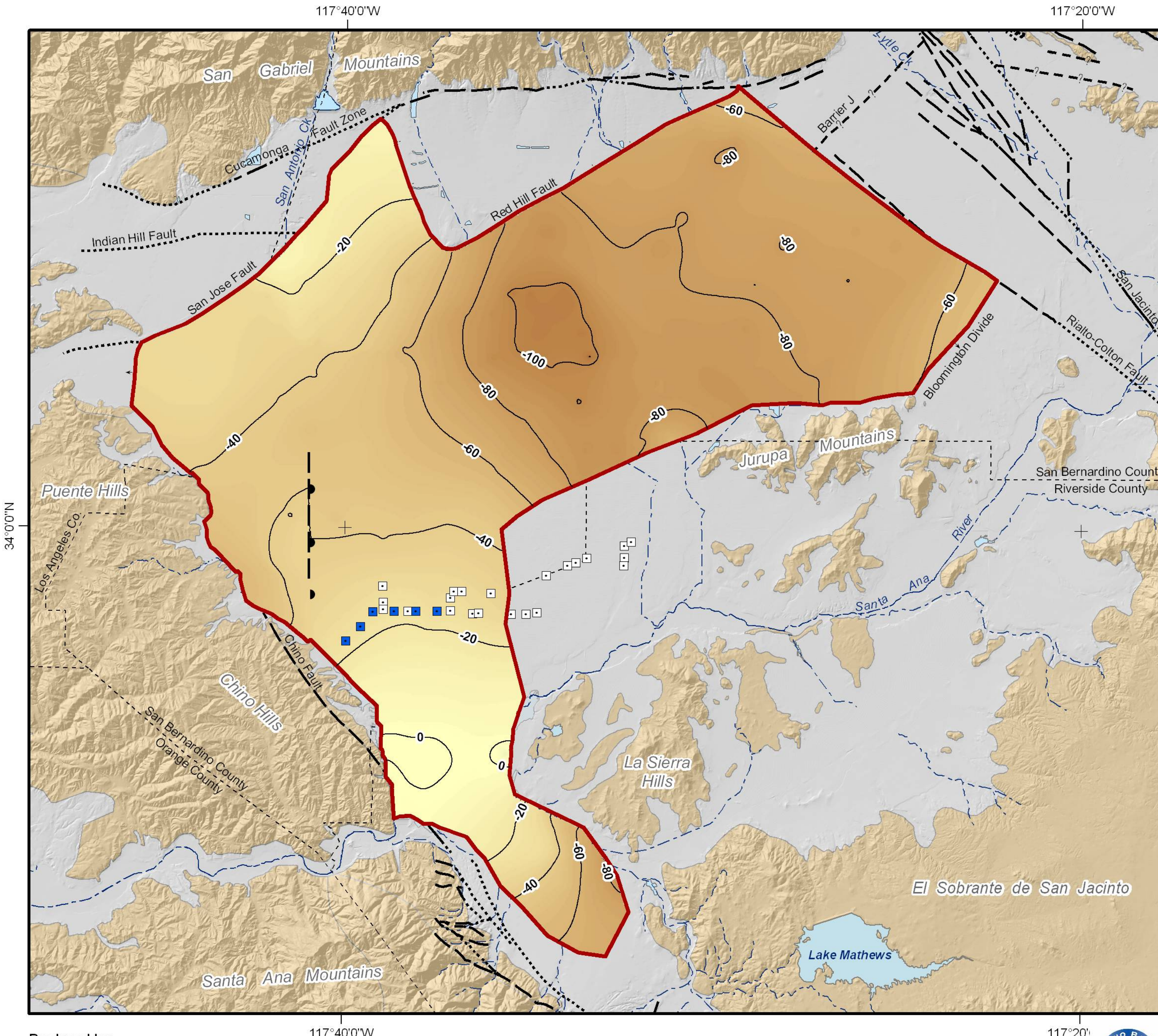

150

Grid of Change in Groundwater-Level *(ft-msl)*

-150

Existing Chino Desalter Well

Proposed Chino Desalter Well

MODFLOW Groundwater Flow Model Boundary

Geology

Water-Bearing Sediments

Quaternary Alluvium

Consolidated Bedrock

Undifferentiated Pre-Tertiary to Early Pleistocene Igneous, Metamorphic, and Sedimentary Rocks

Faults

- Location Certain
- Location Approximate
- Location Concealed
- Location Uncertain
- Approximate Location of Groundwater Barrier

Other Features

- Groundwater Divides
- Flood Control/Conservation Basins
- Streams, Rivers, and Channels

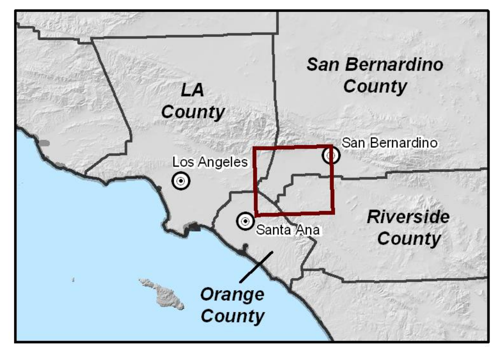

Produced by:

WILDERMUTH ENVIRONMENTAL INC.

23692 Birtcher Drive
Lake Forest, CA 92630
949.420.3030
www.wildermuthenvironmental.com

Author: MJC

Date: 20071030

File: Figure_E-33.mxd

0 1 2 3 4 Miles

0 2 4 6 KM

2007 CBWM Groundwater Model Documentation and Evaluation of the Peace II Project Description

Groundwater Elevation Maps

Change in Groundwater Elevations for Layer 3

Alternative 1B 2005 - 2023

Figure E-33

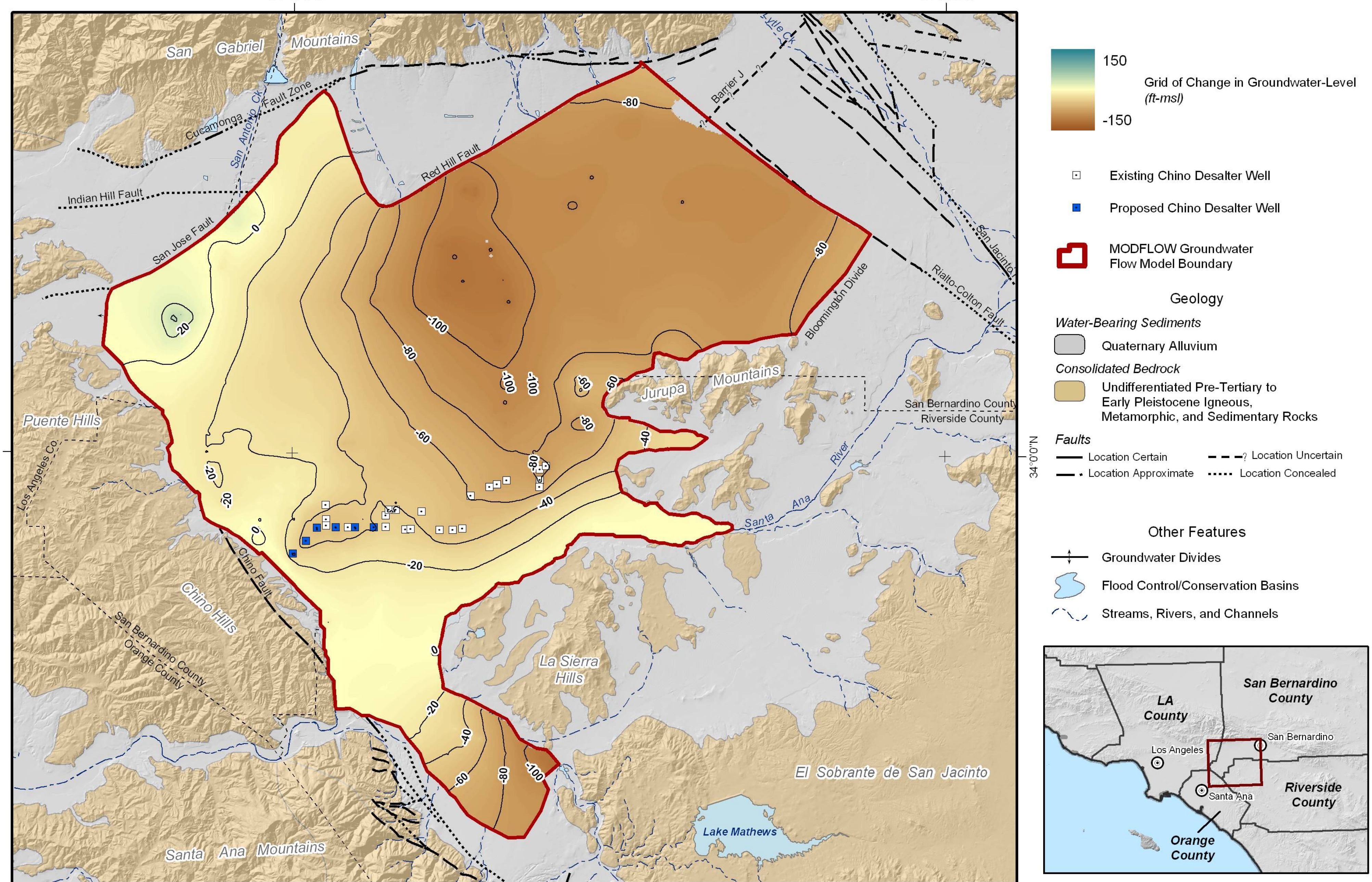

Produced by:

WILDERMUTH ENVIRONMENTAL INC.

23692 Birtcher Drive
Lake Forest, CA 92630
949.420.3030
www.wildermuthenvironmental.com

Author: MJC

Date: 20071030

File: Figure_E-34.mxd

2007 CBWM Groundwater Model Documentation and Evaluation of the Peace II Project Description

Groundwater Elevation Maps

Change in Groundwater Elevations for Layer 1

Alternative 1B 2005 - 2053

Figure E-34

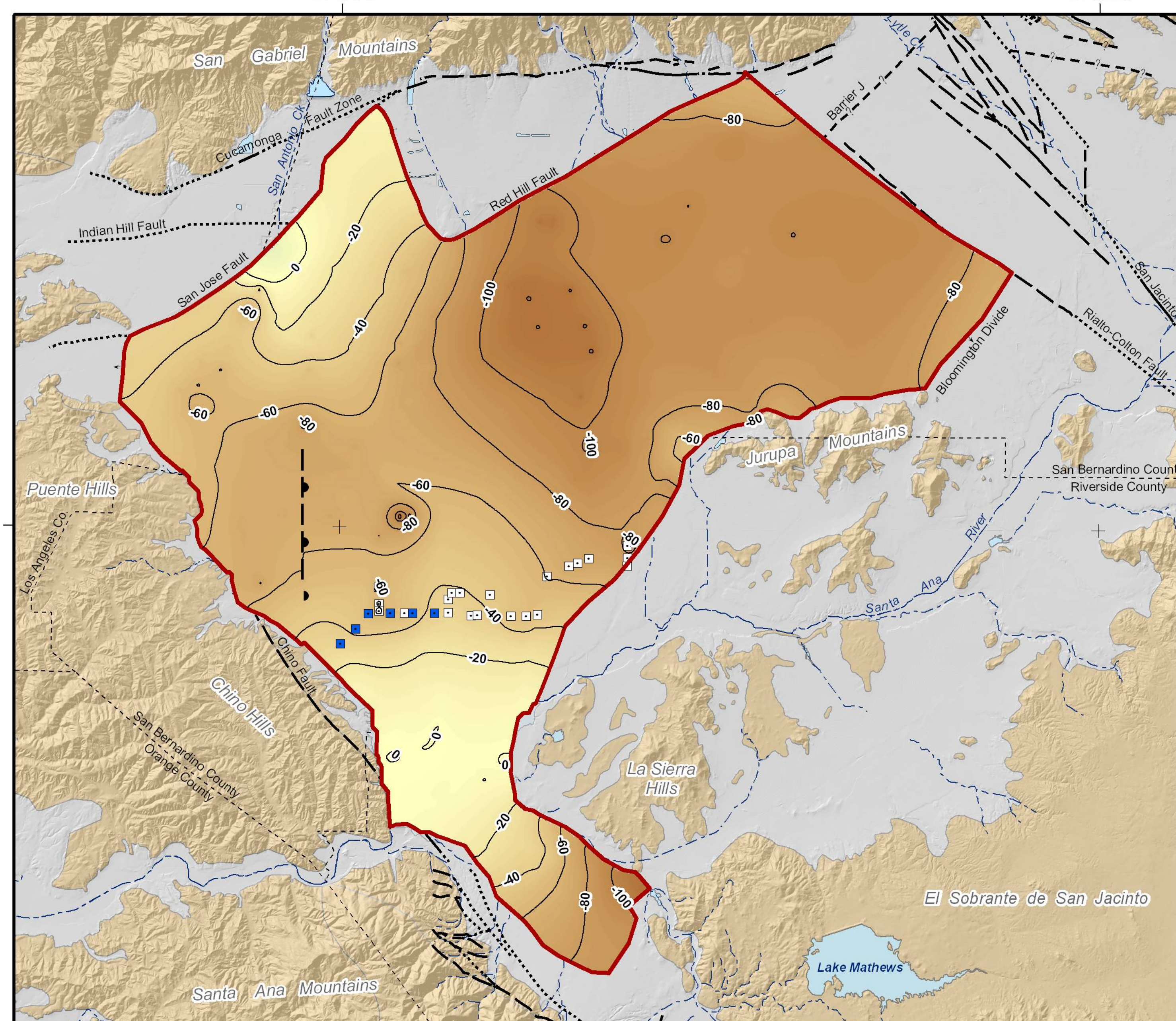

Grid of Change in Groundwater-Level *(ft-msl)*

150

-150

- Existing Chino Desalter Well
- Proposed Chino Desalter Well
- MODFLOW Groundwater Flow Model Boundary

Geology

Water-Bearing Sediments

- Quaternary Alluvium

Consolidated Bedrock

- Undifferentiated Pre-Tertiary to Early Pleistocene Igneous, Metamorphic, and Sedimentary Rocks

Faults

- Location Certain
- Location Approximate
- Location Concealed
- Location Uncertain
- Approximate Location of Groundwater Barrier

Other Features

- Groundwater Divides
- Flood Control/Conservation Basins
- Streams, Rivers, and Channels

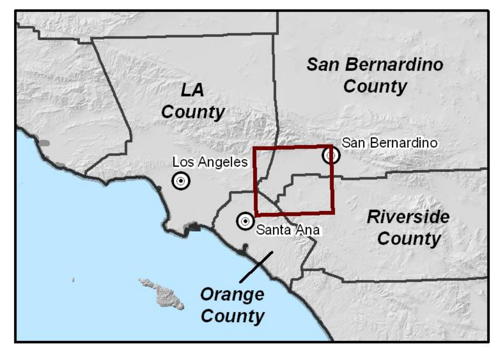

Produced by:

WILDERMUTH ENVIRONMENTAL INC.

23692 Birtcher Drive
Lake Forest, CA 92630
949.420.3030
www.wildermuthenvironmental.com

Author: MJC

Date: 20071030

File: Figure_E-35.mxd

0 1 2 3 4 Miles

0 2 4 6 KM

2007 CBWM Groundwater Model Documentation and Evaluation of the Peace II Project Description

Groundwater Elevation Maps

Change in Groundwater Elevations for Layer 2

Alternative 1B 2005 - 2053

Figure E-35

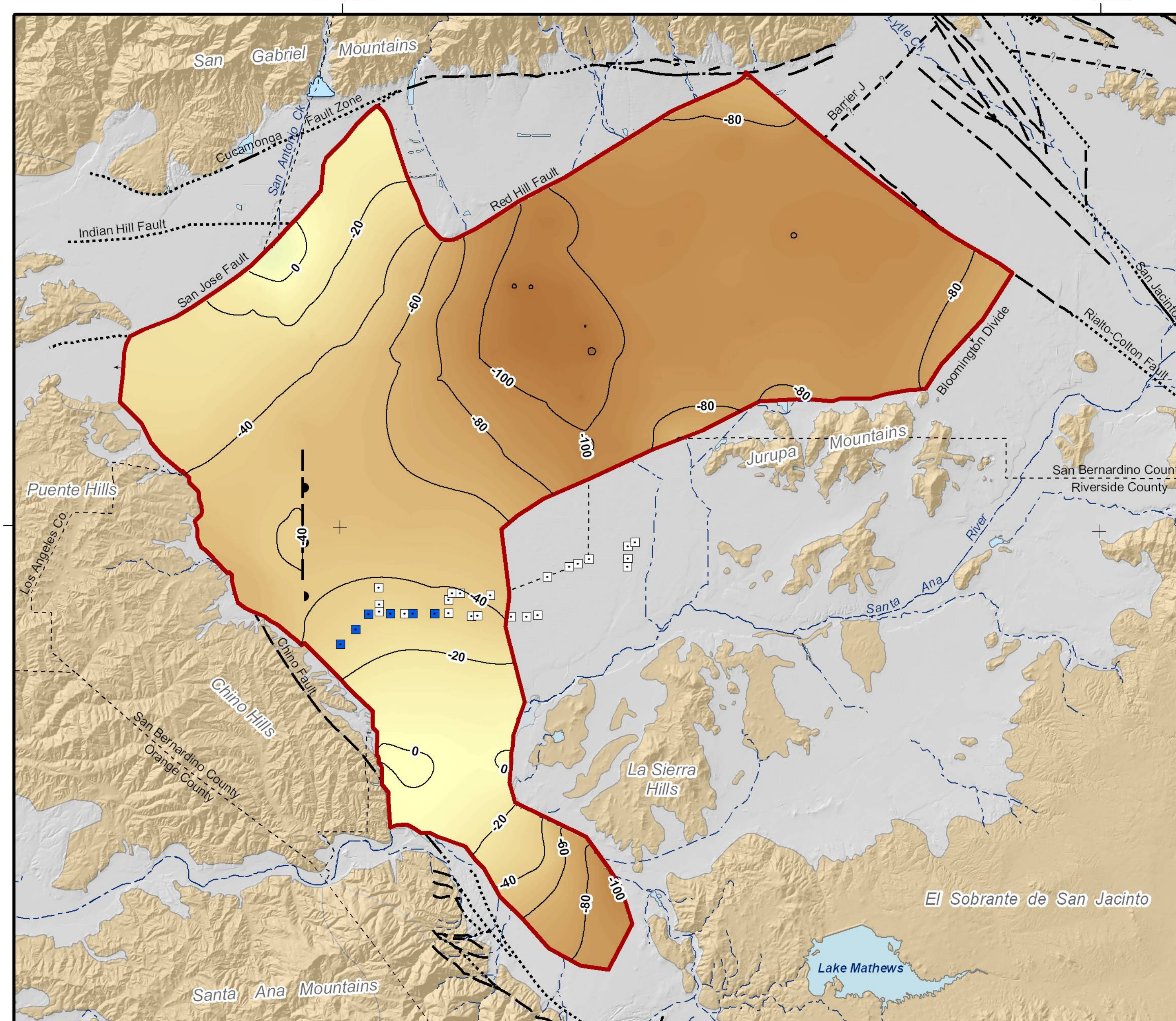

Grid of Change in Groundwater-Level *(ft-msl)*
150
-150

Existing Chino Desalter Well

Proposed Chino Desalter Well

MODFLOW Groundwater Flow Model Boundary

Geology

Water-Bearing Sediments

Quaternary Alluvium

Consolidated Bedrock

Undifferentiated Pre-Tertiary to Early Pleistocene Igneous, Metamorphic, and Sedimentary Rocks

Faults

Location Certain

Location Approximate

Location Concealed

Location Uncertain

Approximate Location of Groundwater Barrier

Other Features

Groundwater Divides

Flood Control/Conservation Basins

Streams, Rivers, and Channels

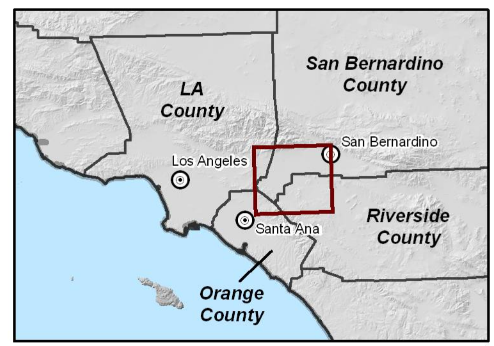

Produced by:

WILDERMUTH ENVIRONMENTAL INC.
23692 Birtcher Drive
Lake Forest, CA 92630
949.420.3030
www.wildermuthenvironmental.com

Author: MJC

Date: 20071030

File: Figure_E-36.mxd

0 1 2 3 4 Miles

0 2 4 6 KM

2007 CBWM Groundwater Model Documentation and Evaluation of the Peace II Project Description

Groundwater Elevation Maps

Change in Groundwater Elevations for Layer 3

Alternative 1B 2005 - 2053

Figure E-36

Appendix F

Groundwater Budgets for Planning Alternatives

Table F-1
Water Budget for Chino North, Chino East, Chino South and Prado Basin Management Zones
Baseline

Period	Inflows							Outflows					Inflow-Outflow
					Artificial Recharge								
	Boundary Inflow	Temescal to PBMZ	Deep Percolation	Stream Recharge	Storm	Replenishment	Subtotal Inflows	Pumping	PBMZ to Temescal	ET	Rising Groundwater	Subtotal Outflow	
2006	32,823	3,118	86,381	26,102	11,830	34,567	194,821	154,078	0	14,768	15,705	184,551	10,270
2007	32,823	3,464	82,131	29,256	11,830	32,960	192,464	168,975	0	14,455	14,168	197,598	-5,134
2008	32,823	3,346	82,540	30,765	11,830	0	161,304	168,653	0	14,366	13,711	196,730	-35,426
2009	32,823	3,121	83,119	31,643	11,830	0	162,536	168,338	0	14,286	13,413	196,037	-33,501
2010	32,823	2,845	81,685	32,225	11,830	0	161,407	168,018	0	14,210	13,216	195,444	-34,036
2011	32,823	2,560	81,397	32,836	11,830	0	161,446	173,787	0	14,105	12,912	200,804	-39,358
2012	32,823	2,265	79,051	33,743	11,830	84,257	243,969	179,560	0	13,961	12,453	205,974	37,995
2013	32,823	2,006	77,836	34,875	11,830	46,453	205,823	185,331	0	13,763	11,880	210,974	-5,151
2014	32,823	1,765	77,415	35,801	11,830	54,778	214,411	191,102	0	13,624	11,500	216,226	-1,815
2015	32,823	1,542	76,682	36,609	11,830	66,012	225,498	196,792	0	13,537	11,259	221,588	3,910
2016	32,823	1,331	75,806	37,179	11,830	64,241	223,210	195,534	0	13,482	11,121	220,137	3,072
2017	32,823	1,135	75,380	37,436	11,830	62,602	221,206	194,274	0	13,452	11,055	218,781	2,425
2018	32,823	954	73,837	37,506	11,830	61,357	218,308	193,018	0	13,440	11,042	217,500	808
2019	32,823	789	73,114	37,467	11,830	60,365	216,388	191,760	0	13,440	11,072	216,272	117
2020	32,823	630	71,198	37,388	11,830	59,509	213,377	190,501	0	13,452	11,132	215,085	-1,708
2021	32,823	486	70,746	37,371	11,830	59,285	212,541	189,738	0	13,464	11,180	214,382	-1,841
2022	32,823	350	69,780	37,450	11,830	59,051	211,284	188,974	0	13,465	11,200	213,639	-2,355
2023	32,823	222	68,382	37,554	11,830	59,000	209,811	188,212	0	13,460	11,203	212,875	-3,064
2024	32,823	99	67,509	37,792	11,830	0	150,053	187,448	0	13,454	11,172	212,074	-62,021
2025	32,823	0	66,570	38,190	11,830	0	149,413	186,687	16	13,430	11,091	211,224	-61,812
2026	32,823	0	65,653	38,763	11,830	0	149,069	186,687	109	13,376	10,917	211,089	-62,020
2027	32,823	0	65,031	39,393	11,830	103,952	253,029	186,687	194	13,306	10,704	210,891	42,138
2028	32,823	0	64,144	39,944	11,830	103,952	252,692	186,687	279	13,242	10,520	210,728	41,965
2029	32,823	0	63,634	40,278	11,830	103,952	252,517	186,687	359	13,191	10,398	210,635	41,882
2030	32,823	0	62,780	40,435	11,830	103,952	251,819	186,687	434	13,157	10,321	210,599	41,221
2031	32,823	0	62,505	40,411	11,830	74,940	222,509	186,687	502	13,134	10,288	210,611	11,899
2032	32,823	0	62,113	40,299	11,830	64,003	211,067	186,687	569	13,125	10,294	210,675	392
2033	32,823	0	61,567	40,139	11,830	64,384	210,743	186,687	629	13,121	10,307	210,744	-1
2034	32,823	0	61,355	39,948	11,830	64,741	210,697	186,687	687	13,121	10,337	210,832	-135
2035	32,823	0	61,088	39,757	11,830	65,102	210,600	186,687	738	13,120	10,364	210,909	-309
2036	32,823	0	60,851	39,602	11,830	65,490	210,596	186,687	789	13,124	10,403	211,003	-407
2037	32,823	0	60,764	39,477	11,830	65,930	210,824	186,687	837	13,127	10,433	211,084	-260
2038	32,823	0	60,480	39,373	11,830	66,398	210,903	186,687	879	13,129	10,460	211,155	-251
2039	32,823	0	60,375	39,335	11,830	0	144,363	186,687	918	13,124	10,462	211,191	-66,828
2040	32,823	0	60,096	39,580	11,830	0	144,328	186,687	957	13,109	10,406	211,159	-66,831
2041	32,823	0	60,057	39,999	11,830	0	144,709	186,687	991	13,077	10,294	211,049	-66,339
2042	32,823	0	59,950	40,541	11,830	103,952	249,096	186,687	1,023	13,031	10,142	210,883	38,213
2043	32,823	0	59,852	40,981	11,830	103,952	249,438	186,687	1,050	12,982	10,009	210,728	38,710
2044	32,823	0	59,764	41,286	11,830	103,952	249,655	186,687	1,082	12,949	9,918	210,636	39,019
2045	32,823	0	59,685	41,386	11,830	103,952	249,676	186,687	1,110	12,933	9,879	210,609	39,067
2046	32,823	0	59,616	41,344	11,830	103,952	249,564	186,687	1,134	12,925	9,873	210,619	38,945
2047	32,823	0	59,556	41,141	11,830	89,202	234,552	186,687	1,156	12,927	9,899	210,669	23,883
2048	32,823	0	59,505	40,888	11,830	67,646	212,692	186,687	1,181	12,939	9,953	210,760	1,932
2049	32,823	0	59,464	40,577	11,830	67,587	212,281	186,687	1,203	12,955	10,013	210,858	1,422
2050	32,823	0	59,432	40,282	11,830	67,568	211,935	186,687	1,223	12,971	10,079	210,960	975
2051	32,823	0	59,404	39,984	11,830	67,639	211,680	186,687	1,240	12,986	10,145	211,058	622
2052	32,823	0	59,379	39,785	11,830	67,811	211,627	186,687	1,261	13,004	10,199	211,151	476
2053	32,823	0	59,356	39,587	11,830	68,058	211,654	186,687	1,278	13,018	10,257	211,240	415
2054	32,823	0	59,337	39,497	11,830	0	143,487	186,687	1,292	13,025	10,286	211,290	-67,802
2055	32,823	0	59,322	39,629	11,830	0	143,603	186,687	1,305	13,019	10,254	211,265	-67,662
2056	32,823	0	59,309	40,038	11,830	0	144,000	186,687	1,319	12,995	10,164	211,165	-67,166
2057	32,823	0	59,299	40,548	11,830	103,952	248,452	186,687	1,331	12,957	10,032	211,007	37,445
2058	32,823	0	59,293	40,985	11,830	103,952	248,883	186,687	1,341	12,918	9,910	210,856	38,026
2059	32,823	0	59,290	41,212	11,830	103,952	249,106	186,687	1,350	12,889	9,842	210,768	38,338
2060	32,823	0	59,290	42,745	11,830	103,952	250,639	186,687	1,390	13,078	9,868	211,023	39,617
Total	1,805,254	32,028	3,643,161	2,108,357	650,650	3,182,307	11,421,756	10,194,825	33,156	732,696	599,115	11,559,792	-138,036
Average	32,823	582	66,239	38,334	11,830	57,860	207,668	185,360	603	13,322	10,893	210,178	-2,510
Maximum	32,823	3,464	86,381	42,745	11,830	103,952	253,029	196,792	1,390	14,768	15,705	221,588	42,138
Minimum	32,823	0	59,290	26,102	11,830	0	143,487	154,078	0	12,889	9,842	184,551	-67,802

Table F-2
Water Budget for Chino North, Chino East, Chino South and Prado Basin Management Zones
Alternative 1A

Period	Inflows							Outflows					Inflow-Outflow
					Artificial Recharge								
	Boundary Inflow	Temescal to PBMZ	Deep Percolation	Stream Recharge	Storm	Replenishment	Subtotal Inflows	Pumping	PBMZ to Temescal	ET	Rising Groundwater	Subtotal Outflow	
2006	32,823	3,118	86,381	26,102	11,830	34,567	194,821	154,078	0	14,768	15,705	184,551	10,270
2007	32,823	3,464	82,131	29,256	11,830	32,960	192,464	168,975	0	14,455	14,168	197,598	-5,134
2008	32,823	3,346	82,540	30,765	11,830	0	161,304	168,653	0	14,366	13,711	196,730	-35,426
2009	32,823	3,121	83,119	31,643	11,830	0	162,536	168,338	0	14,286	13,413	196,037	-33,501
2010	32,823	2,845	81,685	32,225	11,830	0	161,407	168,018	0	14,210	13,216	195,444	-34,036
2011	32,823	2,560	81,397	32,829	11,830	0	161,439	173,787	0	14,105	12,915	200,807	-39,368
2012	32,823	2,267	79,051	33,803	11,830	0	159,774	179,560	0	13,957	12,439	205,956	-46,182
2013	32,823	2,008	77,836	35,222	11,830	0	159,719	185,331	0	13,742	11,785	210,858	-51,139
2014	32,823	1,769	77,415	36,573	11,830	0	160,410	191,102	0	13,574	11,306	215,982	-55,573
2015	32,823	1,545	76,682	37,957	11,830	0	160,837	196,792	0	13,448	10,928	221,168	-60,331
2016	32,823	1,336	75,806	39,230	11,830	23,227	184,252	195,534	0	13,340	10,616	219,490	-35,238
2017	32,823	1,141	75,380	40,238	11,830	23,202	184,614	194,274	0	13,252	10,367	217,893	-33,279
2018	32,823	963	73,837	41,079	11,830	24,232	184,765	193,018	0	13,180	10,166	216,364	-31,600
2019	32,823	798	73,114	41,765	11,830	38,545	198,875	191,760	0	13,123	10,009	214,892	-16,016
2020	32,823	641	71,198	42,329	11,830	37,689	196,509	190,501	0	13,082	9,905	213,488	-16,979
2021	32,823	496	70,746	42,919	11,830	37,465	196,279	189,738	0	13,049	9,803	212,590	-16,311
2022	32,823	359	69,780	43,509	11,830	37,231	195,532	188,974	0	13,012	9,702	211,688	-16,156
2023	32,823	233	68,382	44,045	11,830	37,180	194,493	188,212	0	12,973	9,607	210,792	-16,299
2024	32,823	109	67,509	44,580	11,830	0	156,851	187,448	0	12,940	9,524	209,912	-53,061
2025	32,823	0	66,570	45,116	11,830	0	156,339	186,687	5	12,901	9,422	209,015	-52,676
2026	32,823	0	65,653	45,629	11,830	0	155,935	186,687	99	12,843	9,299	208,928	-52,993
2027	32,823	0	65,031	46,119	11,830	103,952	259,755	185,579	185	12,776	9,170	207,710	52,045
2028	32,823	0	64,144	46,493	11,830	88,514	243,804	185,579	272	12,720	9,067	207,638	36,166
2029	32,823	0	63,634	46,691	11,830	40,729	195,707	185,579	351	12,678	8,997	207,605	-11,897
2030	32,823	0	62,780	46,899	11,830	41,250	195,582	185,579	425	12,642	8,935	207,581	-11,999
2031	32,823	0	62,505	47,086	11,830	51,742	205,986	185,579	495	12,610	8,882	207,566	-1,581
2032	32,823	0	62,113	47,243	11,830	52,183	206,191	185,579	562	12,586	8,842	207,569	-1,378
2033	32,823	0	61,567	47,293	11,830	52,564	206,077	185,579	623	12,567	8,813	207,582	-1,505
2034	32,823	0	61,355	47,281	11,830	52,921	206,210	185,579	679	12,554	8,796	207,608	-1,398
2035	32,823	0	61,088	47,232	11,830	53,282	206,255	185,579	730	12,542	8,783	207,634	-1,379
2036	32,823	0	60,851	47,201	11,830	53,670	206,375	183,755	782	12,538	8,781	205,856	519
2037	32,823	0	60,764	47,130	11,830	54,110	206,657	183,755	830	12,535	8,782	205,902	755
2038	32,823	0	60,480	47,061	11,830	54,578	206,771	183,755	872	12,532	8,784	205,943	828
2039	32,823	0	60,375	47,003	11,830	0	152,031	183,755	911	12,526	8,778	205,970	-53,939
2040	32,823	0	60,096	47,113	11,830	0	151,861	183,755	951	12,516	8,758	205,980	-54,119
2041	32,823	0	60,057	47,369	11,830	0	152,079	183,755	986	12,492	8,705	205,938	-53,859
2042	32,823	0	59,950	47,731	11,830	103,952	256,286	183,755	1,018	12,458	8,633	205,864	50,422
2043	32,823	0	59,852	48,015	11,830	103,952	256,472	183,755	1,046	12,421	8,566	205,788	50,684
2044	32,823	0	59,764	48,188	11,830	103,952	256,557	183,755	1,078	12,399	8,527	205,759	50,798
2045	32,823	0	59,685	48,201	11,830	78,818	231,357	183,755	1,105	12,388	8,515	205,763	25,594
2046	32,823	0	59,616	48,122	11,830	55,994	208,384	183,755	1,131	12,384	8,514	205,784	2,600
2047	32,823	0	59,556	47,970	11,830	55,914	208,093	183,755	1,153	12,383	8,519	205,810	2,283
2048	32,823	0	59,505	47,832	11,830	55,826	207,816	183,755	1,179	12,391	8,535	205,860	1,956
2049	32,823	0	59,464	47,652	11,830	55,767	207,536	183,755	1,201	12,400	8,556	205,912	1,624
2050	32,823	0	59,432	47,472	11,830	55,748	207,305	183,755	1,220	12,410	8,581	205,966	1,339
2051	32,823	0	59,404	47,291	11,830	55,819	207,167	183,755	1,238	12,418	8,601	206,012	1,154
2052	32,823	0	59,379	47,151	11,830	55,991	207,173	183,755	1,259	12,431	8,626	206,071	1,102
2053	32,823	0	59,356	47,007	11,830	56,238	207,254	183,755	1,275	12,442	8,650	206,122	1,132
2054	32,823	0	59,337	46,910	11,830	0	150,900	183,755	1,290	12,449	8,668	206,162	-55,262
2055	32,823	0	59,322	46,967	11,830	0	150,941	183,755	1,303	12,444	8,653	206,155	-55,213
2056	32,823	0	59,309	47,246	11,830	0	151,208	183,755	1,318	12,428	8,610	206,111	-54,903
2057	32,823	0	59,299	47,614	11,830	103,952	255,518	183,755	1,328	12,398	8,545	206,026	49,492
2058	32,823	0	59,293	47,932	11,830	103,952	255,830	183,755	1,340	12,368	8,487	205,950	49,880
2059	32,823	0	59,290	48,059	11,830	103,952	255,953	183,755	1,349	12,346	8,454	205,904	50,049
2060	32,823	0	59,290	49,676	11,830	87,078	240,697	183,755	1,389	12,552	8,480	206,176	34,521
Total	1,805,254	32,119	3,643,161	2,409,064	650,650	2,262,695	10,802,942	10,111,553	32,978	709,328	533,599	11,387,458	-584,516
Average	32,823	584	66,239	43,801	11,830	41,140	196,417	183,846	600	12,897	9,702	207,045	-10,628
Maximum	32,823	3,464	86,381	49,676	11,830	103,952	259,755	196,792	1,389	14,768	15,705	221,168	52,045
Minimum	32,823	0	59,290	26,102	11,830	0	150,900	154,078	0	12,346	8,454	184,551	-60,331

Table F-3
Water Budget for Chino North, Chino East, Chino South and Prado Basin Management Zones
Alternative 1B

Period	Inflows							Outflows					Inflow-Outflow
	Boundary Inflow	Temescal to PBMZ	Deep Percolation	Stream Recharge	Artificial Recharge: Storm	Artificial Recharge: Replenishment	Subtotal Inflows	Pumping	PBMZ to Temescal	ET	Rising Groundwater	Subtotal Outflow	
2006	32,823	3,118	86,381	26,102	11,830	34,567	194,821	154,078	0	14,768	15,705	184,551	10,270
2007	32,823	3,464	82,131	29,256	11,830	32,960	192,464	168,975	0	14,455	14,168	197,598	-5,134
2008	32,823	3,346	82,540	30,765	11,830	0	161,304	168,653	0	14,366	13,711	196,730	-35,426
2009	32,823	3,121	83,119	31,643	11,830	0	162,536	168,338	0	14,286	13,413	196,037	-33,501
2010	32,823	2,845	81,685	32,225	11,830	0	161,407	168,018	0	14,210	13,216	195,444	-34,036
2011	32,823	2,560	81,397	32,829	11,830	0	161,439	173,787	0	14,105	12,915	200,807	-39,368
2012	32,823	2,267	79,051	33,804	11,830	0	159,775	179,560	0	13,957	12,438	205,955	-46,180
2013	32,823	2,008	77,836	35,204	11,830	12,054	171,756	185,331	0	13,743	11,794	210,868	-39,113
2014	32,823	1,769	77,415	36,560	11,830	22,838	183,235	191,102	0	13,577	11,311	215,990	-32,755
2015	32,823	1,546	76,682	37,836	11,830	34,073	194,790	196,792	0	13,458	10,967	221,217	-26,427
2016	32,823	1,334	75,806	38,973	11,830	32,301	193,067	195,534	0	13,367	10,698	219,599	-26,532
2017	32,823	1,139	75,380	39,760	11,830	30,663	191,595	194,274	0	13,298	10,507	218,079	-26,484
2018	32,823	960	73,837	40,380	11,830	29,418	189,248	193,018	0	13,245	10,359	216,622	-27,374
2019	32,823	795	73,114	40,834	11,830	28,426	187,822	191,760	0	13,208	10,259	215,227	-27,405
2020	32,823	639	71,198	41,236	11,830	27,569	185,295	190,501	0	13,182	10,187	213,870	-28,575
2021	32,823	494	70,746	41,710	11,830	27,346	184,948	189,738	0	13,155	10,105	212,998	-28,050
2022	32,823	358	69,780	42,236	11,830	27,112	184,139	188,974	0	13,122	10,010	212,106	-27,967
2023	32,823	231	68,382	42,796	11,830	27,061	183,123	188,212	0	13,082	9,899	211,193	-28,070
2024	32,823	106	67,509	43,425	11,830	0	155,693	187,448	0	13,041	9,785	210,274	-54,581
2025	32,823	0	66,570	44,076	11,830	0	155,299	186,687	6	12,991	9,653	209,337	-54,038
2026	32,823	0	65,653	44,700	11,830	0	155,006	186,687	99	12,923	9,499	209,208	-54,202
2027	32,823	0	65,031	45,337	11,830	103,952	258,973	186,687	185	12,846	9,331	209,049	49,923
2028	32,823	0	64,144	45,906	11,830	37,918	192,620	186,687	272	12,781	9,191	208,931	-16,311
2029	32,823	0	63,634	46,358	11,830	30,610	185,255	185,579	351	12,723	9,085	207,738	-22,483
2030	32,823	0	62,780	46,763	11,830	31,131	185,327	185,579	425	12,670	8,983	207,657	-22,331
2031	32,823	0	62,505	47,118	11,830	51,742	206,018	185,579	493	12,618	8,894	207,584	-1,567
2032	32,823	0	62,113	47,408	11,830	52,183	206,356	185,579	559	12,579	8,826	207,543	-1,187
2033	32,823	0	61,567	47,562	11,830	52,564	206,346	183,755	620	12,551	8,779	205,705	641
2034	32,823	0	61,355	47,646	11,830	52,921	206,575	183,755	677	12,529	8,743	205,704	871
2035	32,823	0	61,088	47,656	11,830	53,282	206,679	183,755	728	12,512	8,720	205,715	964
2036	32,823	0	60,851	47,671	11,830	53,670	206,845	183,755	780	12,503	8,707	205,745	1,100
2037	32,823	0	60,764	47,637	11,830	54,110	207,164	183,755	827	12,497	8,700	205,779	1,386
2038	32,823	0	60,480	47,587	11,830	54,578	207,297	183,755	870	12,492	8,696	205,813	1,484
2039	32,823	0	60,375	47,538	11,830	0	152,566	183,755	909	12,484	8,691	205,839	-53,273
2040	32,823	0	60,096	47,661	11,830	0	152,409	183,755	949	12,473	8,665	205,842	-53,432
2041	32,823	0	60,057	47,912	11,830	0	152,622	182,003	984	12,449	8,614	204,050	-51,427
2042	32,823	0	59,950	48,272	11,830	103,952	256,827	182,003	1,016	12,414	8,543	203,976	52,851
2043	32,823	0	59,852	48,543	11,830	103,952	257,000	182,003	1,045	12,378	8,482	203,908	53,092
2044	32,823	0	59,764	48,705	11,830	103,952	257,074	182,003	1,077	12,357	8,448	203,885	53,189
2045	32,823	0	59,685	48,711	11,830	78,818	231,867	182,003	1,104	12,346	8,432	203,885	27,982
2046	32,823	0	59,616	48,602	11,830	55,994	208,864	182,003	1,131	12,344	8,438	203,916	4,948
2047	32,823	0	59,556	48,427	11,830	55,914	208,550	182,003	1,153	12,347	8,446	203,949	4,601
2048	32,823	0	59,505	48,251	11,830	55,826	208,235	182,003	1,179	12,357	8,468	204,007	4,228
2049	32,823	0	59,464	48,058	11,830	55,767	207,942	182,003	1,200	12,366	8,488	204,057	3,884
2050	32,823	0	59,432	47,837	11,830	55,748	207,670	182,003	1,220	12,380	8,520	204,123	3,547
2051	32,823	0	59,404	47,637	11,830	55,819	207,513	182,003	1,238	12,390	8,538	204,169	3,343
2052	32,823	0	59,379	47,456	11,830	55,991	207,478	182,003	1,258	12,405	8,574	204,240	3,238
2053	32,823	0	59,356	47,296	11,830	56,238	207,543	182,003	1,275	12,417	8,596	204,291	3,252
2054	32,823	0	59,337	47,158	11,830	0	151,148	182,003	1,290	12,428	8,620	204,341	-53,193
2055	32,823	0	59,322	47,182	11,830	0	151,156	182,003	1,302	12,425	8,612	204,342	-53,186
2056	32,823	0	59,309	47,422	11,830	0	151,384	182,003	1,318	12,412	8,578	204,311	-52,927
2057	32,823	0	59,299	47,757	11,830	103,952	255,661	182,003	1,330	12,385	8,523	204,241	51,420
2058	32,823	0	59,293	48,035	11,830	103,952	255,933	182,003	1,340	12,358	8,472	204,173	51,760
2059	32,823	0	59,290	48,150	11,830	103,952	256,044	182,003	1,349	12,339	8,441	204,132	51,912
2060	32,823	0	59,290	49,727	11,830	87,078	240,748	182,003	1,391	12,547	8,473	204,414	36,334
Total	1,805,254	32,100	3,643,161	2,407,336	650,650	2,231,949	10,770,450	10,073,257	32,950	709,640	534,916	11,350,763	-580,313
Average	32,823	584	66,239	43,770	11,830	40,581	195,826	183,150	599	12,903	9,726	206,378	-10,551
Maximum	32,823	3,464	86,381	49,727	11,830	103,952	258,973	196,792	1,391	14,768	15,705	221,217	53,189
Minimum	32,823	0	59,290	26,102	11,830	0	151,148	154,078	0	12,339	8,432	184,551	-54,581

Table F-4
Water Budget for Chino North, Chino East, Chino South and Prado Basin Management Zones
Baseline with Dry Year Yield Program

Period	Inflows							Outflows					Inflow-Outflow
					Artificial Recharge								
	Boundary Inflow	Temescal to PBMZ	Deep Percolation	Stream Recharge	Storm	Replenishment	Subtotal Inflows	Pumping	PBMZ to Temescal	ET	Rising Groundwater	Subtotal Outflow	
2006	32,823	3,118	86,381	26,102	11,830	34,567	194,821	154,078	0	14,767	15,705	184,550	10,271
2007	32,823	3,464	82,131	29,256	11,830	32,960	192,464	168,975	0	14,455	14,168	197,598	-5,134
2008	32,823	3,346	82,540	30,765	11,830	0	161,304	168,653	0	14,363	13,711	196,727	-35,423
2009	32,823	3,121	83,119	31,643	11,830	0	162,536	168,338	0	14,270	13,413	196,021	-33,485
2010	32,823	2,845	81,685	32,225	11,830	0	161,407	168,018	0	14,164	13,216	195,398	-33,991
2011	32,823	2,560	81,397	32,836	11,830	0	161,446	173,787	0	14,018	12,912	200,717	-39,271
2012	32,823	2,265	79,051	33,743	11,830	84,257	243,969	179,560	0	13,842	12,453	205,855	38,114
2013	32,823	2,006	77,836	34,875	11,830	46,453	205,823	185,331	0	13,641	11,880	210,852	-5,028
2014	32,823	1,765	77,415	35,801	11,830	54,778	214,411	191,102	0	13,521	11,500	216,123	-1,712
2015	32,823	1,542	76,682	36,609	11,830	66,012	225,498	196,792	0	13,466	11,259	221,517	3,981
2016	32,823	1,331	75,806	37,179	11,830	64,241	223,210	195,534	0	13,445	11,121	220,100	3,110
2017	32,823	1,135	75,380	37,436	11,830	62,602	221,206	194,274	0	13,437	11,055	218,766	2,440
2018	32,823	954	73,837	37,506	11,830	61,357	218,308	193,018	0	13,431	11,042	217,491	816
2019	32,823	789	73,114	37,467	11,830	60,365	216,388	191,760	0	13,432	11,072	216,264	124
2020	32,823	630	71,198	37,388	11,830	59,509	213,377	190,501	0	13,445	11,132	215,078	-1,701
2021	32,823	486	70,746	37,371	11,830	59,285	212,541	189,738	0	13,457	11,180	214,375	-1,834
2022	32,823	350	69,780	37,450	11,830	59,051	211,284	188,974	0	13,458	11,200	213,632	-2,348
2023	32,823	222	68,382	37,554	11,830	59,000	209,811	188,212	0	13,454	11,203	212,869	-3,058
2024	32,823	99	67,509	37,792	11,830	0	150,053	187,448	0	13,432	11,172	212,052	-61,999
2025	32,823	0	66,570	38,190	11,830	0	149,413	186,687	16	13,380	11,091	211,174	-61,761
2026	32,823	0	65,653	38,763	11,830	0	149,069	186,687	109	13,288	10,917	211,001	-61,932
2027	32,823	0	65,031	39,393	11,830	103,952	253,029	186,687	194	13,188	10,704	210,773	42,256
2028	32,823	0	64,144	39,944	11,830	103,952	252,692	186,687	279	13,121	10,520	210,607	42,085
2029	32,823	0	63,634	40,278	11,830	103,952	252,517	186,687	359	13,092	10,398	210,536	41,981
2030	32,823	0	62,780	40,435	11,830	103,952	251,819	186,687	434	13,090	10,321	210,532	41,288
2031	32,823	0	62,505	40,411	11,830	74,940	222,509	186,687	502	13,104	10,288	210,581	11,928
2032	32,823	0	62,113	40,299	11,830	64,003	211,067	186,687	569	13,120	10,294	210,670	397
2033	32,823	0	61,567	40,139	11,830	64,384	210,743	186,687	629	13,127	10,307	210,750	-7
2034	32,823	0	61,355	39,948	11,830	64,741	210,697	186,687	687	13,131	10,337	210,842	-145
2035	32,823	0	61,088	39,757	11,830	65,102	210,600	186,687	738	13,133	10,364	210,922	-322
2036	32,823	0	60,851	39,602	11,830	65,490	210,596	186,687	789	13,136	10,403	211,015	-419
2037	32,823	0	60,764	39,477	11,830	65,930	210,824	186,687	837	13,136	10,433	211,093	-269
2038	32,823	0	60,480	39,373	11,830	66,398	210,903	186,687	879	13,135	10,460	211,161	-258
2039	32,823	0	60,375	39,335	11,830	0	144,363	186,687	918	13,118	10,462	211,185	-66,822
2040	32,823	0	60,096	39,580	11,830	0	144,328	186,687	957	13,074	10,406	211,124	-66,796
2041	32,823	0	60,057	39,999	11,830	0	144,709	186,687	991	13,003	10,294	210,975	-66,265
2042	32,823	0	59,950	40,541	11,830	103,952	249,096	186,687	1,023	12,925	10,142	210,777	38,319
2043	32,823	0	59,852	40,981	11,830	103,952	249,438	186,687	1,050	12,875	10,009	210,621	38,817
2044	32,823	0	59,764	41,286	11,830	103,952	249,655	186,687	1,082	12,864	9,918	210,551	39,104
2045	32,823	0	59,685	41,386	11,830	103,952	249,676	186,687	1,110	12,877	9,879	210,553	39,123
2046	32,823	0	59,616	41,344	11,830	103,952	249,564	186,687	1,134	12,907	9,873	210,601	38,963
2047	32,823	0	59,556	41,141	11,830	89,202	234,552	186,687	1,156	12,935	9,899	210,677	23,875
2048	32,823	0	59,505	40,888	11,830	67,646	212,692	186,687	1,181	12,958	9,953	210,779	1,913
2049	32,823	0	59,464	40,577	11,830	67,587	212,281	186,687	1,203	12,977	10,013	210,880	1,401
2050	32,823	0	59,432	40,282	11,830	67,568	211,935	186,687	1,223	12,995	10,079	210,984	951
2051	32,823	0	59,404	39,984	11,830	67,639	211,680	186,687	1,240	13,008	10,145	211,080	600
2052	32,823	0	59,379	39,785	11,830	67,811	211,627	186,687	1,261	13,023	10,199	211,170	457
2053	32,823	0	59,356	39,587	11,830	68,058	211,654	186,687	1,278	13,035	10,257	211,257	397
2054	32,823	0	59,337	39,497	11,830	0	143,487	186,687	1,292	13,030	10,286	211,295	-67,808
2055	32,823	0	59,322	39,629	11,830	0	143,603	186,687	1,305	12,992	10,254	211,238	-67,635
2056	32,823	0	59,309	40,038	11,830	0	144,000	186,687	1,319	12,930	10,164	211,100	-67,100
2057	32,823	0	59,299	40,548	11,830	103,952	248,452	186,687	1,331	12,861	10,032	210,911	37,541
2058	32,823	0	59,293	40,985	11,830	103,952	248,883	186,687	1,341	12,804	9,910	210,742	38,140
2059	32,823	0	59,290	41,212	11,830	103,952	249,106	186,687	1,350	12,768	9,842	210,647	38,459
2060	32,823	0	59,290	42,745	11,830	103,952	250,639	186,687	1,390	12,956	9,868	210,901	39,739
Total	1,805,254	32,028	3,643,161	2,108,357	650,650	3,182,307	11,421,756	10,194,825	33,156	730,593	599,115	11,557,689	-135,933
Average	32,823	582	66,239	38,334	11,830	57,860	207,668	185,360	603	13,284	10,893	210,140	-2,472
Maximum	32,823	3,464	86,381	42,745	11,830	103,952	253,029	196,792	1,390	14,767	15,705	221,517	42,256
Minimum	32,823	0	59,290	26,102	11,830	0	143,487	154,078	0	12,768	9,842	184,550	-67,808

Table F-5
Water Budget for Chino North, Chino East, Chino South and Prado Basin Management Zones
Alternative 1A with Dry Year Yield Program

Period	Inflows							Outflows					Inflow-Outflow
					Artificial Recharge								
	Boundary Inflow	Temescal to PBMZ	Deep Percolation	Stream Recharge	Storm	Replenishment	Subtotal Inflows	Pumping	PBMZ to Temescal	ET	Rising Groundwater	Subtotal Outflow	
2006	32,823	3,119	86,381	26,110	11,830	34,567	194,830	154,078	0	14,767	15,700	184,545	10,285
2007	32,823	3,464	82,131	29,261	11,830	32,960	192,469	168,975	0	14,455	14,161	197,591	-5,122
2008	32,823	3,345	82,540	30,772	11,830	0	161,310	168,653	0	14,363	13,701	196,717	-35,407
2009	32,823	3,121	83,119	31,823	11,830	0	162,716	201,333	0	14,270	13,335	228,938	-66,222
2010	32,823	2,845	81,685	32,821	11,830	0	162,003	201,012	0	14,164	12,988	228,164	-66,161
2011	32,823	2,563	81,397	33,946	11,830	0	162,559	206,781	0	14,017	12,521	233,319	-70,760
2012	32,823	2,271	79,051	35,297	11,830	0	161,272	179,560	0	13,839	11,955	205,354	-44,082
2013	32,823	2,012	77,836	36,717	11,830	0	161,218	160,316	0	13,625	11,368	185,309	-24,091
2014	32,823	1,771	77,415	37,808	11,830	0	161,647	166,088	0	13,480	10,987	190,555	-28,908
2015	32,823	1,547	76,682	38,798	11,830	0	161,680	171,780	0	13,385	10,724	195,889	-34,209
2016	32,823	1,335	75,806	39,611	11,830	23,227	184,632	170,521	0	13,315	10,537	194,373	-9,741
2017	32,823	1,140	75,380	40,263	11,830	23,202	184,638	194,274	0	13,254	10,380	217,908	-33,270
2018	32,823	960	73,837	40,898	11,830	24,232	184,581	193,018	0	13,195	10,219	216,432	-31,851
2019	32,823	797	73,114	41,450	11,830	38,545	198,559	191,760	0	13,144	10,087	214,991	-16,431
2020	32,823	640	71,198	41,974	11,830	37,689	196,153	190,501	0	13,107	9,975	213,583	-17,430
2021	32,823	493	70,746	42,521	11,830	37,465	195,878	189,738	0	13,076	9,880	212,694	-16,816
2022	32,823	358	69,780	43,055	11,830	37,231	195,077	188,974	0	13,040	9,789	211,803	-16,726
2023	32,823	232	68,382	43,606	11,830	37,180	194,053	188,212	0	13,000	9,683	210,895	-16,842
2024	32,823	109	67,509	44,311	11,830	0	156,582	217,880	0	12,954	9,556	240,390	-83,808
2025	32,823	0	66,570	45,232	11,830	0	156,455	214,657	5	12,886	9,377	236,925	-80,471
2026	32,823	0	65,653	46,214	11,830	0	156,520	213,448	98	12,791	9,172	235,509	-78,989
2027	32,823	0	65,031	47,046	11,830	103,952	260,682	182,003	181	12,694	8,990	203,868	56,814
2028	32,823	0	64,144	47,473	11,830	88,514	244,784	156,989	268	12,634	8,889	178,780	66,003
2029	32,823	0	63,634	47,496	11,830	40,729	196,512	156,989	349	12,608	8,858	178,804	17,708
2030	32,823	0	62,780	47,369	11,830	41,250	196,052	156,989	425	12,600	8,860	178,874	17,178
2031	32,823	0	62,505	47,136	11,830	51,742	206,036	156,989	495	12,601	8,876	178,961	27,074
2032	32,823	0	62,113	46,948	11,830	52,183	205,896	182,003	562	12,603	8,888	204,056	1,841
2033	32,823	0	61,567	46,751	11,830	52,564	205,535	182,003	626	12,601	8,894	204,124	1,411
2034	32,823	0	61,355	46,590	11,830	52,921	205,519	182,003	681	12,598	8,893	204,175	1,344
2035	32,823	0	61,088	46,400	11,830	53,282	205,423	182,003	732	12,597	8,905	204,237	1,186
2036	32,823	0	60,851	46,280	11,830	53,670	205,454	182,003	785	12,599	8,913	204,300	1,154
2037	32,823	0	60,764	46,147	11,830	54,110	205,674	182,003	831	12,599	8,928	204,361	1,313
2038	32,823	0	60,480	46,065	11,830	54,578	205,775	182,003	874	12,599	8,926	204,402	1,373
2039	32,823	0	60,375	46,126	11,830	0	151,154	213,448	913	12,584	8,901	235,846	-84,692
2040	32,823	0	60,096	46,621	11,830	0	151,369	213,448	952	12,548	8,813	235,761	-84,392
2041	32,823	0	60,057	47,348	11,830	0	152,058	206,785	986	12,489	8,686	228,946	-76,887
2042	32,823	0	59,950	48,082	11,830	103,952	256,637	177,259	1,017	12,424	8,557	199,257	57,380
2043	32,823	0	59,852	48,385	11,830	103,952	256,842	152,245	1,044	12,384	8,493	174,166	82,676
2044	32,823	0	59,764	48,324	11,830	103,952	256,693	152,245	1,077	12,382	8,501	174,205	82,487
2045	32,823	0	59,685	47,975	11,830	78,818	231,131	152,245	1,106	12,403	8,552	174,306	56,825
2046	32,823	0	59,616	47,458	11,830	55,994	207,720	152,245	1,133	12,436	8,625	174,439	33,281
2047	32,823	0	59,556	46,941	11,830	55,914	207,064	177,259	1,157	12,464	8,693	199,573	7,491
2048	32,823	0	59,505	46,537	11,830	55,826	206,521	177,259	1,183	12,490	8,746	199,678	6,842
2049	32,823	0	59,464	46,149	11,830	55,767	206,033	177,259	1,204	12,515	8,799	199,777	6,256
2050	32,823	0	59,432	45,794	11,830	55,748	205,627	177,259	1,225	12,536	8,854	199,874	5,753
2051	32,823	0	59,404	45,473	11,830	55,819	205,349	177,259	1,242	12,554	8,900	199,955	5,394
2052	32,823	0	59,379	45,217	11,830	55,991	205,239	177,259	1,262	12,575	8,953	200,049	5,190
2053	32,823	0	59,356	44,973	11,830	56,238	205,220	177,259	1,278	12,593	8,999	200,129	5,092
2054	32,823	0	59,337	44,957	11,830	0	148,947	206,785	1,294	12,594	9,001	229,674	-80,727
2055	32,823	0	59,322	45,311	11,830	0	149,285	206,785	1,306	12,570	8,930	229,591	-80,305
2056	32,823	0	59,309	46,004	11,830	0	149,966	206,785	1,319	12,523	8,804	229,431	-79,465
2057	32,823	0	59,299	46,679	11,830	103,952	254,583	177,259	1,329	12,470	8,686	199,744	54,839
2058	32,823	0	59,293	47,076	11,830	103,952	254,974	177,259	1,339	12,430	8,613	199,641	55,333
2059	32,823	0	59,290	47,221	11,830	103,952	255,115	177,259	1,348	12,405	8,573	199,585	55,531
2060	32,823	0	59,290	48,759	11,830	87,078	239,780	177,259	1,388	12,609	8,612	199,868	39,912
Total	1,805,254	32,122	3,643,161	2,391,599	650,650	2,262,695	10,785,480	10,005,663	33,014	710,439	535,206	11,284,322	-498,842
Average	32,823	584	66,239	43,484	11,830	41,140	196,100	181,921	600	12,917	9,731	205,169	-9,070
Maximum	32,823	3,464	86,381	48,759	11,830	103,952	260,682	217,880	1,388	14,767	15,700	240,390	82,676
Minimum	32,823	0	59,290	26,110	11,830	0	148,947	152,245	0	12,382	8,493	174,166	-84,692

Table F-6
Water Budget for Chino North, Chino East, Chino South and Prado Basin Management Zones
Alternative 1B with Dry Year Yield Program

Period	Inflows							Outflows					Inflow-Outflow
					Artificial Recharge								
	Boundary Inflow	Temescal to PBMZ	Deep Percolation	Stream Recharge	Storm	Replenishment	Subtotal Inflows	Pumping	PBMZ to Temescal	ET	Rising Groundwater	Subtotal Outflow	
2006	32,823	3,119	86,381	26,110	11,830	34,567	194,830	154,078	0	14,767	15,700	184,545	10,285
2007	32,823	3,464	82,131	29,261	11,830	32,960	192,469	168,975	0	14,455	14,161	197,591	-5,122
2008	32,823	3,345	82,540	30,772	11,830	0	161,310	168,653	0	14,363	13,701	196,717	-35,407
2009	32,823	3,121	83,119	31,823	11,830	0	162,716	201,333	0	14,270	13,335	228,938	-66,222
2010	32,823	2,845	81,685	32,821	11,830	0	162,003	201,012	0	14,164	12,988	228,164	-66,161
2011	32,823	2,563	81,397	33,946	11,830	0	162,559	206,781	0	14,017	12,521	233,319	-70,760
2012	32,823	2,271	79,051	35,297	11,830	0	161,272	179,560	0	13,839	11,956	205,355	-44,082
2013	32,823	2,012	77,836	36,693	11,830	12,054	173,249	160,316	0	13,625	11,373	185,314	-12,065
2014	32,823	1,773	77,415	37,734	11,830	22,838	184,413	166,088	0	13,481	11,000	190,569	-6,156
2015	32,823	1,548	76,682	38,587	11,830	34,073	195,543	171,780	0	13,397	10,772	195,949	-406
2016	32,823	1,335	75,806	39,205	11,830	32,301	193,300	170,521	0	13,344	10,639	194,504	-1,203
2017	32,823	1,139	75,380	39,669	11,830	30,663	191,504	194,274	0	13,300	10,528	218,102	-26,598
2018	32,823	960	73,837	40,104	11,830	29,418	188,972	193,018	0	13,261	10,418	216,697	-27,725
2019	32,823	794	73,114	40,491	11,830	28,426	187,478	191,760	0	13,226	10,324	215,310	-27,832
2020	32,823	638	71,198	40,859	11,830	27,569	184,917	190,501	0	13,201	10,252	213,954	-29,038
2021	32,823	493	70,746	41,319	11,830	27,346	184,556	189,738	0	13,175	10,170	213,083	-28,527
2022	32,823	358	69,780	41,845	11,830	27,112	183,748	188,974	0	13,140	10,075	212,189	-28,442
2023	32,823	231	68,382	42,432	11,830	27,061	182,759	188,212	0	13,097	9,953	211,262	-28,503
2024	32,823	107	67,509	43,246	11,830	0	155,515	217,880	0	13,044	9,794	240,718	-85,203
2025	32,823	0	66,570	44,296	11,830	0	155,519	214,657	6	12,966	9,579	237,208	-81,689
2026	32,823	0	65,653	45,394	11,830	0	155,700	213,448	97	12,860	9,328	235,733	-80,033
2027	32,823	0	65,031	46,322	11,830	103,952	259,958	182,003	182	12,755	9,117	204,057	55,901
2028	32,823	0	64,144	46,837	11,830	37,918	193,551	156,989	268	12,688	8,999	178,944	14,607
2029	32,823	0	63,634	47,011	11,830	30,610	185,908	156,989	348	12,653	8,946	178,936	6,972
2030	32,823	0	62,780	47,057	11,830	31,131	185,621	156,989	424	12,632	8,917	178,962	6,659
2031	32,823	0	62,505	46,966	11,830	51,742	205,866	156,989	493	12,621	8,913	179,016	26,850
2032	32,823	0	62,113	46,922	11,830	52,183	205,870	182,003	562	12,610	8,901	204,076	1,794
2033	32,823	0	61,567	46,896	11,830	52,564	205,680	182,003	621	12,592	8,871	204,087	1,593
2034	32,823	0	61,355	46,850	11,830	52,921	205,779	182,003	680	12,580	8,856	204,119	1,660
2035	32,823	0	61,088	46,770	11,830	53,282	205,793	182,003	732	12,571	8,847	204,153	1,640
2036	32,823	0	60,851	46,733	11,830	53,670	205,907	182,003	784	12,566	8,840	204,193	1,714
2037	32,823	0	60,764	46,671	11,830	54,110	206,198	182,003	829	12,561	8,837	204,230	1,968
2038	32,823	0	60,480	46,632	11,830	54,578	206,342	182,003	872	12,555	8,830	204,260	2,082
2039	32,823	0	60,375	46,730	11,830	0	151,758	213,448	911	12,537	8,798	235,694	-83,935
2040	32,823	0	60,096	47,233	11,830	0	151,981	210,680	950	12,499	8,709	232,838	-80,857
2041	32,823	0	60,057	47,957	11,830	0	152,667	206,785	982	12,439	8,587	228,793	-76,125
2042	32,823	0	59,950	48,681	11,830	103,952	257,236	177,259	1,014	12,374	8,462	199,109	58,127
2043	32,823	0	59,852	48,981	11,830	103,952	257,438	152,245	1,043	12,334	8,398	174,020	83,418
2044	32,823	0	59,764	48,921	11,830	103,952	257,290	152,245	1,075	12,333	8,407	174,060	83,230
2045	32,823	0	59,685	48,576	11,830	78,818	231,732	152,245	1,104	12,353	8,454	174,156	57,575
2046	32,823	0	59,616	48,051	11,830	55,994	208,313	152,245	1,131	12,388	8,529	174,293	34,020
2047	32,823	0	59,556	47,540	11,830	55,914	207,663	177,259	1,156	12,416	8,596	199,427	8,236
2048	32,823	0	59,505	47,144	11,830	55,826	207,128	177,259	1,183	12,442	8,645	199,529	7,599
2049	32,823	0	59,464	46,770	11,830	55,767	206,654	177,259	1,204	12,464	8,692	199,619	7,035
2050	32,823	0	59,432	46,413	11,830	55,748	206,246	177,259	1,224	12,488	8,743	199,714	6,532
2051	32,823	0	59,404	46,069	11,830	55,819	205,945	177,259	1,242	12,508	8,790	199,799	6,146
2052	32,823	0	59,379	45,797	11,830	55,991	205,819	177,259	1,261	12,529	8,844	199,893	5,926
2053	32,823	0	59,356	45,561	11,830	56,238	205,808	177,259	1,277	12,546	8,884	199,966	5,843
2054	32,823	0	59,337	45,524	11,830	0	149,514	206,785	1,294	12,550	8,892	229,521	-80,006
2055	32,823	0	59,322	45,877	11,830	0	149,851	206,785	1,304	12,524	8,819	229,432	-79,581
2056	32,823	0	59,309	46,546	11,830	0	150,508	206,785	1,318	12,479	8,710	229,292	-78,784
2057	32,823	0	59,299	47,204	11,830	103,952	255,108	177,259	1,328	12,427	8,600	199,614	55,494
2058	32,823	0	59,293	47,608	11,830	103,952	255,506	177,259	1,340	12,387	8,527	199,513	55,993
2059	32,823	0	59,290	47,740	11,830	103,952	255,634	177,259	1,347	12,362	8,489	199,457	56,178
2060	32,823	0	59,290	49,303	11,830	87,078	240,324	177,259	1,388	12,568	8,523	199,738	40,586
Total	1,805,254	32,116	3,643,161	2,393,797	650,650	2,231,949	10,756,927	10,002,895	32,974	710,321	535,539	11,281,729	-524,802
Average	32,823	584	66,239	43,524	11,830	40,581	195,580	181,871	600	12,915	9,737	205,122	-9,542
Maximum	32,823	3,464	86,381	49,303	11,830	103,952	259,958	217,880	1,388	14,767	15,700	240,718	83,418
Minimum	32,823	0	59,290	26,110	11,830	0	149,514	152,245	0	12,333	8,398	174,020	-85,203